

# **MicroRNA in Neural Crest development and Neurocristopathies**

**Marco Antonaci**

Thesis submitted for the degree of Doctor of Philosophy

University of East Anglia  
School of Biological Sciences  
Norwich

Word count: 35570

©This copy of the thesis has been supplied on condition that anyone who consults it is understood to recognise that its copyright rests with the author and that use of any information derived there from must be in accordance current UK Copyright Law. In addition, any quotation or extract must include full attribution.

## **Abstract**

The neural crest (NC) is a multipotent population of cells, unique for vertebrates, that originates during late gastrulation/early neurulation. The origin of this population of cells is in the region between the neural ectoderm and the non-neural ectoderm. During the development of the embryo, neural crest cells (NCCs) undergo different waves of migration thanks to a process called epithelial to mesenchymal transition (EMT). This process allows NCCs to migrate towards the whole developing embryo.

At the end of this process, NCCs differentiate to give rise to an astonishing number of derivatives in the adult organism. These derivatives range from the craniofacial skeleton, teeth, cardiac cells, chromaffin cells of the adrenal gland, enteric ganglia, and pigment cells. Because of this, failure during NC development can cause a variety of diseases, often syndromic. These diseases are globally called neurocristopathies (NCPs).

In recent years, the attention of research has moved from the coding regions of the genome to the non-coding regions. This includes long non-coding RNAs (lncRNAs), Piwi-interacting RNAs (piRNAs) and micro RNAs (miRNAs). In particular, miRNAs are small RNA molecules (~22nt in length) that are mainly involved in post-transcriptional regulation of gene expression. As for the mechanism of action, they mainly target the 3' untranslated region (UTR) of mRNAs in a sequence-specific manner and promote their degradation, resulting in the downregulation of gene expression.

The aim of my research is to investigate how miRNAs regulate the development of the NC, and to identify possible miRNAs that might be involved in the onset of NCPs. To do this, I mainly used the African clawed frog *Xenopus tropicalis* as model organism, and tuned the expression of specific miRNAs to investigate any NC-specific phenotype. By doing so, we described a novel molecular mechanism involving the role of *xtr-miR-204-1* during *Xenopus tropicalis* eye development. These findings open to the exciting possibility that miRNAs might be involved in more molecular processes than previously thought, highlighting the importance of studying these genetic regulators during physiological and pathological conditions.

## **Access Condition and Agreement**

Each deposit in UEA Digital Repository is protected by copyright and other intellectual property rights, and duplication or sale of all or part of any of the Data Collections is not permitted, except that material may be duplicated by you for your research use or for educational purposes in electronic or print form. You must obtain permission from the copyright holder, usually the author, for any other use. Exceptions only apply where a deposit may be explicitly provided under a stated licence, such as a Creative Commons licence or Open Government licence.

Electronic or print copies may not be offered, whether for sale or otherwise to anyone, unless explicitly stated under a Creative Commons or Open Government license. Unauthorised reproduction, editing or reformatting for resale purposes is explicitly prohibited (except where approved by the copyright holder themselves) and UEA reserves the right to take immediate 'take down' action on behalf of the copyright and/or rights holder if this Access condition of the UEA Digital Repository is breached. Any material in this database has been supplied on the understanding that it is copyright material and that no quotation from the material may be published without proper acknowledgement.

# **Table of Contents**

<b>Abstract.....</b>	<b>2</b>
<b>Table of contents.....</b>	<b>3</b>
<b>Index.....</b>	<b>4</b>
<b>List of figures.....</b>	<b>8</b>
<b>List of tables.....</b>	<b>10</b>
<b>Abbreviations.....</b>	<b>10</b>
<b>Chapter 1: Introduction.....</b>	<b>13</b>
<b>Chapter 2: Materials and methods.....</b>	<b>44</b>
<b>Chapter 3: Identification and knock-down of micro RNAs potentially with neural crest development.....</b>	<b>61</b>
<b>Chapter 4: Investigation on <i>xtr-miR-204-1</i> developmental role.....</b>	<b>85</b>
<b>Chapter 5: Investigation on <i>xtr-miR-204-1</i> Gene Regulatory Network.....</b>	<b>107</b>
<b>Chapter 6: General discussion and concluding remarks.....</b>	<b>139</b>
<b>Acknowledgements.....</b>	<b>160</b>
<b>References.....</b>	<b>161</b>
<b>Publications.....</b>	<b>178</b>

## **Chapter 1: Introduction**

<b>1.1 NEUcrest project.....</b>	<b>13</b>
<b>1.2 Neural Crest.....</b>	<b>14</b>
<i>1.2.1 Specification of the NC.....</i>	<i>14</i>
<i>1.2.2 NC epithelial-to-mesenchymal transition and migration.....</i>	<i>15</i>
<i>1.2.3 NC differentiation.....</i>	<i>18</i>
<i>1.2.4 Neurocristopathies.....</i>	<i>19</i>
<b>1.3 Eye development.....</b>	<b>22</b>
<i>1.3.1 Induction of the optic vesicle and formation of the optic cup.....</i>	<i>22</i>
<i>1.3.2 Lens development.....</i>	<i>25</i>
<i>1.3.3 Retinal development.....</i>	<i>26</i>
<i>1.3.4 NC contribution to eye development.....</i>	<i>27</i>
<b>1.4 Micro RNAs.....</b>	<b>30</b>
<i>1.4.1 From primary transcripts to mature miRNAs.....</i>	<i>31</i>
<i>1.4.2 RNA interference.....</i>	<i>35</i>
<i>1.4.3 miRNAs in other pathways.....</i>	<i>37</i>
<i>1.4.4 The role of miRNAs in the embryo development.....</i>	<i>38</i>
<i>1.4.5 miRNAs and neurocristopathies.....</i>	<i>40</i>
<b>1.5 Aim of the project.....</b>	<b>42</b>

## **Chapter 2: Materials and methods**

<b>2.1 Collection of <i>Xenopus laevis</i> eggs.....</b>	<b>44</b>
<b>2.2 Fertilisation of <i>Xenopus laevis</i> eggs.....</b>	<b>44</b>
<b>2.3 Collection of <i>Xenopus tropicalis</i> eggs.....</b>	<b>44</b>
<b>2.4 Fertilisation of <i>Xenopus tropicalis</i> eggs.....</b>	<b>44</b>
<b>2.5 Fixation of <i>Xenopus</i> sp embryos.....</b>	<b>45</b>
<b>2.6 Sperm freezing.....</b>	<b>45</b>

<i>2.6.1 Xenopus tropicalis</i> .....	45
<i>2.6.2 Xenopus laevis</i> .....	45
<b>2.7 Transformation of bacteria</b> .....	<b>46</b>
<b>2.8 Cloning for in situ probes</b> .....	<b>46</b>
<i>2.8.1 Primers design</i> .....	46
<i>2.8.2 RNA extraction and cDNA synthesis</i> .....	47
<i>2.8.3 Amplification of the gene of interest and cloning</i> .....	47
<i>2.8.4 Transformation and colony PCR</i> .....	49
<i>2.8.5 MINI and sequencing</i> .....	50
<b>2.9 WISH probe synthesis</b> .....	<b>50</b>
<i>2.9.1 By plasmid linearisation</i> .....	50
<i>2.9.2 By PCR reaction</i> .....	51
<b>2.10 mRNA synthesis</b> .....	<b>52</b>
<i>2.10.1 Using SP6 mMessage mMachine kit</i> .....	52
<i>2.10.2 Recovery of mRNA</i> .....	52
<b>2.11 Whole-mount in-situ hybridisation</b> .....	<b>53</b>
<b>2.12 LNA Whole-mount in-situ hybridisation</b> .....	<b>54</b>
<b>2.13 CRISPR/Cas9</b> .....	<b>55</b>
<i>2.13.1 sgRNA synthesis</i> .....	55
<i>2.13.2 Microinjector settings</i> .....	56
<i>2.13.3 Injection solution loading</i> .....	56
<i>2.13.4 Microinjections</i> .....	56
<i>2.13.5 Microinjection solution</i> .....	57
<i>2.13.6 Genomic DNA extraction</i> .....	57
<i>2.13.7 T7 endonuclease assay</i> .....	57
<b>2.14 Figure making</b> .....	<b>58</b>

2.15 Statistical analysis.....	58
2.16 Solutions.....	59

## **Chapter 3: Identification and knock-down of micro RNAs potentially involved with neural crest development**

3.1 Rescue of the knock-down phenotypes by using miRNA mimics in <i>Xenopus tropicalis</i> .....	61
3.1.1 Assessment of the overexpression of miR-219 phenotype.....	62
3.1.2 Rescue of the knock-down phenotype of miR-219.....	65
3.2 Bioinformatical analysis to discover new miRNAs involved in NC development and NCPs.....	67
3.2.1 In-silico approaches to predict important miRNAs involved in NC development...	67
3.2.2 Strategy to predict miRNAs involved in the etiopathogenesis of craniosynostosis.	71
3.3 gRNAs testing and first screening of the knock-down phenotype.....	74
3.1.1 guide RNA design strategy and targets.....	74
3.3.2 miR-218-2.....	76
3.3.3 miR-10b.....	79
3.3.4 miR-208.....	82

## **Chapter 4: The role of *xtr-miR-204-1* in development**

4.1 <i>xtr-miR-204-1</i> and <i>trpm1</i> expression.....	87
4.2 Preliminary gRNAs testing and <i>xtr-miR-204-1</i> knock-down.....	91
4.3 <i>xtr-miR-204-1</i> knock-down phenotype.....	93
4.4 <i>xtr-miR-204-1-5p</i> overexpression.....	95
4.5 <i>xtr-miR-204-1-5p</i> rescue.....	97
4.6 <i>xtr-miR-204-1-3p</i> overexpression.....	99
4.7 <i>xtr-miR-204-1-3p</i> rescue.....	101
4.8 sgRNA individually injected.....	103
4.9 <i>Trpm1</i> knock-down.....	104

## **Chapter 5: The effect of *xtr-miR-204-1* knock-down**

<b>5.1 Expanding known gene regulatory networks with miRNAs.....</b>	<b>107</b>
<b>5.2 Effect of <i>xtr-miR-204-1</i> knock-down on selected predicted targets expressed in the developing eye.....</b>	<b>108</b>
<i>5.2.1 Sox4 expression in WT embryos and xtr-miR-204-1 knock-down embryos.....</i>	<i>108</i>
<i>5.2.2 Tfp2a expression in WT embryos and xtr-miR-204-1 knock-down embryos.....</i>	<i>109</i>
<i>5.2.3 Tfp2b expression in WT embryos and xtr-miR-204-1 knock-down embryos.....</i>	<i>112</i>
<i>5.2.4 Hmx1 expression in WT embryos and xtr-miR-204-1 knock-down embryos.....</i>	<i>114</i>
<i>5.2.5 Vax2 expression in WT embryos and xtr-miR-204-1 knock-down embryos.....</i>	<i>116</i>
<b>5.3 Effect of <i>xtr-miR-204-1</i> knock-down on the expression of genes that play a role in eye development.....</b>	<b>119</b>
<i>5.3.1 Trpm1 expression in WT embryos and xtr-miR-204-1 knock-down embryos .....</i>	<i>119</i>
<i>5.3.2 Pax6 expression in WT embryos and xtr-miR-204-1 knock-down embryos.....</i>	<i>121</i>
<i>5.3.3 Sox2 expression in WT embryos and xtr-miR-204-1 knock-down embryos.....</i>	<i>123</i>
<i>5.3.4 Tyr expression in WT embryos and xtr-miR-204-1 knock-down embryos.....</i>	<i>125</i>
<i>5.3.5 Tbx5 expression in WT embryos and xtr-miR-204-1 knock-down embryos.....</i>	<i>126</i>
<i>5.3.6 Pax2 expression in WT embryos and xtr-miR-204-1 knock-down embryos.....</i>	<i>128</i>
<b>5.4 Effect of <i>xtr-miR-204-1</i> knock-down on the expression of NC specifiers.....</b>	<b>130</b>
<i>5.4.1 Sox10 expression in WT embryos and xtr-miR-204-1 knock-down embryos.....</i>	<i>130</i>
<i>5.4.2 Snai2 expression in WT embryos and xtr-miR-204-1 knock-down embryos.....</i>	<i>133</i>
<b>5.5 Effect of <i>xtr-miR-204-1</i> knock-down on the expression of selected predicted targets expressed in the pronephric kidney.....</b>	<b>134</b>
<i>5.5.1 Cox5a expression in WT embryos and xtr-miR-204-1 knock-down embryos.....</i>	<i>135</i>
<i>5.5.2 Ndr3 expression in WT embryos and xtr-miR-204-1 knock-down embryos.....</i>	<i>137</i>

## **Chapter 6: General discussion and concluding remarks**

<b>6.1 miRNAs during embryogenesis.....</b>	<b>140</b>
<b>6.2 The dual role of <i>xtr-miR-204-1</i> during development.....</b>	<b>145</b>
<b>6.3 <i>Xtr-miR-204-1</i> GRN.....</b>	<b>149</b>
<b>6.4 Future work.....</b>	<b>153</b>

### **List of figures**

<i>Fig. 1: Neural Crest development.....</i>	<i>17</i>
<i>Fig. 2: Neural crest contribution in the adult organism.....</i>	<i>19</i>
<i>Fig. 3: Overview of vertebrate eye development.....</i>	<i>24</i>
<i>Fig. 4: Retinal progenitor cells derivatives.....</i>	<i>27</i>
<i>Fig. 5: Neural crest contribution to eye development.....</i>	<i>29</i>
<i>Fig. 6: Canonical miRNAs biosynthesis.....</i>	<i>34</i>
<i>Fig. 7: Pri-miRNA common features.....</i>	<i>35</i>
<i>Fig. 8: The overexpression of <i>xtr-miR-219-5p</i> in <i>Xenopus tropicalis</i> embryos produces craniofacial defects.....</i>	<i>64</i>
<i>Fig. 9: The loss of endogenous <i>xtr-miR-219</i> can be rescued by introducing a synthetic <i>xtr-miR-219-5p</i>.....</i>	<i>66</i>
<i>Fig. 10: Conservation of <i>xla-nov-12a-1</i> between <i>Xenopus laevis</i> and <i>Xenopus tropicalis</i>.....</i>	<i>68</i>
<i>Fig. 11: Example of the output generated by TargetScan8.0 using two highly conserved miRNAs among vertebrates.....</i>	<i>70</i>
<i>Fig. 12: Unilateral coronal Craniosynostosis.....</i>	<i>71</i>
<i>Fig. 13: Distribution of miRNAs fold increase.....</i>	<i>73</i>
<i>Fig. 14: MiRNAs with fold increase significantly higher than control.....</i>	<i>74</i>
<i>Fig. 15: MiRNA knock-down strategy.....</i>	<i>75</i>
<i>Fig. 16: Specificity of <i>xtr-miR-218-2</i> in NC-induced <i>Xenopus</i>' animal caps.....</i>	<i>76</i>
<i>Fig. 17: <i>Xtr-miR-218-2</i> knock-down.....</i>	<i>78</i>
<i>Fig. 18: Specificity of <i>xtr-miR-10b</i> in NC-induced <i>Xenopus</i>' animal caps.....</i>	<i>79</i>
<i>Fig. 19: <i>Xtr-miR-10b</i> knock-down.....</i>	<i>81</i>
<i>Fig. 20: <i>Xtr-miR-208</i> knock-down.....</i>	<i>83</i>
<i>Fig. 21: List of miRNAs described as involved in NC development.....</i>	<i>87</i>

Fig. 22: Expression pattern of <i>trpm1</i> and <i>xtr-miR-204-1-3p</i> in <i>Xenopus</i> embryos.....	89
Fig. 23: Preliminary data from <i>xtr-miR-204-1</i> knock-down experiment.....	92
Fig. 24: <i>Xtr-miR-204-1</i> knock-down.....	94
Fig. 25: <i>miR-204</i> family conservation of the guide strand and overexpression of <i>xtr-miR-204-1-5p</i> .....	96
Fig. 26: <i>Xtr-miR-204-1</i> knock-down rescued with <i>xtr-miR-204-1-5p</i> .....	98
Fig. 27: <i>miR-204</i> family conservation of the passenger strand and overexpression of <i>xtr-miR-204-1-3p</i> .....	100
Fig. 28: <i>Xtr-miR-204-1</i> knock-down rescued with <i>xtr-miR-204-1-3p</i> .....	102
Fig. 29: Assessment of the effect of the gRNAs individually injected.....	104
Fig. 30: Assessment of the effect of <i>trpm1</i> knock-down.....	106
Fig. 31: Expression of <i>sox4</i> mRNA following <i>xtr-miR-204-1</i> knock-down.....	109
Fig. 32: Effect of loss of <i>xtr-miR-204-1</i> on <i>tfap2a</i> mRNA expression.....	111
Fig. 33: Effect of loss of <i>xtr-miR-204-1</i> on <i>tfap2β</i> mRNA expression.....	113
Fig. 34: Effect of loss of <i>xtr-miR-204-1</i> on <i>hmx1</i> mRNA expression.....	115
Fig. 35: Effect of loss of <i>xtr-miR-204-1</i> on <i>vax2</i> mRNA expression.....	118
Fig. 36: Effect of loss of <i>xtr-miR-204-1</i> on <i>trpm1</i> mRNA expression.....	121
Fig. 37: Effect of loss of <i>xtr-miR-204-1</i> on <i>pax6</i> mRNA expression.....	123
Fig. 38: Expression of <i>sox2</i> mRNA following <i>xtr-miR-204-1</i> knock-down.....	124
Fig. 39: Expression of <i>tyr</i> mRNA following <i>xtr-miR-204-1</i> knock-down.....	126
Fig. 40: Effect of loss of <i>xtr-miR-204-1</i> on <i>tbx5</i> mRNA expression.....	127
Fig. 41: Effect of loss of <i>xtr-miR-204-1</i> on <i>pax2</i> mRNA expression.....	129
Fig. 42: Effect of loss of <i>xtr-miR-204-1</i> on <i>sox10</i> mRNA expression.....	132
Fig. 43: Effect of loss of <i>xtr-miR-204-1</i> on <i>snai2</i> mRNA expression.....	134
Fig. 44: Effect of loss of <i>xtr-miR-204-1</i> on <i>cox5a</i> mRNA expression.....	136
Fig. 45: Effect of loss of <i>xtr-miR-204-1</i> on <i>ndrg3</i> mRNA expression.....	138
Fig. 46: Members of the <i>miR-10</i> family in <i>Xenopus tropicalis</i> .....	143
Fig. 47: 3-D structure of <i>slit2</i> intron that hosts <i>xla-miR-nov-12a-1</i> .....	145
Fig. 48: Proposed mechanism of action for <i>xtr-miR-204-1</i> .....	149
Fig. 49: Comparison between the passenger strand of <i>miR-204</i> family members.....	158

## **List of tables**

<i>Table 1: Table of NCPs and associated miRNAs.....</i>	<i>43</i>
<i>Table 2: List of primers.....</i>	<i>60</i>
<i>Table 3: List of gRNAs.....</i>	<i>84</i>
<i>Table 4: Syndromes and conditions associated with mutations in the genes that are regulated by xtr-miR-204-1.....</i>	<i>154</i>

## **Abbreviations**

BMP - Bone Morphogenic Pathway

BOFS - Branchio-Oculo-Facial Syndrome

CCHS - Congenital Central Hyperventilation Syndrome

circ-RNA - circular RNA

cNC - cranial Neural Crest

CNS - Central Nervous System

COX - Cytochrome C Oxidase

DDR - DNA Damage Response

DSB - Double Strand Break

EMT - Epithelial to Mesenchymal Transition

ENS - Enteric Nervous System

ESC - Embryonic Stem Cell

FGF - Fibroblast Growth Factor

Fw - Forward

gDNA - genomic DNA

GRN - Gene Regulatory Network

HD - Hirschsprung Disease

L-DOPA - 3,4-dihydroxyphenylalanine

LNA - Locked Nucleic Acid

lncRNA - long non-coding RNA

MHB - Midbrain Hindbrain Boundary  
miRNA - micro RNA  
MITF – Melanocyte-Inducing Transcription Factor  
MRE - Micro-RNA Recognition Element  
NB - Neuroblastoma  
NC - Neural Crest  
NCC - Neural Crest Cell  
NCP - Neurocristopathy  
NDRG - N-Myc Downstream-Regulated Gene  
NF - Nieuwkoop and Faber  
OCACS - Oculo-Auricular Syndrome  
PAX - Paired box  
piRNA - PIWI-interacting RNA  
PNS - Peripheral Nervous System  
Pre-miRNA - precursor micro-RNA  
Pri-miRNA - primary micro-RNA  
RISC - RNA Induced Silencing Complex  
RITA - RNA Induced Transcription Activator  
RPE - Retinal Pigment Epithelium  
Rv - Reverse  
sNC - sacral Neural Crest  
SOX - SRY-related HMG-box  
TBX - T-box transcription factor  
TFAP2 - Transcription Factor AP-2  
tNC - trunk Neural Crest  
TRPM - Transient Receptor Potential Melastatin  
TYR - Tyrosinase  
UTR - Untranslated Region  
UV - Ultra Violet

VAX - Ventral Anterior homeobox

vNC - vagal Neural Crest

WES - Whole Exon Sequencing

WGS - Whole Genome Sequencing

WISH – Whole-mount in Situ Hybridisation

Wnt - Wingless/ $\beta$ -catenin pathway

# **Chapter 1: Introduction**

## **1.1 NEUcrest project**

This project is presented as part of the bigger “NEUcrest” project, whose official title is “*NEUcrest - Training European Experts in Multiscale Studies of Neural Crest Development and Disorders: from Patient to Model Systems and Back again*” (<https://neucrest.curie.fr/index>). The NEUcrest project is an EU-funded project that started in 2019, with the collaboration of eleven partners, which range from academical to industrial institutions. The aim of NEUcrest is to study various aspects of the neural crest on a multiscale level. In particular, fifteen PhD students were recruited to study this tissue using several model organisms, ranging from hiPSCs to animal models such as frogs and mice.

The final goal is to elucidate the mechanisms that give rise to diseases of the neural crest, also called neurocristopathies, and to apply this knowledge to improve the quality of life of people affected by such conditions.

While some of the PhD students projects focused more on the fundamental mechanisms that underly the origin of this cellular tissue, other projects where more focused on the understanding of the pathological mechanisms that give rise to neurocristopathies.

The following project aimed to investigate the role of micro RNAs in the context of neural crest development, and their role in the etiopathogenesis of neurocristopathies, of which not much is known.

To do this, we used the animal model *Xenopus tropicalis*, or African clawed frog. This organism has been used for decades due to its numerous advantages, such as the ease of generating embryos, which develop externally to the mother womb. Large number of embryos that can be generated in a single experiment, with mothers that can lay hundreds of eggs in a single day. Also, it is possible to control the speed of development by simply changing the incubation temperature of the embryos. Finally, *Xenopus tropicalis* genome is relatively similar to the human genome, resulting in the possibility to mimic, in frogs, roughly 70% of human genetic conditions (Blum and Ott, 2018).

## 1.2 Neural crest

The neural crest (NC) is a transient cell type that originates during late gastrulation/early neurulation of a developing embryo. During development, neural crest cells (NCCs) are induced at the neural plate border, and then undergo a process called epithelial to mesenchymal transition (EMT), which will allow them to delaminate from the neuroectoderm and to migrate throughout the embryo (Fig. 1A). These cells then differentiate into an astonishing number of derivatives, which include (but are not limited to) craniofacial skeleton, dentine of teeth, eye, melanocytes and enteric ganglia (Bronner and LeDouarin, 2012). Such an incredible cell population is necessarily controlled by very complex gene regulatory networks (GRNs), which are constantly being updated with the addition of new transcription factors, signalling molecules and non-coding RNAs (Antonaci and Wheeler, 2022; Pla and Monsoro-Burq, 2018; Seal and Monsoro-Burq, 2020; Simoes-Costa and Bronner, 2013, 2015).

### 1.2.1 Specification of the NC

The NC, sometimes referred as the “fourth germ layer”, is a multipotent population of cells that originate in the region between the neural and non-neural ectoderm of the developing embryo as the neural plate develops (Simoes-Costa and Bronner, 2013, 2015). The NC is specific to vertebrates and is required for the formation of many types of cells and tissues as mentioned above, including the craniofacial skeleton, chondrocytes, cardiac septa, the peripheral nervous system, adrenal medulla, and pigment cells (Martik and Bronner, 2017; Mayor and Theveneau, 2013; Theveneau and Mayor, 2012b).

Tissue interactions play an essential role in the induction of the NC tissue. These interactions derive from the neural ectoderm, the non-neural ectoderm and the underlying mesoderm. There are three main signalling pathways involved in this process: Wnt/ $\beta$ -catenin (Wnt), Bone Morphogenic Protein (BMP) and Fibroblast Growth Factor (FGF) (Fig. 1B)(Simoes-Costa and Bronner, 2015). It has been shown in several models that the activation of each of these is required but not sufficient for the induction and specification of the NC, and the activation of all three is essential. Retinoic acid and Notch signalling are also involved in the expression of neural plate border (NPB)

specifiers, although these two factors play different roles among various species (Hochgreb-Hagele and Bronner, 2013; Hockman et al., 2019; Hutchins and Bronner, 2018; Simoes-Costa and Bronner, 2015).

During neurulation, BMP signals are secreted by the non-neural ectoderm in order to maintain the non-neural fate, an action that is also exerted by Wnt as well (Faure et al., 2002; Garcia-Castro et al., 2002). In turn, the axial mesoderm and the neural plate secrete BMP antagonists, creating a BMP gradient that is able to induce the neural plate border specifiers (Plouhinec et al., 2013). At the same time, species specific Wnt signals, derived from the non-neural ectoderm, create the right concentrations to induce the NC specifiers at the level of the neural plate border (Monsoro-Burq et al., 2003). Minor contributions in the induction of the neural plate border derive from hedgehog and retinoic signalling as well, however, these factors have not been fully integrated into the current NC-GRN yet (Hovland et al., 2020; Martik and Bronner, 2017).

All of these gradients of signalling pathways induce the activation of a series of transcription factors. Among the most important there are *Tfap2a*, *Msx1/2*, *Zic1*, and *Pax3/7*. These first neural plate border specifiers trigger the expression of the NC specification module, which include *Tfap2β*, *Snai1/2*, *FoxD3*, *Twist* and the SoxE group of genes (*Sox8/9/10*) (Fig. 1B) (Simoes-Costa and Bronner, 2015).

### 1.2.2 NC epithelial-to-mesenchymal transition and migration

Following induction and specification of the NC tissue, at the end of neurulation, NCCs switch from their original epithelial state into a mesenchymal state. This process, essential for the migration and subsequential differentiation of the NCCs into their numerous derivatives, has been called epithelial-to-mesenchymal transition (EMT) (Nieto et al., 2016).

In order for NCCs to switch into a mesenchymal state, they have to lose their epithelial characteristics, such as the cell-cell adhesion and apicobasal polarity, in order to gain a more mesenchymal-like state, which include a typical elongated shape, with an antero-posterior polarity (Lamouille et al., 2014).

The induction of EMT is initiated by the expression of EMT transcription factors such as Snai1/2, Twist1/2, Zeb1 and Prrx1/2, which repress the transcription of cell-cell adhesion proteins like E-cadherin, and activate mesenchymal proteins, such as Cadherin7/11. Another impressive change that needs to happen during this stage, is the change of the cell morphology, which requires a global cytoskeletal rearrangement (Zhao and Trainor, 2023).

Even though EMT is generally known to be an embryonic process, it is also activated in pathological conditions, including cancer. Melanoma is a particularly important example, in which melanoma cells undergo to EMT before becoming metastatic. It is known in the literature that the expression of EMT markers in melanoma, but also in other types of cancers, is associated with a worse prognosis and with a higher aggressiveness of the cancer (Castro-Perez et al., 2023; Rastrelli et al., 2014). Pigment cells, which give rise to melanoma, are NC derived. Interestingly, melanoma cells often turn on genes associated with their NC origins (White et al., 2011).

Following EMT, NCCs are ready to migrate into the developing embryo, before differentiating into their final derivatives. This migration process is extremely complex, and requires a series of intrinsic (transcription factors, mainly) and extrinsic (signalling molecules, extracellular matrix and contact inhibition) cues that the migrating NCCs can follow (Sauka-Spengler and Bronner-Fraser, 2008).

Other morphogenic cues provided by Wnt, Notch, FGF, Hox, and BMP allow the migrating NCCs to further migrate and differentiate into their final derivatives (Theveneau and Mayor, 2012a, b).

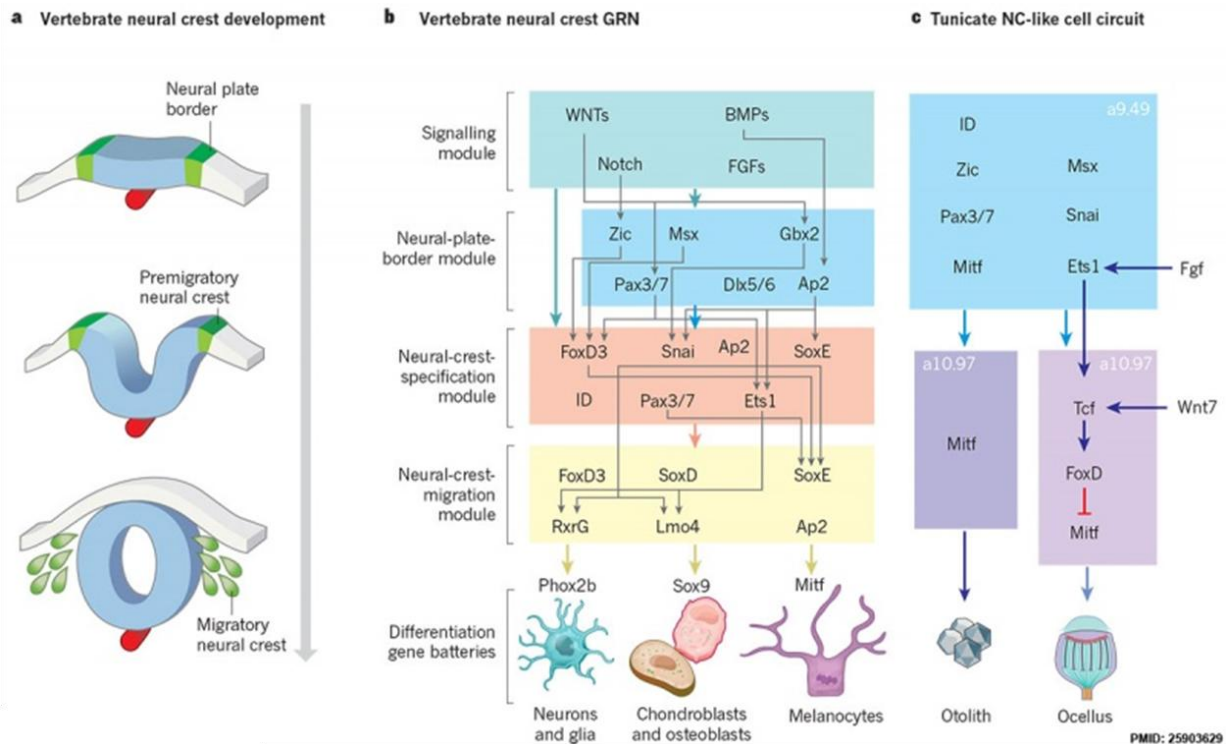


**Fig. 1: Neural crest development: A)** Induction to migration of the neural crest (NC). The induction of the neural crest (green) starts between the neural (light blue) and non-neural (grey) ectoderm, thanks to gradients of Wnt, BMP, and FGF signalling coming from the neural and non-neural ectoderm, as well as from the mesoderm. Following induction, the NCCs undergo a process called epithelial to mesenchymal transition (EMT), in which they ingress the embryo, just before going to a migration process that will see NCCs invading the whole embryo. **B)** For all of these processes to happen, NCCs are controlled by an incredibly complex gene regulatory network (GRN). This network includes multiple different factors, from protein coding transcription factors (the better characterised are included in the figure), non-coding RNAs, signalling molecules and, likely mechanical cues and ion gradients. Figure modified from Green, Simoes-Costa and Bronner, 2015 (Simoes-Costa and Bronner, 2015).

### 1.2.3 NC differentiation

Once the NCCs have migrated throughout the body, they differentiate into a wide range of derivatives. This process is strictly connected to the type of NC subpopulation that the NCCs belong to. There are four main NC populations: cranial, vagal (which include the cardiac NC as well), trunk and sacral NC. Each of these populations have the same differentiation potential, however, according to their position within the embryo, and according to the external signalling that they receive, they will differentiate into different cell types, during development (Fig. 2).

In the case of cranial NC (cNC), this subpopulation is known to differentiate into the craniofacial skeleton, cranial ganglia, odontoblasts, thyroid, chondrocytes, skin and melanocytes (Martik and Bronner, 2021), as well as providing an essential contribution to the development of the eye (Grocott et al., 2011). In particular, the NCCs provide essential contributions in the formation of the choroid, sclera and the cornea (see section 1.3.4 and Fig. 5). Given this, it is not surprising that a number of diseases affecting the NC development, display eye phenotypes as well (Sato et al., 2019; Usman and Sur, 2021).

Vagal NC (vNC) has the potential to give rise to several components of the cardiovascular system, in particular to smooth muscle cells, cardiac septa, and pericytes (cells that regulate blood flow by interacting with the smaller blood vessels, the capillaries). However, an important contribution of the vagal NC is also provided for the enteric nervous system (ENS), which is deputed to the innervation of the pancreas, lungs and the guts ganglia (Hutchins et al., 2018).

The trunk NC (tNC) is the subpopulation of cells that will give rise to the adrenal medulla, sensory neurons, Schwann cells, enteric nervous system, and melanocytes (Kastriti et al., 2022; Vega-Lopez et al., 2017).

In a similar way, the sacral NC (sNC) gives rise to glia and enteric neurons that innervate the hindgut and colon in the adult organism (Burns and Douarin, 1998; Fan et al., 2023; Wang et al., 2011).

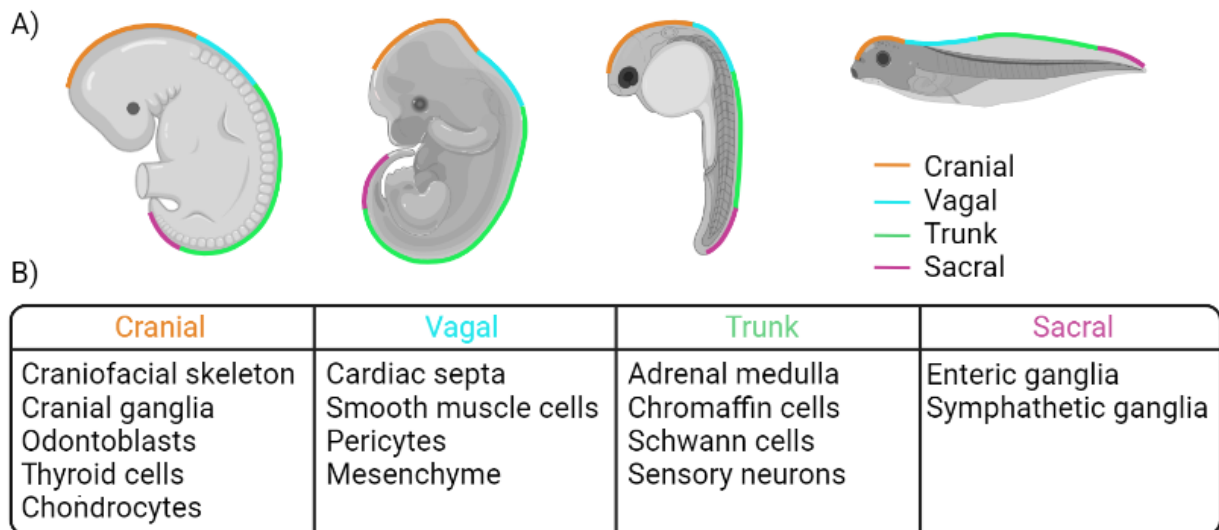


**Fig. 2: Neural Crest contribution in the adult organism. A)** Neural crest populations in different animal models during embryogenesis (from the left: human, mouse, zebrafish and frog). **B)** Neural crest contributions in the adult organism, specific for each subpopulation of the neural crest. All of the subpopulations can give rise to melanocytes.

#### 1.2.4 Neurocristopathies

Since the NC gives rise to so many tissues and cell types in the adult body, and the signals that lead to the correct development of the many different NC derived cell types have to be strictly regulated, it is not surprising that a large number of genetic diseases, often syndromic are due to a defect in the migration, differentiation or survival of this cell population. Such conditions are globally called neurocristopathies (NCPs). Many genes have been associated with NCPs, several of these with a well-established role in NC development. However, because of the variety of these conditions, and the complexity of the NC-GRN, not all the genes involved in the etiopathogenesis of NCPs have been discovered yet (A Vega-Lopez and J Aybar, 2018; Sato et al., 2019; Vega-Lopez et al., 2018).

Some of the most well-known NCPs include cleft palate, congenital heart defects, piebaldism, neurofibromatosis, and craniosynostosis. But also syndromes such as CHARGE, Axenfeld-Rieger, or the DiGeorge syndrome. Here, we are going to discuss some of them.

The most common NCP is craniosynostosis, a condition that arises when two or more bones of the skull fuse prematurely during development. This condition, more than

causing craniofacial abnormalities, often does not allow enough room for the brain to grow and, if not treated timely by surgery, can cause intellectual disabilities. Many genes have been implicated in this heterogeneous condition, suggesting the interesting possibility that some of these NCPs might be caused by multiple genes, interacting with each other, and/or by mutations in the non-coding regions of the genome, which are often not sequenced (Goos and Mathijssen, 2019; Lattanzi et al., 2017; Twigg and Wilkie, 2015).

CHARGE syndrome is a rare disease mainly caused by mutations in the *CHD7* gene. The characteristics of this syndrome include coloboma of the eye, heart defects, atresia of the choanae, intellectual disability, genital and ear abnormalities. All these features give the name to the syndrome, however, not all of them have to be present at once, highlighting how this syndrome can be particularly complex, from a genetic point of view (Usman and Sur, 2021).

DiGeorge syndrome, often called 22q11 deletion syndrome, is characterised by a spectrum of problems, ranging from learning disabilities, speech and hearing problems, heart defects, and cleft palate. This condition is the result of the deletion of a portion of the long arm of chromosome 22. There are two main causative genes involved in this syndrome, *DGCR8* and *TBX1* (Lackey and Muzio, 2021).

Hirschsprung disease is a condition that mainly affects the colon. It is the result of lack of enteric neurons in the intestine, which will result in a variety of signs and symptoms, from swollen belly, vomiting, constipation, failure to thrive and fatigue. It is usually treated by surgical removal of the interested part of the intestine. The genes involved are usually *RET*, *EDNRB*, *SOX10* and *EDN*, however, not all the genes that cause this condition have been identified yet, and some of the people affected by Hirschsprung disease might have mutations in more than one gene, making the molecular diagnosis particularly complicated. More recent evidence have pointed the attention to the effect that non-coding RNAs, and micro RNAs in particular, might play a role in the etiopathogenesis of Hirschsprung disease. (Bondurand and Sham, 2013; Lotfollahzadeh et al., 2021; Wu et al., 2021; Zhu et al., 2020).

Waardenburg syndrome is characterised by hearing loss and loss of pigmentation on the skin, iris and hair. Divided in four types, the main distinction is due to the dystopia Cantorum, or telecanthus (a condition refers to an increased distance between the inner corners of the eyelids in respect to the pupils, while the inter-pupillary distance is still normal (Mustarde, 1963)), abnormalities of the upper limbs, and Hirschsprung disease. Most people affected by Waardenburg syndrome have mutations in *PAX3*, *MITF* and *SOX10* genes however, like many NCPs, not all the causative genes have been discovered yet (Bertani-Torres et al., 2023; Huang et al., 2022).

Microphthalmia is a condition that affects the physiological growth of the eye. This can occur if the neural tissue that forms the optic cup doesn't develop properly, or if there are problems with the correct signalling operated by the NC (Harding and Moosajee, 2019). Because of this, not all microphthalmias can be considered NCPs. For more information about eye development, see section: 1.3.

Coloboma is another developmental defect that affects the eye. In this case, there is a defect in the closure of the choroid fissure. This will result in an open iris, which is unable to regulate the amount of light passing through the pupil. This can result in blindness due to light-damage to the retina. Some cases of colobomas can be considered as NCPs, since the closure of the choroid fissure requires signalling from the NC (Lingam et al., 2021). People with NCPs, such as CHARGE syndrome, branchio-oculo-facial syndrome, Waardenburg syndrome type II can display colobomas and microphthalmia.

Some cancers can be classed as NCPs, if the cells that become cancerous are derivatives of the NC. Within these types of cancers, some are very important from a clinical point of view. Here, we describe two of them, melanoma and neuroblastoma, which arise from melanocytes and sympathoadrenal cells, respectively.

Melanoma is a type of skin cancer that begins in melanocytes and can affect people of every age. Is one of the most common cancers and is mainly triggered by excessive exposure to sunlight. However, genetic factors, such as mutations of *MITF* or *SOX10* genes, can facilitate the onset of this disease. Our lab and others have shown that melanoma cells often express NC genes showing a differentiation to a more stem cell like proliferative and migratory state (White et al., 2011).

Neuroblastoma is one of the most common and aggressive cancers in children. It arises from the sympathoadrenal lineage derived from tNCC, and among the genetic causes, there are mutations in ALK, MYCN and PHOX2B (Wulf et al., 2021).

### **1.3 Eye development**

The eyes are complex organs that allow animals to acquire electromagnetic radiations coming from the environment. These are then processed by the nervous system and translated into images, that animals can use to orientate themselves in the environment.

Eyes in different species can be very different; from the simple eyes of planarians, which can only detect variations in the intensity of the light; to the human eye, which allows us to distinguish colours that range from ~380nm to ~700nm wavelengths; moving through other different type of eyes, like bees' eye, which allow them to perceive the ultraviolet (UV) lights.

To develop such a complicated organ requires a tight interaction and coordinated signalling between different tissues. These include interactions between the placodes, neural tissue, neural crest and the mesenchyme, in a complex process that begins during early neurulation.

#### 1.3.1 Induction of the optic vesicle and formation of the optic cup

During late gastrulation/early neurulation the neural ectoderm, the NC, the placode and the non-neural ectoderm are specified. At this stage, the anterior region of the embryo forms two “presumptive retinal ectoderms”. These regions are characterised by positive FGF signalling, and inhibitors of Wnt and BMP signalling pathways. At this stage, an already complex network of transcription factors have to be specified in the presumptive retinal epithelium. Such transcription factors include Pax6, Rx, Otx2, Sox2, Hes1 and Six3 (Grocott et al., 2020; Macdonald et al., 1995; Zuber et al., 2003).

The presumptive retinal epithelium, at this stage, is composed by a single field in the anterior region of the neural plate, and only thanks to the action of the signalling of Shh, it gets confined and divided into the two distinct retinal fields. Each of the retinal field will then thicken and eventually develop into the optic vesicle (Fig. 3) (Chiang et al., 1996).

Following closure of the neural tube, the optic vesicles grow bilaterally until they get in touch with the surrounding ectoderm. Those cells that get in contact with the growing optic vesicle are the cells that will then give rise to the lens. At this point, the two tissues (optic cup and lens placode) start interacting with each other. In fact, it is essential for the neural epithelium that forms the optic vesicle to receive the signalling from the pre-lens ectoderm, in order to start the formation of the optic cup. On the other hand, the pre-lens placode needs signals from the optic vesicle in order to develop (Ashery-Padan et al., 2000; Hyer et al., 2003).

These events lead to the invagination of the lens placode, with the lens placode cells changing their morphology and detaching from the ectoderm. This will produce a vesicle/like structure with a hollow cavity, surrounded by lens cells, which takes the name of lens vesicle. It is important to know that in the model organisms *Xenopus laevis* and *Danio rerio* the lens cavity is not hollow, but presents itself as a conglomerate of cells (Fig. 3) (Altmann et al., 1997; Oliver et al., 1996).

While the vesicle forms, the optic vesicle starts invaginating itself to form the optic cup, still connected to the rest of the developing brain by the optic stalk. At this stage, four main tissues will form; cells from the inner layer of the optic cup will give rise to the neural retina, while the ones in the outer layer will give rise to the retinal pigmented epithelium; on the other hand, cells from the posterior-ventral region of the optic stalk will give rise to the optic nerve, and the cells on the anterior rim will give rise to the ciliary body and to the iris (Lachke and Maas, 2010).

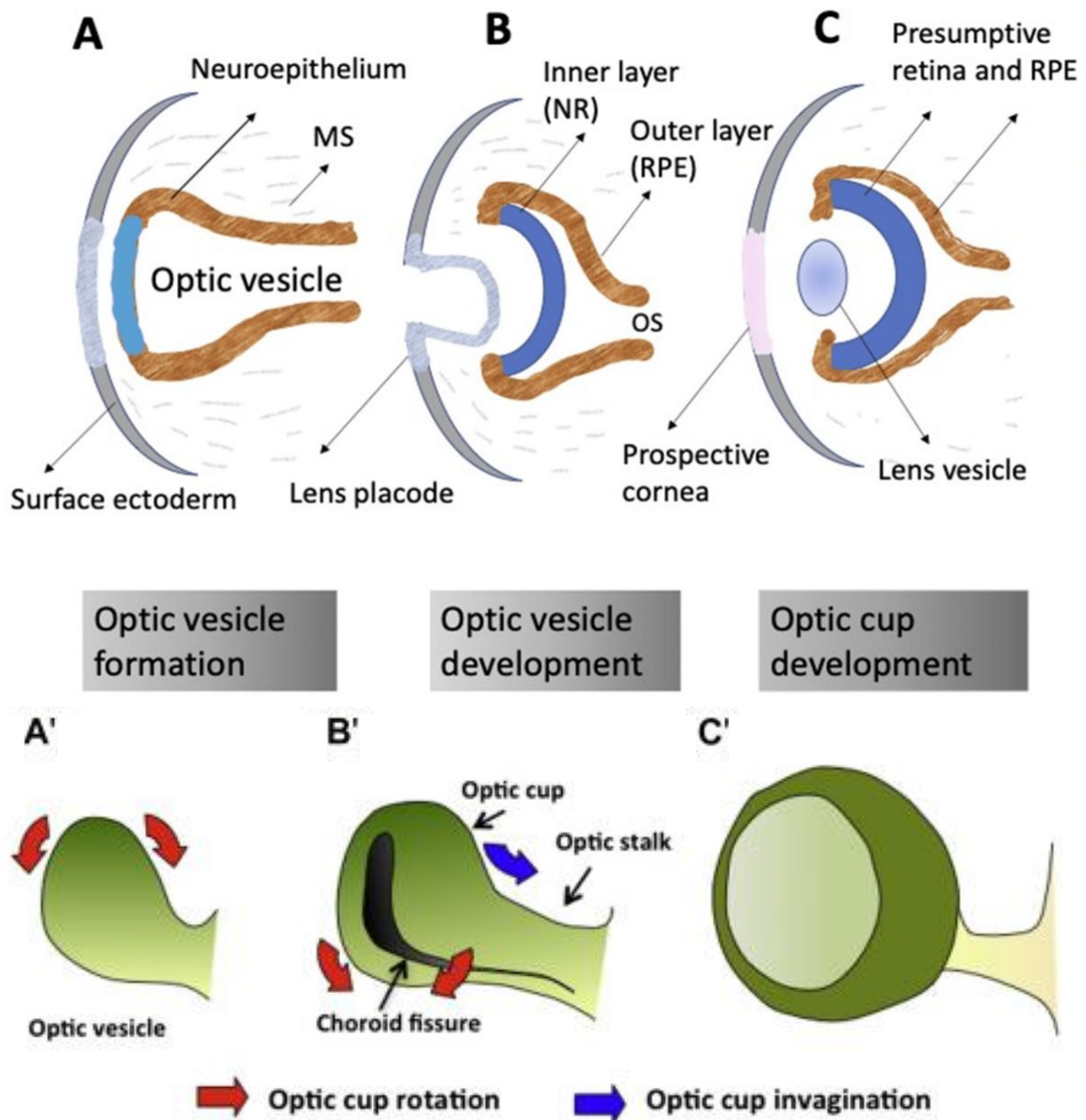


**Fig. 3: Overview of vertebrate eye development:** Overview of vertebrate eye development, from early stage embryo to later stages, in which the optic cup and the lens has formed. **A)** The first stages of eye development see an extrusion of the developing diencephalon, to form the optic vesicle. The optic vesicle will extrude until it reaches the proximity of the surface ectoderm, which will give rise to the lens. **B)** Once the optic vesicle and lens placode get in contact with each other, they will both invaginate. **C)** The lens placode will continue invaginating until it will form a vesicle (lens vesicle). On the other hand, the optic vesicle will keep invaginating until it will form a cup, open on the ventral side to allow the passage of the hyaloid vases and the optic nerve. **D)** The double layered retina will differentiate into its derivatives, and the lens cells will thicken and start producing crystallin. **A')**, **B')** and **C')** show the developing optic vesicle and cup at the same time points of **A)**, **B)** and **C)** (respectively), as seen from the antero-lateral side of the embryo. It is visible, in **B')** the choroid fissure and the typical “cup” shape in **C')**. Images modified from Grigoryan, 2022 (Grigoryan, 2022) and Bovolenta and colleagues, 2010 in the book “Encyclopaedia of the eye”.

### 1.3.2 Lens development

Key players, when it comes to lens development, are the two transcription factors Pax6 and Six3. It has been shown that in permissive tissues, the ectopic expression of Pax6 can, on its own, drive the formation of an ectopic lens (Altmann et al., 1997). However, the epistatic relationship between these two transcription factors is complex, since studies have shown that Pax6 is essential for the sustained expression of Six3, while Six3 seems to be activating Pax6 by interacting with multiple enhancers in the lens placode, suggesting a positive feedback that involves these two key players (Goudreau et al., 2002; Liu et al., 2006; Purcell et al., 2005).

Downstream of Pax6, there are other genes that are involved in the organogenesis of the lenses. Such genes are Sox2, Oct1, and Foxe3, which work by inducing the lens specifiers, regulating proliferation, lens vesicle closure and maintaining the lens cells in a more undifferentiated state (by negatively regulating Prox1 expression). The maintenance of a more undifferentiated state might be required in order to prevent the premature synthesis of crystallin by the mature lens cells. Within this GRN, the transcription factor Tfp2 $\alpha$  plays a role as well. Its role is to regulate factors involved in the adhesion of lens cells, which plays a critical role in the lens vesicle separation (Blixt et al., 2000; Brownell et al., 2000; Donner et al., 2007; Pontoriero et al., 2008; Wigle et al., 1999).

Secreted signalling molecules also play a role in lens development. For example, at early stages of development, Bmp7 is expressed in the lens placodal ectoderm, and necessary for maintaining the expression of Pax6 in this tissue. On the other hand, in the optic vesicle there is high expression of Bmp4, which is required for the induction of lens placodal specifiers during the contact between the optic cup and the lens placodal ectoderm, highlighting an important role for BMP signalling pathway during oculogenesis (Belecky-Adams et al., 2002; Furuta and Hogan, 1998).

Other signalling pathways are also involved in the formation of the lens. For example, FGF pathway is essential for early expression of Pax6 in early placode, while Wnt signalling initially has a negative regulatory role in lens induction in the ectoderm. Also

Notch can play a role in lens development, with its activation able to produce eye duplication in *Xenopus* (Onuma et al., 2002; Robinson, 2006; Song et al., 2007).

### 1.3.3 Retinal development

The developing bi-layered optic cup contains retinal progenitor cells, which are multipotent cells capable of differentiating into all the type of neurons present in the adult retina. These include ganglion, amacrine, horizontal and bipolar cells, rods, cones, and Müller glia, which are the seven cell types present in the adult retina (Fig. 4) (Lachke and Maas, 2010).

Topologically, the posterior part of this bi-layered optic cup will form the retinal pigment epithelium (RPE), while the anterior layer will form the neuroretina. These two tissues are strictly connected to each other, and failure in the development of one of the two will result in developmental defects of the other as well (Cvekl and Mitton, 2010; Livesey and Cepko, 2001).

The differentiation of retinal progenitor cells into their final derivatives begins in the central area of the inner layer of the optic cup, and it continues towards the periphery of the optic cup. There are four main steps in the formation of the mature retinal cells, which include the proliferation of the progenitors, the exit from the cell cycle, the commitment to a particular cell fate and, eventually, the execution of the commitment (Chow and Lang, 2001).

In order to differentiate into the different mature retinal cells, it is required the action of several transcription factors. Proteins like Pax6 are involved in the differentiation into more than one cell type, such as ganglion, amacrine cells, and horizontal cells. Another example is the transcription factor Otx2, involved in the differentiation into both rods and cones. On the other hand, other transcription factors are specific for a single cell type. An example of it is the one of Hes1, which is only involved in the differentiation into Müller cells (Cvekl and Mitton, 2010).

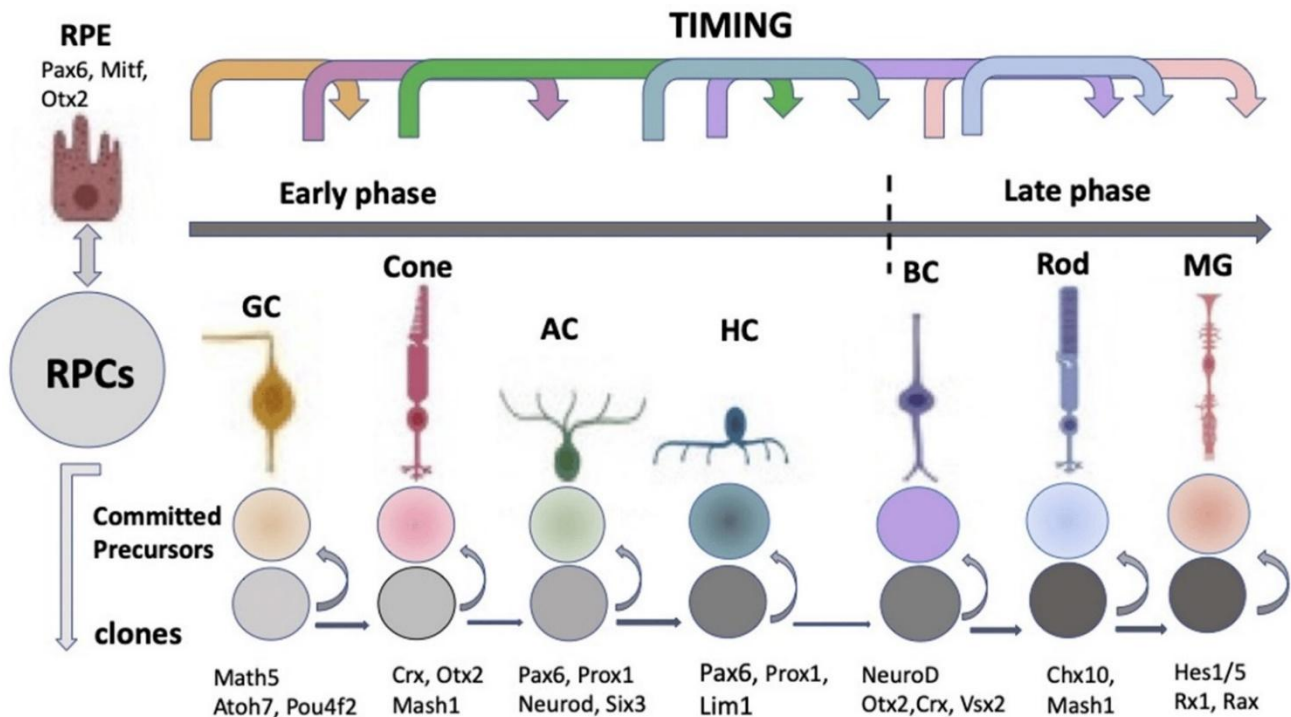


**Fig. 4: Retinal progenitor cells derivatives.** Retinal progenitor cells will give rise to a number of different derivatives that are involved in the acquisition of the environmental light. Each differentiated cell type requires a number of different transcription factors, and are generated at specific times, during development. RPCs-Retinal progenitor cells, GC-Ganglion cells, AC-Amacrine cells, HC-Horizontal cells, BC-Bipolar cells, MG-Müller glia, RPE-Retinal pigment epithelium. Image taken from Grigoryan, 2022 (Grigoryan, 2022).

#### 1.3.4 NC contribution to eye development

NCCs directly contribute to numerous structures in the eye, including cornea, iris, sclera, and ciliary body (Gage et al., 2005). Other than this direct contribution, the NC plays a role in orchestrating interactions between the neural ectoderm that forms the optic cup and the lens placode, and also the surrounding mesenchyme (Gage et al., 2005; Grocott et al., 2011).

This underrated role of the NC, if not fulfilled properly, can lead to particular eye conditions, such as microphthalmia (small-eye), anophthalmia (absent-eye) or coloboma (incomplete closure of the choroid fissure in the ventral region of the eye (Harding and Moosajee, 2019; Lingam et al., 2021). As common in the context of NC development, conditions that affect the eye might present themselves in a spectrum of diseases, such in the case of Axenfeld-Rieger syndrome, or CHARGE syndrome, in which

several tissues are affected, mostly associated with NC derivatives (Michels and Bohnsack, 2023; Usman and Sur, 2021). Unfortunately, to date, the specific interactions between NC and the optic cup remain mostly obscure.

During the formation of the optic cup, NCCs migrate into the periocular mesoderm and enter the structure of the eye *via* two ways: the choroid fissure on the ventral side of the optic cup and between the optic cup and the surface ectoderm (Gage et al., 2005; Weigele and Bohnsack, 2020). The numbers of waves in which NCCs migrate into the developing eye is species specific. In human, for example, there are three waves of migration, while in chicken there is a single continuous migration (Sauka-Spengler and Bronner-Fraser, 2006). By using electron scan microscopy, it has been suggested that, in *Xenopus*, NCCs migrate to the optic cup in a single wave, similarly to what happens in chick. At tailbud stage, they then start to separate and move more freely to invade the eye field (Sadaghiani and Thiebaud, 1987). Once the NCCs are in the developing eye, the signalling that leads to the terminal differentiation is poorly understood, however, it is known that genes such as *FoxC1*, *Eya1/2*, *Sox10* and *Pitx2* are involved in this process (Fig. 5) (Harris and Erickson, 2007; Krispin et al., 2010; Lukoseviciute et al., 2018).

During early stages of eye development, NCCs migrate around the optic vesicle following a gradient of thyroid hormone, while the degradation of iodothyronine operated by the enzyme Dio3 is necessary for the final steps of their migration in the frontonasal process of the developing embryo. The refinement of this migration pattern is finally made possible by an increased gradient of retinoic acid. Another important regulator of NCCs migration into the optic cup is *Pitx2*, which has been associated with Axenfeld-Rieger syndrome, and which display severe eye phenotypes, including anophthalmia and microphthalmia, and that has been considered as a NCP, since the same phenotype has been observed by generating NC-specific knock-out of *Pitx2* (Bohnsack and Kahana, 2013; Bohnsack et al., 2012; Liu and Semina, 2012; Williams and Bohnsack, 2020).

Important function of the migrating NCCs in the periocular mesoderm is to inhibit lens specification, and their ablation is known to produce ectopic lens formation. In chick embryos, NCCs also secrete TGF $\beta$  factors which will, in turn, activate WNT signalling, inducing the expression of *Wnt2b* in the non-lens ectoderm (Bailey et al., 2006; Grocott et al., 2011).

Using animal models, it has been observed that NCCs are also important for the formation of periocular muscle formation by regulating the expression of genes such *Myf5*, *Myog* and *Myod1*, proving the versatile function of the NC in the coordination of eye development (Diehl et al., 2006; Zacharias et al., 2011).

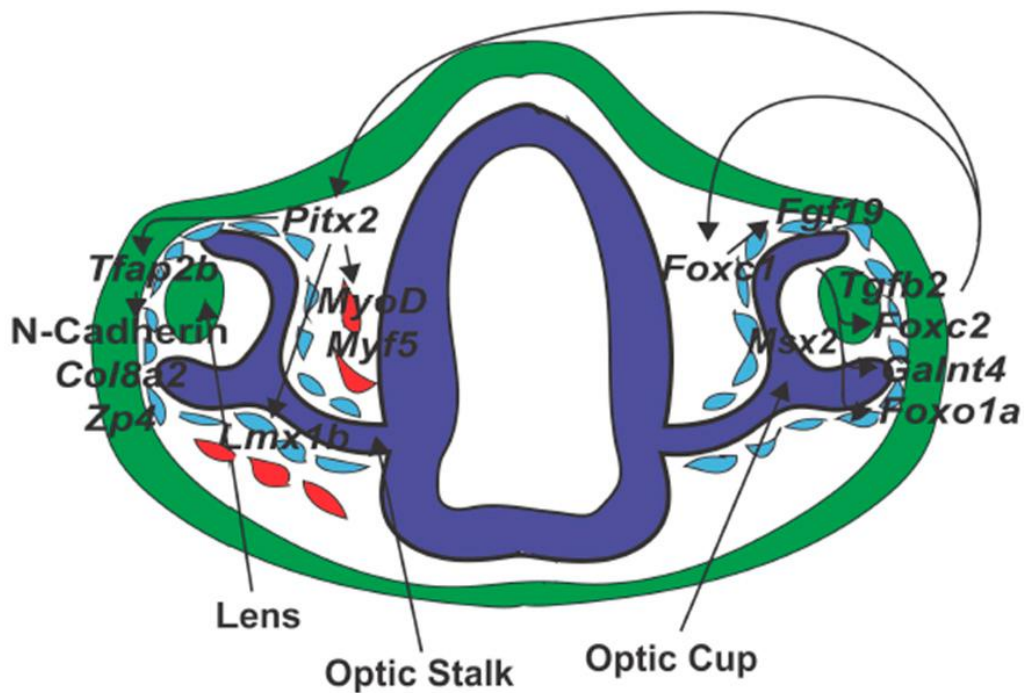


**Fig. 5: Neural crest contribution to eye development.** Coronal section of an embryo after the lens, the lens vesicles and the optic cups have formed. The surface ectoderm is shown in green, which can give rise to the lenses. Dark blue labels the neural tissue and its derivate optic cups and stalks. In red are the mesodermal cells, which will form the extraocular myofibers. The NCCs are in light blue, , which ingress the structure of the developing eye and will coordinate the cross-talk between tissues, promoting the formation of periocular muscular cells, and the formation of the cornea, iris, sclera and ciliary body. Image taken from Weigele and Bohnsack, 2020 (Weigele and Bohnsack, 2020).

## 1.4 micro RNAs

Micro RNAs (miRNAs) are short RNA molecules of around 22nt involved in the control of gene regulation. They act mainly as repressors of gene expression by binding to the untranslated region at the 3' end of a targeted mRNA and either promoting the stalling of the ribosome, or directly promoting the degradation of the targeted mRNA.

MiRNAs were first discovered in *C. elegans* by Lee and colleagues in 1993 (Lee et al., 1993). Since their discovery, well over a thousand miRNAs have been characterised, together with evidence of their important role in gene expression (Saliminejad et al., 2019).

The synthesis of miRNAs starts with the action of the RNA-PolIII that transcribes for a long primary transcript, called pri-miRNA. In most cases, the pri-miRNA has more than one loop, which are recognised by RNaseIII DROSHA which, together with DGCR8, cleaves the pri-miRNA, generating a smaller hairpin of around 70nt. This RNA molecule is called precursor miRNA (pre-miRNA) and is exported to the cytoplasm by the action of Exportin 5. Here, the pre-miRNA is cleaved again by another RNaseIII, Dicer, which generates a double stranded RNA molecule of around 22nt. Generally, only one strand of RNA is used as mature miRNA, while the other is degraded (Fig. 6).

The mature miRNA is loaded in the RISC (RNA-induced silencing complex), which recognises the mRNA target and allows pairing between the “seed” sequence of the miRNA (usually 8nt) and the 3' UTR of the mRNA. This pairing between the two leads to the repression of translation by one of two mechanisms: either the removal of the poly-A tail of the mRNA (and the subsequent degradation by exonucleases activity), or the blocking of translation by stalling the ribosomal complex. The stalled ribosome then moves to subcellular organelles called P-bodies. Here, the complex can either be stored or degraded (Fabian et al., 2010; Murchison and Hannon, 2004; Winter et al., 2009; Xiao and MacRae, 2019).

It is also important to note that the same miRNAs can target more than one mRNA species, and *vice versa*. This kind of mechanism allows a fine regulation of gene

expression, as the presence of more miRNAs on a single mRNA generates a stronger silencing effect (Bartel, 2004).

#### 1.4.1 From primary transcripts to mature miRNAs

There are several ways of biosynthesis of miRNAs. The canonical one, which was the first to be discovered, involves the action of the RNA PolIII, which binds to the promoter of the miRNA gene, and starts transcribing a long primary transcript (or pri-miRNA). This pri-miRNA has a particular hairpin structure, which is recognised by a specific complex containing an RNA endonuclease (RNase III), called DROSHA. DROSHA is able to cleave at the base of the hairpin, producing a precursor miRNA (pre-miRNA) of ~80-90nt in length. This pre-miRNA still possesses the typical hairpin structure, which is recognised by an exportin, called Exportin 5, that has the role of translocating it from the nucleus of the cell to the cytoplasm.

In the cytoplasm, the pre-miRNA is further cleaved by a second endonuclease, type III, called Dicer. Differently from DROSHA, which cleaves at the stem of the hairpin, Dicer cleaves the pre-miRNA at the level of the loop, leaving a double stranded RNA of ~20-25nt (the mature miRNA) as a product (Fig. 6).

It is important to remember that not every hairpin-like RNA structure is recognised by the two endonucleases DROSHA and Dicer. In fact, there are some specific sequences that the hairpin needs in order to be recognised, and that are common to each pri-miRNA. These sequences allow these hairpins to be recognised as miRNAs and to be processed accordingly (Fig. 7) (O'Brien et al., 2018).

There are other ways in which miRNAs can be synthesised in cells. Despite the fact that these methods have been discovered later, these alternative ways represent more the rule than the exception. Two mechanisms in particular are quite common: the synthesis of a long non-coding RNA (lncRNA) that hosts two or more miRNAs in tandem; and the synthesis of miRNAs from circular RNA (circRNAs), usually produced as a consequence of splicing of mRNA, which have been named “mirtrons”, and are discussed in more detail later in this chapter.

For the first case, it is not uncommon to see miRNA genes located in tandem within the genomes. A very common example of a cluster of miRNAs is “miR-132-212”, a well-conserved cluster of two miRNAs, *miR-212* and *miR-132*. A more extreme situation is the cluster “miR-17~92”. This is a conserved cluster that contains six miRNAs in tandem: *miR-17*, *miR-18*, *miR-19a*, *miR-19b*, *miR-20* and *miR-92*. The way these miRNAs are synthesised is similar to the canonical pathway described above. The difference is in the length of the pri-miRNA, which can span for several thousands of nucleotides, and for the fact that from the same pri-miRNA, more than one mature miRNA is produced.

There is virtually no upper limit to the number of miRNAs that can be located in the same cluster. For example, one of the biggest known clusters is located on chromosome 4 of zebrafish, with over 50 miRNAs of the family *dre-miR-430* (Thatcher et al., 2008). Cells have some advantages, in using this strategy: first, they can use the same promoter for more than one miRNA, reducing the amount of space needed in the genome; second, the length of the pri-RNA of a cluster is shorter than multiple pri-miRNAs transcribed separately, this saving energy, and third, the same RNA PolIII can transcribe more than one miRNA per time, maximising the processivity of the enzyme.

The second way a cell can use to synthesise a miRNA is by taking advantage of protein-coding genes. In the eukaryotic domain a large number of genes have at least one intron. These portions of the mRNA are then spliced out, forming a circRNA which can have regulatory functions. In some situations, miRNA genes can be located in introns of protein-coding genes, and their transcription is then coupled with the transcription of the “host” gene. In this case, these miRNAs are called “mirtrons”. The advantages of having miRNA genes within introns of protein-coding genes are similar to the ones discussed for the clusters of miRNAs: reduced amount of space needed within the genome, and no need for a specific RNA PolIII for the miRNA, since the transcription occurs together with the transcription of the host gene (Salim et al., 2022).

A further advantage of mirtrons is the fact that, in some cases, they possess promoters themselves, within the host gene. This promoter allows the synthesis of the miRNA independently from the synthesis of the host gene, giving to this specific type of miRNAs an incredibly versatile function (Luo et al., 2024).

The existence of mirtrons is strictly connected to their evolutionary diversification. In fact, a recent theory suggests that miRNAs originated within introns and then, following whole genome duplication, the host genes that become pseudogenes let the miRNAs that they are hosting free to diversify (Mercuri et al., 2023).

In synthesis, even though the way to explain how miRNAs originate is usually limited to the canonical one, we now know that the reality is more complicated than this. There are several ways that allow the synthesis of a miRNA, and these ways can be interconnected, allowing extremely versatile production of these molecules.

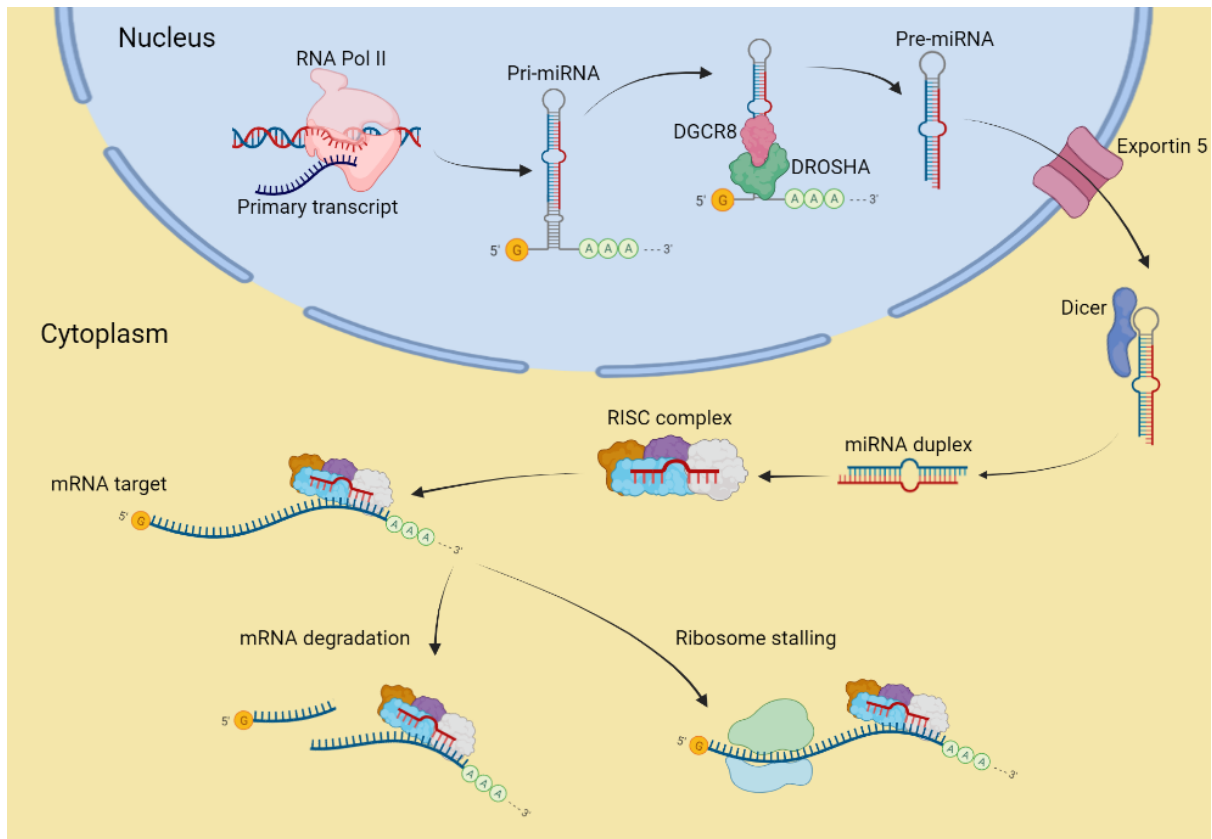


**Fig. 6: Canonical miRNAs biosynthesis.** In the canonical pathway, the biosynthesis of miRNAs starts with the action of the RNA PolII, which like a classical protein-coding gene, produces a primary transcript (pri-miRNA) that can be a few hundreds of nucleotides long. This primary transcript is characterised by a particular hairpin 3D-structure which allows it to be recognised by a complex of proteins which include the endonuclease type III DROSHA. DROSHA removes the base of the hairpin loop from the pri-miRNA, generating a miRNA precursor (pre-miRNA). The pre-miRNA is exported from the nucleus to the cytoplasm by the Exportin 5 and, in the cytoplasm, processed further by a second endonuclease type III, Dicer, which removes the loop of the hairpin. This second cleavage leaves behind the mature miRNA, a short RNA duplex of around 20nt. Once the miRNA gets processed for the second time by Dicer, it is ready to be loaded in the RNA-induced silencing complex (RISC), which scans the cytoplasm for mRNA species that possess, in their 3' UTR, a sequence that is able to make Watson-Crick base pairing with the seed sequence of the miRNA. Once the miRNA/RISC complex finds that mRNA target, it promotes either the degradation of the mRNA *via* removal of the poly-A tail, or it promotes the stalling of the ribosomal complex.

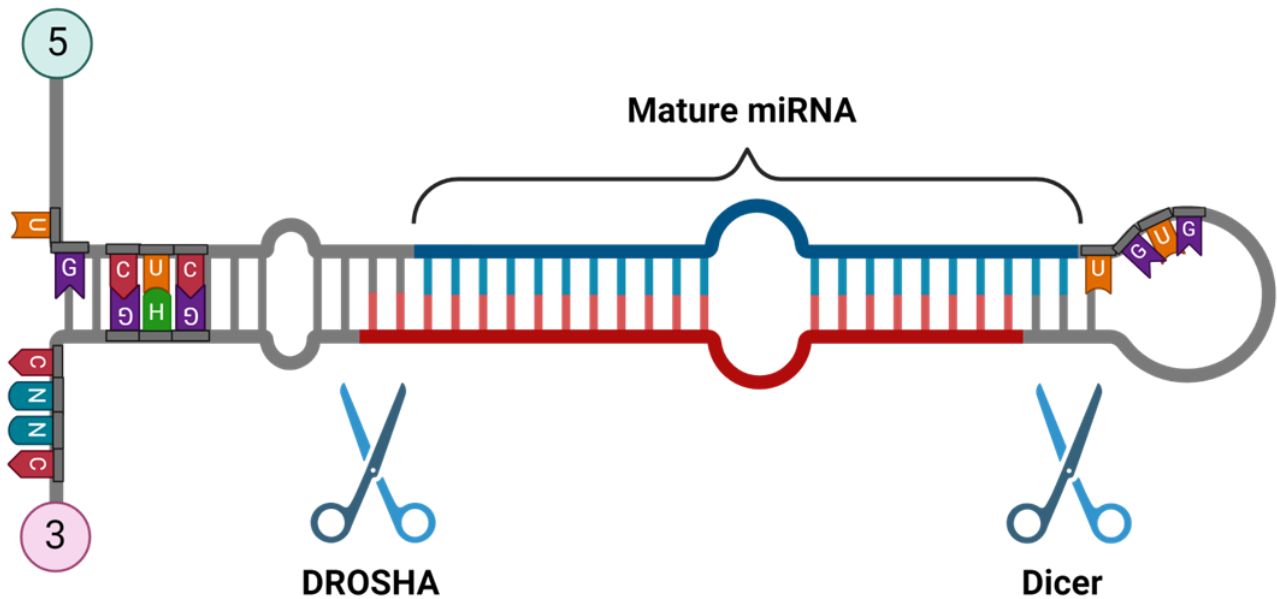


**Fig. 7: Pri-miRNA common features.** Structure of a pri-miRNA. Some features are common to most miRNAs, these include the secondary structure, which is a hairpin of ~40nt in length from the base to the loop, and a mismatch in proximity of the base of the hairpin, and within the mature miRNA duplex. Pri-miRNAs also share some sequence-specific features, in particular to the base of the hairpin, which is important for the cleavage operated by DROSHA (pri-miRNA to pre-miRNA), and a typical UGUG motif on the loop, which is needed for the cleavage operated by Dicer (pre-miRNA to mature miRNA).

#### 1.4.2 RNA interference

The most studied pathway in which miRNAs are involved is called RNA interference, or RNAi. This pathway involves the use of miRNAs to downregulate the expression of specific genes by repressing the translation of the mRNA. This mechanism can occur by either directly degrading the targeted mRNA, or by promoting the stalling of the ribosomal complex, with the targeted mRNA already loaded in it.

To exert its function, the mature miRNA needs to be loaded into a multiprotein complex called RISC (RNA induced silencing complex). Only when the miRNA is inside the RISC complex, it can “search” within the cytoplasm for mRNAs that can form a Watson-Crick base pairing from the “seed” sequence of the miRNA, and the miRNA recognition element (MRE) of the mRNA.

The seed sequence is the portion of the miRNA that is located between the second and the eighth nucleotides of the miRNA, and it is historically speaking, the functional part of the miRNA, in animals. However, in recent years, evidence suggests that the 3' half of the mature miRNA might be involved in the stability of the miRNA itself (Chipman and Pasquinelli, 2019).

The MRE of a mRNA is the part of the mRNA that pairs with the miRNA that is targeting it. Usually, this region is located in the 3' UTR of the mRNA, in proximity with the polyadenylated region. The sequence of the MRE does not have to display any particular feature, other than being complementary for the seed sequence of the miRNA. Also, the short length of the seed sequence (~8nt) in comparison to the 3' UTR of a mRNA, which can easily span over 1kb, gives the possibility to several different miRNAs/RISC to target the same mRNA molecule. When this happens, there is an additive effect of the silencing activity of the miRNAs on that specific mRNA. This mechanism allows a very fine regulation of gene expression, that can be tuned down at different ranges, according to the number of miRNAs that are targeting that specific gene.

An especially important group of proteins involved in the RNAi machinery is the Argonaute proteins. These proteins can interact with the 3' end of the miRNA, once it is loaded into the RISC, and help with the correct orientation of the miRNA to its mRNA target. Some AGO proteins, and in particular AGO2, possess a nuclease activity which is, on its own, able to cleave the mRNA. However, other AGO proteins have the role of recruiting additional proteins to exert the silencing of the mRNA. It is interesting to note that the fate of the mRNA, after it has been targeted by the miRNA, is heavily reliant on the type of pairing between the two. For example, it has been shown that a perfect matching of the miRNA with the MRE is more likely to result in the direct cleavage of the mRNA. On the other hand, imperfect matching between the miRNA and the MRE will likely result in the block of translation *via* steric interaction with the ribosomal complex. Either way, the pairing of the seed sequence is pivotal in this process, without it, none of the two types of repression are possible (Fig. 6).

### 1.4.3 miRNAs in other pathways

Despite the fact that RNAi is the most common and the best characterised pathway involving miRNA, these molecules can exert different and less known roles in the cell.

One of these pathways is the DNA damage response (DDR), in which miRNAs seem to play an important role in delivering the effectors of the DDR into the locus of DNA damage. The exact mechanism is still unclear; however, it seems that following double strand break (DSB) of the DNA helix, the active form of the RNA PolII is translocated to the site of the DSB, and it starts to produce RNA molecules of the length of a pre-miRNA. These particular miRNAs are then processed by Dicer and translocated back to the nucleus, where they accumulate to the locus of DDR (Francia et al., 2012).

Interestingly, knock-down of Dicer, as well as inhibition of the RNA PolII reduces the capacity of the cells to repair DSB of the DNA. This happens because the effectors of the DDR are either not recruited to the DDR locus, or because they are not retained long enough to repair the DNA in an efficient manner (Francia et al., 2012).

Another nuclear function of miRNA is associated with the enhancement of transcriptional activity. It has been observed that miRNAs can interact with active enhancers in the nucleus, as proven by active histone marker modifications such as the acetylation of lysine 27 of histone 3 (H3K27ac). This action leads to the activation of the enhancer and to higher levels of transcription of the gene regulated by that enhancer (Liu et al., 2018).

The theory that miRNAs can promote gene expression by interacting with enhancers is corroborated by the observation that AGO2 has been observed in the nucleus of cells, and that it can interact with a complex of proteins that shares similarities with the RISC, which has been called RNA induced transcriptional activator complex (RITA complex). Not all the proteins involved in this complex have been identified, but it has been seen that helicases are associated with it, presumably to allow the binding between the miRNA and the enhancer sequence of the DNA (Portnoy et al., 2016).

In conclusion, it is remarkable the number of functions that such short RNA molecules can play withing cell biology. From gene silencing to gene activation, passing though the

maintenance of the integrity of the DNA, miRNAs play a key role in cellular function that still need to be fully elucidated.

#### 1.4.4 The role of miRNAs in the developing embryo

A role for miRNAs during development was first noted in 2003, when Bernstein and colleagues deleted Dicer in mice (Bernstein et al., 2003). Disruption of Dicer leads to disruption of miRNAs biogenesis, since this enzyme is essential for the processing of pre-miRNA to mature miRNA, in the cytoplasm. It was observed that knock-out of Dicer leads to early embryonic lethality. This effect was due to extensive NCCs death, which lead to absence of NC derived tissues (Huang et al., 2010; Zehir et al., 2010). Similar effects were observed by deleting DGCR8, an important cofactor of DROSHA, which is the second endonuclease involved in miRNA biogenesis by processing the pri-miRNA into the pre-miRNA (Chapnik et al., 2012). That was not surprising since, in human, deletion of DGCR8 causes the DiGeorge syndrome, a NCP, that affects 1:4000 children (Lackey and Muzio, 2021). These studies led the way to prove a strict connection between miRNA biology and NC biology.

Following these studies, many individual miRNAs have been associated with specific steps of development. For example, in the context of NC development, Gessert and colleagues carried out excellent work in identifying several miRNAs that are associated with the early moment of NC development, in *Xenopus laevis*. These miRNAs include *xla-miR-130a*, *xla-miR-219*, *xla-miR-23b*, *xla-miR-200b*, *xla-miR-96* and *xla-miR-196a*. Using a morpholino knock-down strategy, they have shown that *xla-miR-130a*, *xla-miR-219* and *xla-miR-23* are important for the correct development of the eye, while *xla-miR-200b*, *xla-miR-96* and *xla-miR-196a* are important, other than for the correct formation of the eye, also for the correct development of craniofacial structures associated with the NC (Gessert et al., 2010).

Still in the context of NC development, Avellino and colleagues have shown that, in medaka fish, *ola-miR-204* is important for the correct migration of NCCs. They were able to regulate the levels of migration of NCCs by modulating the expression level of this miRNA (Avellino et al., 2013).

Both these studies were corroborated by the work of Ward and colleagues. They used *Xenopus laevis* induced organoids, called animal caps, to generate NC, neural or blastula tissues, and then performed small RNA sequencing to identify those miRNAs that are NC specific, when compared with the other two tissues (Ward et al., 2018).

Besides NC development, other groups have gone on to show miRNAs to be important in many developmental processes, such as muscle development. In this case, of particular interest are the so-called “myomiRs”, or miRNAs that are required for the correct homeostasis and development of muscles. These myomiRs include *gga-miR-1*, *gga-miR-133* and *gga-miR-206*, which have been shown to be involved in the correct development of the myotome, in chick (Goljanek-Whysall et al., 2014; Mok et al., 2017).

Another tissue whose correct development is heavily reliant on miRNA biology, is the neural tube. For example, inhibition of miR-9 and miR-124a can result in a reduced neuronal component in the adult organism, while overexpressing these miRNAs can limit the astrocytic development, highlighting the importance of the right concentration of these translational regulators (Delaloy et al., 2010; Krichevsky et al., 2006).

Another example in which miRNAs play an important role is bones. In 2009, Li and colleagues found that *mmu-miR-2861*, is able to control bone differentiation in mice by repressing the expression of the histone deacetylase 5 (HDAC5). This enzyme is able to control the expression of Runx2 by promoting its degradation. Therefore, in the absence of *mmu-miR-2861*, HDAC5 will be overexpressed and will repress Runx2, leading to loss of bone formation. To reinforce this hypothesis, this miRNA is conserved in human as well, and homozygous mutations in *hsa-miR-2861* that block its expression were shown to cause primary osteoporosis in two adolescents (Li et al., 2009).

The mentioned studies are just some examples of the extensive literature that associates miRNAs biology with development, showing their importance during embryogenesis.

#### 1.4.5 miRNAs and Neurocristopathies

Despite the numerous evidence that links miRNAs and embryo development, the literature that shows their involvement with human diseases is relatively scarce, though not completely absent.

For example, as mentioned above, homozygous mutations that block the expression of *hsa-miR-2861* have been shown to be associated with the onset of primary osteoporosis in at least two subjects (Li et al., 2009).

More related to NC development, loss of DGCR8, an important co-factor of DROSHA (the first endonuclease that processes pri-miRNAs into pre-miRNAs) causes an NCP called DiGeorge syndrome. This syndrome affects 1:4000 children and is characterised by cardiac defects, abnormal facies, cleft palate, and hypoplastic or absent thymus. Other common features of the DiGeorge syndrome are renal abnormalities, hearing loss and skeletal abnormalities. Most of these features are associated with NC developmental defects, highlighting the importance of the RNAi pathway in NC development (Du et al., 2019; Lackey and Muzio, 2021).

In recent years, de-regulated miRNAs have been associated with different types of NCPs and NC-derived cancers (Table 1) (Ayers et al., 2015; Lorusso et al., 2020; Ooi et al., 2018; Roth et al., 2018; Stallings, 2009). Some types of cancers, in particular neuroblastoma (NB) and melanoma, are considered NCPs, as they derive from NC tissues. MiRNAs that promote tumour growth are called oncomiRs, while miRNAs known to suppress the malignancy of the tumoral mass are called anti-oncomiRs (Svoronos et al., 2016).

Among the oncomiRs, we can include the cluster of miRNAs miR-17~92, which include six miRNAs: *miR-17*, *miR-18*, *miR-19a*, *miR-19b*, *miR-20* and *miR-92*. The overexpression of this cluster in NB is associated with high proliferation and invasiveness, while down-regulation of it reduces the invasiveness and increases the apoptotic levels in these cells (Svoronos et al., 2016).

On the other hand, *hsa-miR-34a* has been shown to play a protective role in cancer progression, as the overexpression of this miRNA induces the arrest of cell proliferation

and apoptosis in NB cells. This effect might be due to the targeting of *E2F3* mRNA by *hsa-miR-34a*, which is known to induce cell cycle progression (Stallings, 2009).

MiRNAs are also known to play a role in melanoma progression. For example, *hsa-miR-21* is considered an oncomiR, as its expression is often up-regulated in melanoma cells. This activation plays a role in the inhibition of cell differentiation and apoptosis. As a proof of it, knock-down of *hsa-miR-34a* in melanoma cells induces apoptosis and enhances the effectiveness of both chemo and radiotherapy. This effect seems to be triggered by the inhibition of the expression of *MCL-1*, an important player of the PI3K-AKT-mTOR pathway (Lorusso et al., 2020).

Partially thanks to these findings, which prove the importance of miRNAs in the etiopathogenesis of human cancers, more and more evidence have been collected linking mutations affecting miRNAs and rare diseases.

An excellent example has been provided by Bachetti and colleagues. In 2021, they identified an association between the miRNA-mediated regulation of *PHOX2B* and the onset of congenital central hypoventilation syndrome (CCHS). This is also an NCP which affects the correct development of the CNS and that can cause sudden infant death via hypoxic crisis during sleep, a condition also known as “Ondine’s Curse”. They observed a mutation in the 3’ UTR of *PHOX2B* in a family affected by this condition. This generates a potential new binding site for *hsa-miR-204/211*, which is already known to be targeting this gene in NB cells (Bachetti et al., 2021; Perri et al., 2021). The authors speculated that the generation of this new binding site might induce a further downregulation of *PHOX2B*, that might contribute to the onset of CCHS (Bachetti et al., 2021).

In recent years, another NCP has been associated with miRNAs deregulation. Hirschsprung disease (HD) is a condition characterised by the absence of enteric ganglia, which causes severe problems to the person affected by it. These include swollen belly, vomiting, chronic constipation, and fatigue. In 2016, a differential miRNA expression analysis was carried out on colon tissue from people affected by HD, highlighting 168 differentially expressed miRNAs (Li et al., 2016; Lotfollahzadeh et al., 2021). A further study showed how a point mutation in the seed sequence of *hsa-miR-100* increases the susceptibility to HD (Zhu et al., 2020).

## 1.5 Aim of the project

As mentioned previously in this chapter, even the most up-to-date GRNs that illustrate how the NC is regulated, do not provide much information about the contribution of miRNAs. Given the important role of miRNAs during development, and supported by previous data obtained in our lab by Dr Nicole Ward (Ward et al., 2018), we hypothesise that miRNAs play an important role in many aspects of NC development and that the current NC-GRNs are lacking information about these molecules.

In this project we aimed to expand the current state of knowledge by identifying miRNAs that are potentially involved in various aspects of NC development. To do so, we used a combination of approaches, ranging from literature reviews to bioinformatical analysis, in order to identify miRNAs that might be of interest for this project. Then, we used the African clawed frog *Xenopus tropicalis* as model organism and downregulated the expression of these miRNAs by using a CRISPR-Cas9 strategy, to investigate any NC-specific phenotype.

This work helps us to increase our knowledge of the NC-GRN, to identify novel markers for NCPs and possibly, to use this knowledge to generate new treatments for these kinds of conditions.

During this project, we identified eighteen miRNAs that we predict to be involved in NC development, by using bioinformatical approaches (*xtr-miR-10b*, *xtr-miR-15a-16a*, *xtr-miR-17~92*, *xtr-miR-30a*, *xtr-miR-99*, *xtr-miR-100*, *xtr-miR-132-212*, *xtr-miR-145*, *xtr-miR-187*, *xtr-miR-194-1*, *xtr-miR-200b*, *xtr-miR-204-1*, *xtr-miR-204-2*, *xtr-miR-208*, *xtr-miR-210*, *xtr-miR-218-2*, *xtr-miR-455*, and *xtr-miR-489*).

Of those miRNAs, we tested *in vivo* the effect of the knock-down on four of them (*xtr-miR-10b*, *xtr-miR-204-1*, *xtr-miR-208*, and *xtr-miR-218-2*), describing interesting developmental defects in *Xenopus tropicalis*.

Finally, we focused our investigation on the developmental role of one of these miRNAs, *xtr-miR-204-1*. We identified some of the genes whose expression is affected by its knock-down and, most importantly, we identified a previously undescribed dual mechanism that is operated by this miRNA. In particular, we suggest that *xtr-miR-204-1*

is able to use both guide strand and passenger strand in order to execute its developmental role.

Neurocristopathy	Symptoms	miRNA/miRNA-related genes	Implicated target/s	Role in NC development
DiGeorge Syndrome	Behaviour problems;	DGCR8	iRNA	General
	Hearing problems;			
	Feeding problems;			
	Congenital heart defects; Hypoparathyroidism			
Neuroblastoma	Adrenal gland tumour	miR-17-92	<i>cdkn1a</i>	Induction, chondrocyte differentiation
		miR-34a	<i>e2f3, mycn, bcl2, cdk6</i>	EMT
		miR-204	<i>bcl2, ntrk2</i>	Specification and migration
		miR-193b	<i>mycn, mcl1, ccnd1</i>	Orofacial development
		miR-188	<i>kif1b</i> (predicted)	
		miR-125-1	<i>e2f3, mcl1</i> (predicted)	Specification
Melanoma	Skin tumour	miR-501	<i>bcl2, e2f3, cdk6, ntrk2</i> (predicted)	
		miR-32	<i>mcl1</i>	
		miR-579-3p	<i>mitf, braf, mdm2</i> (predicted)	
		miR-200c	<i>bmi1, zeb2, tubb3, abcg5, mdr1</i>	Specification
		miR-7	<i>egfr, igf1r, craf</i>	Tooth development
		miR-21	<i>pten</i>	Shwann cells differentiation
		miR-638	<i>tp53inp2</i>	
		miR-34a	<i>bcl2, cdk6, e2f3, mycn</i>	EMT
		miR-100	<i>trim71</i>	EMT
		miR-125b	<i>bak1, bcl2, e2f3</i>	
		miR-192	<i>zeb2</i>	
miR-193b	<i>cdk6, mcl1, bmi1</i> (predicted)	Orofacial development		
miR-514a	<i>nf1</i>			
CCHS	CNS development delay; Hypoxic crisis	miR-204	<i>phox2b</i>	Specification and migration
Hirschsprung Disease	Swollen belly; Vomiting; Chronic constipation; Fatigue	miR-100	<i>ednrb</i>	EMT
		miR-206	<i>scdpr</i>	Orofacial development
		miR-214	<i>plagl2</i>	
		miR-483	<i>fh11</i>	
		miR-124	<i>sox9</i>	
Craniosynostosis	Premature fusion of two or more skull bones	miR-23b	<i>smad3, smad5</i>	Induction
		miR-133b	<i>egfr, fgfr1</i>	Chondrocyte differentiation
CHARGE Syndrome	Coloboma; Heart defects; Atresia choanae; Growth retardation; Genital abnormalities; Ear abnormalities	let-7	<i>chd7</i>	Chondrocyte differentiation
		let-7b	<i>lin28b</i>	Chondrocyte differentiation
		miR-143	<i>bcl2, fgf1, igfbp5, camk1d</i>	Cardiac differentiation
		miR-145	<i>tgfr2, apc, cmyc</i>	Cardiac differentiation
		miR-135	<i>lzts1, lats2, ndr2, btrc</i>	
Neurofibromatosis	Peripheral nerves and Schwann cells tumour	miR-889	<i>apc</i>	
		miR-128	<i>nf1</i>	
		miR-137	<i>nf1</i>	
		miR-103	<i>nf1</i>	
		miR-140	<i>pdgfra</i>	Chondrocyte differentiation
		miR-17-92	<i>tbx1, tbx3</i>	Induction, chondrocyte differentiation
Cleft palate	Incomplete fusion of the bilateral palatal shelves	miR-200b	<i>smad2, snai2, zeb1, zeb2</i>	Specification

**Table 1: Table of NCPs and associated miRNAs.** Schematic of NCPs (first column) and related phenotype (second column). For each NCP there is one or more associated miRNAs (third column) and the gene that they regulate in that pathological context (forth column) and in which step of NC differentiation that gene acts (fifth column). Adapted from: (Antonaci and Wheeler, 2022).

## **Chapter 2: Material and methods**

### **2.1 Collection of *Xenopus laevis* eggs:**

Females of *Xenopus laevis* were primed with an injection of 200U (200µl) PMSG onto one lymph sac from 3 to 7 days before eggs collection. Frogs are not fed during this time. Induction is was then performed ~16h before eggs collection with an injection of 500U (500µl) of Chorulon onto one lymph sac. Once the first eggs are naturally released, frogs were gently squeezed in order to collect eggs in a petri dish.

### **2.2 Fertilisation of *Xenopus laevis* eggs:**

*Xenopus laevis* frozen sperm was collected from the -80°C and thawed for 30sec in a 37°C water bath doing an “8” movement. Then, 125µl of 1X MMR was added to the frozen sperm and gently mixed with a pre-cut tip, the mixture was then pipetted on the eggs. The eggs were then incubated at 18°C for 10min. After this incubation, the plate was flooded with 0.1X MMR and incubated for 20min more at 18°C. At this point, fertilised eggs will turn with the animal pole (pigmented side) on the top and vegetal pole (non-pigmented side) on the bottom. The embryos were then de-jellied by removing 0.1X MMR and adding Cysteine solution for 7min. During this incubation, it is possible to improve the process by gently swirling the embryos clock-wise and anti-clock-wise. At the end of the 7min, Cysteine solution was removed by washing the embryos twice with 1X MMR and twice with 0.1X MMR.

### **2.3 Collection of *Xenopus tropicalis* eggs:**

Females of *Xenopus tropicalis* were primed with an injection of 10U (100µl) Chorulon onto one lymph sac 24h-72h before eggs collection. Frogs are not fed during this time. Induction was then performed ~5h before eggs collection with an injection of 200U (200µl) of Chorulon onto one lymph sac. Once the first eggs were naturally released, frogs were gently squeezed in order to collect eggs in a petri dish.

### **2.4 Fertilisation of *Xenopus tropicalis* eggs:**

*Xenopus tropicalis* frozen sperm was collected from the -80°C and thawed for 30sec in a 37°C water bath doing an “8” movement. Then, 125µl of 0.1X MMR was added to the

frozen sperm and gently mixed with a pre-cut tip, the mixture was then pipetted on the eggs. The eggs were then incubated at 26°C for 15min. After this incubation, the plate was flooded with 0.05X MMR and incubated for 25min more at 26°C. At this points, fertilised eggs will contract the pigmentation on the animal pole, making it darker than the one of unfertilised eggs. The embryos were then de-jellied by removing 0.05X MMR and adding Cysteine solution for 7min on gentle agitation. At the end of the 7min, Cysteine solution was removed by washing the embryos twice with 0.1X MMR and twice with 0.05X MMR and plated on BSA coated Petri dishes.

## **2.5 Fixation of *Xenopus* sp embryos:**

Fertilised embryos were let to develop at 16-21°C (*X. laevis*) or 26°C (*X. tropicalis*). Once they reached the desired stage, embryos were collected and fixed in MEMFA for 2h at RT with gentle rocking, or ON at 4°C with gentle rocking. Once fixed, embryos were washed three times with 100% Ethanol. At this point, we proceeded with the desired protocol, or stored the embryos at -20°C indefinitely.

## **2.6 Sperm Freezing**

2.6.1 *Xenopus tropicalis*: All cryopreservation steps were performed immediately after removing the testes.

Testes were transferred on a 1.5ml tube with 500µl L15 media supplemented with 1% calf serum (or FBS) and L-glutamine 2µM, then homogenised with a pestle. Immediately after, we added the same volume of ice cold cryoprotectant (500µl) and made 125µl aliquots.

2.6.2 *Xenopus laevis*: All cryopreservation steps were completed immediately after the removal of the testes.

Testes were transferred on a 6cm petri dish with 1ml L15 media supplemented with 1% calf serum (or FBS) and L-glutamine 2µM, then homogenise with two tweezers. Immediately after, we added the same volume of ice cold cryoprotectant (1ml) and made 125µl aliquots.

Solution A: One egg yolk (~15ml) with the same volume of dH<sub>2</sub>O;

Solution B: 0.4M Sucrose, 10mM NaHCO<sub>3</sub>, 2mM pentoxifylline;

Cryoprotectant was prepared by mixing 20% of solution A and 80% of solution B. Then, centrifuged at 32000g for 20min, then the supernatant was collected, and the pellet was discarded. Aliquots of cryoprotectant were made in 1ml volume and stored at -20°C.

The 125µl aliquots of sperm were frozen immediately by keeping them in a polystyrene box covered with an aluminium foil at -80°C. The day after, we removed them from the box and stored in a normal box.

## **2.7 Transformation of Bacteria**

Competent cells were thawed on ice (from the -80°C). Once they were starting to thaw, we pipetted 4µl of plasmid in the tube with competent cells (100µl aliquots of competent cells) and incubated on ice for 30min. In the meanwhile, we set the heat block at 42°C and the heat shaker at 37°C. We then performed heat shock at 42°C for 90sec, flicking the tubes every 15sec. Then, we put back on ice for 2min more. We added 900µl of antibiotic-free LB and incubated at 37°C, 250rpm for 1h in the heat shaker. We centrifuged for 5min at 6000g to pellet bacteria. Then, we removed 950µl of the supernatant and resuspended the bacteria pellet in the remaining 50µl with the pipette. Finally, we plated the 50µl in an LB-agar plate with the appropriate antibiotic and incubated upside-down ON at 37°C.

The day after, we took a single colony from the plate and incubated in 100ml of LB with the appropriate antibiotic for ~16h at 37°C and 180rpm. Then, we pelleted the bacteria by centrifugation at 6000g for 15min at 4°C and proceed with the MIDI protocol according to the manufacturer protocol.

## **2.8 Cloning for in situ probes**

2.8.1 Primers design: To design primers for amplifying the fragment of mRNA of interest, we accessed <https://www.xenbase.org/entry/> and searched for the gene of interest. We searched under “Expression” to determine if the gene was overexpressed at specific stages and, if so, which chromosomal variant was more expressed (*L.* or *S.*; this applied only to *X. laevis*). We then navigated to “Summary” and selected the CDS of interest (*X.*

*tropicalis*, *X. laevis* L., or *X. laevis* S.). The CDS sequence was copied and pasted into the [NCBI Primer-BLAST tool: https://www.ncbi.nlm.nih.gov/tools/primer-blast/](https://www.ncbi.nlm.nih.gov/tools/primer-blast/)

The following parameters were used:

- PCR product size: Ideally between 500 and 1000bp
- Primer melting temperature: Min – 59.0°C; Opt – 60.0°C; Max – 61.0°C
- Organism: Either *X. tropicalis* or *X. laevis*

Primers were designed by clicking “Set primers,” which took some time to complete. The optimal pair of primers was selected based on the number of possible non-specific products and the desired product length, and the primers were ordered accordingly.

2.8.2 RNA extraction and cDNA synthesis: Tadpole stages were collected, where the mRNA of the gene of interest is highly expressed. Approximately 3–4 tadpoles were placed in a 1.5 ml Eppendorf tube, and as much media as possible was removed without leaving the embryos completely dry. The samples were snap-frozen in liquid nitrogen for ~30sec and either stored immediately at -80°C or processed further.

RNA extraction was performed using the *RNeasy Micro Kit* from Qiagen (cat. No. 74004) following the manufacturer’s protocol. RNA was quantified using a Nanodrop spectrophotometer, and samples were stored at -80°C or used immediately for cDNA synthesis. cDNA was synthesized using *SuperScript™ IV Reverse Transcriptase 10,000U* from Invitrogen (cat. No. 18090010) according to the manufacturer’s protocol. The cDNA was either stored at -20°C or used immediately.

2.8.3 Amplification of the gene of interest and cloning: The PCR reaction was set as follows: 12.5µl of 2X TaqBiomix, 2µl cDNA, 1µl of primer mix (Forward and Reverse, both 10µM), 9.5µl nuclease-free water.

The thermocycler was set as follows:

Step	Cycle	Temperature	Time (min:sec)
1	1	95°C	05:00
2	37	95°C	00:30
		*	00:30
		72°C	**
3	1	72°C	07:00
4	1	10°C	∞

\* Annealing temperature is specific for the pair of primers (it should be between 59°C and 61°C);

\*\* Taq polymerase can process ~1000bp/min, so the elongation time was calculated accordingly (usually the minimum was 1min, even if the fragment was smaller than 1000bp).

We run 4µl of the PCR reaction on a 1.5% agarose gel for 40min at 90V and image. If only the specific band was visible, it was possible to proceed with the next step.

The PCR reaction was purified by using the “QIAquick PCR purification kit” from Qiagen (ref. 28104) according to the manufacturer protocol. We then quantified the purified fragment on the Nanodrop. At this point, we wither stored the fragment at -20°C or proceeded to the next step.

To clone the fragment, we used the “pGEM-T Easy Vector System” from Promega (cat. no. A1360), setting up the reaction as follows: 5µl of 2X Rapid Ligation Buffer - T4 DNA Ligase, 0.5µl pGEM-T Easy Vector (50ng), 1µl T4 DNA Ligase, \*µl PCR product, up to 10µl nuclease-free water.

\*To determine the amount of µl of PCR product, we used <https://nebiocalculator.neb.com/#!/ligation> and set the following parameters: “Insert DNA length” – the length of the PCR product; “Vector DNA length” – pGEM-T is 3015bp; “Vector DNA mass” – in the reaction we used 25ng. NB: Change the scale from “kb” to “bp” according to what we needed.

The ng of insert to use are written in the “Required insert mass” table, it was useful to start with the ratio 3:1. By using the concentration obtained on the Nanodrop, we calculated the volume of insert that was needed for the reaction.

We then incubated the reaction at RT for 2h or at 4°C ON. At this point, it was possible to store the ligation product at -20°C or to proceed immediately to the next step.

2.8.4 Transformation and colony PCR: We prepared enough LB-agar plates with the specific antibiotic and X-Gal. To make X-Gal plates, we poured 50µl of X-Gal onto an already made LB-agar plate and spread it until it dried.

Then, we performed transformation as stated before. The difference was that, at the end, blue and white colonies were visible on the plate the day after. Only the white be the ones with the insert.

We set the PCR reactions as follows: 10µl of 2X TaqBiomix, 1µl of M13Fw/M13Rv mix (10µM each), 9µl nuclease-free water. With a 10µl tip, we gently scratched one of the white colonies and pipetted up and down on the PCR reaction mix. Not all the colony were removed from the plate, as it will needs to grow again ON at 37°C. At least three colonies each plate were tested.

Step	Cycle	Temperature	Time (min:sec)
1	1	95°C	05:00
2	35	95°C	00:30
		59°C	00:30
		72°C	*
3	1	72°C	07:00
4	1	10°C	∞

\*The elongation temperature was calculates as before, but considering the insert as it is 200bp longer than the insert.

The PCR product was run on a 1.5% agarose gel for 40min at 90V. If a single band of the size of the insert + 200bp was visible, we grew the remaining of the colony in 5ml of LB broth with ampicillin.

2.8.5 MINI and sequencing: The day after, we controlled if the colony grew in the LB (the media should be cloudy). If so, we performed a MINI following the manufacturer protocol.

The sample was then sent for sequencing using either M13Fw or M13Rv as primer to check the directionality of the insert.

Once the result of the sequencing came back, we proceeded with the probe synthesis.

## **2.9 WISH probes synthesis**

2.9.1 By plasmid linearisation: We checked the appropriate plasmid and the appropriate restriction enzyme. Then we set the restriction reaction.

Linearization was set in a final volume of 25 $\mu$ l: 2.5 $\mu$ g of plasmid, 2.5 $\mu$ l of appropriate 10X Restriction Buffer, 2.5 $\mu$ l of appropriate Restriction Enzyme, nuclease free water to a final volume of 25 $\mu$ l.

Incubated at 37°C ON (for normal restriction enzymes) or for 2h for (HF and time-saving restriction enzymes).

We then run a 1% agarose gel with 100ng (1 $\mu$ l) of linearisation product and 100ng of circular plasmid to check the linearisation (circular and linear plasmids have different sizes). For gel loading, we added 2 $\mu$ l of 6X Loading dye, 1 $\mu$ l of linearised plasmid and 7 $\mu$ l of water. For circular plasmids, we added 2 $\mu$ l of Loading dye, 100ng of plasmid and water to a final volume of 10 $\mu$ l.

By using the QioQuick PCR purification kit, we followed the instructions to purify the linearised plasmid. Then, we eluted it in nuclease-free water.

For the riboprobe synthesis, we assembled the reaction in the following way: To a final volume of 20 $\mu$ l: 4 $\mu$ l of 5X transcription buffer, 2 $\mu$ l DTT (100mM), 2 $\mu$ l DIG, 1 $\mu$ l RNA inhibitor (RNasin), 2 $\mu$ l appropriate RNA polymerase (T7, T3, SP6) and 9 $\mu$ l of linearised plasmid.

If using T7 polymerase, we incubated ON at 37°C;

If using T3 polymerase, we incubated 3h at 37°C;

If using SP6 polymerase, we incubated 4h at 40°C.

We then run a 1.5% agarose gel with 1µl of reaction product to check the quality of the reaction. For gel loading, we added 2µl of 6X Loading dye, 1µl of riboprobe and 7µl of water.

If the probe was visible, we proceeded with the purification using G50 Purification columns (Illustra, ProbeQuant G-50 Micro Columns – GE Healthcare) following the manufacturer instructions.

The purified riboprobe was quantified on the Nanodrop and then diluted in Hybridisation buffer at a concentration of 1µg/ml at -20°C.

2.9.2 By PCR reaction: By using the appropriate plasmid, we set 25µl of reaction as follows: 12.5µl TaqBiomix 2X, 1µl of appropriate primers (usually M13 Fw and M13 Rv) 10µM, 100ng of plasmid, nuclease-free water to a volume of 25µl.

The thermocycler was set as follows:

Step	Cycle	Temperature	Time (min:sec)
1	1	95°C	05:00
2	35	95°C	00:30
		59°C	00:30
		72°C	1:30
3	1	72°C	07:00
4	1	10°C	∞

5µl of PCR product were loaded on a 1.5% agarose gel for 30-40min. If the PCR product was visible, we proceeded with the purification by using QIAquick PCR purification kit following the manufacturer instructions.

The sample was then quantified on the Nanodrop (twice with 1µl and calculating the average).

For the riboprobe synthesis, the reaction was assembled in the following way: To a final volume of 20µl: 4µl of 5X transcription buffer, 2µl DTT (100mM), 2µl DIG, 1µl RNA inhibitor (RNasin), 2µl appropriate RNA polymerase (T7, T3, SP6), 100ng of PCR product and H<sub>2</sub>O to a final volume of 20µl.

If using T7 polymerase, we incubated ON at 37°C;

If using T3 polymerase, we incubated 3h at 37°C;

If using SP6 polymerase, we incubated 4h at 40°C.

We run a 1.5% agarose gel with 1µl of reaction product to check the quality of the reaction. For gel loading, we added 2µl of 6X Loading dye, 1µl of riboprobe and 7µl of water.

If the probe was visible, we proceeded with the purification using G50 Purification columns (Illustra, ProbeQuant G-50 Micro Columns – GE Healthcare) following the manufacturer instructions.

The purified riboprobe was quantified on the Nanodrop and diluted in Hybridisation buffer at a concentration of 1µg/ml at -20°C.

## **2.10 mRNA synthesis**

2.10.1 Using SP6 mMessage mMachine Kit: Frozen reagent, including RNA Pol, were thawed on ice. Briefly vortexed the 10X Reaction Buffer and the 2X NTP/CAP and microfuged both of them.

The reaction was prepared at room temperature to a final volume of 20µl (it can be scaled up, if needed).

The reaction was set as follows: 10µl 2X NTP/CAP, 2µl 10X Reaction Buffer, 1µg of linearised plasmid or 0.2µg of PCR product, 2µl Enzyme Mix, H<sub>2</sub>O to a final volume of 20µl.

The reaction was mixed well by pipetting up and down and incubated for 2h at 37°C.

2.10.2 Recovery of mRNA: 30µl of LiCl Solution were added, mixed well and stored at -20°C for at least 30min.

Sample was centrifuged at >15,000g at 4°C for 15min and the supernatant was carefully removed. We washed once with 70% ethanol and centrifuged again with the same settings. The supernatant was removed and the pellet resuspended in 50µl of nuclease free water, quantified on the Nanodrop and stored at -80°C.

## 2.11 Whole-Mount in-situ Hybridisation

All steps were carried out at RT and with gentle rocking, unless otherwise specified.

The embryos were first washed sequentially in ethanol solutions of decreasing concentration, prepared in DEPC-treated PBST. Washes were performed for 5 minutes each in 75%, 50%, and 25% ethanol, followed by two additional washes in DEPC-PBST for 5 minutes each.

Proteinase K treatment was performed using a solution of 20 µg/ml Proteinase K in DEPC-PBST, with the incubation time adjusted according to Table 1. This step was carried out without rocking. The embryos were then washed twice with DEPC-PBST for 5 minutes to remove residual Proteinase K, followed by fixation in 3.7% paraformaldehyde (PFA) in DEPC-PBS for 20min. Fixation was followed by two more washes with DEPC-PBST for 5min each.

Pre-heated hybridization buffer (60°C) was added, and the embryos were incubated until they settled to the bottom of the vial without rocking. The hybridization buffer was replaced with fresh buffer, and the embryos were incubated at 60°C for at least 1h. The probe solution was added, and the embryos were incubated overnight (ON) at 60°C.

The next day, the embryos were washed once with hybridization buffer for 10min at 60°C, followed by three washes with 2X SSC for 20min each at 60°C. RNase A treatment was performed by incubating the embryos in a solution of 10ng/ml RNase A in 2X SSC for 30 min at 37°C. This was followed by one wash in 2X SSC for 10min and two washes in 0.2X SSC for 30min each at 60°C.

Embryos were then washed with MAB for 10min and blocked in blocking solution (2% Boehringer Blocking Reagent (BBR) in MAB) for at least 1h. The embryos were incubated overnight at 4°C in blocking solution containing α-Digoxigenin-AP (1:3000).

The following day, embryos were washed twice with MAB for 5min, six times with MAB for 30min each, and overnight in MAB at 4°C. Additional washes were performed three times with MAB for 5min each, followed by two washes with NTMT for 10min.

Colour development was performed using a solution of 35µl BCIP and 9µl NBT in 10ml NTMT, protected from light. The embryos were monitored until the probe developed a

clear signal or the sense control began to show staining. The colour solution was replaced if it turned purple to accelerate the reaction and reduce background staining.

The reaction was stopped with three washes in PBST for 10min each. Optionally, embryos were bleached in a bleaching solution for 2h, followed by three washes in PBST. Embryos were stored overnight in 100% methanol at 4°C, washed three times in PBST for 10min each, and imaged on a 2% agarose plate with water.

The embryos were stored in 100% methanol at -20°C or in PBS with sodium azide at 4°C.

## **2.12 LNA-Whole-Mount in-situ Hybridisation**

The LNA-WISH protocol largely follows the same steps as described for the WISH protocol, with specific modifications for the hybridization and washing conditions, as detailed below:

After sequential washes in ethanol solutions and Proteinase K treatment, fixation, and initial washes (see WISH protocol 2.11), pre-heated hybridization buffer at 54°C was added. The embryos were incubated until they settled to the bottom of the vial without rocking. The hybridization buffer was replaced with fresh buffer, and the embryos were incubated at 54°C for at least 3h.

The LNA probe solution was added, and the embryos were incubated ON at 54°C. The next day, the embryos were washed once with hybridization buffer for 10min at 54°C, followed by three washes with 2X SSC for 20min each at 54°C, and two washes with 0.2X SSC for 30min each at 54°C.

Subsequent blocking, antibody incubation, and colour development were performed as described in the WISH protocol, with the same washing steps. The reaction was stopped, and embryos were optionally bleached, stored in methanol or PBS with sodium azide, and imaged according to the WISH protocol.

These minor adjustments in temperature and hybridization times accommodate the properties of LNA probes while maintaining overall consistency with the WISH protocol.

Time in minutes of incubation with Proteinase K solution. The staging is performed according to the standard Nieuwkoop and Faber staging system.

<b>Stage (NF)</b>	1-10	10.5-12	13-16	17-20	21-25	26-30	31-33	34-36	37-40	41-45
<b>Time (min)</b>	0.5	1	2	3	4	5	6	8	18	20

## 2.13 CRISPR/Cas9

2.13.1 sgRNA synthesis: Oligos were resuspended to a final concentration on 100µM and then we set the following reaction:

Final volume: 25µl: 12.5µl Taq polymerase 2X, 0.5µl MgCl<sub>2</sub> (50mM), 0.5µl specific oligo (100µM), 0.5µl universal CRISPR oligo (100µM) (AAAAGCACCGACTCGGTGCCACTTTTTCAAGTTGATAACGGACTAGCCTTATTTAACTTGC TATTTCTAGCTCTAAAC), 11µl nuclease free water.

Before starting the PCR reaction, we took 3µl from each sample and keep it on ice.

- The following PCR was run:

Step	Cycle	Temperature	Time (min:sec)
1	1	95°C	05:00
2	13	95°C	00:20
		65°C	00:20
		68°C	00:15
3	30	94°C	00:20
		58°C	00:20
		68°C	00:15
4	1	68°C	05:00
5	1	4°C	∞

A 1.2% agarose gel was made, and 3µl of PCR product and 3µl of the reaction mix as a negative control were loaded. The negative control was less bright than the PCR product.

sgRNAs were synthesized using the MEGAscript T7 Transcription Kit (Invitrogen-ThermoFisher Scientific). All components, except the T7 Enzyme mix, were thawed at room temperature, while the T7 Enzyme mix was thawed at 4°C. The reaction was assembled at room temperature in 1.5ml Eppendorf tubes. The final volume was 20µl,

consisting of 2µl of T7 10X Reaction buffer, 2µl of T7 ATP Solution, 2µl of T7 CTP Solution, 2µl of T7 GTP Solution, 2µl of T7 UTP Solution, 2µl of T7 Enzyme mix, and 8µl of DNA template. The reaction was mixed by pipetting and microfuged, then incubated overnight at 37°C.

After incubation, 1µl of DNase I was added, and the reaction was incubated for an additional 15min at 37°C. The reaction was stopped by adding 115µl of nuclease-free water and 15µl of sodium acetate (3M), then vortexed for 10sec. RNA was precipitated by adding 300µl of 100% ethanol, mixed by pipetting, and chilled for at least 2h at -20°C.

The sample was centrifuged at 4°C for 15min at >10,000g, and the supernatant was removed. The RNA pellet was resuspended in 50µl of nuclease-free water. The sgRNA was quantified using a Nanodrop and stored at -80°C.

2.13.2 Microinjector settings: All microinjections were performed using an Harvard apparatus PLS-1 system. The needles were produced pulling borosilicate filaments (OD 1mm, ID 0.58mm, 15cm length) from Multichannel System (product code G100F-6). The microinjector is set on according to the following parameters:

- $P_{\text{inject}}$ : Between 8.5psi and 10.5psi;
- $P_{\text{balance}}$ : Between 1.2psi and 1.4psi;
- Injection time: Between 500ms and 900ms.

2.13.3 Injection solution loading: A drop of 1.4µl of injection solution was pipetted on parafilm and, by using the microscope, we filled the needle with it.

2.13.4 Microinjections: On a Petri-dish with the net on the bottom, we filled with Ficoll solution, gently put ~20-25 embryos and orientate them with the animal pole on the top. We slowly removed all the solution and started the injections using the rows on the grid to orientate and to keep track of the injected embryos. Once all the embryos were injected, we moved them to the appropriate Petri-dish filled with Ficoll solution and left them there for at least 30min at the appropriate temperature (16°C -22°C for *X. laevis* and 24°C-26°C for *X. tropicalis*). Then, we changed the solution with MMR at the appropriate concentration (0.1X for *X. laevis* and 0.05X for *X. tropicalis*).

2.13.5 Microinjection solution: We incubated 0.8µl EnGen Spy Cas9 NLS from NEB (cat. no. #M0646M) and 300ng < X < 1500ng of sgRNA in a final volume of 4µl of injection solution for at least 30min. We injected 4nl of injection solution each embryo at 1-2 cells stage on the animal pole (we also co-injected a tracer like mRNA for GFP or LacZ to a final concentration of 100ng in the 4µl of injection solution).

2.13.6 Genomic DNA extraction: We digested *Xenopus* tissue (usually 1 tadpole at stage 35) in 60µl of Lysis buffer at 56°C for 2h. We pipetted well up and down to help the lysis, then, we inactivated Proteinase K at 95°C for 15min. Sample was then centrifuged at 1,000g for 1min at RT and we collected the supernatant and quantified on the Nanodrop. After that, we either used it immediately for genotyping or stored at -20°C.

2.13.7 T7 endonuclease assay: Template gDNA was amplified using the specific primers (product size should be ~700nt and the region cleaved by the Cas9 should produce two different sized fragments). Final volume 20µl: 10µl Taq polymerase 2X, 1µl Fw primer (10µM), 1µl Rv primer (10µM), ~50ng gDNA, up to 20µl with nuclease free water.

Step	Cycle	Temperature	Time (min:sec)
1	1	95°C	05:00
2	40	95°C	00:30
		*	00:30
		72°C	**
3	1	72°C	07:00
4	1	10°C	∞

\* The annealing temperature of the specific pair of primers is set between 59°C and 61°C);

\*\* Taq polymerase can process ~1000bp/min, so the elongation time was calculated accordingly (usually the minimum is 1min, even if the fragment is smaller than 1000bp).

3-5µl of PCR product was loaded on 1-2% agarose gel to check the amplification.

“T7 endonuclease reaction on a final volume of 20µl: 2µl NEB buffer 10X, 3µl PCR product, 14µl Nuclease free water, 1µl T7 (10U) (to add after)”.

Step	Cycle	Temperature	Time (min:sec)
1	1	95°C	05:00
2	1	85°C	05:00
3	1	25°C	05:00
4	1	4°C	05:00
Add T7 endonuclease to sample			
5	1	37°C	15:00
		10°C	∞

We run the PCR product on a 1-2% agarose gel. If the Cas9 cleaved the DNA, on the gel will be visible both bands of the DNA. After validation by T7 endonuclease assay, sequencing of the PCR product was performed in order to identify the indel generated by the Cas9.

## 2.14 Figure making

Illustrations and diagrams shown in Chapter 1, Fig. 2, 6, 7 and Chapter 6, Fig. 3, were produced by using the online tool BioRender© (<https://www.biorender.com/>) .

For figures that were taken by other publications, the original publication has been referenced in the didascaly of the figure.

## 2.15 Statistical analysis

Each experiment, excluding *xtr-miR-10b* and *xtr-miR-218-2* knock-down, where performed at least in biological triplicate, and the female frogs used for the experiments produced a similar number of viable embryos, across experiments. The final number of embryos for each experimental group is indicated in each graph.

For assessing microphthalmia phenotypes, we measured the diameter of each eye of the same tadpole and, if the diameter of one of the eyes was <80% than the other, we considered it as positive to microphthalmia. For all the other phenotypes, we used a double blind approach, in which a colleague scored the presence or absence of a phenotype without knowing the name of the sample.

Statistically significant differences between groups have been assessed using t-test, which assesses the likelihood that an event occurs in two separate groups. In each graph, \* indicates  $p < 0.05$ , \*\* indicates  $p < 0.01$  and \*\*\* indicates  $p < 0.001$ .

## 2.16 Solutions

Bleaching solution: 0.5X SSC, 5% H<sub>2</sub>O<sub>2</sub>, 5% Formamide in dH<sub>2</sub>O.

BSA coating solution: 4% Bovine Serum Albumin in dH<sub>2</sub>O.

Cysteine: 2% L-Cysteine, pH 7.6 in 0.1X MMR (laevis) or 0.05X MMR (tropicalis).

DEPC-solutions: 200µl DEPC every litre of solution.

Ficoll: 3% Ficoll in 0.1X MMR (laevis) or 0.05X MMR (tropicalis).

Hybridisation buffer: 50% Formamide, 5X SSC, 1mg/ml Torula RNA, 100µg/ml Heparin, 1X Denharts, 0.1% Tween-20, 0.1% CHAPS, 5mM EDTA (pH 8.0) in dH<sub>2</sub>O.

LB – LB agar: 10g NaCl, 5g Yeast Extract, 10g Tryptone in 1l of dH<sub>2</sub>O (1.5% Agar for LB-Agar).

LB ampicillin – LB agar ampicillin: 1:1000 Ampicillin from the 50mg/ml stock solution in LB or LB-agar.

Lysis buffer: 50mM Tris HCl pH 8.5, 1mM EDTA (pH 8.0), 0.5% Tween-20, 100µg/ml Proteinase K-to add fresh every time in dH<sub>2</sub>O.

10X MAB: 1M Maleic Acid, 1.5M NaCl, 40g NaOH, pH 7.5 in dH<sub>2</sub>O.

10X MEM salts: 1M MOPS, 20mM EGTA (pH 8.0), 10mM MgSO<sub>4</sub>-H<sub>2</sub>O, pH 7.4 in dH<sub>2</sub>O.

MEMFA: 1X MEM salts, 3.7% formaldehyde in DEPC-H<sub>2</sub>O.

10X MMR: 1M NaCl, 20mM KCl, 10mM MgCl<sub>2</sub>, 20mM CaCl<sub>2</sub>, 50mM HEPES, pH 7.5 in dH<sub>2</sub>O.

Na-Azide solution: 1:1000 Na-Azide from the 20% w/v stock solution.

NTMT: 100mM Tris-HCl pH 9.5, 100mM NaCl, 50mM MgCl<sub>2</sub>, 1% Tween20 in dH<sub>2</sub>O.

PBS(T): 10 PBS tablets in 1l of dH<sub>2</sub>O (or DEPC-H<sub>2</sub>O), 0.1% Tween-20.

20X SSC: 3M NaCl, 0.3M Sodium Citrate, pH 7 in dH<sub>2</sub>O.

50X TAE: 2M Tris Base, 1M Glacial Acetic Acid, 50mM EDTA (pH 8.0) in dH<sub>2</sub>O.

Name	Sequence	NCBI Ref Number
M13 Fw	GTA AACGACGGCCAG	
M13 Rv	CAGGAAACAGCTATGAC	
Xtr.miR-10b Fw	GCTGACTTAAGGCGTTATGATGT	NR_049541.1
Xtr.miR-10b Rv	AGTGTCATGAAGCCCACCAG	
Xtr.miR-204 Fw	AGTGAAATTACGGCGCCAGT	NR_049693.1
Xtr.miR-204 Rv	TCGACGATGAGAGCAACCAC	
Xtr.miR-218-2 Fw	GAACAGATTGGCAGGTCTTGG	NR_049616.1
Xtr.miR-218-2 Rv	CTCCTTGGTCCTGGCTTCAA	
Xtr.miR-208 Fw	GCTTCCATTGAGCGAGAACCCT	NR_049695.1
Xtr.miR-208 Rv	GAGACTGACGCCATCCAAAGA	
Xtr.trpm1 Fw	TTAATGAACGCTCCCGTGCT	XM_031899154.1
Xtr.trpm1 Rv	TAGTTGCAAGCTCAGGGCTC	
Xtr.cox5a fw T7	TAATACGACTCACTATAGccgctttctagtcacctgc	NM_001017049.3
Xtr.cox5a rv SP6	ATTTAGGTGACACTATAGttcttctggggtggagatgc	
Xtr.ndrg3 fw T7	TAATACGACTCACTATAGgctcacagagataaagccgc	NM_001006793.1
Xtr.ndrg3 rv SP6	ATTTAGGTGACACTATAGgtgttgggtgggagtactgga	
Xtr.sox4 fw T7	TAATACGACTCACTATAGcccggaagaaggtaagctct	NM_001045619.2
Xtr.sox4 rv SP6	ATTTAGGTGACACTATAGatcatctcgctcacctcagg	
Xtr.tfap2a fw T7	TAATACGACTCACTATAGCCGCCCTACCAGCCAATATA	NM_001037258.1
Xtr.tfap2a rv SP6	ATTTAGGTGACACTATAGTTGTCCAGCTTCTCCCTCAG	
Xtr.tfap2b fw T7	TAATACGACTCACTATAGCTCTCATGTCAACGACCCCT	NM_001045644.1
Xtr.tfap2b rv SP6	ATTTAGGTGACACTATAGTTTTCCAGCCTCTCCCTCAG	
Xtr.tyr fw T7	TAATACGACTCACTATAGTCTGACCAGCTCTGCTACT	NM_001103048.1
Xtr.tyr rv SP6	ATTTAGGTGACACTATAGGGGCATCTCTCCAATCCCAG	
Xtr.tbx5 Fw T7	TAATACGACTCACTATAGAGATTGACTGAGCATTCCACAAGA	NM_001198768.1
Xtr.tbx5 Rv SP6	ATTTAGGTGACACTATAGTTACCCCATGCACAGAGTGG	
Xtr. Hmx1 Fw T7	TAATACGACTCACTATAGCCCAGAGATCGCAGAAGCAG	XM_002940218.3
Xtr. Hmx1 Rv SP6	ATTTAGGTGACACTATAGGACATGGGGCAAGTTGAAGC	
Xtr.Pax2.Fw.SP6	AAAATTTAGGTGACACTATAGTCCAAGCTTCCTGACTTGCC	NM_001044423.1
Xtr.Pax2.Rv.T7	AAATAATACGACTCACTATAGAACGCCTCGTAATCCTGACC	
Xtr.Vax2.SP6	AAAATTTAGGTGACACTATAGCAGCCACAGAACGAGTCAGA	XM_002938396.5
Xtr.Vax2.Rv.T7	AAATAATACGACTCACTATAGTGGTGAAGTGCTTCCCGATG	

**Table 2: List of primers.** List of primers that have been used in this project. The first column lists the name of primers (Xtr stands for *Xenopus tropicalis*). Some of the primers have been designed with a T7 or SP6 promoter sequence for a quicker synthesis of the WISH riboprobe.

## **Chapter 3: Identification and knock-down of micro RNAs potentially involved with neural crest development**

The initial aim of this project was to find miRNAs that are involved in the development of the NC of *Xenopus tropicalis*, and that could be of medical interest for the development or treatment of NCPs. Because of this, we used a combination of known literature and bioinformatical approaches to generate a list of miRNAs that can potentially be of medical interest.

In order to determine the effect of these miRNAs, we decided to use a knock-down/overexpression approach. To knock-down the expression of the miRNAs of interest, we used a double CRISPR/Cas9 strategy that consists in the complete removal of the miRNA gene from the genome of the injected *Xenopus* embryos. Since we carried out all the experiments in F0, the developing tadpoles will be mosaics, with some cells being wild type, some being heterozygous, and some other being fully knocked-out for the specific miRNA (Godden et al., 2022).

Also, in order to assess the specificity of the knock-down strategy, we need to establish a robust rescue experiment. To do so, we used synthetic miRNAs, called miRNA mimics, and injected them together with the solution used to knock-down the miRNAs of interest.

In this chapter, we will discuss the strategy that we developed to rescue the miRNAs knock-down in *Xenopus tropicalis*, how we generated the list of miRNAs that were selected as potentially interesting from a medical point of view and, finally, determine the phenotype caused by the knock-down of some of these miRNAs.

### **3.1 Rescue of the knock-down phenotypes by using miRNA mimics in *Xenopus tropicalis***

Once a CRISPR method for knocking down miRNAs in *Xenopus tropicalis* was obtained in our laboratory, the next step was to set up a method to rescue the observed phenotype. To do so, we decided to take advantage of synthetic miRNAs, called miRNA mimics (Qiagen), that were used as a tool to overexpress specific miRNAs. To determine

the efficacy of this approach, we decided to rescue the phenotype of a miRNA that has already been studied in our laboratory, *xtr-miR-219*.

MiR-219 is a family of miRNAs that include, in Homo sapiens, hsa-miR-219A-1 and hsa-miR-219A-2 while, in Xenopus tropicalis, only one member (*xtr-miR-219*) has been identified, so far.

From literature, it is known that miR-219 is expressed in the brain of adult mice (Kasai et al., 2016). However, it is also known from other model organisms that miR-219 is also important for the development of the neural tissue, in particular with respect to the differentiation of neural precursors into oligodendrocytes (Li et al., 2019a; Wu et al., 2017).

With respect to human disease, miR-219 has been associated with several types of tumours, however, the role that this miRNA plays in this context is cancer-specific, and it can act as an oncosuppressor in some types of cancers, and as an oncogene in other types, highlighting the importance of understanding this miRNA biology in depth and in different environments (Xing et al., 2018; Yang et al., 2018).

### 3.1.1 Assessment of the overexpression of miR-219 phenotype

Once the phenotype produced by the knock-down of *xtr-miR-219* was confirmed by a previous PhD student (Godden et al., 2022), the next step was to identify the phenotype produced by the overexpression of this miRNA. To determine it, we microinjected three groups of embryos at stage NF2, one with Cas9 on its own, one with a control mimic (*cel-miR-39-3p*), which should not affect the development of the embryo, and one with *xtr-miR-219-5p* (Fig. 8).

A total of 65 embryos were injected for the Cas9 group, and 6% of them produced a visible craniofacial phenotype. Of the 72 embryos injected for the control miRNA mimic, 10% produced a craniofacial phenotype, and no statistically significant difference was observed between these two groups, as shown by chi-squared statistical analysis. On the other hand, of the 76 embryos that were injected with *xtr-miR-219-5p* mimic, more than 20% of them produced an appreciable craniofacial phenotype. Compared to the

control mimic group, this difference was statistically significant after chi-squared analysis ( $p=0.00041$ ) (Fig. 8).

The observation that the overexpression of *xtr-miR-219-5p* produces craniofacial phenotypes, in a similar way to the knock-down of the endogenous miRNA, was not surprising. In fact, it is reasonable to speculate that, since miRNAs are fine posttranscriptional regulators of gene expression, their overexpression might cause an excessive downregulation of their target genes. This might produce the same final phenotype of the knock-down, as the genes that will be directly involved will be the same.

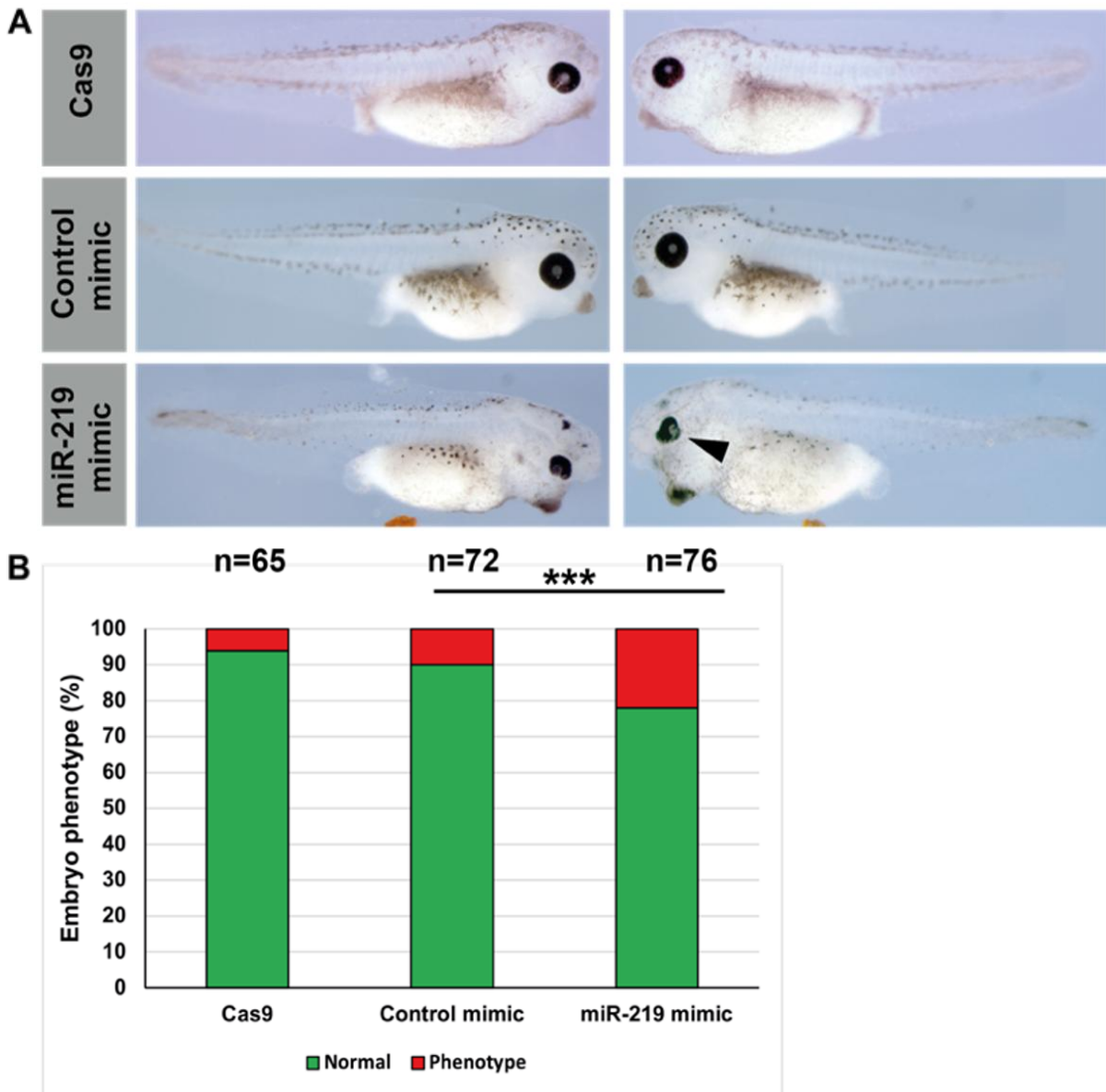


**Fig. 8: The overexpression of *xtr-miR-219-5p* in *Xenopus tropicalis* embryos produces craniofacial defects. A)** To determine the effect of the overexpression of *xtr-miR-219-5p*, three groups of embryos were injected. One group was only injected with Cas9, one with a control miRNA mimic (*cel-miR-39-3p*), and one with the actual *xtr-miR-219-5p* mimic. On the left, there is the non-injected side of the embryos, and on the right the injected side. The side of the injection was determined according to GFP expression. As indicated by the black arrowhead, the overexpression of *xtr-miR-219-5p* produced a characteristic craniofacial phenotype. **B)** Quantification of the craniofacial phenotype of the injected tadpoles. No difference was observed between Cas9 and control mimic groups, while a significant ( $p=0.00041$ ) difference was observed between control mimic and miR-219 mimic groups.

### 3.1.2 Rescue of the knock-down phenotype of *miR-219*

Next, the actual rescue experiment was performed to assess the recovery of the phenotype when *xtr-miR-219* is knocked-down. To do so, four groups of embryos were microinjected in 1 blastomere of a stage NF2 embryo. The first group injected was the control (injected with Cas9 and control mimic). The second group was an internal control to show that the knock-down of *xtr-miR-219* worked properly during the experiment. The third group was the control of the rescue experiment, in which the endogenous loss of *xtr-miR-219* was rescued by the control mimic (*cel-miR-39-3p*). The last group was the proper rescue, in which the endogenous *xtr-miR-219* was knocked-down, and the synthetic *xtr-miR-219-5p* mimic was introduced to rescue that loss. As shown in Fig. 9, the loss of endogenous *xtr-miR-219* produced craniofacial phenotypes ( $p=0.0008$ ), when compared to the control group.

Interestingly, while the control mimic on its own did not produce any appreciable phenotype (Fig. 8), its co-injection with the gRNAs and Cas9 to knock-down the endogenous *xtr-miR-219* had an additive effect on the number of tadpoles displaying craniofacial defects. A possible reason for this might be because the excess of exogenous RNA (gRNAs, control mimic and *Gfp* mRNA) might induce RNA toxicity in the developing embryo. Another possible explanation might be due to the fact that the excess of RNA could interfere with the endogenous processes of DNA damage repair, making the CRISPR-editing more efficient. Of course, a combination of both could explain the result as well. When we analysed the number of tadpoles that displayed a craniofacial phenotype in the rescue group, we noticed that this number was significantly reduced ( $p=0.001$ ) in comparison to the group of embryos injected with *xtr-miR-219* gRNAs and *xtr-miR-219-5p* mimic. This result indicated that, in *Xenopus tropicalis*, it is possible to produce miRNA knock-down using CRISPR-Cas9 genome editing, and that it is possible to rescue this knock-down by introducing that synthetic miRNA.

Also, this experiment showed that it is possible to increase the effect of a CRISPR-induced knock-down by co-injecting a miRNA mimic that, on its own, does not produce any visible phenotype. However, for the aim of this project, this effect was not further investigated.

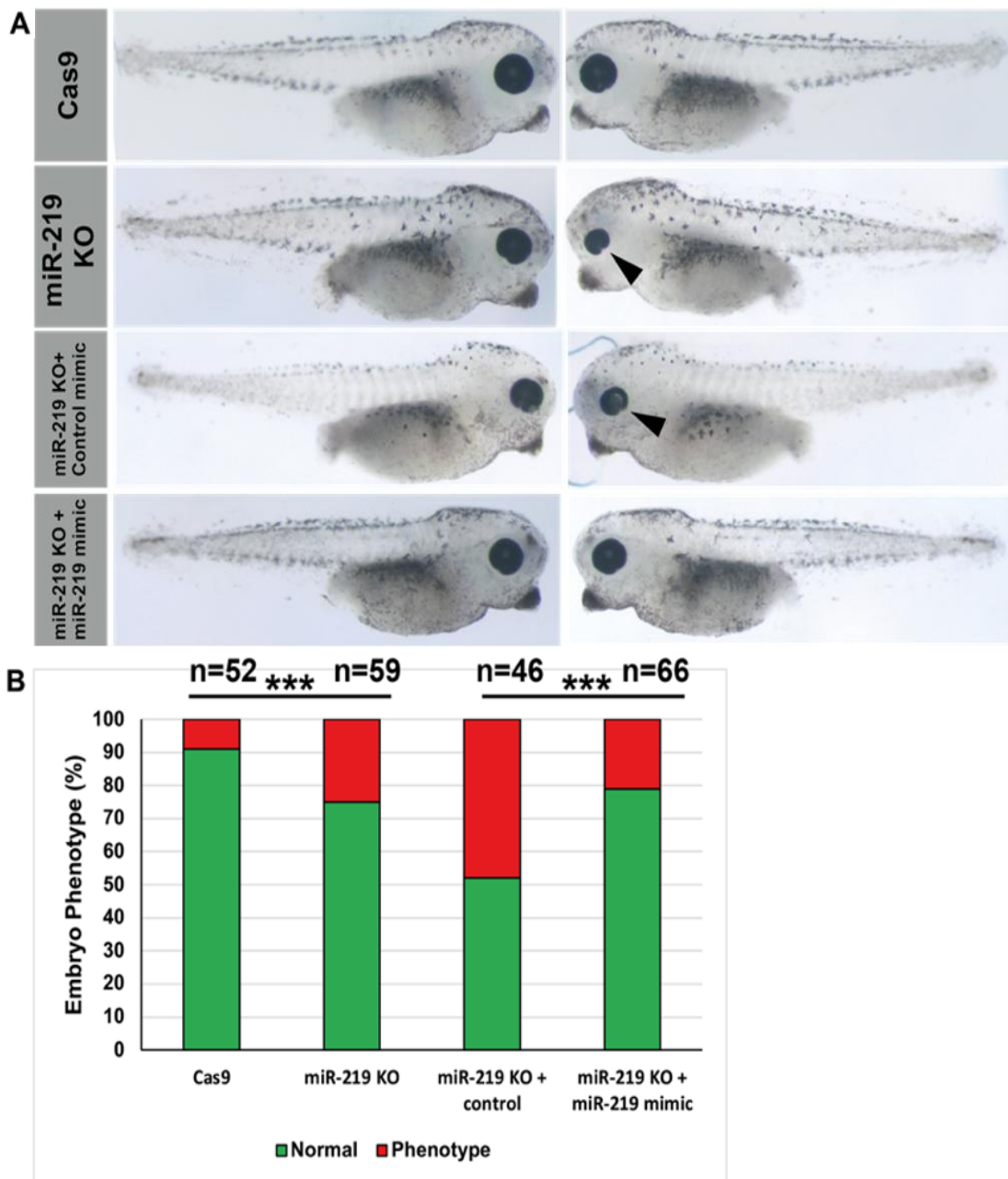


**Fig. 9: The loss of endogenous *xtr-miR-219* can be rescued by introducing a synthetic *xtr-miR-219-5p*. **A)** On the left side, the non-injected side of the tadpole, and on the right side, the injected side. As shown by the black arrowheads, knock-down of *xtr-miR-219* produces craniofacial phenotypes in both miR-219 knock-down ( $p=0.0008$  in comparison to Cas9 group) and miR-219 knock-down together with control mimic. This phenotype was rescued if, instead of the control mimic, the embryos were injected with *xtr-miR-219-5p* mimic ( $p=0.001$ ). **B)** Quantification of the rescue experiment, shown as a percentage of tadpoles displaying craniofacial defects.**

### **3.2 Bioinformatical analysis to discover new miRNAs involved in NC development and NCPs**

As part of the project, we wanted to identify novel miRNAs involved in *Xenopus*' NC development. To do so, we used different in-silico approaches (in section 3.2.1) and an extensive literature analysis.

An important point that we kept in consideration while searching for candidate miRNAs, was the conservation among species and, in particular, conservation between *Xenopus* and *Homo sapiens*. This was particularly important because of the nature of the NEUcrest project, which is aimed at the study of NC development (see section 1.3). The aim of the NEUcrest is, in fact, to provide clinicians with better tools to investigate neurocristopathies, and the people affected by such conditions with better care.

#### 3.2.1 In-silico approaches to predict important miRNAs involved in NC development

The first approach undertaken to identify new miRNAs that might play a role in NC development, was to search in a database that was previously generated in the Wheeler laboratory by Dr Nicole Ward (Ward et al., 2018). In summary, she took advantage of a *Xenopus laevis* organoid model, called animal cap, that she induced to become neural, NC, or undifferentiated tissue. She then collected the total small RNAs in these samples and carried out small RNA sequencing. She then carried out a comparative analysis to identify those miRNAs that were enriched in the NC-induced animal cap samples. The main two enriched miRNAs were *xla-miR-219* and *xla-miR-196a*, which were then further investigated in our laboratory (Godden et al., 2022). Other miRNAs identified included *xla-miR-nov-12a-1*, *xla-miR-338-3*, *xla-miR-218-2*, *xla-miR-10b*, *xla-miR-204a*, *xla-miR-130b/c*, *xla-miR-23* and *xla-miR-24*.

After a conservation analysis, we found that *xla-miR-nov-12a-1* was not conserved in human, and only partially conserved in *Xenopus tropicalis*, therefore it was discarded from the list of possible miRNAs to further investigate (Fig. 10).

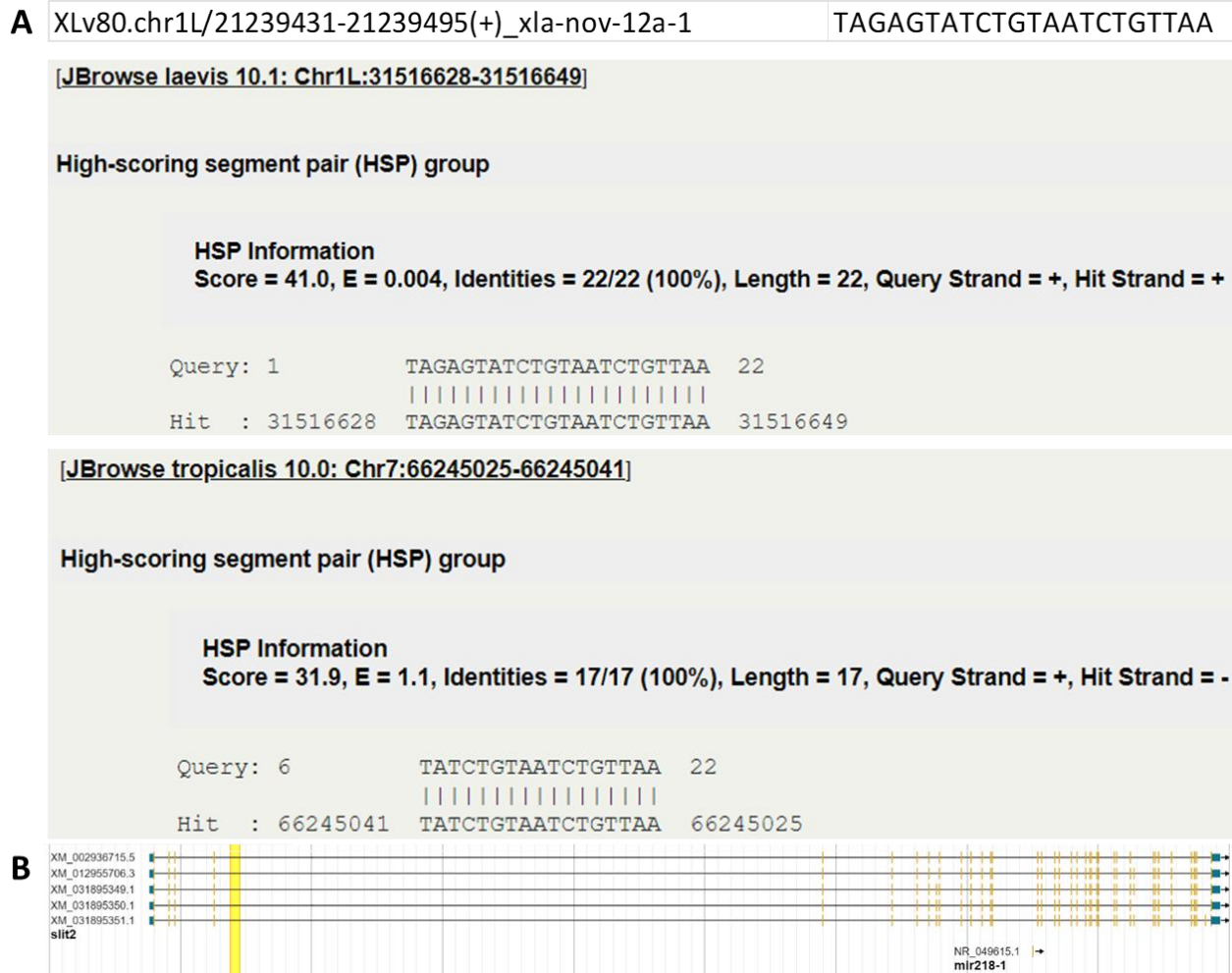


**Fig. 10: Conservation of *sla-nov-12a-1* between *Xenopus laevis* and *Xenopus tropicalis*.** **A)** On top, there is the name and genomic locus (*Xenopus laevis* V9.1) of the novel miRNA *sla-nov-12a-1* and its cDNA as sequenced from the short RNA sequencing performed by Dr Nicole Ward (Ward et al., 2018). When blasted on *Xenopus laevis* genome (V.10.1), we obtain a match on a different genomic locus on the same chromosome (from Chr1L:21239431-21239495 to Chr1L:31516628-31516649), which might be due to slight variations between different genome versions. If blasted on *Xenopus tropicalis* genome, we can only find a match by reducing the e-value to the minimum, since the first match misses six of the twenty-two nucleotides of *sla-nov-12a-1*. This indicates that this miRNA is not conserved in *Xenopus sp.* **B)** In *Xenopus laevis*, *sla-nov-12a-1* is a mirtron of the gene *slit2*, which also hosts *sla-miR-218-1*.

It is important to note that even if *Xenopus* induced-animal caps experiments are well-established models in the field of developmental biology, they might not be completely physiological. In fact, the induction of the specific tissue is induced by overexpression of different concentrations of Wnt and Noggin. This will result in neural and NC-like tissues. They will express some of the markers for the specific tissues, but it will not necessarily recapitulate the exact chromatin landscape, transcriptome, and proteome of the in-vivo tissue. Therefore, other approaches were needed to identify other miRNAs or to confirm this small RNA sequence data.

There are several online free-to-use tools to identify potential targets of specific miRNAs. These tools, such as TargetScan8.0 ([https://www.targetscan.org/vert\\_80/](https://www.targetscan.org/vert_80/)), DIANA (<http://diana.imis.athena-innovation.gr/DianaTools/index.php>), or miRDB (<http://www.mirdb.org/>), use algorithms that identify, within the 3' UTR of the transcriptome of a specific species, potential binding sites for the specific miRNA.

These websites are of incredible use to scientists interested in miRNA biology, as they provide quick lists of genes that might be post-transcriptionally regulated by miRNAs. Most of these tools, however, do not take into account the spatial-temporal localization of the miRNA and the mRNA, as they might not be expressed at the same time, or even in the same cell type. Given this, it is not surprising that the output of these kind of tools include a large number of false-positive targets. In fact, lists of predicted targets of one miRNA can range from few hundreds (f.e. 449 predicted targets of *hsa-miR-219-5p* in human using TargetScan8.0) to several thousands of them (f.e. 1207 predicted targets of *hsa-miR-let-7c-5p* in human using TargetScan8.0)(Fig. 11). Importantly, for all the bioinformatical analysis that we carried out during this project, we decided to use *Homo sapiens* RNA ref seq. The reason of it is because the 3' UTR of *Xenopus*' genes are not particularly well-annotated.

**Human | miR-219-5p**

449 transcripts with conserved sites, containing a total of 479 conserved sites and 97 poorly conserved sites.

Please note that these predicted targets include some false positives. [\[Read more\]](#)

Genes with only poorly conserved sites are not shown. [\[View top predicted targets, irrespective of site conservation\]](#)

Table sorted by cumulative weighted context++ score [\[Sort table by predicted occupancy\]](#) [\[Sort table by aggregate P<sub>CT</sub>\]](#)

The table shows at most one transcript per gene, selected for being the most prevalent, based on 3P-seq tags. [\[Download table\]](#)

Target gene	Representative transcript	Gene name	Number of 3P-seq tags supporting UTR + 5	Link to sites in UTRs	Conserved sites				Poorly conserved sites				6mer sites	Representative miRNA	Predicted occupancy		
					total	8mer	7mer-m8	7mer-A1	total	8mer	7mer-m8	7mer-A1			mod miRNA	high miRNA	transfected miRNA
ZBTB18	0358704.4	zinc finger and BTB domain containing 18	935	Sites in UTR	2	2	0	0	0	0	0	0	0	hsa-miR-219a-5p	0.1546	0.7612	1.6337
RORB	0376896.3	RAR-related orphan receptor B	5	Sites in UTR	3	3	0	0	2	0	0	2	3	hsa-miR-219a-5p	0.2811	1.3029	3.1062
GXYLT1	0398675.3	glucoside xylosyltransferase 1	126	Sites in UTR	2	1	1	0	2	0	0	2	0	hsa-miR-219a-5p	0.2181	0.9643	2.1910

**Human | let-7-5p/miR-98-5p**

1207 transcripts with conserved sites, containing a total of 1386 conserved sites and 243 poorly conserved sites.

Please note that these predicted targets include some false positives. [\[Read more\]](#)

Genes with only poorly conserved sites are not shown. [\[View top predicted targets, irrespective of site conservation\]](#)

Table sorted by cumulative weighted context++ score [\[Sort table by predicted occupancy\]](#) [\[Sort table by aggregate P<sub>CT</sub>\]](#)

The table shows at most one transcript per gene, selected for being the most prevalent, based on 3P-seq tags. [\[Download table\]](#)

Target gene	Representative transcript	Gene name	Number of 3P-seq tags supporting UTR + 5	Link to sites in UTRs	Conserved sites				Poorly conserved sites				6mer sites	Representative miRNA	Predicted occupancy		
					total	8mer	7mer-m8	7mer-A1	total	8mer	7mer-m8	7mer-A1			mod miRNA	high miRNA	transfected miRNA
HMGA2	0403681.2	high mobility group AT-hook 2	8021	Sites in UTR	7	1	3	3	0	0	0	0	1	hsa-let-7d-5p	0.5314	2.4035	5.4009
ARID3B	0346246.5	AT rich interactive domain 3B (BRIGHT-like)	11	Sites in UTR	5	0	1	4	0	0	0	0	0	hsa-let-7d-5p	0.2676	1.4166	3.9617
LIN28B	0345080.4	lin-28 homolog B (C. elegans)	118	Sites in UTR	4	2	2	0	1	0	0	1	0	hsa-let-7d-5p	0.3064	1.5398	3.8461

**Fig. 11: Example of the output generated by TargetScan8.0 using two highly conserved miRNAs among vertebrates. A) Number of predicted targets of *hsa-miR-219-5p* and B) *hsa-let-7-5p*, two highly conserved miRNAs among vertebrates. *Hsa-miR-219-5p* has 449 predicted targets, almost one third of *hsa-let-7-5p*, which has 1207 predicted targets. These data show the variability in the number of possible targets that different miRNAs can have.**

### 3.2.2 Strategy to predict miRNAs involved in the etiopathogenesis of craniosynostosis

Craniosynostosis is the most common physical malformation in a child. This condition occurs when two or more of the cranial bones fuse together too early during development. This will result in craniofacial malformations, which can be only partially solved by invasive surgery. Typically, these operations have to be repeated periodically during the life of the person affected by it, as they are only rarely resolutive. Moreover, if not treated in time, craniosynostosis can cause intellectual disability, since the premature closure of the skull sutures can interfere with the proper growth of the brain (Fig. 12).

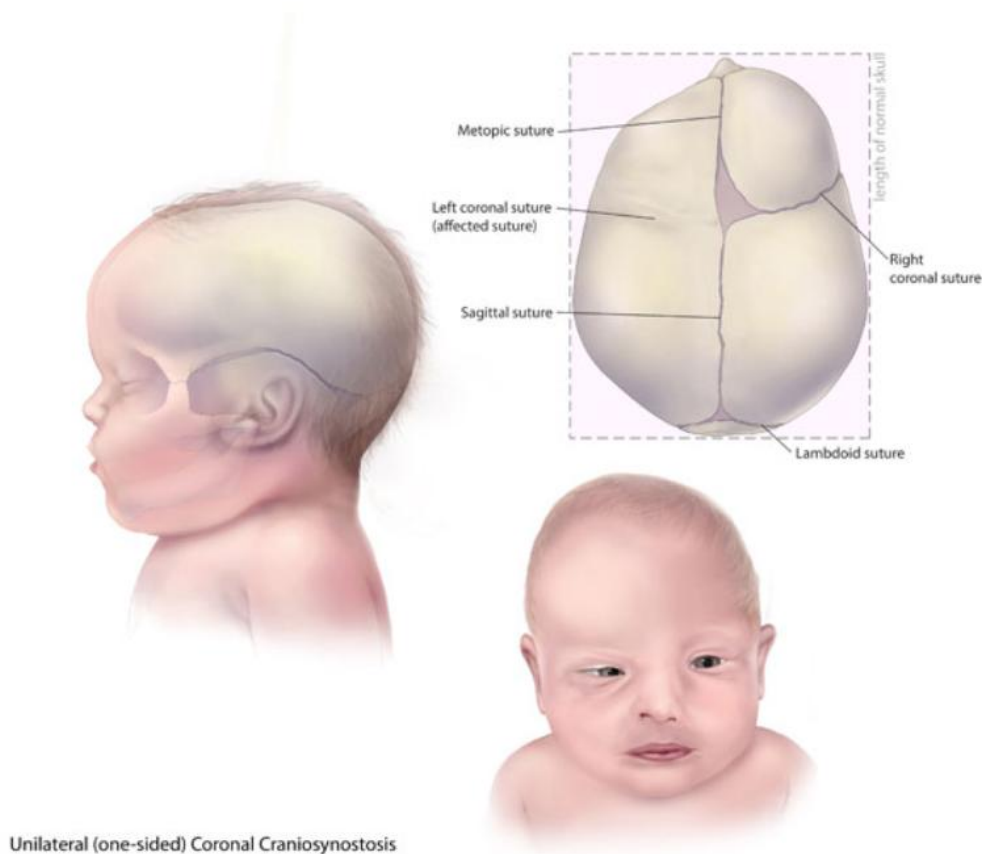


**Fig. 12: Unilateral coronal craniosynostosis.** Representation of unilateral coronal Craniosynostosis. In this specific case of craniosynostosis, the parietal and frontal bones of the skull fuse too early. This will cause craniofacial defects, if not surgically treated on time.

One of the reasons why craniosynostosis occurs is due to defects during NC development since this population of cells will give rise to the craniofacial skeleton and cartilages (Goos and Mathijssen, 2019).

To identify potential miRNAs involved in craniosynostosis, we used a list of 309 genes that have already been associated with this particular condition. This list of genes was kindly provided by Ana Filipa Duarte (Erasmus Medical Centre, Rotterdam, Han van Neck and Irene Mathijssen laboratory) and, to date, it has not been published.

The idea of this analysis was to find miRNAs whose binding sites are enriched in this pool of 309 genes. For example, if a miRNA is predicted to target 10% of the genes in the genome, then it is expected to be targeting 10% of the genes that are presumably involved in craniosynostosis. If, however, the miRNA is involved in craniosynostosis, this number would appear to be higher than that. To assess that this statistical analysis is correct, the results were compared to a pool of control miRNAs that are involved in other biological processes and that are not involved with NC development. For this control, nine miRNAs were selected, that are known to be involved in muscle, liver or lung development. These miRNAs are: *hsa-miR-486-5p*, *hsa-miR-1-5p*, *hsa-miR-155-5p*, *hsa-miR-199-5p*, *hsa-miR-122-5p*, *hsa-miR-15-5p*, *hsa-miR-133-3p.1*, *hsa-miR-29a-5p* and *hsa-miR-200ab-5p*.

The percentage of predicted targets of a specific miRNA in comparison to the number of genes in the genome was calculated using the formula:  $Nt/Ng \times 100$ , where  $Nt$  is the number of predicted targets, and  $Ng$  is the number of genes in the genome (this number is variable according to the different definitions that we can give to a gene, in this case, we used 25.000 genes in the human genome).

Then, the same was done for the genes associated with craniosynostosis (in this case,  $Ng=309$ ). This gave us two values: WG (%) (percentage of genes in the whole genome) and CA (%) (percentage of craniosynostosis-associated genes).

Next, we calculated the ratio between the percentage of genes that are predicted to be targeted by a miRNA in the whole genome and the percentage of genes that are predicted to be targeted by that same miRNA, but in the list of genes involved in craniosynostosis. To calculate this, we used the formula:  $CA (\%)/WG (\%)$ . This calculation gave us the

normalised values that we used to do the statistics downstream, which we called Fold Increase (FI).

The first result was that 105 miRNAs conserved among vertebrates had at least one predicted binding site for at least one of these genes associated with craniosynostosis. For each of these miRNAs, we calculated the FI. Then we calculated the mean value and the standard deviation of the FI, which accounted to Mean value=3.50, St. Dev=1.98 (Fig. 13).

In order to shortlist these miRNAs, we had to set a cut-off that was equal to the mean FI +  $\frac{1}{2}$  St. Dev, which gave us a value of 4.49. All those miRNAs whose FI was higher than that value, were considered of interest for NC development and, some of them, further investigated (Fig. 14).

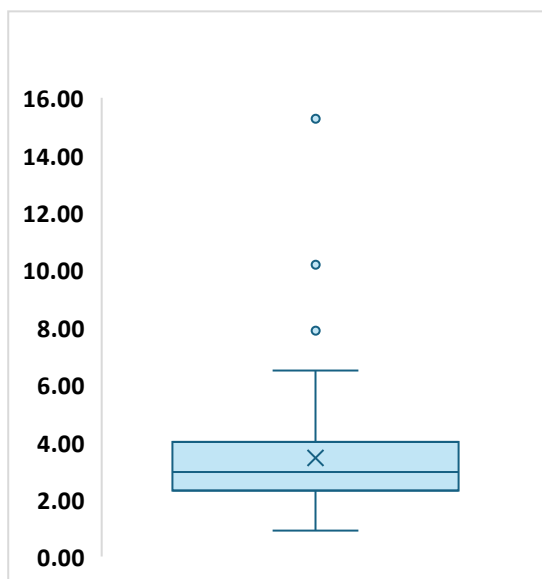


**Fig. 13: Distribution of miRNAs fold increase.** Box and whiskers graph representing the distribution of the Fold Increase values (FI) for the 105 miRNAs conserved among vertebrates that were predicted to bind at least one of the craniosynostosis-associated genes. Mean=3.50; St. dev.=1.98.

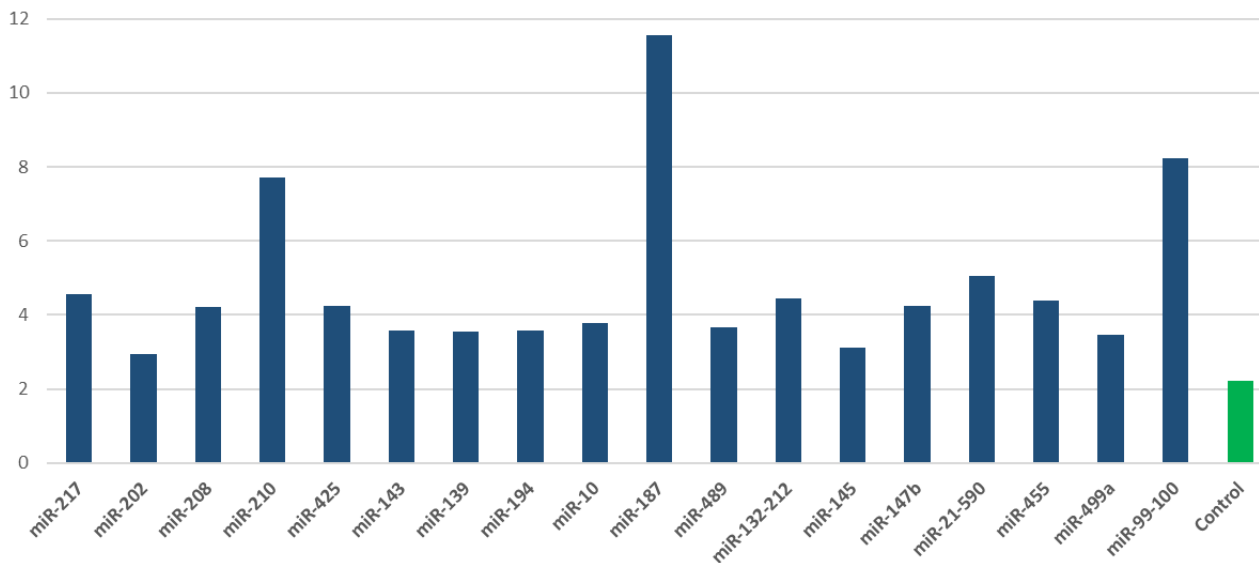


**Fig. 14: MiRNAs with fold increase significantly higher than control.** On the X axes, all the miRNAs with a fold increase higher than the control one, plus  $\frac{1}{2}$  of its standard deviation. On the Y axes, the fold increase of each of these miRNAs. In green, the mean value of the fold increase for nine miRNAs that are not involved in NC and craniofacial development.

### 3.3 gRNAs testing and first screening of the knock-down phenotype

#### 3.1.1 guide RNA design strategy and targets

Short gRNAs were designed to target *xtr-miR-10b*, *xtr-miR-15a-16a*, *xtr-miR-17~92*, *xtr-miR-30a*, *xtr-miR-99*, *xtr-miR-100*, *xtr-miR-132-212*, *xtr-miR-145*, *xtr-miR-187*, *xtr-miR-194-1*, *xtr-miR-200b*, *xtr-miR-204-1*, *xtr-miR-204-2*, *xtr-miR-208*, *xtr-miR-210*, *xtr-miR-218-2*, *xtr-miR-455*, and *xtr-miR-489* (Table 3). In particular, we designed four gRNAs for each miRNA (two gRNAs targeting upstream of the miRNA gene, and two gRNAs targeting downstream of the miRNA gene, which we called Fw1, Fw2, Rv1 and Rv2). The only exception was done for *xtr-miR-204-1*, for which we could only design one gRNA upstream of the gene, because of the intronic nature of this miRNA. In fact, *xtr-miR-204-1*, is located inside an intron of *trpm1* gene, in the proximity of the upstream exon. In order to avoid mutations in the coding region of *trpm1*, we decided to not design gRNAs closer than ~50nt to any coding sequences, which reduced the number of gRNAs that we could use for our purpose (Fig. 15). To knock down the expression of our targeted miRNA, we injected all the possible combinations of gRNAs (usually four combinations in total, Fw1/Rv1, Fw1/Rv2, Fw2/Rv1 and Fw2/Rv2)(Fig. 15).

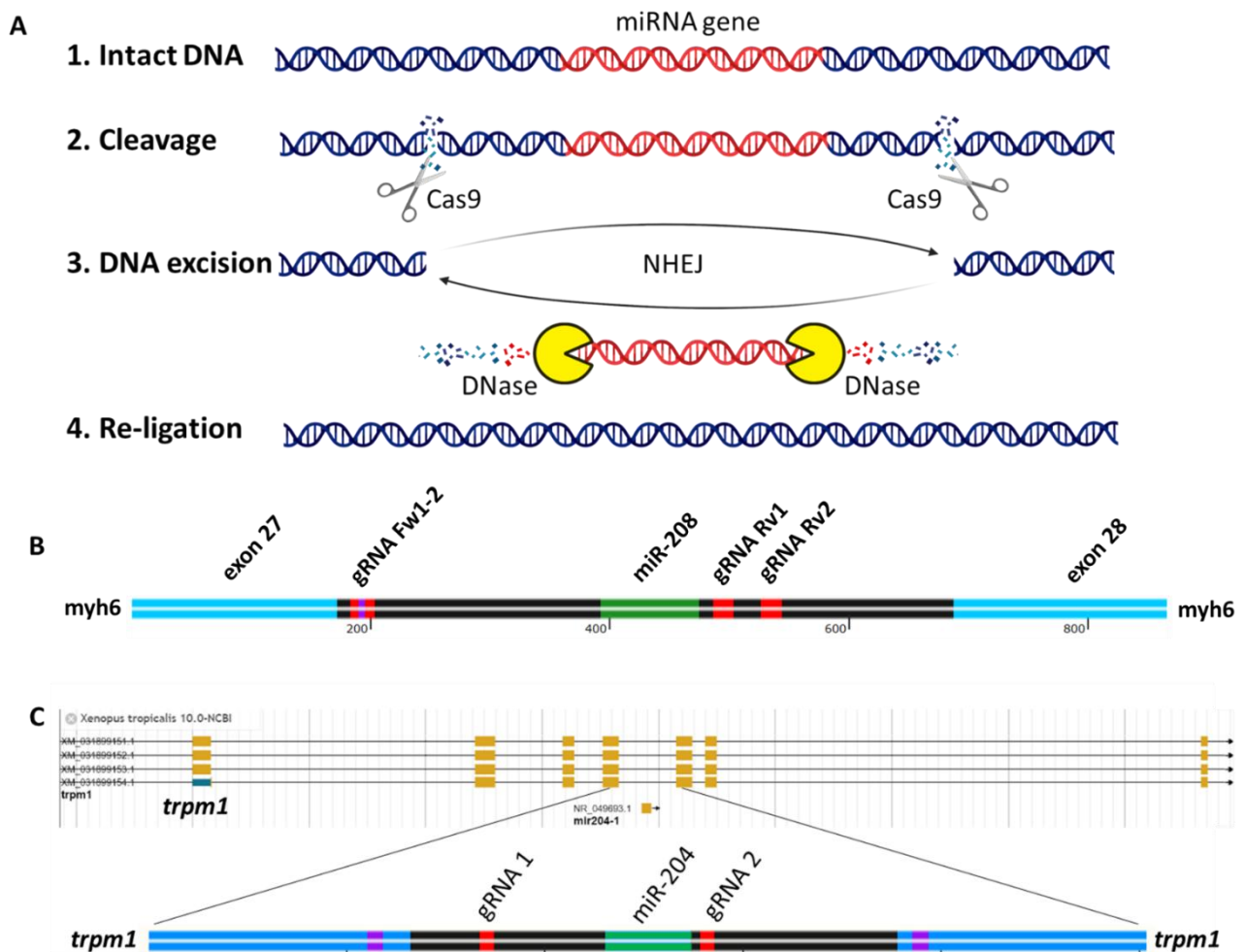


**Fig. 15: MiRNA knock-down strategy. A)** To knock-down miRNAs in *Xenopus tropicalis* embryos, we use the double gRNAs CRISPR-Cas9 approach shown here. In red, on the DNA filament, there is the representation of the target miRNA gene (1). We target the DNA upstream and downstream of the miRNA gene using the Cas9 conjugated with two different gRNAs and injecting it at the same time (2). If the cleavage of the DNA operated by the Cas9 protein occurs at the same time, there is the possibility that the whole locus between the two double strand break is excised from the genome. For this to occur, the cell has to repair the DNA damage by non-homologous end-joining (3). At the end of the DNA damage repair process, the two broken ends are re-ligated together and the DNA locus that contains the miRNA gene will be degraded by DNases (4). **B)** Schematic representation of *Xenopus tropicalis myh6* gene, magnified on the intron that contains *xtr-miR-208*. In light blue, there are the exons of *myh6*; in green, *xtr-miR-208*; in black the intron where *xtr-miR-208* is located; in red the region of the DNA that is targeted by the gRNAs; in purple there is a partial overlap between gRNA Fw1 and gRNA Fw2 binding site. **C)** Screenshot of *Xenopus tropicalis* genome browser (V10.0) that highlights *trpm1* gene (top). On the bottom, a magnification of the intron that contains *xtr-miR-204-1*. In blue, the exons of *trpm1*; in green, *xtr-miR-204-1* gene; in red, the binding sites of the gRNAs that have been used for the experiments; and in purple the region bound by the primers used for genotyping.

### 3.3.2 *miR-218-2*

Mir-218-2 is one of the miRNAs that was selected from the small RNA sequencing experiment (Ward et al., 2018) (Fig. 16). This miRNA belongs to the miR-218 family, which includes *miR-218-1* and *miR-218-2*. Both these miRNAs belong to the class of mirtrons (see: “1.1.3 From primary transcripts to mature miRNA”), and are localised inside of introns of *slit2* and *slit3* genes, respectively. The slit genes (*slit1*, *slit2* and *slit3*) act in the SLIT/ROBO pathway, which has historically been associated to the axon guidance and neural development (Rothberg et al., 1988). More recently, this pathway has also been associated with other organ development, such as the kidney and the heart (Fan et al., 2012; Medioni et al., 2010). Mir-218 family’s expression has been associated with neuropsychiatric disorders and with depression/anxiety (Schell et al., 2022). The fact that this miRNA family has never been associated with NC development, but was highly upregulated in NC-induced *Xenopus*’ animal caps, made it an excellent candidate for further investigation.

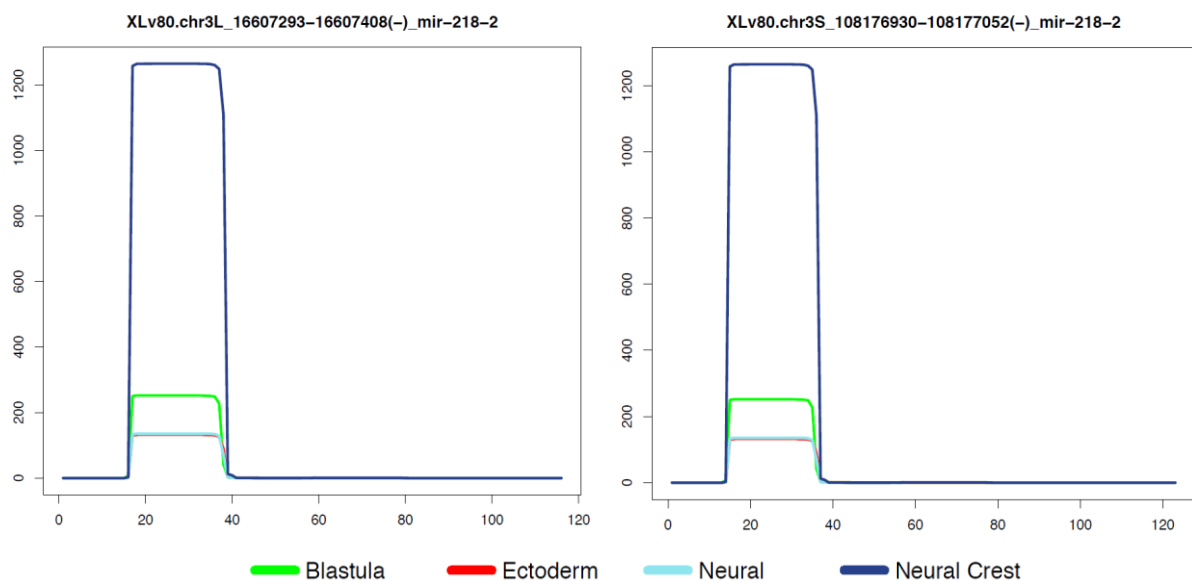


**Fig. 16: Specificity of *xtr-miR-218-2* in NC-induced *Xenopus*’ animal caps.** Modified from Ward et al (2018). Number of reads of *miR-218-2* (from S and L chromosomes) in *Xenopus*’ animal caps induced to become Neural (light blue) or NC (dark blue), or from blastula (green) and ectoderm (red). The graph indicates that both S and L isoforms of *miR-218-2* are specifically upregulated in the NC sample.

To knock-down *xtr-miR-218-2*, all the possible combinations of gRNAs were injected in one blastomere of a NF2 stage *Xenopus tropicalis* embryo, and then we observed the phenotype. The gRNAs were named “Fw” and “Rv” to indicate the gRNAs targeting the genomic region upstream the miRNA gene (Fw) and downstream the miRNA gene (Rv). Having two gRNAs upstream and two downstream of the miRNA gene, the possible combinations to inject are four in total (Fw1/Rv1, Fw2/Rv1, Fw1/Rv2 and Fw2/Rv2) (Fig. 15B).

Following knock-down of *xtr-miR-218-2*, the only observed phenotypes were different degrees of edema. This phenotype was only present in those tadpoles that were injected with the gRNA Rv2 (Fig. 17).

Edema is a condition in which the organism cannot properly balance the level of body fluids, therefore the swelling of the affected area. In vertebrates, this homeostasis is orchestrated by the kidneys, but these problems might arise also due to failure in heart or vasculature development. Both these tissues are of mesodermal origin. For this reason, edema is a phenotype that is usually not associated with defects of NC development (Rehman and Ahmed, 2023).

Since the only observed phenotype was not related to NC development for all the gRNAs combinations, we decided to not further characterise the knock-down animals, and to continue searching for candidate miRNAs.

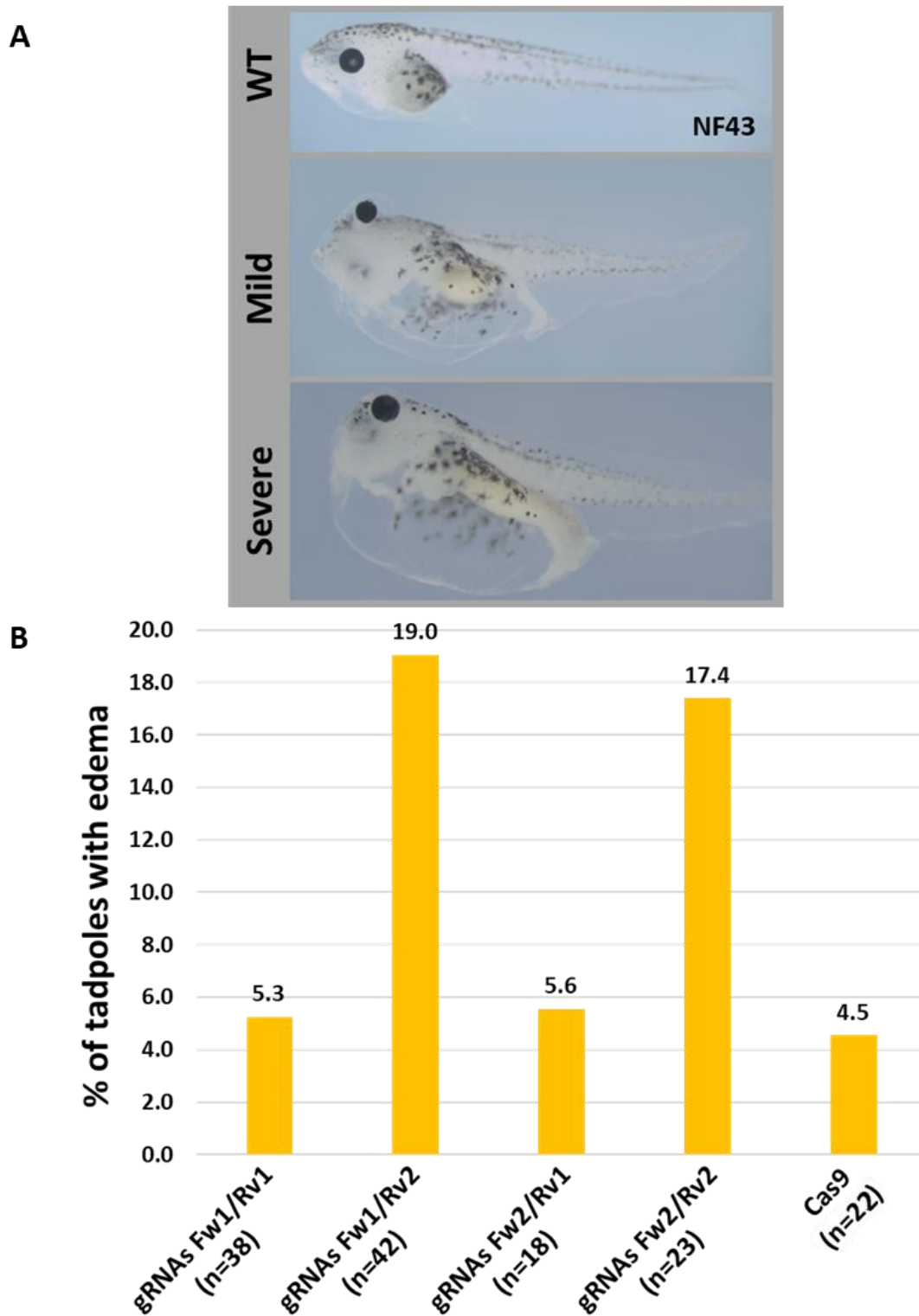


**Fig. 17: *Xtr-miR-218-2* knock-down.** **A)** Representative images showing edema following injection of the gRNAs to knock-down *xtr-miR-218-2* and **B)** quantification. Statistical analysis could not be performed due to low experimental numbers. Embryos were injected in one blastomere of a NF2 stage embryos. Embryos injected without using any gRNA (Cas9 group) were used as a control.

### 3.3.3 *miR-10b*

*Xtr-miR-10b* was selected as a possible candidate for two reasons: firstly, it was one of the miRNAs specifically expressed in the *Xenopus*' animal cap induced NC (Ward et al., 2018) (Fig. 11); secondly, it is one of the miRNAs that was flagged from the bioinformatical analysis carried out using the genes that are associated with the aetiopathogenesis of craniosynostosis (Fig. 7).

*Mir-10b* belongs to a conserved miRNA family that includes, in human, two members: *hsa-miR-10a* and *hsa-miR-10b*. In frog, there is also a third member, *xtr-miR-10c*. These miRNAs are all localised within the HOX genes clusters, in particular, *hsa-miR-10b* gene is localised upstream the *HOXD4* locus (approximately 1200bp upstream the beginning of the coding sequence of *HOXD4*).

*Mir-10b* has been shown to negatively regulate the expression of different HOX genes, including *HOXB3A* and *HOXD10A* (Giusti et al., 2016). So far, *hsa-miR-10b* has been mainly associated with cancer progression, and not many studies were conducted on this miRNA in the context of developmental biology, which made it a good candidate for further investigation in *Xenopus* (Biagioni et al., 2013; Sheedy and Medarova, 2018).

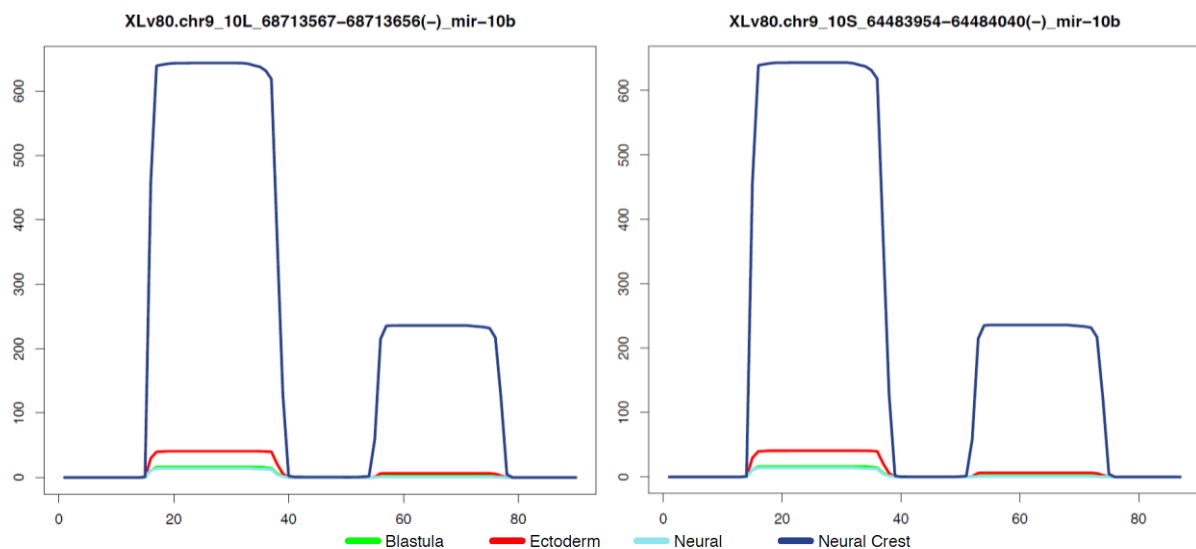


**Fig. 18: Specificity of *xtr-miR-10b* in NC-induced *Xenopus*' animal caps.** Modified from Ward et al (2018). Number of reads of *miR-10b* (from S and L chromosome) in *Xenopus*' animal caps induced to become Neural (light blue) or NC (dark blue), or from blastula (green) and ectoderm (red). The graph indicates that both S and L isoforms of *miR-10b* are specifically upregulated in the NC sample.

Also for *xtr-miR-10b*, all the combinations of gRNAs were injected at 2-cell stage of *Xenopus tropicalis*, and then observed the phenotype, for a total of four different combinations (Fig. 15B, Table 3).

Following knock-down of *xtr-miR-10b*, we observed two separate phenotypes using all combinations of gRNAs, apart from the combination “Fw1/Rv2”. The phenotypes include a characteristic craniofacial malformation (“flat” head), and defects during melanocyte development (melanocytes were rounded and/or lower in number)(Fig. 19A, B).

Since chondrocytes and melanocytes are both NC derivatives, craniofacial malformations and pigmentation defects both strongly suggest problems during NC development.

Unfortunately, while these experiments were performed, a new version of *Xenopus tropicalis* genome was released (V10.0). In this version, *xtr-miR-10b* got incorporated into the 5'UTR of *hoxd4*. This change implicates that the deletion of the miRNA locus affects the entire 5'UTR of *hoxd4* gene, resulting in the impossibility of knowing if the observed phenotype was caused by the loss of *xtr-miR-10b* or by the loss of *hoxd4* 5'UTR (Fig. 19C).

Because of this, the dual CRISPR-Cas9 approach to excise the miRNA locus, was not suitable for *xtr-miR-10b*, and the effect of this miRNA during NC development was no longer investigated. However, more investigations on this miRNA using different type of tools, such as morpholinos, as well as using rescue experiments with miRNA mimics and, potentially, generating stable genetically modified *Xenopus tropicalis* lines that carry point mutations within the seed sequence of *xtr-miR-10b* might help in the understanding the biology of this gene in the context of *Xenopus* development.

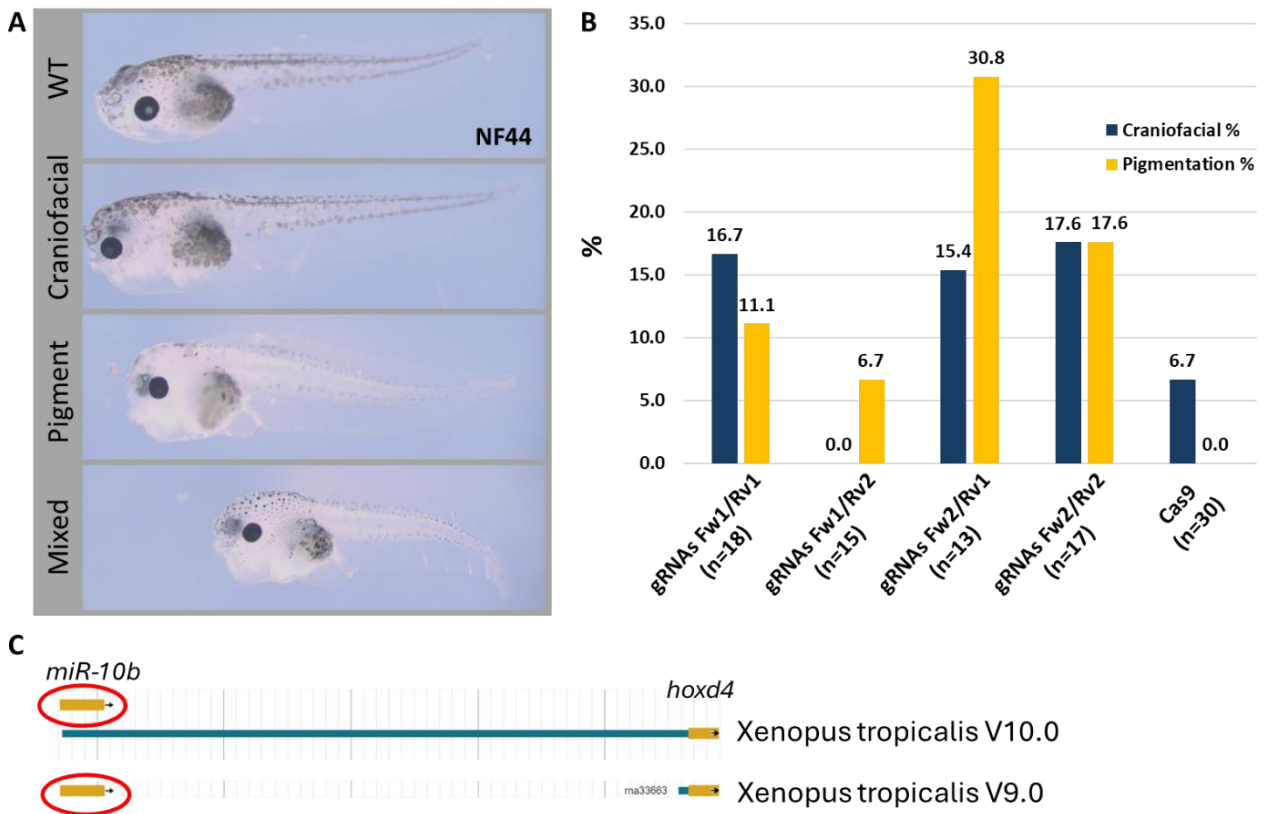


**Fig. 19: *Xtr-miR-10b* knock-down.** Effect of *xtr-miR-10b* knock-down in *Xenopus tropicalis*. **A)** The observed phenotypes are related to both craniofacial development and pigment development. In particular, the head of the tadpoles look shorter than the wild type, while the melanocytes look immature (round shape) or lower in number in most gRNAs combinations, apart from the combination Fw1/Rv2. Statistical analysis could not be performed due to low experimental numbers **B)**. **C)** Changes in the *hoXd4* locus from V9.0 to V10.0. The blue line represents the 5'UTR of *hoXd4*, showing that *xtr-miR-10b* and *hoXd4* are produced as a long single transcript, and not separately.

### 3.3.4 miR-208

There is extensive literature on the role of *hsa-miR-208* in cardiac physiology, and about its use as biomarker for detecting cardiac injury (Huang et al., 2021; Ji et al., 2009; Liu et al., 2023; Zhao et al., 2020).

Even though the role of this miRNA has been studied extensively on adult tissues, there is a lack of knowledge involving *miR-208* during development. The fact that *miR-208* was flagged up from the bioinformatical analysis conducted using genes associated with craniosynostosis (Fig. 14) was quite surprising, since this miRNA has always been associated with cardiac function. This is the reason why *xtr-miR-208* was selected as a possible candidate for craniofacial development.

To further justify a *xtr-miR-208* knock-down experiment, we decided to perform an LNA-WISH using a probe for *xtr-miR-208* in *Xenopus laevis* at early stages of development and check if this particular miRNA is expressed in tissues other than the heart (Fig. 20A). Results show that *xtr-miR-208* is, as expected, expressed in the heart field. However, it seems to be expressed also in the otic vesicle, migrating NC and in the eye, making this miRNA an interesting candidate for further investigation.

Following a preliminary knock-down experiment, we noticed that all the gRNAs combinations apart from Fw1/Rv2 led to a very low survival rate (data not shown). Considering that the combination Fw1/Rv2 consistently produced a deletion of *xtr-miR-208* locus in over 60% of the injected embryos (n=16) (Fig. 20B), we decided to perform the rest of the experiments using only this combination of gRNAs. By using the other combinations, we noticed a lower deletion rate in the combination Fw1/Rv1 (40%, n=5), and Fw2/Rv1 (43%, n=7). For the combination of gRNAs Fw2/Rv2, only one of the injected embryos survived, making this combination of gRNAs non suitable for further experiments.

We observed a “twisted” phenotype in almost 40% of the injected embryos, probably due to failure during the extension of the musculature (Fig. 20C, D).

Because we observed no obvious phenotype that could be associated with defects in NC development, we decided to not continue with this miRNA for further investigation with respect to NC development.

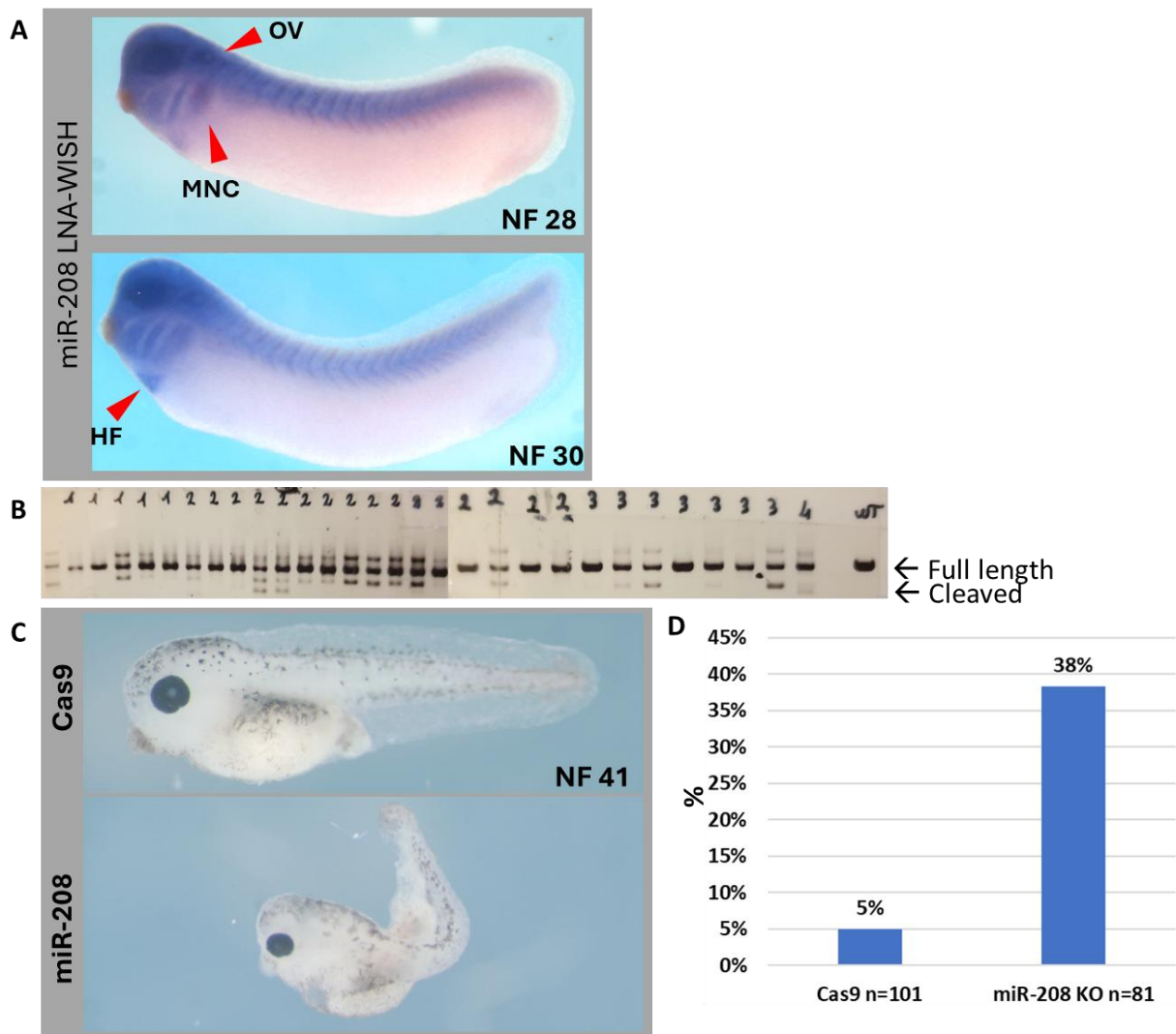


**Fig. 20: *Xtr-miR-208* knock-down. A)** The expression pattern of *xtr-miR-208* in *Xenopus laevis* tailbud was determined by LNA-WISH. As pointed out by the red arrows, at early stages it is possible to detect expression in the otic vesicle and in migrating NC, while later during development, the expression of *xtr-miR-208* becomes visible in the heart field (red arrow). **B)** Genomic DNA PCR on single tadpoles that were injected with the different combinations of gRNAs (1=Fw1/Rv1, 2=Fw1/Rv2, 3=Fw2/Rv1, 4=Fw2/Rv2 and WT is a noninjected control embryo). The wild type band is at approximately 800bp, while the deletion produces a band at approximately 500bp. Most tadpoles had a certain degree of mosaicism, especially on sample number 2. **C)** The knock-down of *xtr-miR-208* on *Xenopus tropicalis* produced a “twisted” phenotype, likely caused by defects during the development and elongation of the musculature **D)** on the injected side in 38% of the injected animals. Figure legend: OV, otic vesicle; MNC, migrating neural crest; HF, heart field.

Target	sgRNA sequence (5' to 3')
miR-10b-Fw1	taatac <b>gactcactata</b> GGGAGAACTTGAGCTACCATg <b>tttttagagctagaa</b>
miR-10b-Rv1	taatac <b>gactcactata</b> GGAATACAATTAGTAGTGAGg <b>tttttagagctagaa</b>
miR-10b-Fw2	taatac <b>gactcactata</b> GGAGAGAGTTTGACTTACAGg <b>tttttagagctagaa</b>
miR-10b-Rv2	taatac <b>gactcactata</b> GGACTGCGGGGGGCATAGCCg <b>tttttagagctagaa</b>
miR-15a-16a-Fw1	taatac <b>gactcactata</b> GGGGGACAGAGCAGCAGCTTg <b>tttttagagctagaa</b>
miR-15a-16a-Rv1	taatac <b>gactcactata</b> GGGTCACCACAGCAACCAATg <b>tttttagagctagaa</b>
miR-15a-16a-Fw2	taatac <b>gactcactata</b> GGATATTCTGAATTTGCAGTg <b>tttttagagctagaa</b>
miR-15a-16a-Rv2	taatac <b>gactcactata</b> GGTAGTGACACACCCCCTTg <b>tttttagagctagaa</b>
miR-17~92 Fw1	ctag <b>ctaatac</b> gactcactataGGTTGGGTCCGCATGCAGCTg <b>tttttagagctagaa</b>
miR-17~92 Fw2	ctag <b>ctaatac</b> gactcactataGGA <b>ACTGATCTGTGGGATGG</b> g <b>tttttagagctagaa</b>
miR-17~92 Rv1	ctag <b>ctaatac</b> gactcactataGGAGTACTTTTTATGCCAGAg <b>tttttagagctagaa</b>
miR-17~92 Rv2	ctag <b>ctaatac</b> gactcactataGGTTGGGTCCGCATGCAGCTg <b>tttttagagctagaa</b>
miR-30a-Fw1	taatac <b>gactcactata</b> GGGAACCATTTGATCCAATGg <b>tttttagagctagaa</b>
miR-30a-Rv1	taatac <b>gactcactata</b> GGTGT <b>CACAGGGATGACAG</b> Ag <b>tttttagagctagaa</b>
miR-30a-Fw2	taatac <b>gactcactata</b> GGCAGTGATGATAGAGTAg <b>tttttagagctagaa</b>
miR-30a-Rv2	taatac <b>gactcactata</b> GGACAACCTGCATTAATTGGg <b>tttttagagctagaa</b>
miR-99 Fw1	ctag <b>ctaatac</b> gactcactataGGAGCCGCCTTTTATAACAg <b>tttttagagctagaa</b>
miR-99 Fw2	ctag <b>ctaatac</b> gactcactataGGCATGATGGGACACAGCTTg <b>tttttagagctagaa</b>
miR-99 Rv1	ctag <b>ctaatac</b> gactcactataGGATATATTAGGATATTTATg <b>tttttagagctagaa</b>
miR-99 Rv2	ctag <b>ctaatac</b> gactcactataGGGTTAATTTGCATTATCAGg <b>tttttagagctagaa</b>
miR-100 Fw1	ctag <b>ctaatac</b> gactcactataGGCAACACACTTCACATCAAg <b>tttttagagctagaa</b>
miR-100 Fw2	ctag <b>ctaatac</b> gactcactataGGTCTGTGTCGGCTTGGCTAg <b>tttttagagctagaa</b>
miR-100 Rv1	ctag <b>ctaatac</b> gactcactataGGTATGCCGGGAAGACAAGGg <b>tttttagagctagaa</b>
miR-100 Rv2	ctag <b>ctaatac</b> gactcactataGGCCTGACGGCTGTGGGTGGg <b>tttttagagctagaa</b>
miR-132-212 Fw1	ctag <b>ctaatac</b> gactcactataGGTAGCCAATGGTGAGAAACg <b>tttttagagctagaa</b>
miR-132-212 Fw2	ctag <b>ctaatac</b> gactcactataGGGGACGCATGGGGAATCTAg <b>tttttagagctagaa</b>
miR-132-212 Rv1	ctag <b>ctaatac</b> gactcactataGGAAGGGATAGGGTATATTGg <b>tttttagagctagaa</b>
miR-132-212 Rv2	ctag <b>ctaatac</b> gactcactataGGCGGATATCTGCAGGCTGGg <b>tttttagagctagaa</b>
miR-145 Fw1	ctag <b>ctaatac</b> gactcactataGGGTCCAGGCCAGCCATTAg <b>tttttagagctagaa</b>
miR-145 Fw2	ctag <b>ctaatac</b> gactcactataGGGAGCAATCCATAATGGCTg <b>tttttagagctagaa</b>
miR-145 Rv1	ctag <b>ctaatac</b> gactcactataGGGGTCTGGGAAAGGCCCTTg <b>tttttagagctagaa</b>
miR-145 Rv2	ctag <b>ctaatac</b> gactcactataGGCTGCTCATTGGTGACCACg <b>tttttagagctagaa</b>
miR-187 Fw1	ctag <b>ctaatac</b> gactcactataGGAAGACCACTCAGTGCTATg <b>tttttagagctagaa</b>
miR-187 Fw2	ctag <b>ctaatac</b> gactcactataGGGTGGTCTTCCATACAGC <b>Ag</b> g <b>tttttagagctagaa</b>
miR-187 Rv1	ctag <b>ctaatac</b> gactcactataGGATCTGGTGATCATGAATGg <b>tttttagagctagaa</b>
miR-187 Rv2	ctag <b>ctaatac</b> gactcactataGGGGCGACAATTCTGTCATGg <b>tttttagagctagaa</b>
miR-194-1 Fw1	ctag <b>ctaatac</b> gactcactataGGGAGACGTTGCGCAGAGCTg <b>tttttagagctagaa</b>
miR-194-1 Fw2	ctag <b>ctaatac</b> gactcactataGGAGACGTTGCGCAGAGCTTg <b>tttttagagctagaa</b>
miR-194-1 Rv1	ctag <b>ctaatac</b> gactcactataGGTGGGGTCCCCACCGACAGg <b>tttttagagctagaa</b>
miR-194-1 Rv2	ctag <b>ctaatac</b> gactcactataGGCTGGGGTCCCCACCGACAg <b>tttttagagctagaa</b>
miR-200b-Fw1	taatac <b>gactcactata</b> GGCCTGAGGTCTAATACAGTg <b>tttttagagctagaa</b>
miR-200b-Rv1	taatac <b>gactcactata</b> GGAATATTGCTGCACATCCg <b>tttttagagctagaa</b>

**Table 3: List of gRNAs.** List of all the designed gRNAs for the miRNAs of interest. On the first column, are the target miRNA as named in *Xenopus tropicalis*. On the second column, are the sequences of the gRNA. Capital letters show the functional binding sites of the gRNA.

## **Chapter 4: The role of *xtr-miR-204-1* in development**

So far, we have investigated the effect of the knock-down of three miRNAs that we predicted to be involved in NC development: *xtr-miR-10b*, *xtr-miR-208* and *xtr-miR-218-2*. These miRNAs were selected according to literature investigations, as well as bioinformatical analysis. However, following preliminary analysis, we decided to not to pursue the investigation of the developmental role of these miRNAs for different reasons, ranging from technical problems related to the CRISPR-Cas9 approach that we were using (*xtr-miR-10b*), to the observation of phenotypes unrelated to NC development (*xtr-miR-208* and *xtr-miR-218-2*). However, during this investigation, we generated a list of miRNAs that are predicted to be involved in NC development, according to the literature (Fig. 21). This list separates miRNAs according to their developmental role/s, starting from the early stages of NC development, of induction and specification, moving towards the EMT and migration, and finishing at the differentiation into specific derivatives, such as craniofacial skeleton or teeth.

*Xtr-miR-204-1* was the last miRNA whose role was assessed during *Xenopus tropicalis* development. This miRNA was selected according to two criteria: firstly, it is one of the miRNAs with the most specific expression in the NC-derived organoids generated in our laboratory by Dr Nicole Ward (Ward et al., 2018); secondly, literature search showed that *hsa-miR-211* (the human homolog of *xtr-miR-204-1*) is highly expressed in melanocytes, which are derived from the NC, and is involved in controlling cellular migration, a key property of NCCs (Cui and Man, 2023; Piacentino et al., 2020). *Xtr-miR-204-1* is a miRNA that belongs to the miR-204 family, which includes *xtr-miR-204-1* and *xtr-miR-204-2* in *Xenopus tropicalis* and *hsa-miR-211* and *hsa-miR-204* in *Homo sapiens*. Both these miRNAs are located into introns of TRPM genes (*trpm1* for *hsa-miR-211/xtr-miR-204-1* and *trpm3* for *hsa-miR-204/xtr-miR-204-2*). TRPM (transient receptor potential melastatin) proteins are transient ion channels that allow the transport of divalent cations, in particular Mg<sup>++</sup> and Ca<sup>++</sup>. There are a total of eight TRPM genes both in human and frog (Huang et al., 2020). *TRPM1*, the host gene of *xtr-miR-204-1*, is expressed in the adult retina and melanocytes (Jia et al., 2020; Su et al., 2020), however, its expression (and, by extension, of *xtr-miR-204-1*) during development is not very well known. The

RNA-seq analysis conducted by Dr Nicole Ward was not able to distinguish between *xtr-miR-204-1* and *xtr-miR-204-2*, since the sequence of the mature RNA is the same. Because of this, for my investigation, I decided to study the role of *xtr-miR-204-1*, because this is the least studied of the two miRNAs.

*Hsa-miR-204* was found to be important for the correct development of the eye in human. In particular, Conte and colleagues have described in six affected members of a British family a heterozygous mutation in the seed sequence of the 5p arm of this gene, which led to retinal dystrophy and coloboma with or without cataract (Conte et al., 2015). Following further investigations in Medaka fish, they managed to recapitulate this phenotype. They also identified increased cellular apoptosis as the main cause of it. It is important to notice that *hsa-miR-204* correspond to *xtr-miR-204-2*, in *Xenopus*. On the other hand, *xtr-miR-204-1* that has been investigated in the next chapters correspond to the human *hsa-miR-211*.

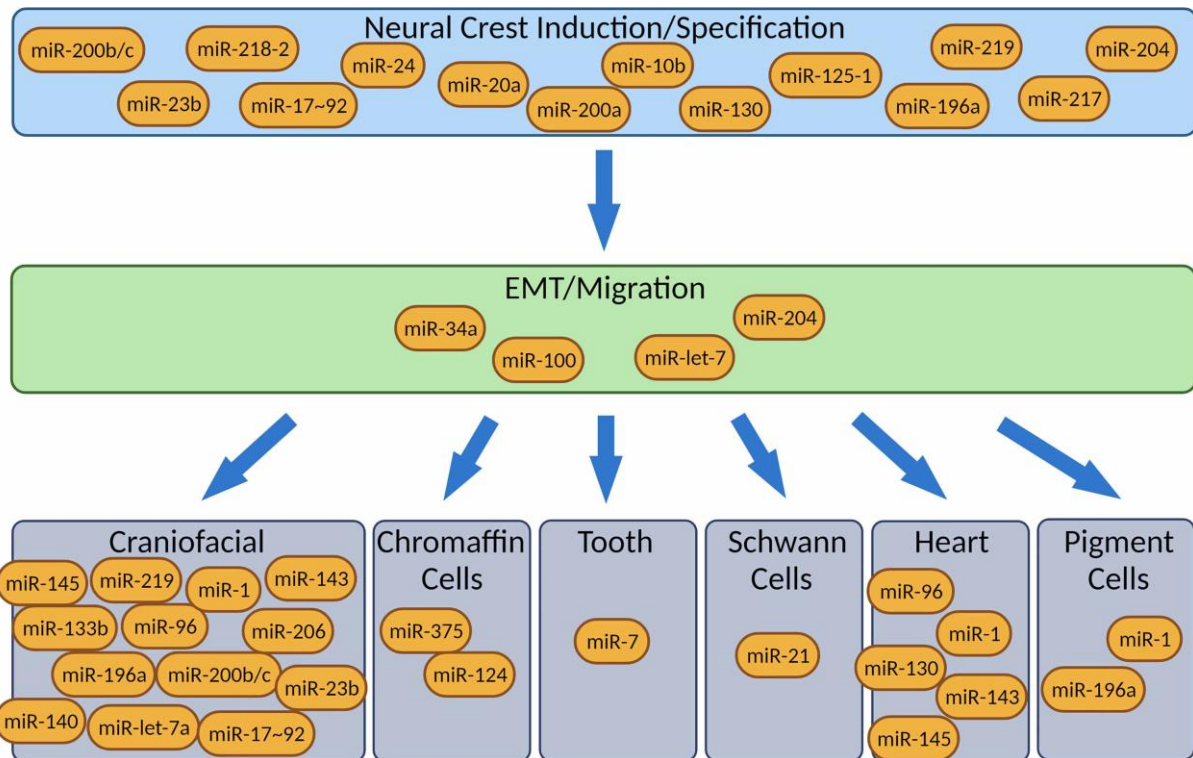


**Figure 21: List of miRNAs described as involved in NC development.** The table represents a schematic of the NC development, divided into boxes according to the different stages of development (top box, induction and specification, middle box, EMT and migration, and differentiation into various derivatives, in the smaller boxes on the bottom). To note how some miRNAs are involved in different aspects of NC development, such as in the case of *miR-219*, involved in the early stages of induction and specification, as well as in craniofacial development. Similarly, *miR-196a* is involved in the early phases of NC development, as well as in pigment cells differentiation. Both *miR-219* and *miR-196a* were investigated in our laboratory (Godden et al., 2022). Image taken from (Antonaci and Wheeler, 2022).

#### 4.1 *xtr-miR-204-1* and *trpm1* expression

To determine the expression pattern of *xtr-miR-204-1*, we carried out several whole-mount in situ hybridisations (WISHs). The first WISH that we performed was a variant of the classic experiment, in which a modified locked nucleic acid (LNA) probe was used. This is also called LNA-WISH, and it is mainly used to investigate the expression of short RNA molecules (Antonaci et al., 2023).

Since miRNAs are extremely short (~22nt), it is not possible to design a regular WISH probe, which is usually hundreds of nucleotides long. To overcome this problem, it is

possible to buy pre-designed probes that are complementary to the miRNA of interest, and that have on both the 5' and 3' ends a nucleotide that is tagged with digoxigenin.

As the sequences of guide strand of *xtr-miR-204-1/2* (*xtr-miR-204-1-5p* and *xtr-miR-204-2-5p*) are the same, in order to distinguish between the expression of the two different miRNAs, we decided to undertake two different approaches: in the first one, and more indirect, we decided to determine the expression pattern of *trpm1*, which should be co-expressed together with *xtr-miR-204-1*; for the second approach, we designed an LNA probe for *xtr-miR-204-1-3p*, which is the annotated passenger strand. In fact, differently from *xtr-miR-204-1-5p* and *xtr-miR-204-2-5p*, the passenger strand of *xtr-miR-204-1* is unique, not sharing the same sequence with *xtr-miR-204-2-3p*.

When hybridised with the *trpm1* probe, the staining was visible on the embryos only after stage NF29, in the dorsal region of the developing eye, in the pineal gland and, to a minor extent, around the otic vesicle, brain, and branchial arches. At later stages of development, *trpm1* is also expressed in the melanocytes, as well as in the retina and in the pineal gland (Fig 21A).

When using the custom *xtr-miR-204-1-3p* LNA probe at different stages of development, the staining was more specific than the one for *xtr-miR-204-1-5p* and *trpm1* probes (Fig. 21A). In particular, while at earlier stages of development there was no detected signal, at stages NF26 it was possible to detect some specific staining in the optic vesicle and putative olfactory placode, with some lower expression in the otic vesicle and migrating NC. Later in development, at stage NF33, the expression in the eye field increased, as well as the expression in the olfactory placode. The expression in the branchial arches becomes sharper, as we expected at this stage of development. An additional staining in the somites, with increased intensity of the staining moving towards the posterior side of the embryos, starts appearing. At late tadpole stage (NF39), the expression in the eye becomes confined to the ciliary marginal zone, and a specific staining in the septum between hindbrain and midbrain (MHB) appears. Finally, at tadpole stage (NF41), the staining becomes more diffuse in the head, in particular in the olfactory placode, branchial arches, and MHB. Also in the somites, the staining became stronger and at a comparable level from antero-posterior axes. Interestingly, later in development, it is possible to appreciate a specific staining in the pronephric tubule and duct (Fig. 21B).

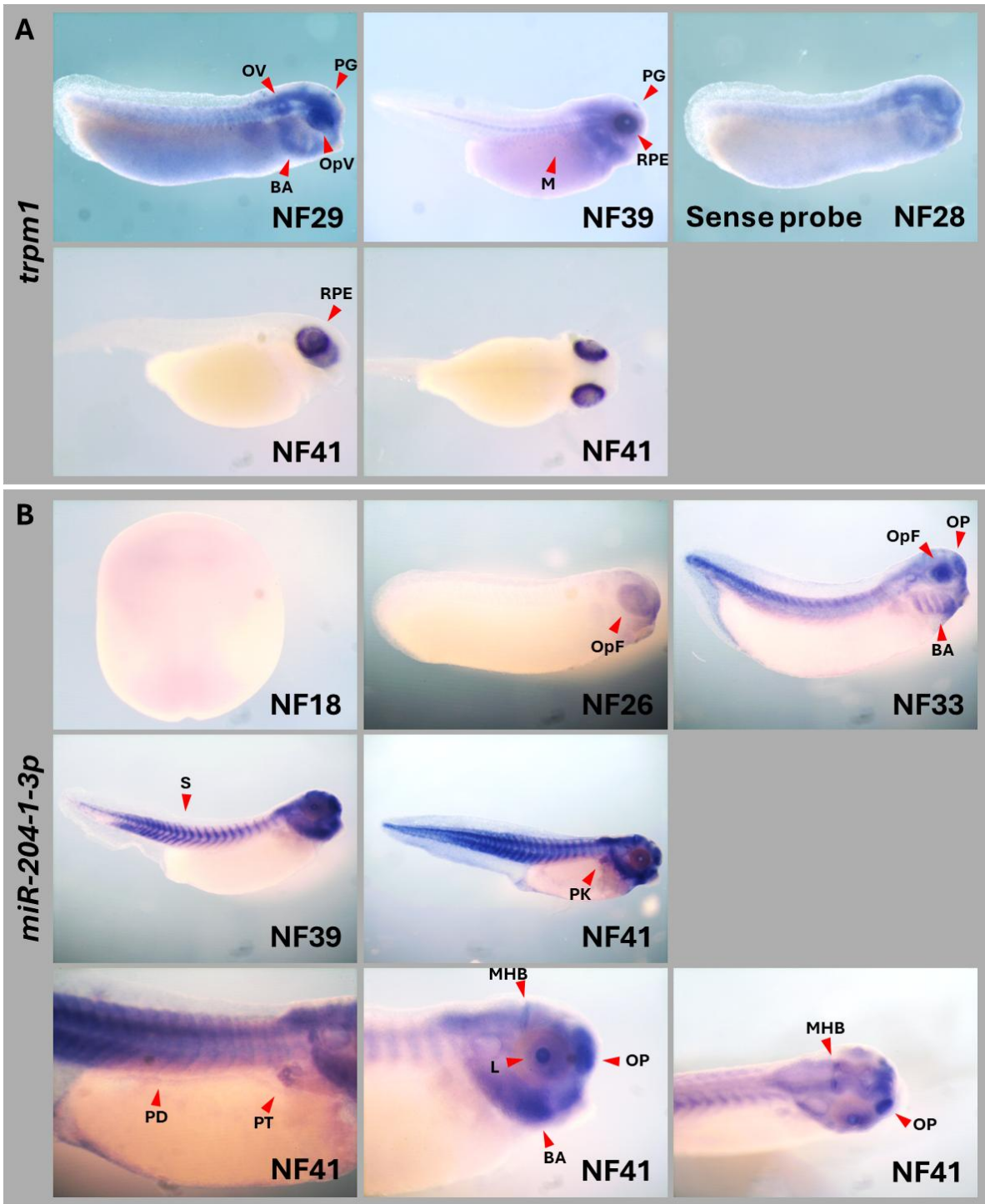


**Fig. 22: Expression pattern of *trpm1* and *xtr-miR-204-1-3p* in *Xenopus* embryos. A)** Expression pattern of *trpm1* at NF29, 39, and 41. Embryos were stained with the sense probe as a control. At NF29, the expression is mainly in the optic cup, with some expression in the branchial arches, pineal gland, and in the otic vesicle. At later stages of development, the expression is mostly in the RPE, pineal gland and melanocytes. **B)** Expression pattern of *xtr-miR-204-1-3p* at different stages of development. The staining starts to be visible at NF26, in the optic vesicle. At later stages of development, the expression starts to be evident in the olfactory placode, somites and branchial arches. At NF41 it is possible to appreciate the expression in the pronephric kidney and tubule as well. On the bottom row, from left to right: details of the expression of *xtr-miR-204-1-3p* in the pronephros; in the head (lateral view), showing the expression in the olfactory placode, branchial arches, ciliary marginal zone and MHB; in the head from the dorsal side, better displaying the expression in the MHB. Figure legend: OV, otic vesicle; PG, pineal gland; OpV, optic vesicle; M, melanocytes; BA, branchial arches; RPE, retinal pigmented epithelium; OF, optic field; S, somites; PK, pronephric kidney; PT, pronephric tubule; PD, pronephric duct; MHB, midbrain-hindbrain boundary; OP, olfactory placode; L, lens. All the embryos are viewed laterally, with the caudal side on the left, and the rostral side on the left. Exceptions are the embryos stained for *xtr-miR-204-1-3p*, stage NF18 (which is seen dorsally, with the rostral side on the top and the caudal side on the bottom), and the last stage NF41 picture, which is a magnification from the dorsal view, oriented caudally on the left and rostrally on the right.

## 4.2 Preliminary gRNAs testing and *xtr-miR-204-1* knock-down

The strategy to knock-down the expression of *xtr-miR-204-1* was the same that we used with the previous miRNAs (*xtr-miR-10b*, *xtr-miR-218-2* and *xtr-miR-208*). The difference was that the intron that hosts *xtr-miR-204-1* is not particularly big (just over 600bp), we only managed to design one sgRNA upstream of the miRNA that would have been to a sufficient distance from the intron/exon boundary of *trpm1* instead of the two we normally tried to design. This resulted in only two possible gRNAs combination for the preliminary result: Fw1/Rv1 and Fw1/Rv2 (Fig. 23A).

Following a preliminary experiment, we noticed that by using the combination of gRNAs Fw1/Rv1, there was a higher level of mortality in comparison to the control embryos. On the other hand, the group of embryos injected with the combination of gRNAs Fw1/Rv2 did not display such a phenotype. In both groups there were eye defects, which we could cluster into two macro-categories: eye size defects (microphthalmia and anophthalmia) and colobomas (of the choroid fissure or superior coloboma). However, the incidence of such phenotypes was higher in the group of embryos injected with the combination of gRNAs Fw1/Rv1 (Fig. 23B, C).

Based on these preliminary results we decided to proceed with the rest of the experiments with the combination of gRNAs Fw1/Rv1.

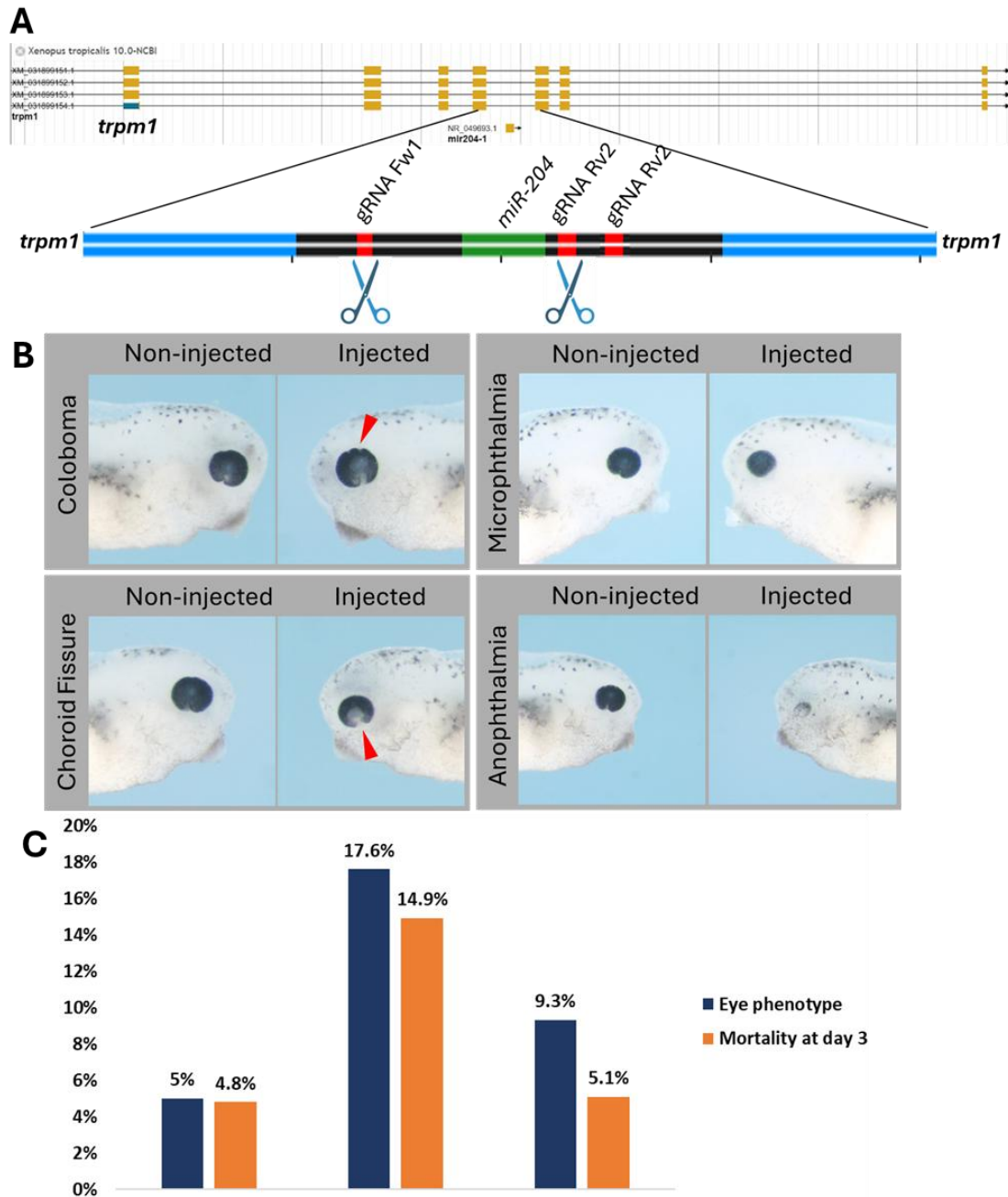


**Fig. 23: Preliminary data from *xtr-miR-204-1* knock-down experiment. A)** On top, screenshot of *Xenopus tropicalis* V10.0 genome browser, showing the locus of *trpm1* that include *xtr-miR-204-1* gene. On the bottom, magnification of the intron of *trpm1* that hosts *xtr-miR-204-1*. In blue, there are the exons of *trpm1* that flank the miRNA gene. In green, *xtr-miR-204-1* gene. In red, the binding site of the gRNAs. **B)** Representative images displaying the four types of eye developmental defects: superior coloboma, coloboma of the choroid fissure, microphthalmia and anophthalmia which will be grouped as coloboma and microphthalmia. Each panel shows the same embryo, with the non-injected side on the left and the injected (knock-down) side on the right. **C)** Quantification of the eye phenotypes and embryos mortality at day 3 post injection. The combination of gRNAs Fw1/Rv1 shows higher levels of eye developmental defects and mortality, when compared to the control group (Cas9) and the second combination of gRNAs (Fw1/Rv2).

### 4.3 *xtr-miR-204-1* knock-down

To assess the effect of *xtr-miR-204-1* knock-down, we performed more experiments using the combination of gRNAs Fw1/Rv1 in biological triplicate. Following these experiments, we confirmed the eye phenotypes. In particular, we observed that 28% of the knock-down embryos displayed coloboma phenotype (in contrast to the 8% of the control group), while 14% had microphthalmia or anophthalmia (in contrast to the 2% of the control group) (Fig. 23A).

We also confirmed that the CRISPR-Cas9 strategy was working on the injected embryos, so we extracted the genomic DNA (gDNA) from individual tadpoles that have been previously injected with the combination of gRNAs and performed a PCR using primers that flank the gRNAs binding site. This way, if the deletion have occurred, we should be able to detect a smaller band on the electrophoresis gel. The length of this smaller band corresponds to the length of the wild-type PCR product minus the portion of DNA that is encompassed between the two gRNAs. In this specific case, the length of the PCR product for the uninjected embryos is 702bp, and the region of DNA between the two gRNAs is about 280bp, therefore the expected PCR product in the knock-down embryos should be of 420bp. What we observed on the electrophoresis gel was a band of exactly the expected size, which was missing in the wild-type embryos gDNA PCR (Fig. 24B, top).

To further confirm the deletion of the DNA locus harbouring *xtr-miR-204-1*, and in order to determine the efficiency of the CRISPR-Cas9 knock-down strategy, we extracted the gDNA from ten different tadpoles that have been injected to knock-down *xtr-miR-204-1*. We then performed a PCR using the same conditions as before and ran the ten samples individually (along with a negative control, a tadpole injected with the Cas9 protein, but without any gRNAs). The result was that all the injected tadpoles displayed a certain degree of deletion, showing that the knock-down strategy works for all the injected tadpoles, but not with the same level of mosaicism (Fig. 24B, bottom).

Finally, we quantified the number of embryos that displayed the four different eye phenotypes (coloboma of the choroid fissure, superior coloboma, microphthalmia and anophthalmia which, from now on, will be classified as coloboma and microphthalmia) (Fig. 24A).

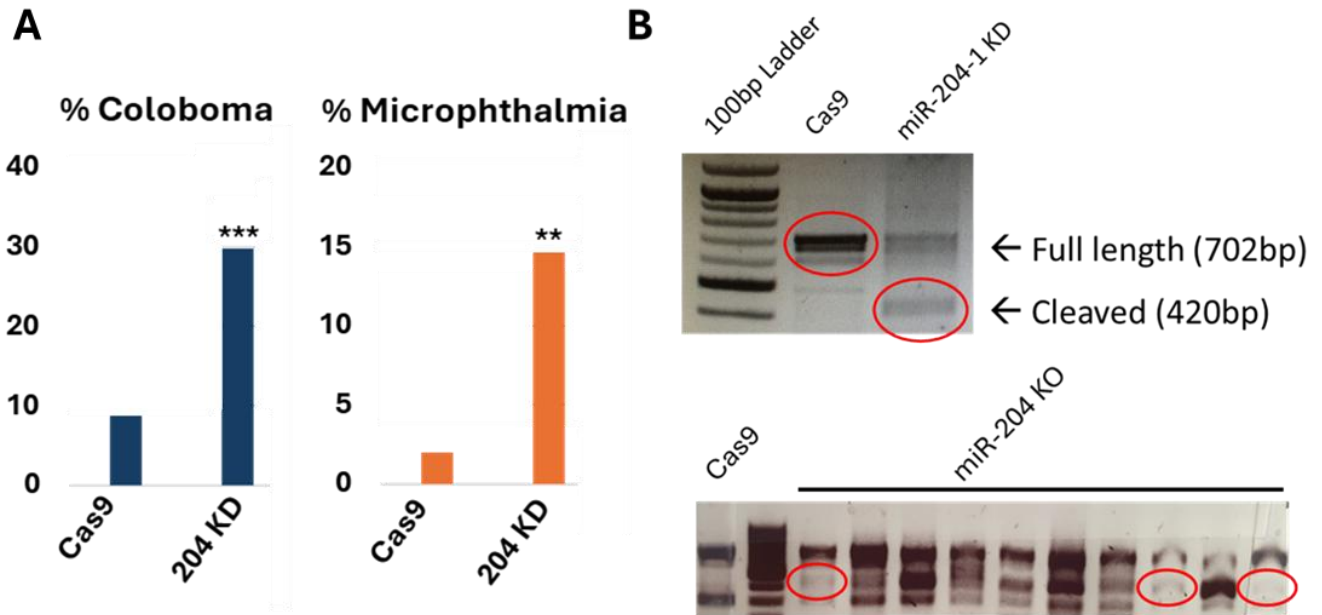


**Fig. 24: *Xtr-miR-204-1* knock-down.** **A)** Bar charts that show the percentage of embryos displaying coloboma (left) or microphthalmia (right) in control group (Cas9, n=119) and in *xtr-miR-204-1* knock-down embryos (n=150). Experiment was performed in triplicate. \*\*p<0.01, \*\*\*p<0.001 **B)** Top image shows a DNA electrophoresis on PCR products using primers that bind outside the whole *trpm1* intron that hosts *xtr-miR-204-1*. Circled in red, in the Cas9 lane, there is the WT band of 702nt. Circled in red, in the miR-204-1 KD lane, there is the cleaved region of the genome, which lack *xtr-miR-204-1* gene, of 420nt. On the bottom gel, ten different embryos have been genotyped in the same way. In comparison to the Cas9 sample (to the left), all the knocked-down embryos show the cleaved DNA fragment (the red circles highlight the fainter bands).

#### 4.4 *xtr-miR-204-1-5p* overexpression

In order to confirm the specificity of the knock-down, and to exclude the possibility of off-target effects of the gRNAs, we needed to perform a rescue experiment. To carry out such an experiment, we had to inject a miRNA mimic. However, before doing that, we needed to assess the effect of the overexpression of *xtr-miR-204-1*.

We injected embryos with a control miRNA mimic (*cel-miR-39-3p*), which should not produce any visible phenotype, and with *xtr-miR-204-1-5p*. The decision of injecting the 5p arm of *xtr-miR-204-1* was taken for different reasons. The first reason is that, in most miRNAs, only the 5p strand of the mature miRNA is loaded into the RISC complex and used in the RNA interference pathway, and it is therefore called the guide strand (Murchison and Hannon, 2004). The second reason is because, also for this miRNA (at least for the human homolog, *hsa-miR-204/211*), the strand that has been represented the most is the 5p. Also, in human, *hsa-miR-204-5p* and *hsa-miR-211-5p* share the same seed sequence, therefore the same predicted targets, while the 3p strands of *hsa-miR-204* and *hsa-miR-211* have different seed sequences. This suggests a conserved function of the 5p strand (Fig. 25A). Finally, in miRbase (the miRNA database that contains all the known miRNAs across different species) there is no mention of *xtr-miR-204-1-3p*. All these clues pointed toward the choice of *xtr-miR-204-1-5p* as a preferred candidate to perform the rescue experiment.

Following overexpression of *xtr-miR-204-1-5p* in *Xenopus tropicalis* tadpoles, we did not observe any obvious phenotype, including any of the observed phenotypes for the knock-down of *xtr-miR-204-1*. Specifically, of the 105 embryos injected with *xtr-miR-204-5p* mimic, only 12% displayed any eye developmental disorder, similarly to the 11% of the 65 embryos in the control group (Fig. 25B).

**A** Hsa-211-5p **TTCCCTTTGT**CATCCTTCGCCT  
 Hsa-204-5p **TTCCCTTTGT**CATCCTATGCCT  
 Xtr-204-1-5p **TTCCCTTTGT**CATCCTATGCCT  
 Xtr-204-2-5p **TTCCCTTTGT**CATCCTATGCCT

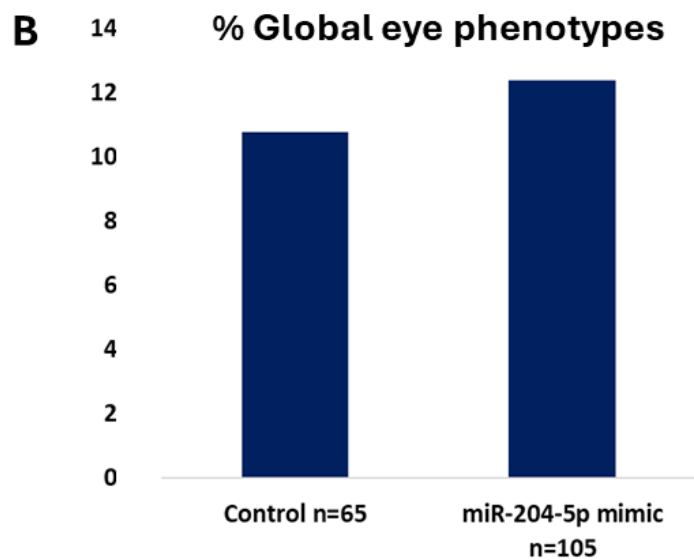


**Fig. 25: miR-204 family conservation of the guide strand and overexpression of *xtr-miR-204-1-5p*.** **A)** Comparison of the mature miR-204 family members in *Homo sapiens* (*hsa-miR-204-5p* and *hsa-miR-211-5p*) and *Xenopus tropicalis* (*xtr-miR-204-1-5p* and *xtr-miR-204-2-5p*). In red there is the seed sequence, while underlined there are the differences between the two strands. **B)** Effect of the overexpression of *xtr-miR-204-1-5p* in *Xenopus tropicalis* embryos on eye development. No significant differences were observed between the control group (injected with *cel-miR-39-3p* mimic) and the group injected with *xtr-miR-204-1-5p* miRNA mimic.

#### 4.5 *xtr-miR-204-1-5p* rescue

Following the assessment of the effect of the overexpression of *xtr-miR-204-1-5p*, we carried out the rescue experiment, in which we tested the specificity of our observed phenotypes. In these experiments, we injected embryos with Cas9 protein and a control miRNA mimic as a negative control, with Cas9 protein and *xtr-miR-204-1* gRNAs as a positive control, and with a mix of Cas9 protein, *xtr-miR-204-1* gRNAs and *xtr-miR-204-1-5p* miRNA mimic as proper rescue experiment.

On an initial assessment of the eye phenotypes, we noticed that there was a global and significant reduction in eye phenotypes in the rescued embryos, when compared to the knocked-down ones. However, when analysing the results in more depth, and assessing the different phenotypes, we noticed that the rescue occurred fully for the coloboma phenotypes, but not for the eye size phenotypes (Fig. 26A, B).

These results indicated that the observed colobomas were caused by the lack of *xtr-miR-204-1-5p*. However, the impossibility of rescuing the eye size defects indicated that the cause of such phenotypes was to be attributed to some other factor, and not to the lack of *xtr-miR-204-1-5p*.

In order to understand the reason why anophthalmias and microphthalmias could not be rescued by using *xtr-miR-204-1-5p*, we had to rule out different hypothesis about the reasons why these phenotypes occurred. We hypothesized three possible scenarios; the first one was that *xtr-miR-204-1* passenger strand, the 3p, is also involved in eye development, and that *xtr-miR-204-1-5p* and *xtr-miR-204-1-3p* play a different role during development. The second hypothesis is that the intron of *trpm1* in which *xtr-miR-204-1* is located is also involved in the regulation of some genes (likely *trpm1* itself), and that might affect the growth of the eye during development. The third and last hypothesis is that one (or both) the gRNAs used to knock-down *xtr-miR-204-1* have some off-targets that are involved in eye development.

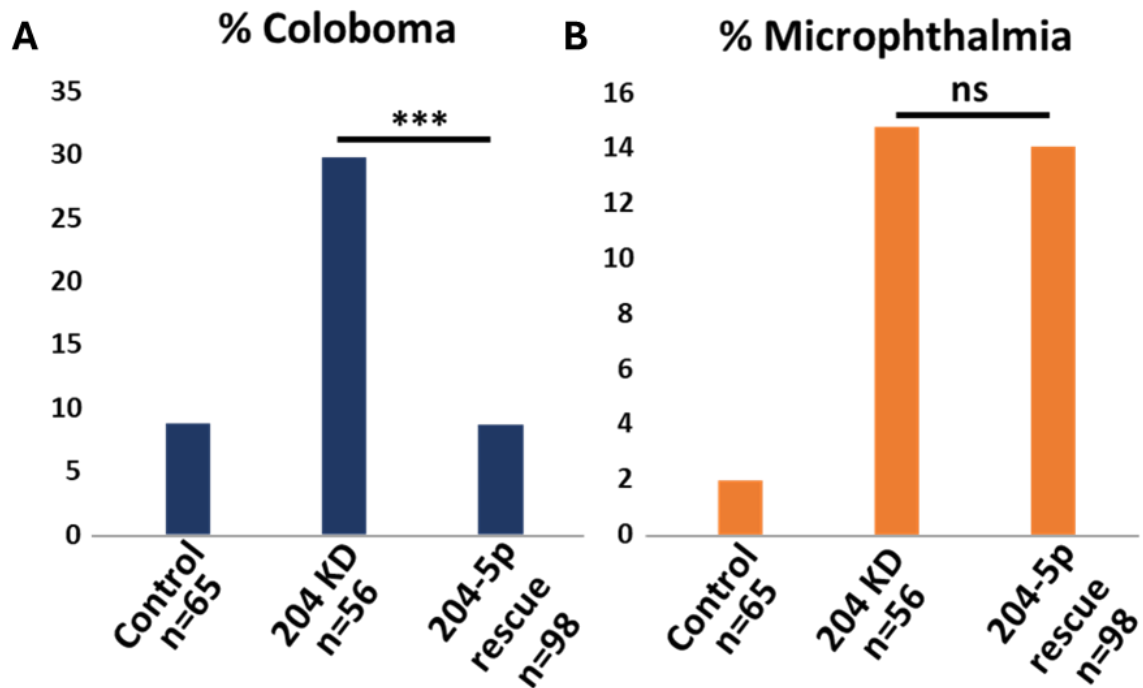


**Fig. 26: *Xtr-miR-204-1* knock-down rescued with *xtr-miR-204-1-5p*.** **A)** Percentages of embryos displaying coloboma phenotypes in the control, *xtr-miR-204-1* knock-down, and rescued groups. \*\*\* $p < 0.001$ . **B)** Percentages of embryos displaying microphthalmia phenotypes in the control, *xtr-miR-204-1* knock-down, and rescued groups. Control embryos were injected with Cas9 protein and *GFP* mRNA, miR-204-1 knock-down were injected with Cas9 protein, *GFP* mRNA, and miR-204-1 gRNAs, while miR-204-5p rescue samples were injected with Cas9 protein, *GFP* mRNA, miR-204-1 gRNAs and *miR-204-1-5p* miRNA mimic.

#### 4.6 *xtr-miR-204-1-3p* overexpression

To test the first hypothesis, in which the passenger strand of *xtr-miR-204-1*, *xtr-miR-204-1-3p*, plays a role in eye development, we performed a rescue experiment exclusively using *xtr-miR-204-1-3p*. Unfortunately, this miRNA has not been annotated in *Xenopus* (only the guide strand has, so far, been annotated). Because of that, we had to design a custom miRNA mimic.

To do so, we extrapolated the sequence of *xtr-miR-204-1-3p* using the sequence of *xtr-pre-miR-204-1* and predicted the sequence of the passenger strand. To confirm this analysis, we also blasted the sequence of *xtr-miR-204-1-3p* that we generated with the human homologous: *hsa-miR-211-3p*. As a result, we obtained an almost perfect match (only one nucleotide of difference between the two mature miRNAs, and not in the seed sequence, meaning that the predicted targets of these miRNAs should be the same (Fig. 27A).

Another interesting point that we could extrapolate is that, if the seed sequence is conserved among species, then this miRNA is probably playing some sort of biological role. In fact, the conservation of the passenger strand of *xtr-miR-204-1* is even higher than the conservation of the guide strand. If we compare the sequences of *hsa-miR-211-5p* with the sequence of *xtr-miR-204-1-5p* we can notice that there are two nucleotides that are different. Also in this case, these differences do not fall within the seed sequence of the miRNA (Fig. 27A).

Once we obtained the sequence of *xtr-miR-204-1-3p*, we overexpressed it in order to have possible information about the effect of this miRNA, before proceeding with the actual rescue experiment. We noted that overexpression of *xtr-miR-204-1-3p* did produce an eye phenotype. In particular, we observed a significant increase of embryos with colobomas and even more embryos displaying microphthalmia, in comparison to the control group (Fig. 27B). From this conclusion we could say that the passenger strand of *xtr-miR-204-1* might be playing a role in controlling eye development during *Xenopus* embryogenesis.

**A**

Xtr-204-1-5p **TTCCCTTTGT**CATCCTATGCCT  
Hsa-211-5p **TTCCCTTTGT**CATCCTTCGCCT

Xtr-204-1-3p **GCAGGGACAGCAAAGGGATGC**  
Hsa-211-3p **GCAGGGACAGCAAAGGGGTGC**

**B**

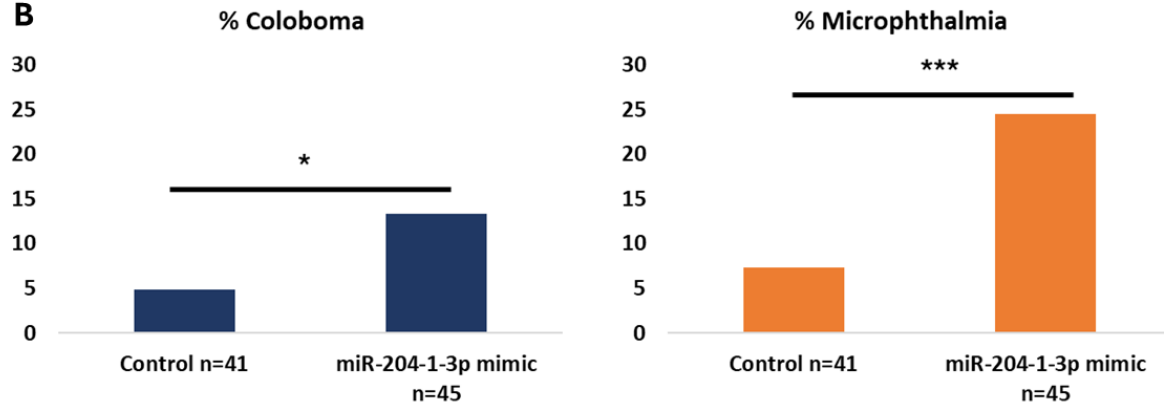


**Fig. 27: miR-204 family conservation of the passenger strand and overexpression of *xtr-miR-204-1-3p*.** **A)** Comparison of the mature miR-204 family members between *Homo sapiens* and *Xenopus tropicalis*. Top, the guide strands of both species (*hsa-miR-211-5p* and *xtr-miR-204-1-5p*) are compared with each other. Bottom, the passenger strands of both species (*hsa-miR-211-3p* and *xtr-miR-204-1-3p*) are compared with each other. In red there are the seed sequences, while underlined there are the differences between the two strands. **B)** Effect of the overexpression of *xtr-miR-204-1-3p* in *Xenopus tropicalis* embryos on eye development. Significant differences were observed between the control group (injected with *cel-miR-39-3p* mimic) and the experimental group, injected with *xtr-miR-204-1-3p*, for both coloboma phenotypes (bar chart on the left) and microphthalmia (bar chart on the right). \* $p < 0.05$ , \*\*\* $p < 0.001$ .

#### 4.7 *xtr-miR-204-1-3p* rescue

Once we assessed the effect of the overexpression of *xtr-miR-204-1-3p* on its own, we proceeded with the rescue experiment. For this experiment we used four different groups: a Control (injected with Cas9 protein, control mimic, and *Gfp* mRNA) and two positive controls, overexpression (injected with *xtr-miR-204-1-3p* mimic, and *Gfp* mRNA) and knock-down (injected with Cas9 protein, gRNAs to knock-down *xtr-miR-204-1*, and *Gfp* mRNA). For the actual experiment, we used the two following groups: Control + knock-down (injected with Cas9 protein, gRNAs to knock-down *xtr-miR-204-1*, control mimic, and *Gfp* mRNA) and Rescue (injected with Cas9 protein, gRNAs to knock-down *xtr-miR-204-1*, *xtr-miR-204-1-3p* mimic, and *Gfp* mRNA).

The reason for the use of the first group (Control) was to have a baseline for the second and third group (Overexpression and Knock-down), which were then used as a technical control. They were proving that all the reagents and the injections *per se* were working. The last two groups, Control + Knock-down and Rescue, were the actual experiment. In the first group (Control + Knock-down), we were supposed to see the microphthalmia and coloboma phenotypes, while in the second group (Rescue), we were expecting to see less microphthalmia phenotypes, in comparison to the previous one.

When we analysed the data taking into account only for the coloboma phenotypes, we did not see any in the group where *xtr-miR-204-1-3p* was overexpressed (as expected from the experiment in section 4.6, Fig. 27B). We also observed a significant increase of colobomas in the knock-down group (also expected, because of the previous experiments), a further increase in the Control + Knock-down group, and a non-significant reduction in the rescued group (Fig. 28A).

On the other hand, what we observed while taking into account only the microphthalmia phenotypes, was an increased number of embryos displaying such phenotypes in the knock-down group, and a non-significant trend for the rescue in comparison to the control group; a further increase in these phenotypes for the fourth group, in which the knock-down was performed together with the overexpression of the control mimic, and a complete rescue of microphthalmia in the rescued group, whose numbers dropped down to the level of the control group (Fig. 28B).

Overall, these data indicate that the rescue experiment using the passenger strand of *xtr-miR-204-1* is working. It also indicates that, while *xtr-miR-204-1-5p* is involved in the coloboma phenotypes, *xtr-miR-204-1-3p* is involved in different biological processes, which include the growth of the eye.

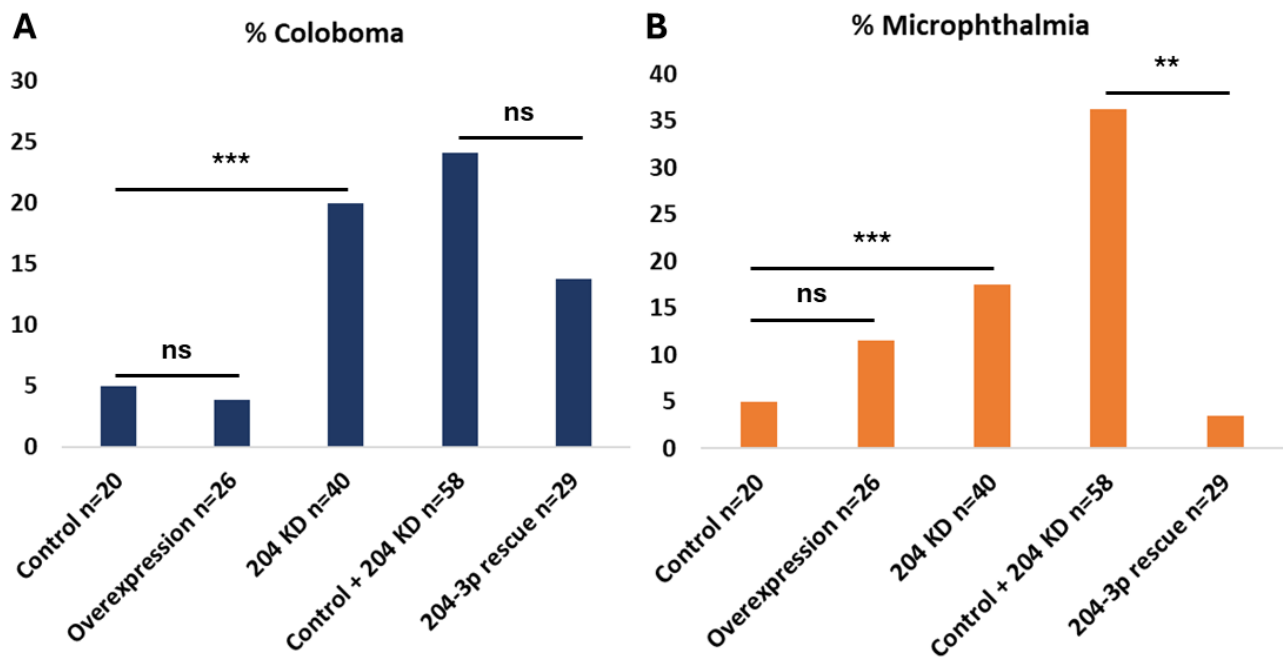


**Fig. 28: *Xtr-miR-204-1* knock-down rescued with *xtr-miR-204-1-3p*.** **A)** Percentages of embryos displaying coloboma phenotypes in the groups: Control, *xtr-miR-204-1-3p* overexpression, *xtr-miR-204-1* knock-down, *xtr-miR-204-1* knock-down rescued with the control mimic (*cel-miR-39-3p*), and rescued with *xtr-miR-204-1-3p* mimic. **B)** Percentages of embryos displaying microphthalmia phenotypes in Control, *xtr-miR-204-1-3p* overexpression, *xtr-miR-204-1* knock-down, *xtr-miR-204-1* knock-down rescued with the control mimic (*cel-miR-39-3p*) and rescued with *xtr-miR-204-1-3p* mimic groups. \*\*p<0.01, \*\*\*p<0.001.

#### 4.8 sgRNA individually injected

To further confirm that the observed eye phenotype was due to loss of *xtr-miR-204-1-3p* and not to any gRNAs off-target, we analysed *in silico* the possible off targets of the gRNAs that have been used for the knock-down experiments. We searched in CRISPRScan the off targets of the two gRNAs using *Xenopus tropicalis* as the species and two number of mismatches. Using these settings, we could not identify any predicted off-target in any protein coding gene (including UTRs or introns).

Therefore, we decided to extend the search using three possible mismatches. Using this setting, the number of off-targets increased (as predicted). However, none of those new off-targets fell into coding genes.

Failing to find any possible off-target using the *in silico* approach, we decided to test the efficacy of our gRNAs by injecting them individually. The idea is that, if at least one of the gRNAs was producing the observed phenotypes, we would have been able to see it even without using both gRNAs at once.

The experiment was performed injecting a total of four groups: a negative control group injected with Cas9 protein and *Gfp* mRNA, a positive control injected with Cas9 protein, both gRNAs (Fw1/Rv1) and *Gfp* mRNA, and the two experimental groups, injected with Cas9 protein, *Gfp* mRNA, and either gRNA Fw1, or gRNA Rv1.

The data shows how the effect of a single gRNA injection does not produce any increase in the eye phenotypes, in comparison to the Cas9 control. On the contrary, as expected, the injection of both gRNAs produced an increase in coloboma and microphthalmia. This experiment indicates that the observed eye developmental defects are likely due to the knock-down of *xtr-miR-204-1*, rather than to off-targets of the gRNAs (Fig. 29A, B).

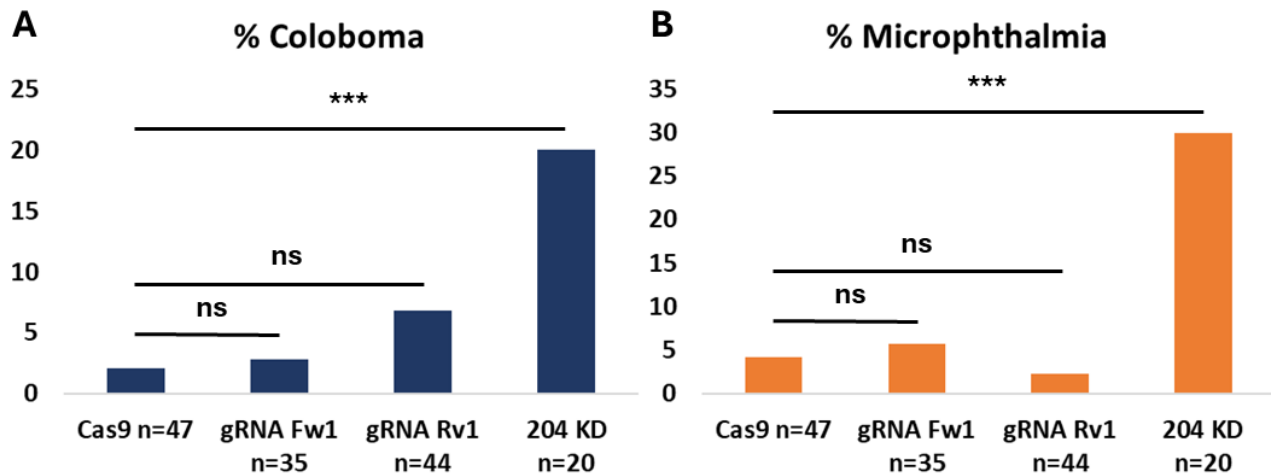


**Fig. 29: Assessment of the effect of the gRNAs individually injected. A)** Percentages of embryos displaying coloboma phenotypes when injected with Cas9 protein alone, with the gRNA Fw1 alone, with the gRNA Rv1 alone, and with a combination of Fw1 and Rv1, which is what it is used to knock-down *xtr-miR-204-1*. \*\*\* $p < 0.001$ . **B)** Percentages of the embryos displaying microphthalmia phenotypes when injected with Cas9 protein alone, with the gRNA Fw1 alone, with the gRNA Rv1 alone, and with a combination of Fw1 and Rv1, which is what it is used to knock-down *xtr-miR-204-1*. \*\*\* $p < 0.001$ .

#### 4.9 *Trpm1* knock-down

In order to determine the specificity of the observed phenotype, we had to perform one last control experiment. As mentioned in the introduction of this chapter, *xtr-miR-204-1* is located within an intron of the gene *trpm1*. The CRISPR/Cas9 approach that we were using to knock-down this miRNA is removing its whole genomic locus, which correspond to almost half of this intron.

Sometimes, introns of protein coding genes can regulate the expression of its host gene (Rose, 2018). This means that, potentially, the loss of part of the intron that hosts *xtr-miR-204-1* could cause a downregulation of *trpm1*, and this loss of *trpm1* could be the cause of coloboma or microphthalmia, or both. In humans, TRPM1 is not involved in either coloboma or microphthalmia, but mutations in this gene are known to cause congenital stationary night blindness (Tsang and Sharma, 2018). However, *Trpm1* in *Xenopus* might be playing a different and unknown developmental role. therefore we needed to assess the effect of *trpm1* knock-down in *Xenopus*, without affecting the expression of *xtr-miR-204-1*.

Since mirtrons are processed as introns in the nucleus of the cell, we decided to use an ATG-morpholino, which is able to block the translation of a target gene by binding to the ATG of the mRNA of such gene and, therefore, sterically blocking the ribosomal complex (Timme-Laragy et al., 2012). This entire phenomenon occurs when the mRNA is in the cytoplasm, while splicing occurs when the mRNA is still in the nucleus. Therefore, by using an ATG morpholino, the splicing of *trpm1* mRNA (and, by extension, the expression of *xtr-miR-204-1*) should occur normally. Since *trpm1* has two transcription starting site (in both *Xenopus tropicalis* and *Homo sapiens*), we decided to design two morpholinos, one for each transcript variant, and to inject both of them at the same time in *Xenopus tropicalis* embryos, along with a control group, injected with a control morpholino that is not predicted to have any target.

The limitation of this experiment is that we could not test the effectiveness of the two morpholinos in knocking-down of *trpm1*. This is because the ATG morpholino do not impact on the mRNA level of the targeted gene, and there are no tested antibodies for *Xenopus Trpm1* that could have been used for Western blot. Because of this, we used the highest recommended concentration of morpholino for *Xenopus tropicalis* embryos (40ng/embryo).

From this experiment, we show that the knock-down of both *trpm1* isoforms in *Xenopus tropicalis* do not produce any visible eye developmental defect (Fig. 30A, B).

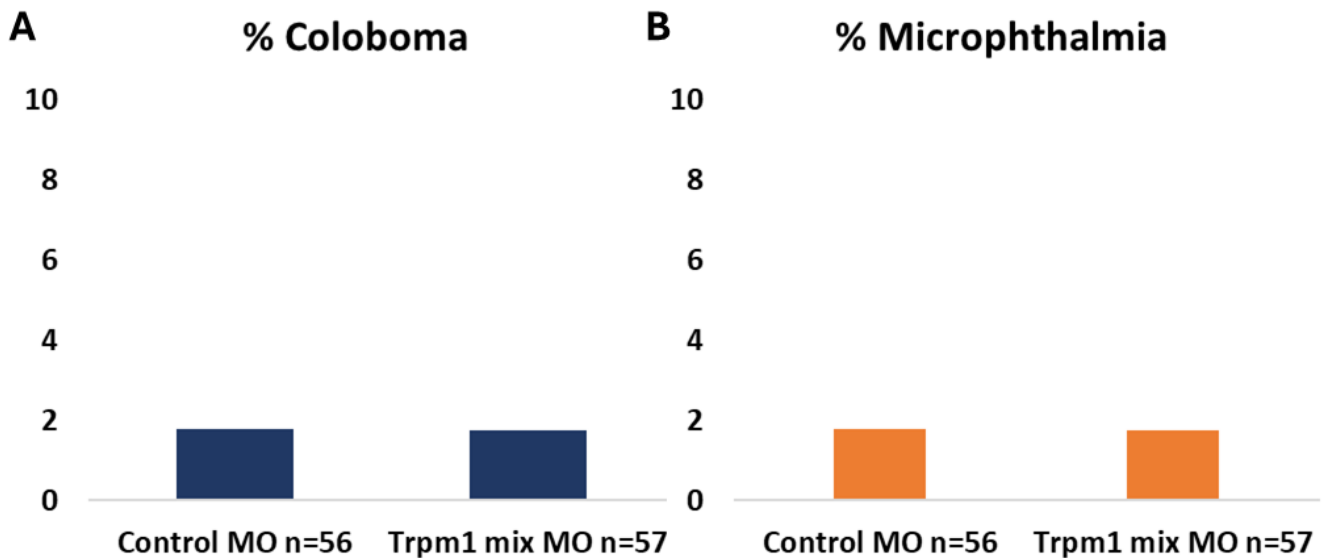


**Fig. 30: Assessment of the effect of *trpm1* knock-down. A)** Percentages of the embryos displaying coloboma phenotypes when injected with control morpholino, or with the combination of *trpm1* morpholinos. **B)** Percentages of the embryos displaying microphthalmia phenotypes when injected with control morpholino, or with the combination of *trpm1* morpholinos.

In summary, we have described how lack of the whole *xtr-miR-204-1* gene is able to trigger severe eye phenotypes, shown as defects in the growth of the eye (microphthalmia and anophthalmia), and defects in the closure of the choroid fissure (shown as coloboma of the choroid fissure and superior colobomas). We have also shown that the annotated guide strand of *xtr-miR-204-1* (*xtr-miR-204-1-5p*) is responsible for the coloboma phenotypes, and that the overexpression of this miRNA does not affect the development of the eye in a critical manner, as shown by the overexpression experiment. On the other hand, we have seen that *xtr-miR-204-3p* (the annotated passenger strand) is responsible for the eye growth phenotypes, and that the sole overexpression of this miRNA is capable of inducing such phenotypes in the developing tadpoles.

## **Chapter 5: The effect of *xtr-miR-204-1* knock-down**

While it is important to identify the phenotype that the loss of the gene of interest produces, as well as the tissues in which this gene is expressed, it is equally important to understand which genes are affected by the deregulation of this gene in order to understand the mechanism underlying the phenotypes. This concept is even more crucial when the subject of the investigation is a regulator of gene expression, such as a transcription factor or, in this specific case, a miRNA.

For this project, we decided to investigate some of the genes that might be impacted by the absence of *xtr-miR-204-1* both directly and indirectly. To do so, we investigated the expression of genes that are important during the development of the eye, including NC-specific genes (such as *snai2* or *sox10*). Some of these genes are computationally predicted to be direct targets of *xtr-miR-204-1*, while others were selected because of their known role in human eye developmental disorders, specifically coloboma and microphthalmia.

In the specific case of *xtr-miR-204-1*, the number of computationally predicted targets for the guide strand (*xtr-miR-204-1-5p*) is relatively low when using the online tool TargetScan8.0 (791 transcripts, using *Homo sapiens* genomic annotations). On the other hand, the number of predicted targets for *hsa-miR-204-1-3p*, the passenger strand, is too high to be considered reliable (5753 total transcripts). Therefore, we decided to consider only the targets of *hsa-miR-204-1-5p* for the decision of which genes to investigate.

### **5.1 Expanding known gene regulatory networks with miRNAs**

In past years, new and more comprehensive gene regulatory networks have been published with respect to NC development. However, these networks are mostly composed of protein-coding transcription factors, and not many other regulatory elements, such as miRNAs, have been included.

The investigation on the genes that are directly and indirectly affected by the expression of *xtr-miR-204-1* is important not only to expand our general knowledge of the GRN of the eye and the NCCs but also to pinpoint the important role that these RNA species play during development.

By proving the importance of *xtr-miR-204-1* in the regulation of the development of the eye, we also wanted to further prove that miRNAs play a central role in development.

## **5.2 Effect of *xtr-miR-204-1* knock-down on selected predicted targets expressed in the developing eye**

To better understand the role of *xtr-miR-204-1* during eye development, we decided to perform WISH experiments on tadpoles that have been previously knocked-down for *xtr-miR-204-1* on one side only. Given the high number of predicted targets (791 predicted targets, using TargetScan 8.0), we shortlisted the ones that are known to be expressed in the developing eye, where we know that *xtr-miR-204-1* is also expressed. What we expected to observe was an increased expression level of these genes in the developing eye of these animals.

The genes that we shortlisted and that are presented here are *sox4*, *tfap2a*, *tfap2β*, *hmx1* and *vax2*.

### 5.2.1 *Sox4* expression in WT embryos and *xtr-miR-204-1* knock-down embryos

SOX4 is a gene that encodes for an SRY-related HMG-box protein, which acts as a transcription factor that plays a fundamental role during embryonic development. In particular, SOX4 is involved in the regulation of neurogenesis, where it directs the differentiation of neural progenitor cells to specific neuronal subtypes (Bergsland et al., 2006).

Given its role in embryo development, it is no surprise that, in the adult organism, it has been implicated in cancer biology. Specifically, it has been observed that SOX4 can play a role in cell proliferation, survival and invasion of cancer cells. However, SOX4 can play a role as tumour suppressor or as an oncogene according to the specific type of cancer (Liu et al., 2021a; Moreno, 2020). This might be due to the fact that SOX4 protein activity is tightly regulated by post-translational acetylation (Jang et al., 2015).

The reason why this gene has been selected for investigation following *xtr-miR-204-1* KD is because it is a predicted target of this miRNA. Also, its expression partially overlaps with the expression pattern of *xtr-miR-204-1/2-5p* RNA. However, human mutations in this gene have not been associated with any eye developmental defects.

In our control experiments, the expression of *sox4* has been observed in neural and neural-derived tissues, mainly in the anterior part of the head, which might indicate forebrain, midbrain and sensory placode expression. Following *xtr-miR-204-1* KD, we did not observe any appreciable variation in the expression of this gene in the injected side of the embryo, neither as expression intensity nor as expression pattern (Fig. 31). This data might indicate that either *xtr-miR-204-1* does not regulate the expression of *sox4* in the developing *Xenopus tropicalis* embryos, or that this gene is indeed regulated by the miR-204/211 family, but from *xtr-miR-204-2*, which is mainly expressed in neural tissues. Since our experimental procedure targets specifically *xtr-miR-204-1*, we are not able to investigate the potential regulation between *xtr-miR-204-2* and *sox4* by using our CRISPR-Cas9 knock-down strategy.

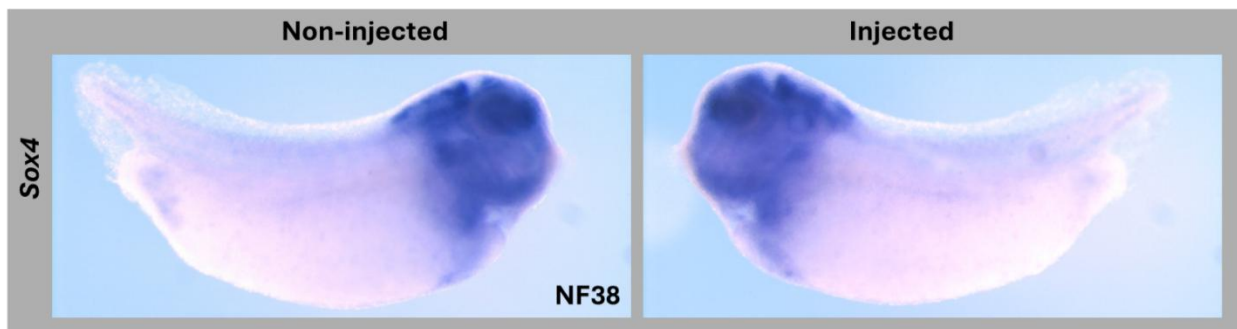


**Fig. 31: Expression of *sox4* mRNA following *xtr-miR-204-1* knock-down.** Representative *xtr-miR-204-1* knocked-down embryo, at stage NF38, imaged from the non-injected side (left) and injected side (right). No obvious differences have been observed between the knock-down and wild type sides of the injected embryos.

### 5.2.2 *Tfap2a* expression in WT embryos and *xtr-miR-204-1* knock-down embryos

*Tfap2a* (Transcription Factor AP-2 Alpha), is a key gene that plays many roles in various biological processes. It belongs to the AP-2 family of transcription factors, which are essential regulators of gene expression in development and differentiation.

The effects of TFAP2 $\alpha$  in the modulation of gene expression ranges from cell proliferation, apoptosis, migration and, importantly, differentiation.

During embryonic development, TFAP2 $\alpha$  plays a crucial role in the NC development, from its induction to the differentiation to different derivatives (Chambers et al., 2019; Liu et

al., 2007; Seberg et al., 2017). However, it has been shown that TFAP2 $\alpha$  is also expressed in the epidermis and mammary glands (Bakiri et al., 2015; Smits et al., 2023).

Alterations in *TFAP2 $\alpha$*  expression levels have been linked to developmental disorders, including craniofacial anomalies and neural tube defects (Dixon et al., 2011; Schorle et al., 1996).

Beyond development, TFAP2 $\alpha$  continues to exert its influence in tissue homeostasis and disease. In the context of cancer, TFAP2 $\alpha$  has been found to exhibit both tumour-suppressive and oncogenic properties depending on the cellular context and tumour type. In some cancers, such as breast and prostate cancer, TFAP2 $\alpha$  functions as a tumour suppressor. Interestingly, in NC-derived cancers, such as melanoma and neuroblastoma, TFAP2 $\alpha$  can promote tumour progression by enhancing cell survival, invasion, and angiogenesis (Jin et al., 2023).

The reason why this gene was selected for further analysis is because *TFAP2 $\alpha$*  is a predicted target of *hsa-miR-204/211-5p* and involved in the Branchio-oculo-facial syndrome (BOFS). Among other signs, BOFS patients can also display coloboma in their phenotypes. Furthermore, it plays an important role during NC development, and because of its expression pattern in *Xenopus tropicalis*, which appears to be at the level of the optic cup at tailbud stage. In particular, the expression of *tfap2 $\alpha$*  is higher in the branchial arches, in the trigeminal nerve, in the presumptive lens, pronephric duct, and several structures of the head (Fig. 32A).

Following *xtr-miR-204-1* knock-down, we observed a disrupted expression pattern in the microinjected side in specific regions of the embryos. In fact, the expression pattern on the first three branchial arches was disrupted and the expression in the presumptive lens reduced in almost half of the injected embryos (41%, n=37)(Fig. 32B, C), while the control group displayed different expression only in 9.1% of the examined embryos (n=33). From these data, we can conclude that *xtr-miR-204-1* is regulating the expression of *tfap2 $\alpha$*  (either directly or indirectly) and that the effect of *xtr-miR-204-1* knock-down on the developing embryos might be, at least in part, associated with an aberrant expression of *tfap2 $\alpha$* .

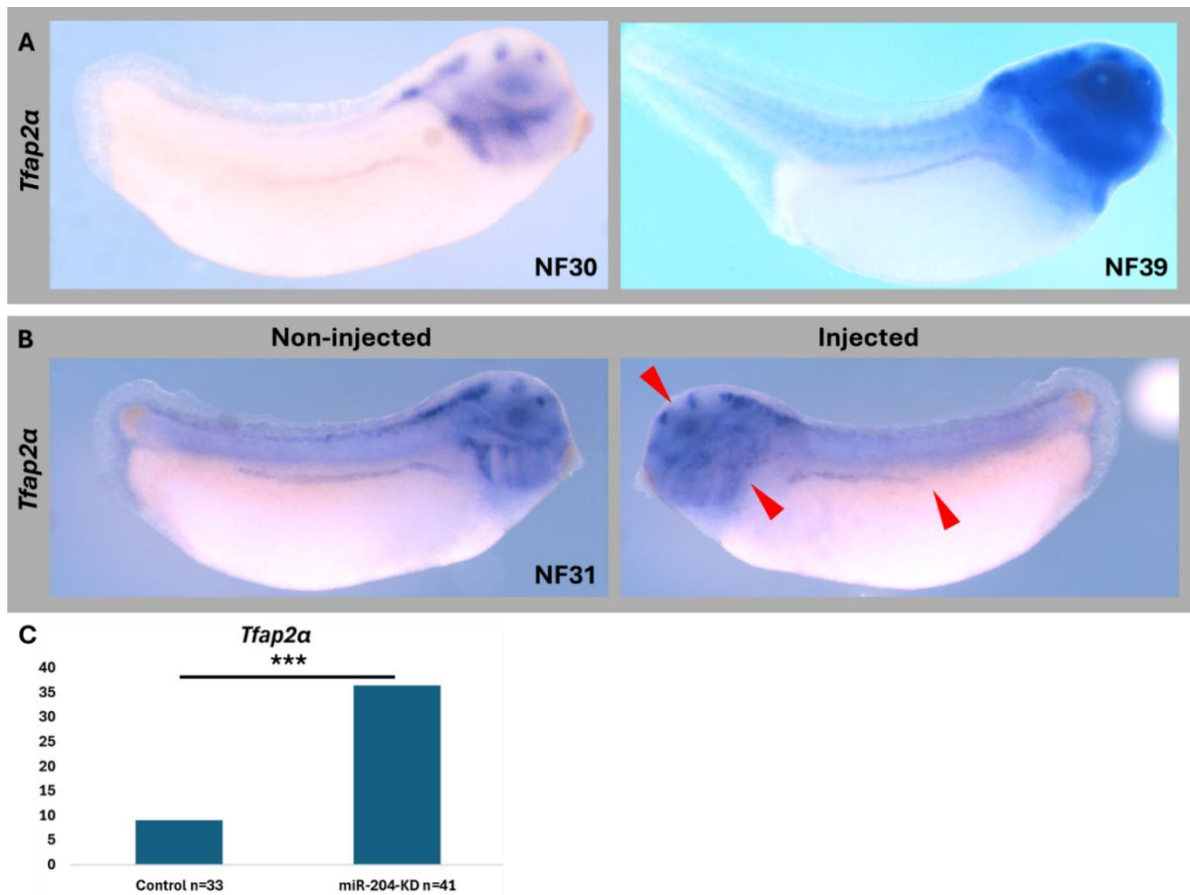


**Fig. 32: Effect of loss of *xtr-miR-204-1* on *tfap2a* mRNA expression.** **A)** Wild type expression of *tfap2a* on tailbud embryos (stage NF30, left picture) and tadpole embryos (stage NF39, right picture). It is possible to see the expression of *tfap2a* in cranial and trunk NC, in the presumptive lens field, and in the pronephric duct, but not in the head of the pronephros. The expression becomes more generalised in the head at tadpole stage. **B)** Representative *xtr-miR-204-1* knocked-down embryo, at stage NF31, imaged from the non-injected side (left) and injected side (right). The expression of *tfap2a* is disrupted in the first branchial arches and in the trigeminal nerve, while reduced in the presumptive lens and in the pronephric tubule, compared to the non-injected side of the embryo. **C)** Percentage of embryos that show a disrupted expression of *tfap2a* on the injected side in control or *xtr-miR-204-1* knock-down. \*\*\* $p < 0.001$ .

### 5.2.3 *Tfap2b* expression in WT embryos and *xtr-miR-204-1* knock-down embryos

*TFAP2β* (Transcription Factor AP-2 Beta), is another member of the AP-2 family of transcription factors with diverse roles in cellular processes. Like *TFAP2α*, *TFAP2β* functions as a transcriptional activator or repressor, regulating the expression of target genes involved in various biological pathways.

In embryonic development, *TFAP2β* plays critical roles in the formation of multiple tissues and organs, including the cardiovascular system and NC derivatives. It regulates the expression of genes necessary for the differentiation and patterning of these tissues, ensuring proper morphogenesis and organogenesis (Raap et al., 2021). *TFAP2β* is particularly crucial for heart development, where it is involved in the specification of cardiac progenitor cells and the regulation of cardiac gene expression (Zhao et al., 2011).

The dysregulation of *TFAP2β* expression has been implicated in various human diseases. Alterations in *TFAP2β* expression levels have been associated with developmental disorders, including congenital heart defects and craniofacial abnormalities (Massaad et al., 2019; Zhao et al., 2011). Also, similar to *TFAP2α*, also *TFAP2β* is a computationally predicted target of *hsa-miR-204/211-5p*. Finally, *TFAP2β* is also known for its dual role in cancer biology, playing as a tumour-suppressor in various type of cancer, but acting as an oncogene in NC-derived cancers (Fu et al., 2019; Jin et al., 2023).

With a similar expression pattern to *tfap2α*, *tfap2β* is also expressed in the presumptive lens, hindbrain, midbrain and midbrain/forebrain boundary, branchial arches and pronephros. However, while the expression of *tfap2α* is stronger in the first three branchial arches and in the pronephric tubule, *tfap2β* expression in these tissues is very different: the pronephric expression is restricted to the head of the pronephros. In the branchial arches, the expression of *tfap2β* is limited to the fourth, fifth and sixth branchial arches, while at later stages of development it is possible to see some staining in a region posterior to the head, and ventral to the pronephric kidney, which we suggest as part of the cardiac outflow tract (Fig. 33A).

Surprisingly, following knock-down of *xtr-miR-204-1*, we observed no changes in the expression patten of this gene in the head region. The only observed phenotype in 4 of the 33 analysed embryos was a reduction of the expression in the head of the pronephric

kidney. From this experiment, we could conclude that, at least in *Xenopus tropicalis*, *xtr-miR-204-1* is not likely to be regulating *tfap2β* in the examined stages of development (Fig. 33B).

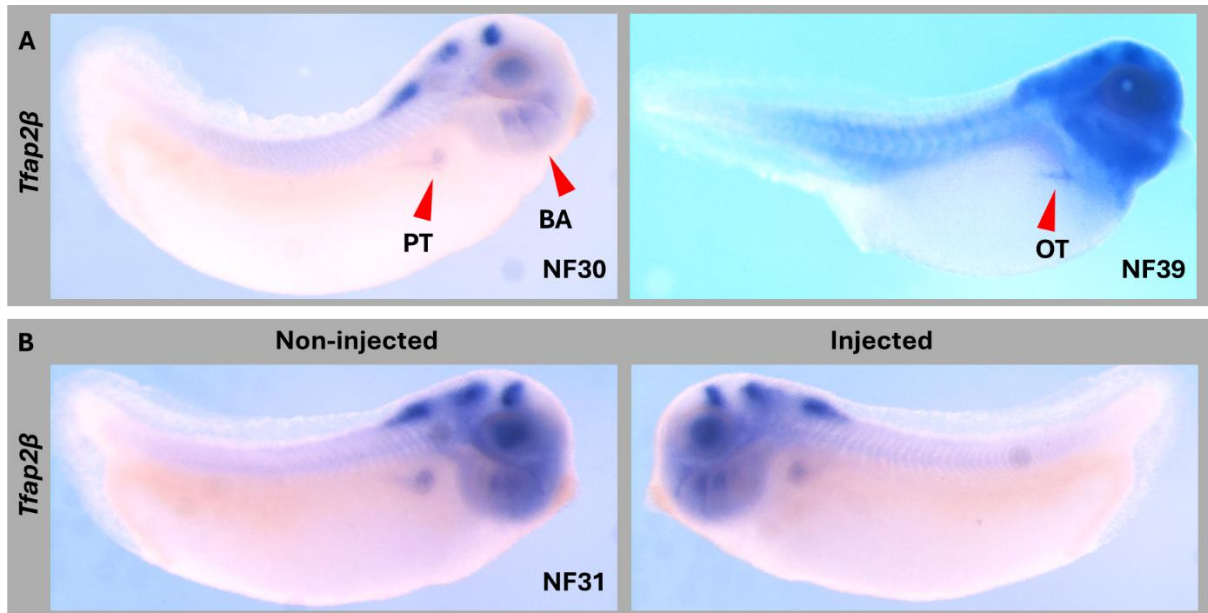


**Fig. 33: Effect of loss of *xtr-miR-204-1* on *tfap2β* mRNA expression. A)** Wild type expression of *tfap2β* on tailbud embryos (stage NF30, left picture) and tadpole embryos (stage NF39, right picture). It is possible to see the expression of *tfap2β* in cranial and trunk NC, in the presumptive lens field, and in the head of the pronephros, but not in the pronephric duct, differently from the pattern of *tfap2α*. Different is also the expression in the branchial arches, which is stronger in the fourth, fifth and sixth, while for *tfap2α* the main expression is seen on the first three branchial arches (Fig. 33A). At tadpole stage, the expression in the head becomes less specific, while some specific staining appears posteriorly to the head and ventrally to the head of the pronephric kidney, which we suggest as part of the cardiac outflow tract (red arrowhead). **B)** Representative *xtr-miR-204-1* knocked-down embryo, at stage NF31, imaged from the non-injected side (left) and injected side (right). No obvious differences in the expression of *tfap2β* have been observed between the knock-down and wild type sides of the injected embryos. Figure legend: BA; branchial arches; PT, pronephric tubule; OT; outflow tract.

#### 5.2.4 *Hmx1* expression in WT embryos and *xtr-miR-204-1* knock-down embryos

*HMX1* gene, also known as *NKX5.3*, belongs to the homeobox family of genes. These genes play crucial roles in embryonic development by regulating the formation of body structures and organs. Specifically, *HMX1* is involved in the development of various tissues and organs, including the eye, inner ear, and craniofacial structures (Kelly and El-Hodiri, 2016).

An important role of this gene during embryonic development involves eye development. In fact, mutations in *HMX1* have been linked to a condition known as oculo-auricular syndrome (OCACS), which is characterized by abnormalities affecting the eyes, ears and, to a minor extent, of the palate. These abnormalities can range from mild to severe and may include underdevelopment or malformation of the eye structures, such as the retina, iris, or optic nerve (Gillespie et al., 2015).

This gene is expressed in very specific cells during development. At early tailbud stage (NF31) the expression is localised in the otic vesicle, trigeminal nerve and around the presumptive lens. Later during development this gene is also expressed in the Schwann cell precursors and ventrally to the head of the pronephric kidney, in a region that we suggest might be within the lung buds. (Fig. 34A).

*Hmx1* has been selected because it is a computationally predicted target of *hsa-miR-204/211-5p*. Also, the phenotype of *xtr-miR-204-1* knock-down in *Xenopus tropicalis* embryos matches really well with the phenotypes that characterise OCACS patients.

Indeed, following knock-down of *xtr-miR-204-1*, we observed an altered expression of *hmx1* between the injected and uninjected sides of the embryos. In particular, we observed in 41% of the embryos an expanded expression of *hmx1* in the region of the choroid fissure, in comparison to just 3% of the control group. In 31% of the embryos we observed a significantly expanded expression in the trigeminal nerve, in comparison to the 13% of the control group. And in 20% of the observed embryos we see an altered expression on the otic vesicle, compared to the 3% of the control group (knock-down n=29, control n=38) (Fig. 34B-F).

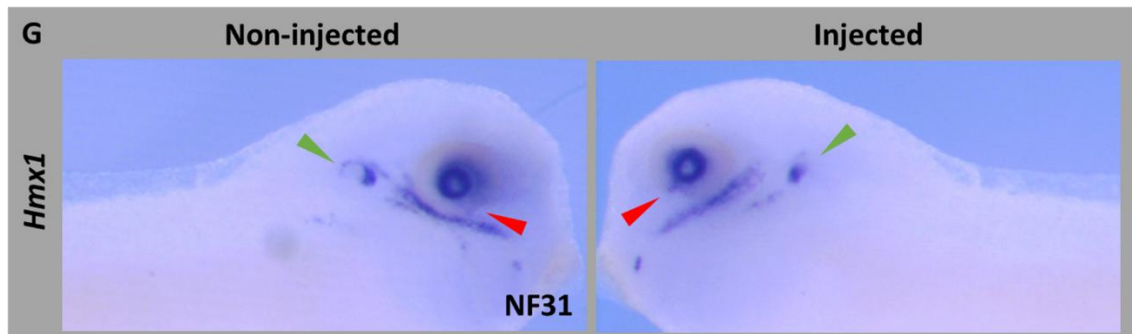
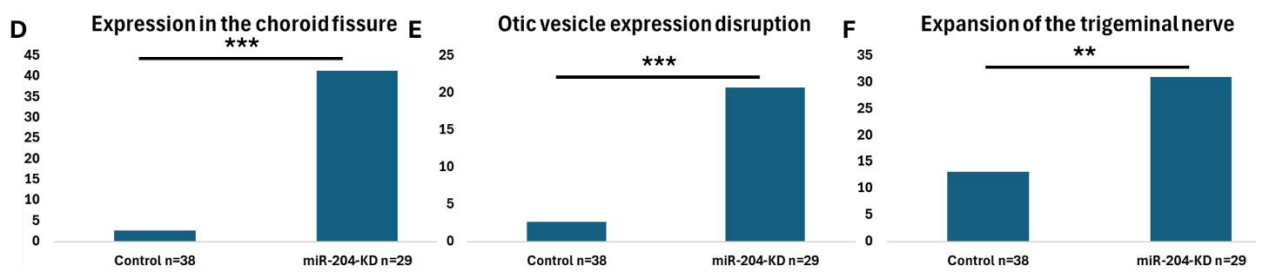
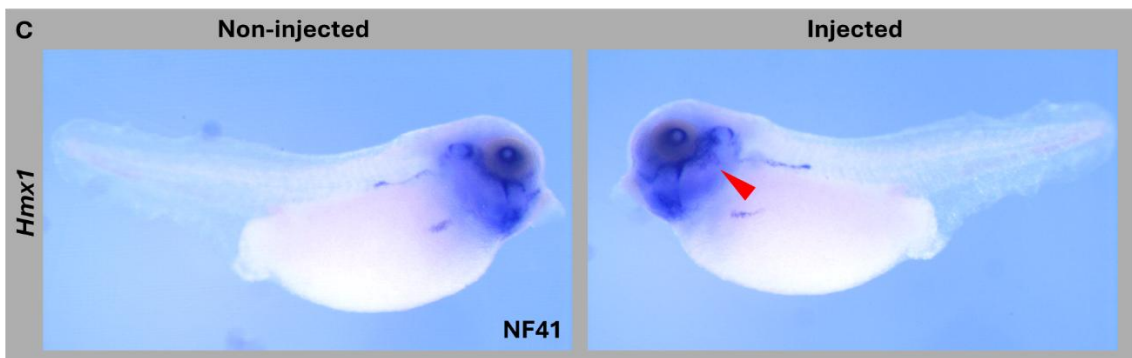
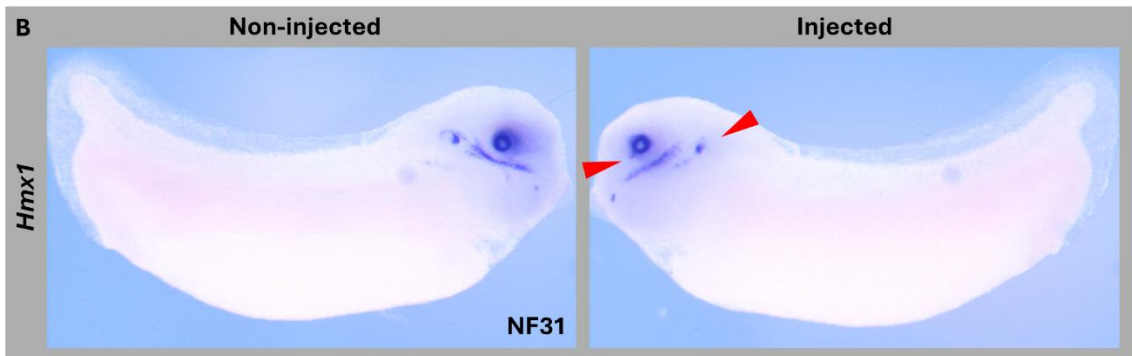
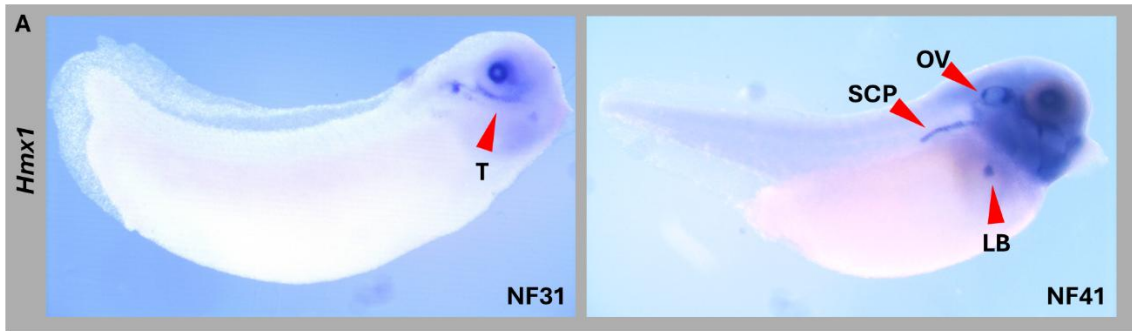


**Fig. 34: Effect of loss of *xtr-miR-204-1* on *hmx1* mRNA expression.** **A)** Wild type expression of *hmx1* on tailbud embryos (stage NF31, left picture) and tadpole embryos (stage NF41, right picture). It is possible to see the expression of *hmx1* around the presumptive lens field, in the trigeminal nerve and around the otic vesicle. At later stages of development, expression of *hmx1* is visible in the Schwann cell precursors and in a region ventral to the head of the pronephric kidney, which we suggest as part of the lung buds (red arrowheads). **B)** Representative *xtr-miR-204-1* knocked-down embryo, at stage NF31, imaged from the non-injected side (left) and injected side (right), showing the reduced expression of *hmx1* mRNA in the otic vesicle and expanded expression of *hmx1* in the choroid fissure (red arrowheads). **C)** Representative *xtr-miR-204-1* knocked-down embryo, at stage NF41, imaged from the non-injected side (left) and injected side (right). We observed an increased thickness of the trigeminal ganglia staining of *hmx1* mRNA (red arrowhead). **D, E, F)** Percentage of embryos that show expression of *hmx1* in the choroid fissure, disrupted expression of *hmx1* in the otic vesicle and expanded expression of *hmx1* staining in the trigeminal nerve, in comparison to the non-injected side of the embryos. **G)** Head magnification of the tadpole illustrated in **B)**. \*\* $p < 0.01$ , \*\*\* $p < 0.001$ . Figure legend: T, trigeminal nerve; OV, otic vesicle; SCP, Schwann cells precursors; LB, lung buds.

#### 5.2.5 *Vax2* expression in WT embryos and *xtr-miR-204-1* knock-down embryos

VAX2 (Ventral Anterior Homeobox 2) plays a crucial role in embryonic development, particularly in the formation of the CNS. It belongs to the family of homeobox genes, which encode transcription factors that regulate the expression of other genes involved in development. VAX2 is specifically involved in the development of the eye and the forebrain.

One of the primary functions of VAX2 is its role in specifying the dorsoventral patterning of the retina during early embryonic development. VAX2 helps to determine the identity of retinal cells, ensuring that they develop into the appropriate cell types necessary for proper vision (Barbieri et al., 1999).

VAX2 is expressed in specific regions of the developing eye, including the optic vesicle and the optic cup (Kim and Lemke, 2006)(Fig. 35A). Its expression is tightly regulated and is influenced by other signalling molecules and transcription factors. Through a complex interplay of genetic interactions, VAX2 helps to establish the precise spatial organization of retinal cell types, such as retinal ganglion cells, amacrine cells, and bipolar cells (Mui et al., 2002).

Mutations or dysregulation of *VAX2* can lead to developmental abnormalities in the eye and brain. For example, *Vax2* inactivation in mice may result in defects in retinal patterning, which will lead to coloboma of the eye (Barbieri et al., 2002).

This gene was selected for analysis following knock-down of *xtr-miR-204-1* because of two reasons: firstly, *VAX2* is a computationally predicted target of *hsa-miR-204/211-5p*. Furthermore, it was selected because the observed deregulation of *tbx5* (Fig. 40), which is specifically expressed in the dorsal region of the eye. Because of that, we wanted to investigate whether *xtr-miR-204-1* can also play a role in the dorso-ventral patterning of the retinal cells. All of these reasons made of *vax2* an excellent candidate to investigate the gene regulatory network of *xtr-miR-204-1*.

As predicted by the bioinformatical analysis, from our preliminary data about the expression of *vax2* mRNA, we observed increased expression of this gene in the region of the choroid fissure, but not in other areas of the RPE, in 40% of the analysed embryos (n=15) (Fig. 35B, C).

However, this data was collected from a single *xtr-miR-204-1* knock-down experiment, and should be considered accordingly.

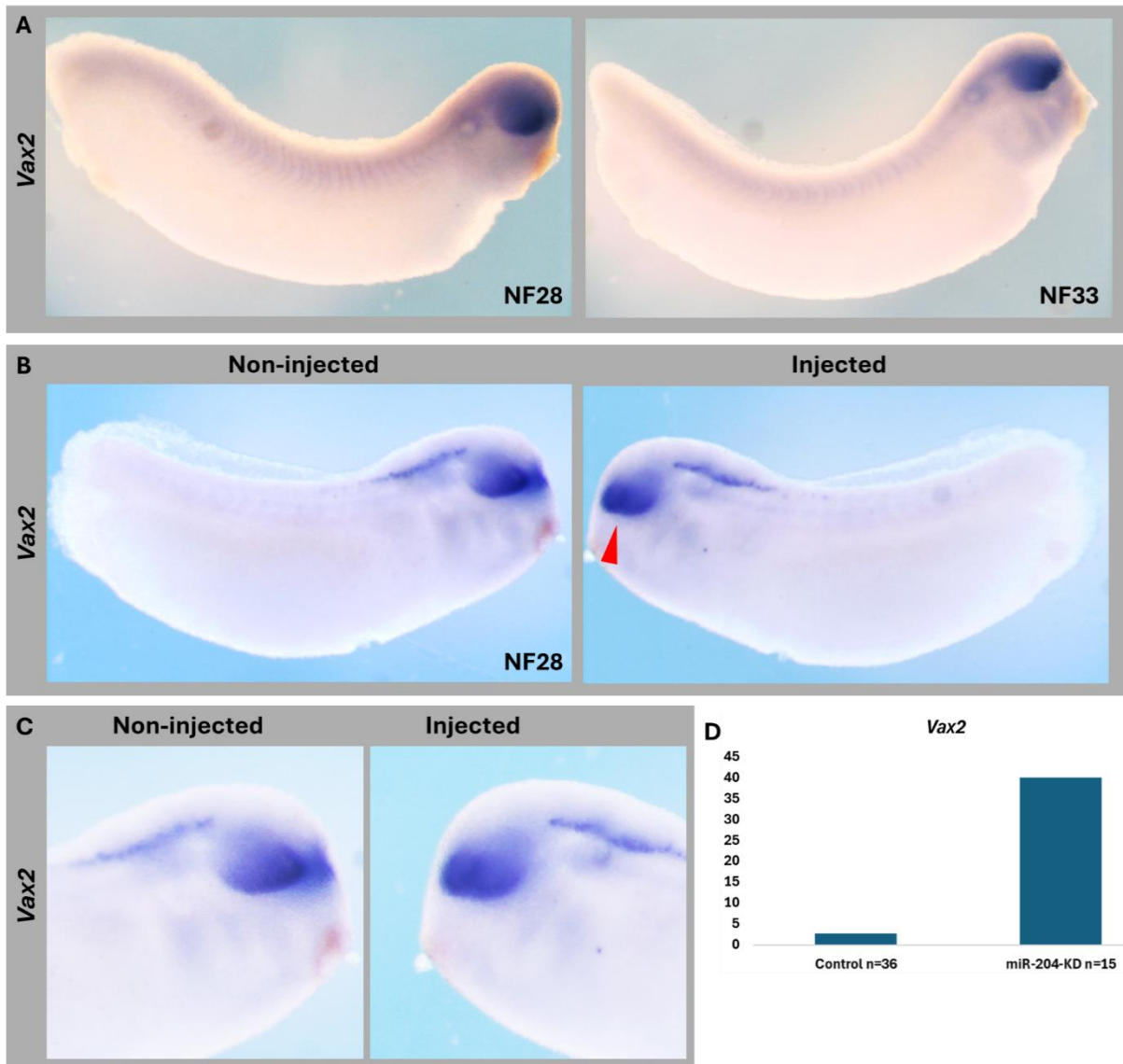


**Fig. 35: Effect of loss of *xtr-miR-204-1* on *vax2* mRNA expression. A)** Wild type expression of *vax2* on tailbud embryos (stage NF28, left picture and stage NF33 to the right). It is possible to appreciate the expression of *vax2* in the ventral side of the optic cup. **B-C)** Representative *xtr-miR-204-1* knocked-down embryo, at stage NF28, imaged from the non-injected side (left) and injected side (right). The expression of *vax2* is stronger in the optic cup of the injected side of the embryo, in particular in the region of the eye where the choroid fissure will form (red arrowhead), when compared to the non-injected side of the embryo. **D)** Percentage of embryos that show an expansion on the expression of *vax2* on the injected side in control or *xtr-miR-204-1* knock-down.

### **5.3 Effect of *xtr-miR-204-1* knock-down on the expression of genes that play a role in eye development**

Given the striking eye phenotypes observed on *Xenopus tropicalis* tadpoles following *xtr-miR-204-1* knock-down, we decided to investigate the expression of some key regulators of eye development in such condition.

The genes presented here are not predicted targets of *xtr-miR-204-1* and, therefore, we could not predict in advance what effect the knock-down of this gene could produce on their expression.

The genes that we selected for this part of the project are *trpm1*, *pax6*, *sox2*, *tyr*, *tbx5* and *pax2*.

#### 5.3.1 *Trpm1* expression in WT embryos and *xtr-miR-204-1* knock-down embryos

TRPM1 (Transient Receptor Potential Cation Channel Melastatin 1) protein is encoded by the *TRPM1* gene. This is a non-selective cation channel primarily expressed in the adult retina and melanocytes. In the retina, it is expressed in the ON bipolar cells, which form synapses with either cones or rods. When there is low light coming from the environment, glutamate is released, and activates mGluR6 which will, in turn, close the TRPM1 channel, preventing the influx of sodium and calcium in the cell, and keeping it polarised.

On the other hand, when there is enough light in the environment, glutamate is not released, mGluR6 is not active, and cannot close TRPM1. This will lead to influx of sodium and calcium in the cells, and to its depolarisation.

This mechanism of light response in which TRPM1 operates is important for night vision, and it is therefore not surprising that mutations in *TRPM1* can lead to stationary night blindness (Chubanov et al., 2024).

By trying to identify genes that might be regulated by *xtr-miR-204-1*, one of the first genes that we decided to assess was *trpm1*. The choice fell on this gene for two distinct reasons; the first one is that TRPM1 can heterodimerise with TRPM3, which has been proven to be targeted by *hsa-miR-204-5p* (*xtr-miR-204-2-5p*, in *Xenopus*) (Huang et al., 2020). Since *xtr-miR-204-1-5p* and *xtr-miR-204-2-5p* share the same sequence, and are both expressed in the RPE, this means that *xtr-miR-204-1-5p* has the same potential to

target *trpm3*. If this is true, it means that in absence of this miRNA, *trpm3* might be overexpressed, and an excess of TRPM3 might promote the repression of its partner, TRPM1.

The second reason why we chose this gene is because it is not uncommon for a mirtron to regulate to some extent the expression of its host gene (Salim et al., 2022), as in the case of *hsa-miR-204* and *trpm3* (Shiels, 2020).

*Trpm1* is not a predicted target of *xtr-miR-204-1-5p* since there are no binding sites in its 3'UTR for this miRNA. Therefore, in case of deregulation of this miRNA, any variation in the expression of *trpm1* could be attributed to some indirect effect, or to the loss of the intron caused by our CRISPR-Cas9 knock-down experiment.

In this case, following knock-down of *xtr-miR-204-1*, we observed a reduction in both intensity and area of expression of *trpm1* expression in the RPE. This happened in 50% of the injected embryos (n=36), while in only 7% of the control embryos there was a mild reduction of the expression of this gene on the injected side (n=28) (Fig. 36). This result might indicate that, even in those tadpoles where microphthalmia is not present, knock-down of *xtr-miR-204-1* might result in vision defects caused by downregulation of *trpm1*.

It is interesting how the expression of *trpm1* positively correlates with the expression of its mirtron, *xtr-miR-204-1*, and it definitely needs further investigation to understand the feedback underlying this regulation.

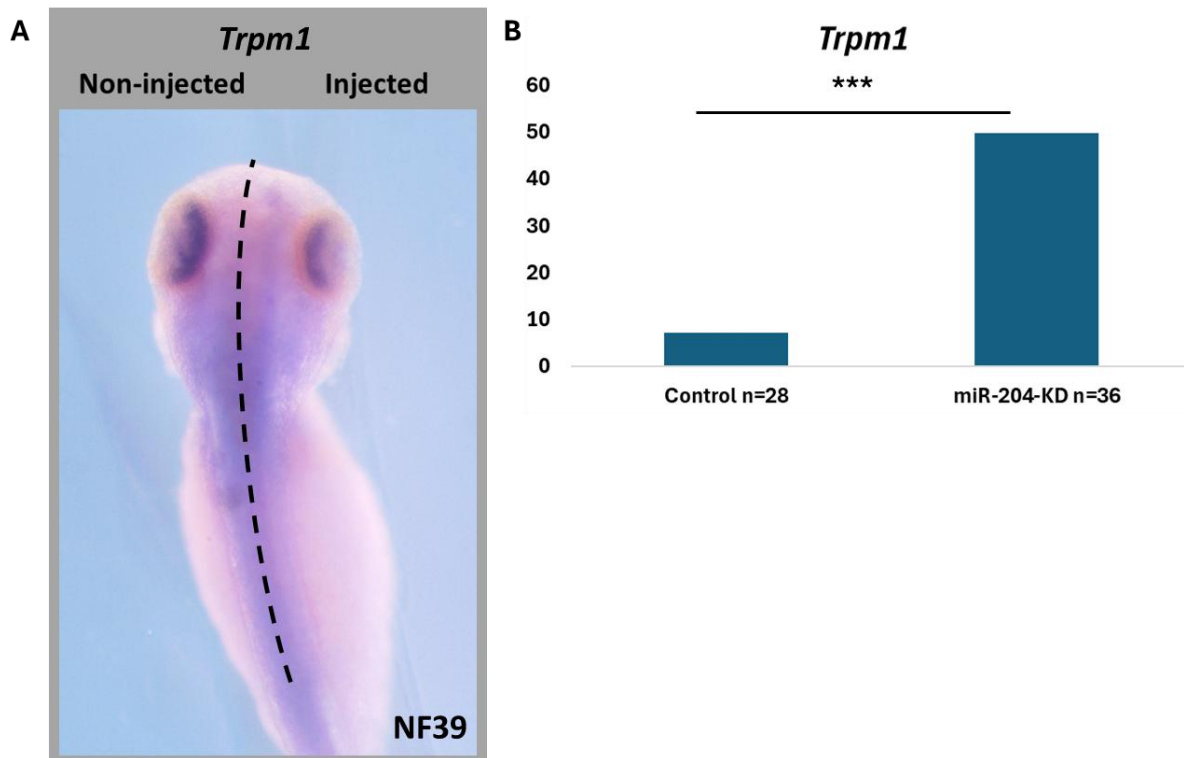


**Fig. 36: Effect of loss of *xtr-miR-204-1* on *trpm1* mRNA expression.** **A)** Dorsal view of representative *xtr-miR-204-1* knocked-down embryo, at stage NF39. Both intensity and extension of the expression of *trpm1* is reduced in the knocked-down side of the embryo, when compared to the control. **B)** Percentage of embryos that show a reduced expression of *trpm1* on the injected side in control or *xtr-miR-204-1* knock-down. \*\*\* $p < 0.001$ .

### 5.3.2 Pax6 expression in WT embryos and *xtr-miR-204-1* knock-down embryos

*PAX6* (Paired Box 6) is a crucial gene that plays a fundamental role in embryonic development, particularly in the development of the eyes and central nervous system (CNS). This gene encodes for a transcription factor, PAX6, which is often referred to as a master regulator of eye development.

One of the most striking aspects of *PAX6* is its evolutionary conservation—it is found in a wide range of organisms, from fruit flies to humans, indicating its critical role in development across species. During embryonic development, *PAX6* is expressed in specific regions that give rise to the eyes and CNS. It plays a pivotal role in the formation of the optic vesicle, which later develops into the retina, and the lens placode, which gives rise to the lens of the eye (Wawersik et al., 2000). Its expression, on its own, can drive the formation of ectopic eyes in permissive tissues (Chow et al., 1999).

In the CNS, PAX6 is essential for the development of the forebrain, including structures such as the cerebral cortex, hippocampus, and olfactory bulb. It regulates the proliferation and differentiation of neural progenitor cells, which give rise to different types of neurons and glial cells. PAX6 also plays a role in establishing regional identity within the developing brain, helping to define the boundaries between different brain regions.

In humans, mutations in the *PAX6* gene have been linked to various eye disorders, including aniridia, and Peters anomaly, which involves abnormalities in the cornea and lens (Lima Cunha et al., 2019).

The choice of this gene as potentially involved in *xtr-miR-204-1* gene regulatory network was driven by the fact that *PAX6* is one of the most important genes involved in eye development, even though this gene is not a computationally predicted target of *hsa-miR-204/211-5p*.

Indeed, following knock-down of *xtr-miR-204-1*, the expression of *pax6* was reduced in the injected side, compared to the uninjected side of the same embryo, in 32% of the analysed tadpoles (n=37). This was significantly higher than the control group, in which only 5% of the embryos showed a reduced expression between injected and uninjected side (n=41) (Fig. 37). From these results, we could conclude that the reduction of the expression of *xtr-miR-204-1* can indirectly impact on the expression levels of *pax6* mRNA.

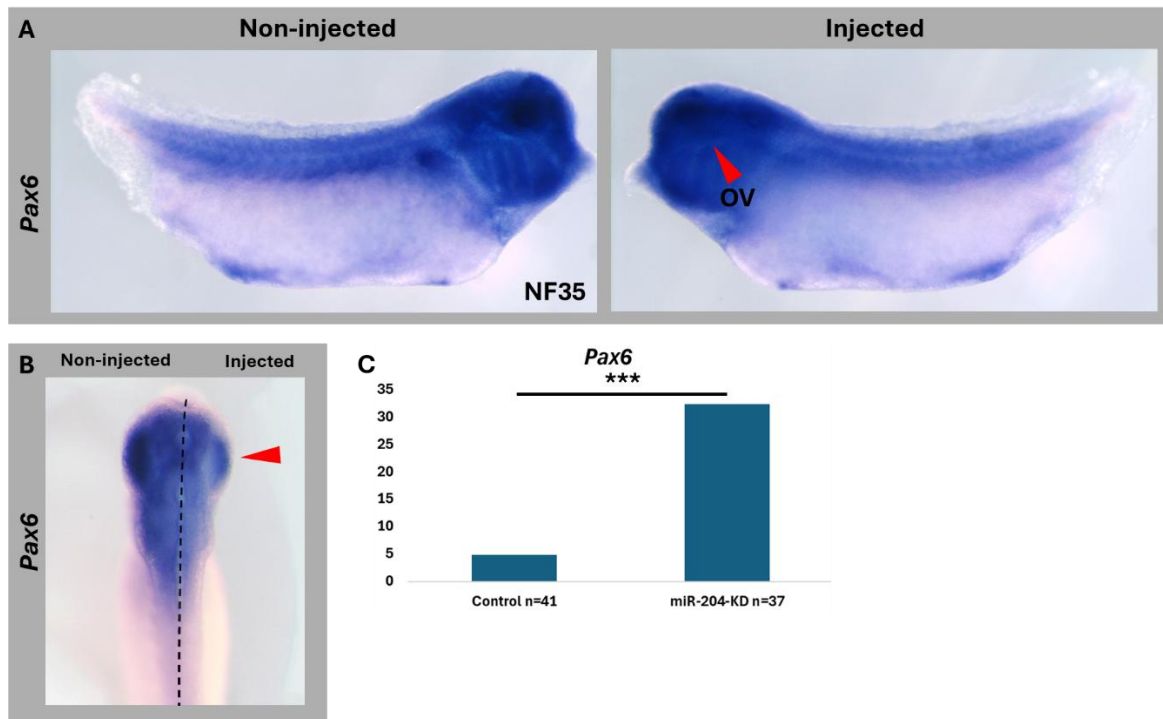


**Fig. 37: Effect of loss of *xtr-miR-204-1* on *pax6* mRNA expression. A)** Representative *xtr-miR-204-1* knocked-down embryo, at stage NF35, imaged from the non-injected side (left) and injected side (right), showing the reduced expression of *pax6* mRNA. It is possible to observe a global reduction of *pax6* expression in the developing eye (red arrowhead). **B)** Representative *xtr-miR-204-1* knocked-down embryo imaged from the dorsal side, which has been knocked-down on the right side. There is a clear reduction of the expression of *pax6* mRNA expression on the injected side, in comparison to the non-injected side. This reduction is particularly evident in the optic cup (red arrowhead). **C)** Percentage of embryos that show a reduced expression of *pax6* in the optic cup in the injected side, in comparison to the non-injected side of the embryos. \*\*\* $p < 0.001$ . Figure legend: OV, optic vesicle.

### 5.3.3 *Sox2* expression in WT embryos and *xtr-miR-204-1* knock-down embryos

SOX2 (SRY-box 2), is a crucial gene that plays a fundamental role in embryonic development and stem cell pluripotency. It belongs to the Sox family of transcription factors, which are characterized by a conserved high-mobility group DNA-binding domain.

SOX2 was first identified as a gene involved in the determination of cell fate in the developing embryo (Uwanogho et al., 1995). It is highly expressed in embryonic stem cells (ESCs) and plays a central role in maintaining their pluripotent state. Along with OCT4, NANOG, and KLF5, SOX2 forms a regulatory network that controls the expression

of genes responsible for maintaining pluripotency while repressing differentiation-related genes. This network is essential for the self-renewal and differentiation capabilities of embryonic stem cells (Takahashi and Yamanaka, 2006).

Additionally, SOX2 is involved in the development of various tissues and organs throughout the body, including the nervous system, eyes, and inner ear (Feng and Wen, 2015).

Mutations or dysregulation of SOX2 expression have been associated with developmental disorders such as anophthalmia, microphthalmia, and other craniofacial abnormalities (Williamson et al., 1993). Furthermore, SOX2 expression has been found to be dysregulated in various types of cancer, including lung cancer, breast cancer, and glioblastoma. In cancer cells, SOX2 can promote tumour growth, invasion, and metastasis (Wuebben and Rizzino, 2017).

Because of its role in the nervous system and eye development, this gene has been selected for further investigation following knock-down of *xtr-miR-204-1*. However, this gene is not a computationally predicted target of this miRNA, and it is not supposed to be expressed in the same cell type as *xtr-miR-204-1* (Ward et al., 2018). Therefore, if present, any alteration in the expression pattern of this gene would likely be attributed to indirect effects.

In fact, following knock-down of *xtr-miR-204-1*, we did not observe any visible changes in the expression pattern or levels of *sox10* mRNA in any of the 24 observed tadpoles (Fig. 38). This indicates that the observed phenotypes of microphthalmia and anophthalmia are likely attributed to the deregulation of other genes.

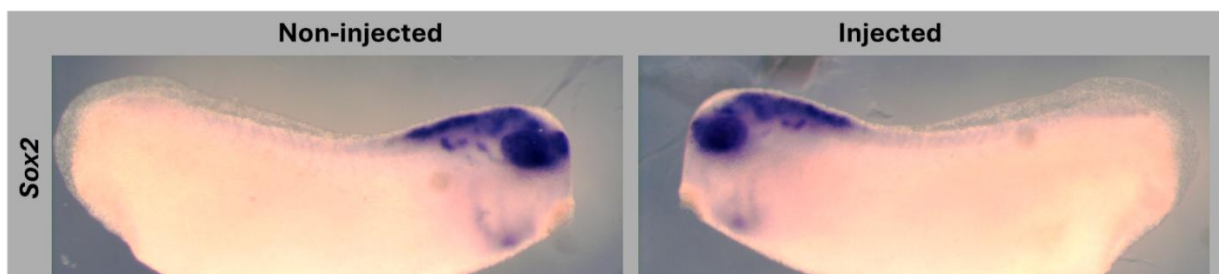


**Fig. 38: Expression of *sox2* mRNA following *xtr-miR-204-1* knock-down.** Representative *xtr-miR-204-1* knocked-down embryo, at stage NF27, imaged from the non-injected side (left) and injected side (right). No obvious differences have been observed in the expression pattern of *sox2* between the knock-down and wild type sides of the injected embryos.

#### 5.3.4 Tyr expression in WT embryos and xtr-miR-204-1 knock-down embryos

*TYR* (tyrosinase) is a critical enzyme involved in melanin biosynthesis, which plays a crucial role in determining the coloration of skin, hair, and eyes in humans and other animals. This enzyme catalyses two key reactions in the melanin synthesis pathway: the hydroxylation of the amino acid tyrosine to form L-DOPA (3,4-dihydroxyphenylalanine), and the subsequent oxidation of L-DOPA to form dopaquinone. These reactions are essential steps in the production of both eumelanin and pheomelanin, the two main types of melanin found in humans (Snyman et al., 2024).

Mutations in the *TYR* can lead to various forms of oculocutaneous albinism, a group of disorders characterized by a reduction or absence of melanin pigment in the skin, hair, and eyes. Individuals with oculocutaneous albinism typically display fair skin, light-coloured hair, and light-sensitive eyes, along with visual impairments due to abnormal development of the retina and optic nerve (Dolinska et al., 2014; Marcon and Maia, 2019). Furthermore, abnormalities in tyrosinase activity have been associated with various skin conditions, including vitiligo, a disorder characterized by the loss of melanocytes and depigmented patches on the skin (Jin et al., 2010). Evidence suggests that tyrosinase may play a role in regulating immune responses, as it is expressed in certain immune cells and has been shown to modulate the production of inflammatory mediators (Montagna et al., 2020).

The reason why this gene was selected for investigation in the context of *xtr-miR-204-1* knock-down is because *TYR* is co-expressed with *TRPM1*, and is also one of the known targets of *MITF* (Goding and Arnheiter, 2019). Its expression in WT embryos is in the melanocytes and in the RPE of the eye.

Following knock-down of *xtr-miR-204-1*, we did not observe any visible de-regulation in either melanocyte or in the RPE (Fig. 39). From this experiment we can conclude that, at least in *Xenopus tropicalis*, the expression of *tyr* is not dependent on the expression of *xtr-miR-204-1*.

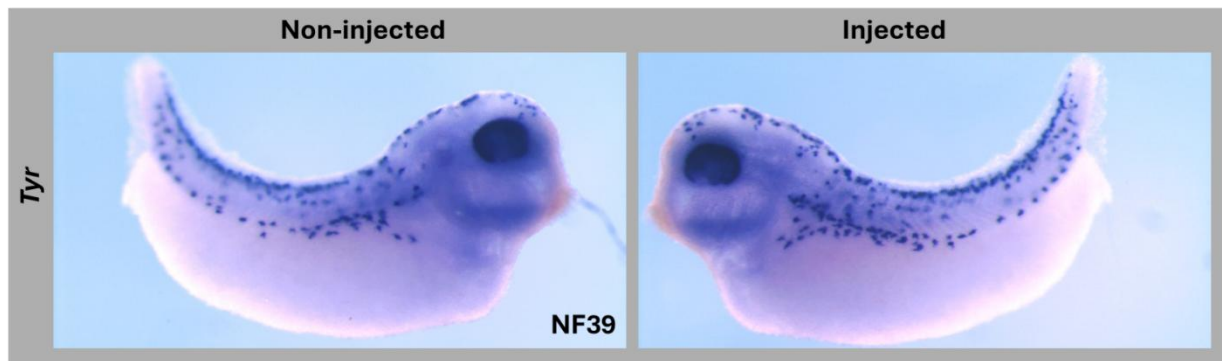


**Fig. 39: Expression of *tyr* mRNA following *xtr-miR-204-1* knock-down.** Representative *xtr-miR-204-1* knocked-down embryo, at stage NF38, imaged from the non-injected side (left) and injected side (right). No obvious differences have been observed in the expression pattern of *tyr* between the knock-down and wild type sides of the injected embryos.

#### 5.3.5 *Tbx5* expression in WT embryos and *xtr-miR-204-1* knock-down embryos

*TBX5* (T-box transcription factor 5) is a crucial gene that plays a pivotal role in embryonic development, particularly in the formation of limbs and the heart. It belongs to the T-box gene family, which encodes transcription factors involved in the regulation of developmental processes. This gene is highly conserved among species, including frogs and humans. Its expression pattern is tightly regulated both spatially and temporally during embryogenesis.

In limb development, *TBX5* is responsible for specifying the anterior-posterior axis and initiating the formation of forelimbs in vertebrates (Agarwal et al., 2003). Moreover, *TBX5* is a key regulator of cardiac morphogenesis, influencing the differentiation and patterning of various cardiac structures during embryonic development. It is particularly vital for the development of the atria and left ventricle. Mutations in *TBX5* have been associated with congenital heart diseases, including atrial and ventricular septal defects (Steimle and Moskowitz, 2017).

Other than its role in limb and heart development, *TBX5* is also involved in the development of the eye, and in particular in the morphological and topographical development of the retina. This gene is, in fact, expressed in the dorsal region of the optic cup and, at later stages of development, in the dorsal side of the retina, other than in the heart field (Fig. 40A). It is important to note that deregulation of *TBX5* can induce a

dorsalisation of the ventral side of the eye, leading to deregulation of ventral markers, such as *PAX2* and *VAX2* (Barbieri et al., 2002).

This gene has been selected to investigation following *xtr-miR-204-1* knock-down since we were interested in knowing if the dorso-ventral axes of the developing eye would have been affected. Indeed, what we observed was that, at later stages of development, 41% (n=29) of the analysed embryos displayed a mild expanded expression of *tbx5* in the eye. This was significantly more than in the control group, in which only 10% (n=29) of the embryos displayed a different expression of this gene between the two developing eyes (Fig. 40B, C).

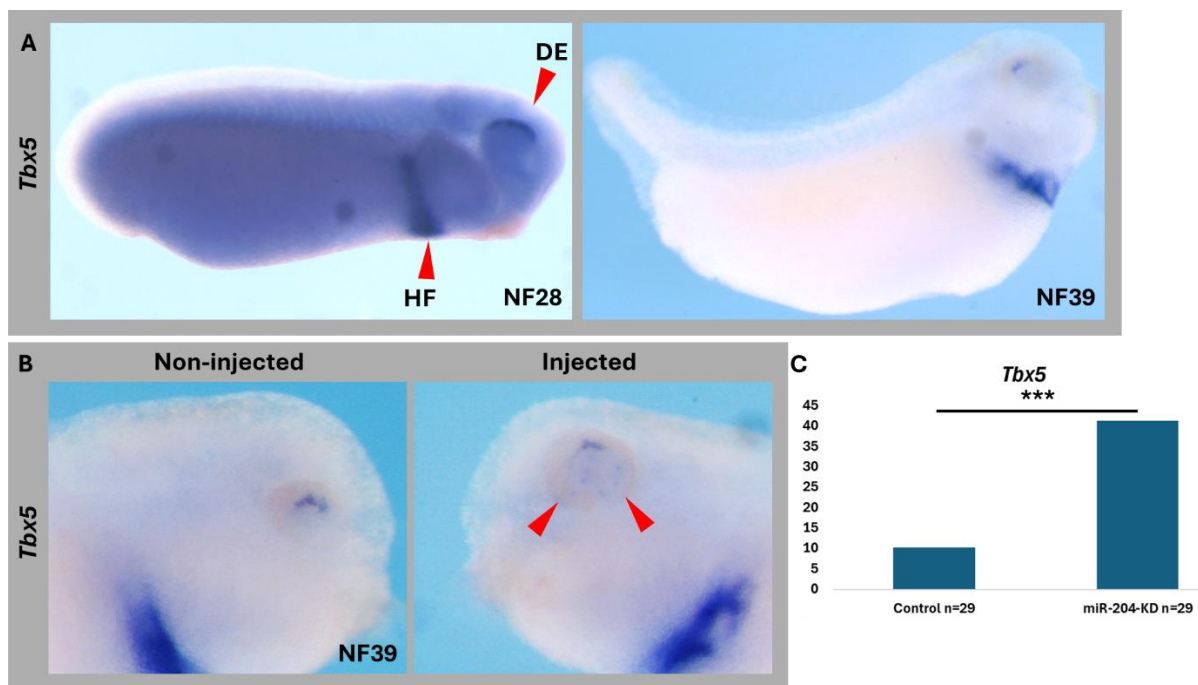


**Fig. 40: Effect of loss of *xtr-miR-204-1* on *tbx5* mRNA expression. A)** Wild type expression of *tbx5* on tailbud embryos (stage NF28, left picture) and tadpole embryos (stage NF39, right picture). It is possible to see the expression of *tbx5* in the heart field and on the dorsal side of the optic cup, at tailbud stage. At tadpole stages, the expression of *tbx5* is consistently in the heart field and in the dorsal side of the RPE. **B)** Detail of the head of a representative *xtr-miR-204-1* knocked-down embryo, at stage NF39, imaged from the non-injected side (left) and injected side (right). The expression of *tbx5* extends from the dorsal side of the RPE to the ventral side (red arrowheads), compared to the non-injected side of the embryo. **C)** Percentage of embryos that show an expansion on the expression of *tbx5* on the injected side in control or *xtr-miR-204-1* knock-down. \*\*\*p<0.001. Figure legend: DE, dorsal eye; HF, heart field.

### 5.3.6 Pax2 expression in WT embryos and xtr-miR-204-1 knock-down embryos

*PAX2* (Paired Box Gene 2), belongs to the PAX gene family, which encodes a group of transcription factors that are vital for the development of multicellular organisms. These genes are highly conserved across species, indicating their fundamental role in evolutionary biology. *PAX2* is primarily involved in the development of several organs during embryogenesis, including the CNS, kidneys, eyes, and ears. It regulates the expression of numerous target genes involved in various cellular processes such as proliferation, differentiation, and apoptosis.

In the embryonic kidney, *PAX2* is expressed in the intermediate mesoderm, where it plays a pivotal role in the formation of the pronephric duct, which later gives rise to the entire urinary system (Eccles et al., 2002). *PAX2* mutations or dysregulation can lead to severe renal abnormalities, such as renal hypoplasia or agenesis (Dressler and Woolf, 1999).

*PAX2* is also crucial for the development of the eye, particularly the formation of the optic nerve, retina, and lens. It regulates the expression of genes involved in eye morphogenesis and differentiation of retinal cell types. Mutations in *PAX2* can cause ocular malformations like coloboma (Bower et al., 2012).

During neural tube development, *PAX2* is expressed in specific regions of the CNS, where it regulates the differentiation of neurons and glial cells. In fact, disruption of *PAX2* might lead to neurodevelopmental disorders such as autism spectrum disorder, seizures, and intellectual disabilities (Lv et al., 2021).

The key role of *PAX2* in the development of the eye, together with its overlapping expression with *xtr-miR-204-3p* made *pax2* an excellent candidate to investigate the role of *xtr-miR-204-1* during *Xenopus* development. Indeed, what we observed from our preliminary data was a general downregulation of *pax2* mRNA expression in all the tissues where this gene is expressed. This include the otic vesicle in 33% of the analysed embryos, in the optic cup in 14% of the embryos, and in the pronephric kidney in 14% of the analysed embryos (n=15 for early tailbud stages, and n=6 for tadpole stages) (Fig. 41B, C).

Similarly to the *vax2* experiment (paragraph 5.1.14), these are preliminary data that were obtained by a single *xtr-miR-204-1* knock-down experiment, and should be confirmed by increasing the number of observations.

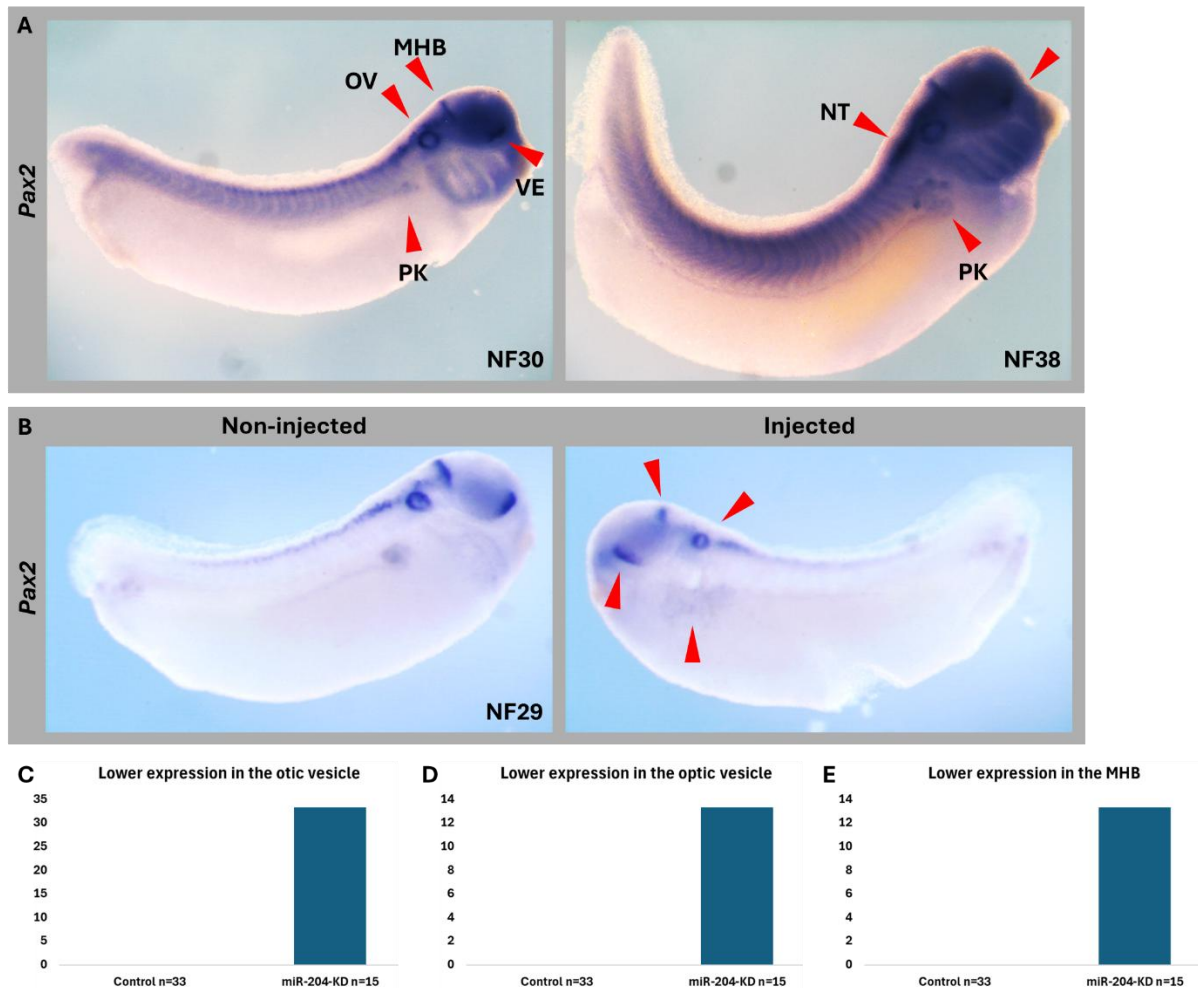


**Fig. 41: Effect of loss of *xtr-miR-204-1* on *pax2* mRNA expression.** **A)** Wild type expression of *pax2* on tailbud (stage NF30, left picture) and tadpole embryos (stage NF38, right picture). It is possible to appreciate the expression of *pax2* in the ventral side of the optic cup, in the neural tube, in the otic vesicle, in the midbrain-hindbrain boundary (MHB) and in the pronephric kidney (red arrowheads) across both developmental stages. **B)** Representative *xtr-miR-204-1* knocked-down embryo, at stage NF29, imaged from the non-injected side (left) and injected side (right). The expression of *pax2* is reduced in the optic cup of the injected side of the embryo, as well as in the MHB, in the otic vesicle and in the pronephric kidney (red arrowheads), when compared to the non-injected side of the embryo. **C-E)** Percentage of embryos that show a reduced expression of *pax2* on the injected side in control or *xtr-miR-204-1* knock-down in the otic vesicle, optic vesicle and in the MHB. Figure legend: OV, otic vesicle; MHB, midbrain-hindbrain boundary; VE, ventral eye; PK, pronephric kidney; NT, neural tube.

#### **5.4 Effect of *xtr-miR-204-1* knock-down on the expression of NC specifiers**

Since *xtr-miR-204-1* was selected from a list of miRNAs that were computationally predicted to be expressed and important during NC development, we decided to test this theory by analysing the expression of two key regulators of NC development, *sox10* and *snai2*.

These two genes, *sox10* and *snai2*, were selected aside from *tfap2a* and *tfap2b*, also known for their role during NC development, since the last two were also computationally predicted to be targets of *xtr-miR-204-1*, and we decided to test more NC-specific genes that might also be affected by the lack of this miRNA, even though in an indirect manner.

What we expected from these experiments was a negative effect on the expression of these genes on one or more NC derivatives, at the investigated stages of development, likely the eye or the melanocytes, where we know from literature that *trpm1* is expressed.

##### 5.4.1 *Sox10* expression in WT embryos and *xtr-miR-204-1* knock-down embryos

*SOX10* (SRY-box 10), encodes a transcription factor that is crucial for the development of the NC. *SOX10* is expressed in NCCs and is essential for their survival, proliferation, migration, and differentiation into different cell types, including glial cells and melanocytes (Pingault et al., 2022).

In the nervous system, *SOX10* is involved in the development of several structures, including the peripheral nervous system (PNS) and enteric nervous system (ENS). It regulates the expression of genes involved in the differentiation of Schwann cells, which are crucial for the myelination of peripheral nerves (Bondurand and Sham, 2013).

*SOX10* also plays a pivotal role in the development of melanocytes, which are responsible for skin, hair, and eye pigmentation (Marathe et al., 2017).

Mutations in *SOX10* can lead to disorders such as Waardenburg syndrome and Hirschsprung disease. Waardenburg syndrome is a genetic disorder characterized by hearing loss and pigmentary abnormalities of the hair, skin, and eyes. Some individuals with Waardenburg syndrome may experience abnormalities in the development of the inner ear, leading to hearing loss (Bertani-Torres et al., 2023). Hirschsprung disease, also

known as congenital aganglionic megacolon, is characterized by the absence of innervation in the colon, resulting in severe constipation or intestinal obstruction (Lotfollahzadeh et al., 2021).

*Sox10* was chosen as potentially involved in *xtr-miR-204-1* GRN because of its pivotal role in NC development. Also, since *SOX10* is co-expressed with *TRPM1* and *hsa-miR-211* in the melanocytes and, with *xtr-miR-204-1* in the otic vesicle, they might regulate each other in one of these tissues.

After knock-down of *xtr-miR-204-1*, we were able to observe only a mild reduction in the expression of *sox10* in the branchial arches and in the otic vesicle in 36% of the injected embryos at earlier stages of development (n=45) (Fig. 42A). However, at later stages of development, we observed a severe loss of *sox10* expression in the melanocytes on the injected side of the embryos, which occurred on 48% of the injected embryos (n=31). This was significantly higher than in the control embryos, where we were not able to observe any significant reduction in any of them (n=39) (Fig. 42B).

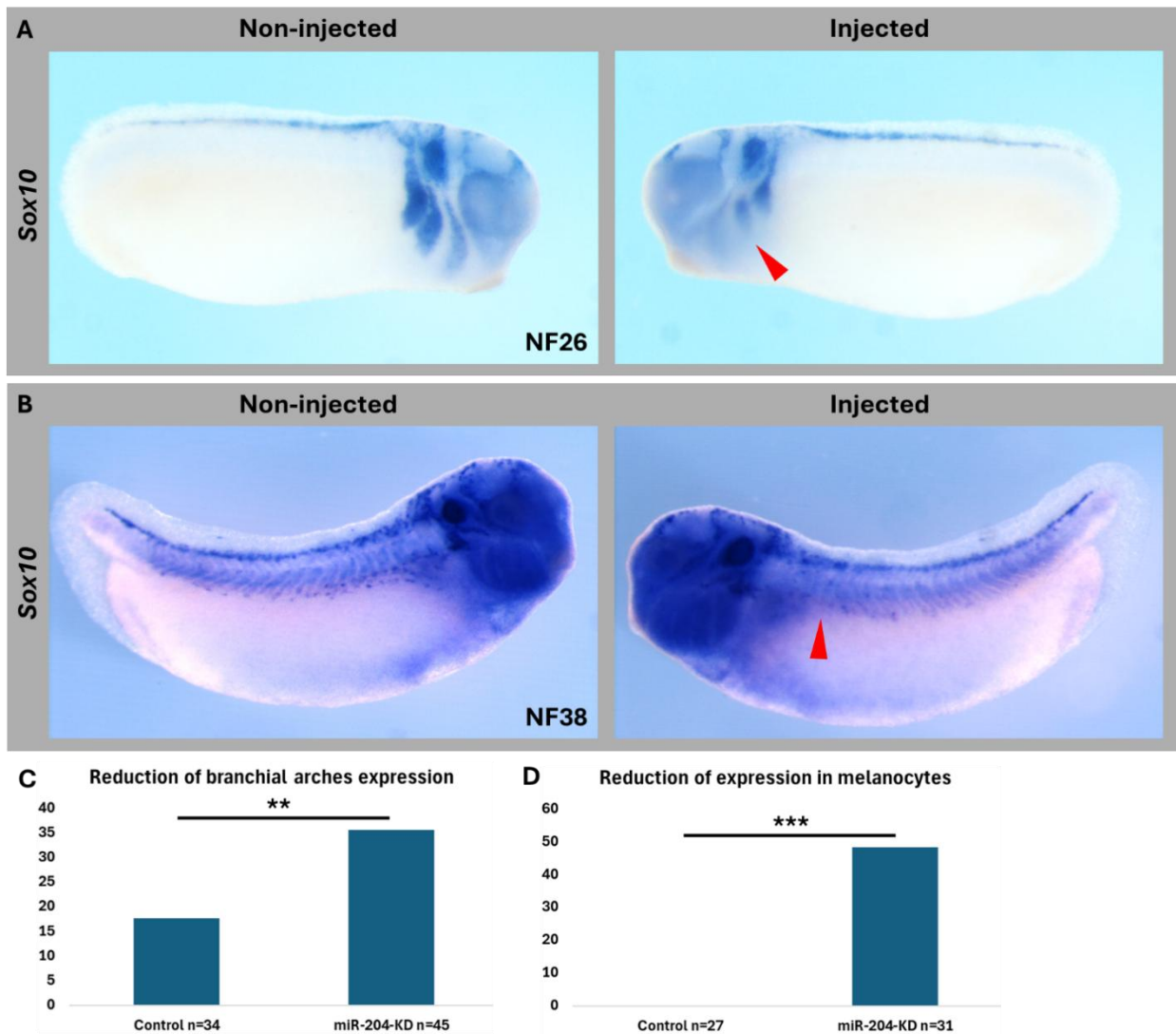


**Fig. 42: Effect of loss of *xtr-miR-204-1* on *sox10* mRNA expression. A)** Representative *xtr-miR-204-1* knocked-down embryo, at stage NF26, imaged from the non-injected side (left) and injected side (right), showing the reduced expression of *sox10* mRNA in the branchial arches (red arrowhead). **B)** Representative *xtr-miR-204-1* knocked-down embryo, at stage NF38, imaged from the non-injected side (left) and injected side (right), showing the reduced expression of *sox10* mRNA in the melanocytes population (red arrowhead). **C-D)** Percentage of embryos that show a reduced expression of *sox10* in the branchial arches in the injected side of stage NF26 embryos, and reduced expression of *sox10* in the population of melanocytes, in comparison to the non-injected side of the embryos. \*\* $p < 0.01$ , \*\*\* $p < 0.001$ .

#### 5.4.2 Snai2 expression in WT embryos and xtr-miR-204-1 knock-down embryos

*SNAI2*, previously known as *SLUG*, is a member of the Snail family of zinc finger transcription factors, which include *SNAI1*, *SNAI2* and *SNAI3*. It plays a crucial role in various biological processes, particularly in embryonic development, tissue differentiation, and cancer progression.

One of the primary functions of *SNAI2* is its involvement in the EMT, a process by which epithelial cells lose their characteristics and acquire properties of mesenchymal cells. EMT is crucial during embryonic development for NCCs migration (Nieto et al., 2016).

In embryonic development, *SNAI2* is mainly expressed in the developing NC, where it regulates cell migration and differentiation. *SNAI2* regulates the delamination and migration of NCCs from the neural tube, which is essential for their proper distribution and differentiation during development (Shi et al., 2011).

In cancer biology, *SNAI2* is often upregulated in various types of cancers, including breast, lung, colon, and prostate cancers. Its overexpression correlates with advanced tumour stage, metastasis, and poor patient prognosis. As in development, in cancer cells, *SNAI2* promotes EMT by repressing the expression of epithelial markers while inducing the expression of mesenchymal markers. This phenotypic switch enhances cancer cell motility, and invasiveness (Alves et al., 2018).

*SNAI2* is often used as a marker for NC development, and its expression correlates well with the expression of *SOX10* (Li et al., 2019b). For this reason, *snai2* has been selected for further investigation following *xtr-miR-204-1* knock-down.

Similarly to *sox10* expression, following *xtr-miR-204-1* knock-down the main effect on the expression pattern of *snai2* was a partial to complete loss of expression in the melanocytic population, which we observed in 27% of the injected embryos (n=27), and that we did not observe in any of the control embryos (n=30) (Fig. 43).

This data, combined with the results of *sox10* expression, indicate that *xtr-miR-204-1* plays an important role in melanocyte development. This role might include the terminal differentiation of melanocytes. However, further studies need to be carried out in order to investigate the exact mechanism underlying this process, especially considering that

the expression of *tyr* and the number of melanocytes in knocked-down tadpoles seem to be unaltered (Fig. 39).

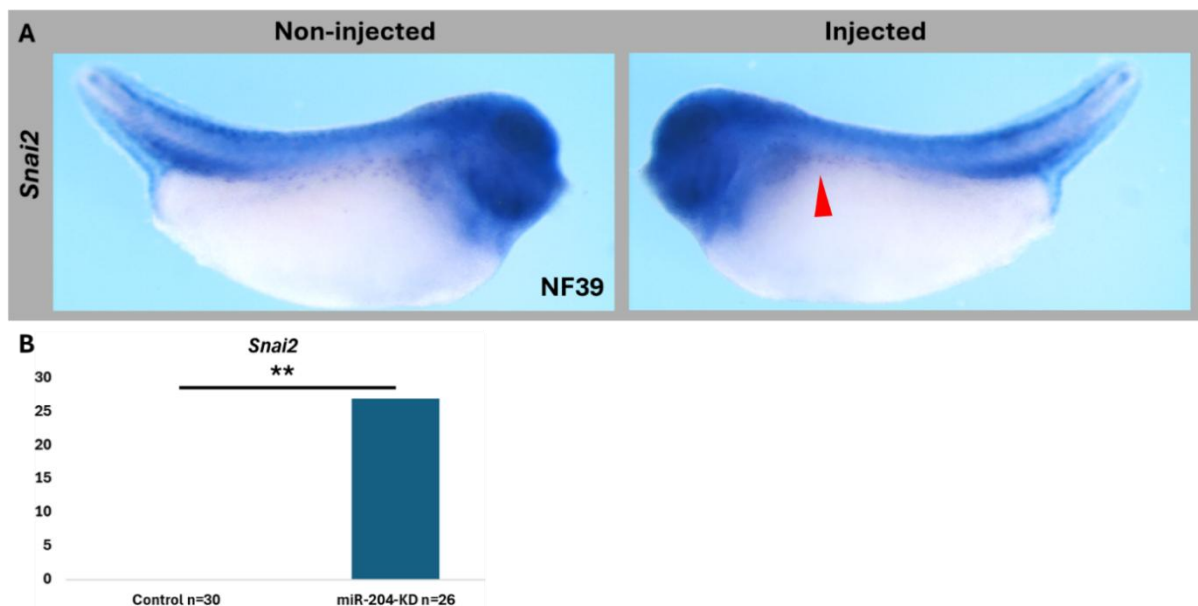


**Fig. 43: Effect of loss of *xtr-miR-204-1* on *snai2* mRNA expression. A)** Representative *xtr-miR-204-1* knocked-down embryo, at stage NF39, imaged from the non-injected side (left) and injected side (right), showing the reduced expression of *snai2* mRNA. It is possible to observe a reduction of *snai2* expression in the population of melanocytes, when comparing to the non-injected side of the embryo (red arrowhead). **B)** Percentage of embryos that show a reduced expression of *snai2* in the population of melanocytes of the injected side, in comparison to the non-injected side of the embryos. \*\* $p < 0.01$ .

### 5.5 Effect of *xtr-miR-204-1* knock-down on the expression of selected predicted targets expressed in the pronephric kidney

Since we observed expression of *xtr-miR-204-1* in the pronephric kidney, and also a variation in the expression of *pax2* in this organ following knock-down of this miRNA, we speculated that it might be playing a role in the pronephric kidney as well.

Because of this, we decided to investigate if *xtr-miR-204-1* might be regulating the expression of some predicted direct targets also in this organ.

To do so, we shortlisted from the list of computationally predicted targets of *xtr-miR-204-1* obtained using TargetScan 8.0 two genes that are known from the literature to be expressed in the pronephros as well. Therefore, we decided to use *cox5a* and *ndrg3*, which answer all these criteria.

### 5.5.1 Cox5a expression in WT embryos and xtr-miR-204-1 knock-down embryos

COX5a (Cytochrome C Oxidase Subunit 5a) is the terminal enzyme of the respiratory chain, and for this reason is mainly expressed in the inner membrane of the mitochondria. This step requires a multiprotein complex that includes 13 subunits (Moe et al., 2023). The metabolic function of the respiratory chain is to produce ATP, after glycolysis and the Krebs cycle (Haddad and Mohiuddin, 2024).

Given the important role in providing cells with energy, it is no surprise that this gene is highly expressed in different tissues. However, by checking the expression of this gene by WISH at tadpole stage, it is possible to appreciate some tissues where this gene is upregulated in comparison to the rest of the embryo. These tissues include several regions of the head, somites, and the pronephric kidney (Fig. 44A).

Loss of function of this protein can result in a wide range of phenotypes, from mild hypotonia and mild muscle weakness to more severe conditions in which also heart, brain and liver are heavily affected.

The reason why this gene was selected is because, by using bioinformatical tools, its transcript is one of the most likely to be targeted by *hsa-miR-204-5p* (within the top 10 predicted targets). Also, the expression pattern partially overlaps with the expression of *xtr-miR-204-1-3p*, with respect to the pronephric and head staining, meaning that these two genes are potentially expressed together (Fig. 44A).

Following *cox5a* WISH on knock-down embryos, we did not observed an obvious increase/expansion of the expression of this gene in the head region, in comparison to the uninjected side. However, in 31% of the observed embryos (n=35), we observed an increase in the staining in the pronephric kidney (in both glomerulus and tubule). This increase was significantly different from the control embryos, in which only in 8% (n=36) there was a difference in the expression level between the injected and uninjected side (Fig. 44B, C).

This data is consistent with the fact that *COX5a* is a predicted target of *hsa-miR-204/211-5p*, and with the fact that *xtr-miR-204-1-3p* WISH stains the pronephros and pronephric duct (Fig. 44). It will be interesting to investigate if the regulation of *cox5a* in the

developing pronephros operated by *xtr-miR-204-1-5p* plays a functional role in the correct development of this organ. Also, further investigation is needed to assess if, in the absence of *xtr-mir-204-1*, *cox5a* is upregulated because of a direct interaction with the miRNA, or because of a secondary effect.

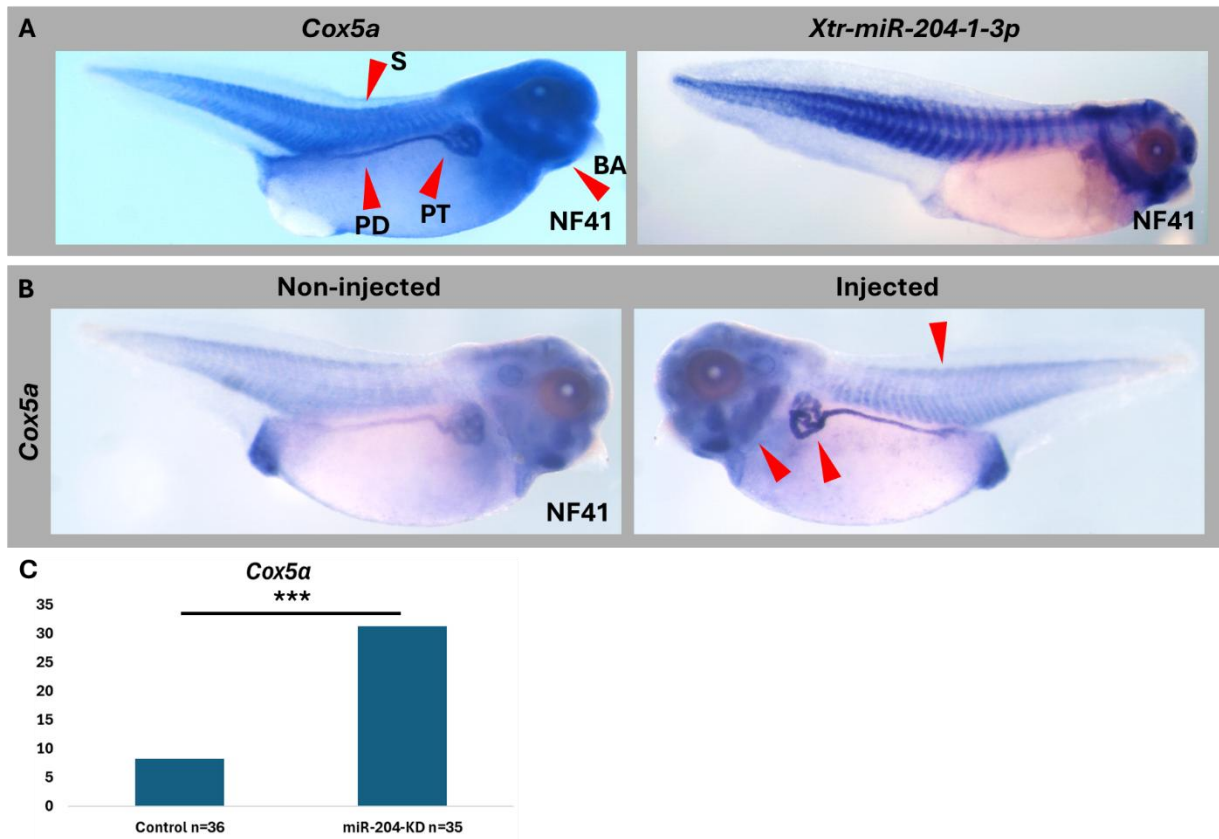


**Fig. 44: Effect of loss of *xtr-miR-204-1* on *cox5a* mRNA expression.** **A)** Wild type expression of *cox5a* (left) and *xtr-miR-204-1-3p* (right) on stage NF41 embryos. As indicated by the red arrowheads, the expression is stronger in the somites, pronephric kidney and duct, and in the branchial arches for both genes. **B)** Representative *xtr-miR-204-1* knocked-down embryo, at stage NF41, imaged from the non-injected side (left) and injected side (right). The expression in the branchial arches, somites and pronephros is stronger in the injected side, in comparison to the non-injected side of the same embryo. **C)** Percentage of embryos that show an increased expression of *cox5a* on the injected side in control or *xtr-miR-204-1* knock-down. \*\*\*p<0. Figure legend: BA, branchial arches; PD, pronephric duct; PT, pronephric tubule; S, somites.

### 5.5.2 *Ndr3* expression in WT embryos and *xtr-miR-204-1* knock-down embryos

NDRG3 (N-Myc Downstream-Regulated Gene 3 Protein) belongs to a family of proteins that includes four members: NDRG1, NDRG2, NDRG3 and NDRG4. This family of protein belongs to the hydrolases superfamily.

Not much is known about the specific role of this gene during development. However, several studies pinpointed the role of *NDRG3* in cancer. In particular, it has been observed that high levels of NDRG3 positively correlates with reduced apoptosis and increased proliferation and migration in gastric cancer and, therefore with poor prognosis of patients with this type of cancer (Jing et al., 2018; Liu et al., 2021b; Wang et al., 2023).

Even though the expression of the *ndrg* genes has been already assessed in several animal models, including *Xenopus tropicalis*, during embryo development (Zhong et al., 2015) the precise, functional role of these genes in development still needs to be elucidated.

The reason why this gene has been selected for further investigation in the *xtr-miR-204-1* knock-down embryos is because it is one of the most promising direct targets of *hsa-miR-204/211-5p* according to bioinformatical tools (TargetScan8.0, MiRanda, DIANA). Also, the expression of this gene partially overlaps with the expression pattern observed for *xtr-miR-204-1-3p* assessed by WISH. In particular, at later stages of development (stage NF 41), it is possible to see expression of this gene in the head region, particularly in the RPE, in the somites, and in the pronephros (Fig. 45A).

Indeed, in *xtr-miR-204-1* knock-down embryos, the expression of *ndrg3* was significantly increased in the injected then in the non-injected side in 45% of the analysed embryos (n=31) in the pronephric kidney and duct in comparison to the control group (6.9%, n=29) (Fig. 45B, C). This increase, however, was not as strong as the signal that we observed for the expression of *cox5a* in the pronephric kidney area (Fig. 44B).

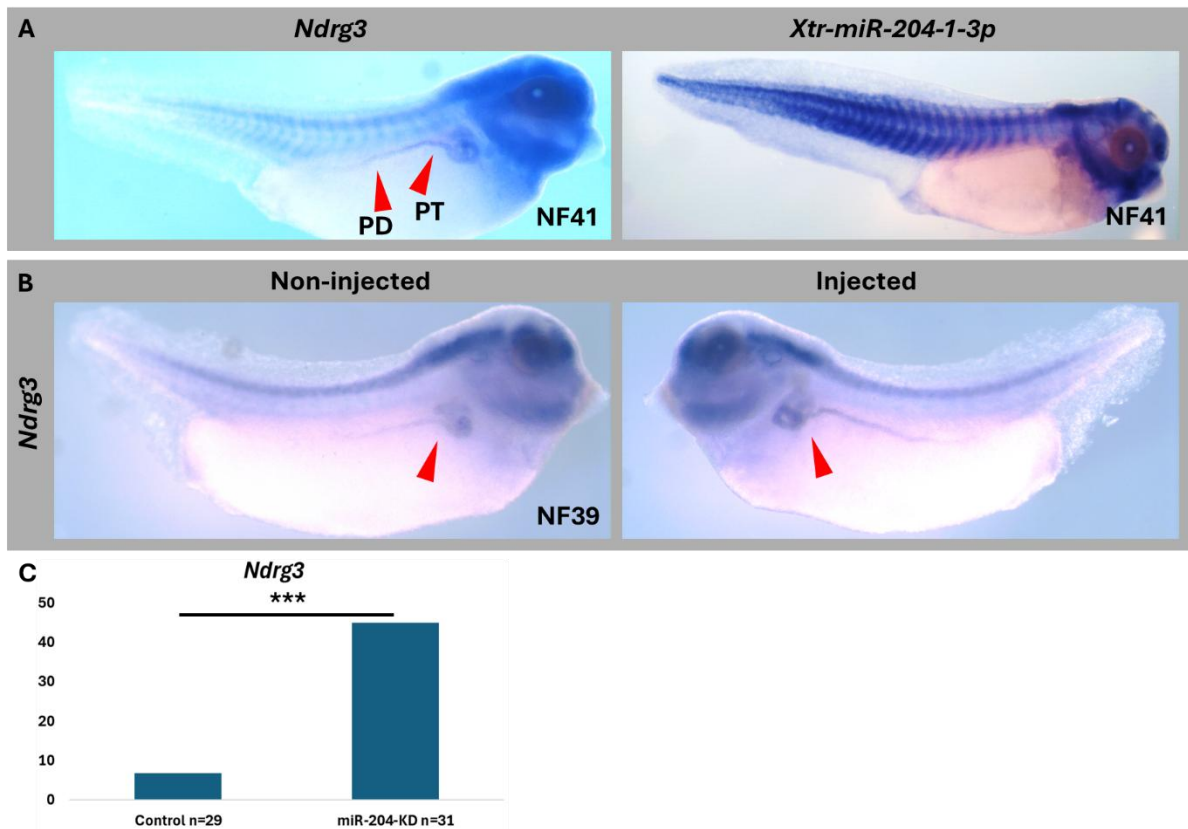


**Fig. 45: Effect of loss of *xtr-miR-204-1* on *ndrg3* mRNA expression. A)** Wild type expression of *ndrg3* (left) and *xtr-miR-204-1-3p* (right) on stage NF41 embryos. As indicated by the red arrowheads, the expression is stronger in the pronephric kidney and duct for both genes. **B)** Representative *xtr-miR-204-1* knocked-down embryo, at stage NF39, imaged from the non-injected side (left) and injected side (right). The expression in the pronephros is stronger, and the duct longer in the injected side, in comparison to the non-injected side of the same embryo. **C)** Percentage of embryos that show an increased expression of *ndrg3* on the injected side in control or *xtr-miR-204-1* knock-down. \*\*\* $p < 0.001$ . Figure legend: PD, pronephric duct; PT, pronephric tubule.

## **Chapter 6: General discussion and concluding remarks**

Increasing evidence has shown how miRNAs can play a central role during embryogenesis both in physiological and pathological contexts. Studies from our lab have shown that the correct development of the NC is also relying on miRNAs (Antonaci and Wheeler, 2022; Godden et al., 2022; Ward et al., 2018). However, to date, the full extent of the role that these molecules play during NC development have not been fully explored.

In this study, we used *Xenopus tropicalis* as a model organism in order to identify miRNAs that play a role during NC development. We had two main reasons to carry out this project. Our first goal was more addressed to expanding our general knowledge of the biology of the NC. Most of the previously published NC-GRNs lack regulatory elements other than protein-coding transcription factors. However, increasing evidence is highlighting the fact that development is more complex than that. There are many elements in the cell, other than protein-coding transcription factors, which have the potential to regulate gene expression. Such elements include miRNAs.

Given this, it will never be possible to generate an extensive and comprehensive NC-GRN without including these other factors, and having a complete NC-GRN will help us in better understanding the biology of the NC.

This leads to the second main point of this study. As mentioned before, problems arising during NC development can lead to pathological conditions. A better understanding on how the NC works can provide us with better tools to promptly identify such pathologies, to provide people affected with better care, and provide more information on the origin of these conditions to families of those involved, and information on how to handle them.

As the project progressed, we identified several miRNAs of interest using a combination of bioinformatical and *in vivo* tools. This preliminary analysis led to the finding of several potential and unexpected candidates, such as *xtr-miR-10b* and *xtr-miR-208*, as well as a longer list of miRNAs that still need to be tested (Chapter 3, Fig. 14).

Eventually, the study led to an investigating the role of *xtr-miR-204-1*, the less known member of the miR-204 family, during embryogenesis. The extensive study of this miRNA

shed light to its role in regulating some of the genes that are essential for eye and NC development, such as *pax6* and *tfap2β*, but also on some genes involved in melanocytes development, such as *sox10* and *snai2*.

However, what is probably the most exciting finding that this project led us to, is the fact that *xtr-miR-204-1* might be playing a dual role in the context of the development of the eye: one that is carried out by its annotated guide strand, *xtr-miR-204-1-5p*, and one carried out by its passenger strand, which has not been annotated in *Xenopus*, as of yet, *xtr-miR-204-1-3p*. While the guide strand might be involved in the closure of the choroid fissure in the eye, and its lack leads to coloboma phenotypes (a hypothesis reinforced by previous literature as well, (Avellino et al., 2013)), lack of the passenger strand seems to be involved in the growth of the eye during development, and its lack can lead to microphthalmia and anophthalmia.

Evidence that the passenger strand might play a biological role has previously been observed in particular physio- and pathological contexts, such as cancer, also in the case of *hsa-miR-211-3p* (Ma et al., 2019; Xu et al., 2017). However, to the best of our knowledge, this is the first time such behaviour has been observed on a miRNA in the context of embryo development.

## 6.1 Micro RNAs during embryogenesis

There is increasing evidence that miRNAs play a fundamental role during embryogenesis. However, our knowledge of such translational regulation is still far from matching what we know about protein-coding genes. Therefore, part of this project has aimed at filling this gap. In doing so, by using a combination of bioinformatical and literature approaches, we shortlisted eighteen miRNAs that might be of potential interest, from a NC development point of view. These included miRNAs: *nov-miR-12a*, *xtr-miR-10b*, *xtr-miR-21/590*, *xtr-miR-23*, *xtr-miR-24*, *xtr-miR-99/100*, *xtr-miR-130b/c*, *xtr-miR-132/212*, *xtr-miR-139*, *xtr-miR-143*, *xtr-miR-145*, *xtr-miR-147b*, *xtr-miR-187*, *xtr-miR-194*, *xtr-miR-202*, *xtr-miR-204-1*, *xtr-miR-208*, *xtr-miR-210*, *xtr-miR-217*, *xtr-miR-218-2*, *xtr-miR-338-3*, *xtr-miR-425*, *xtr-miR-455*, and *xtr-miR-499a*.

These miRNAs were found independently from the ones already described in the literature as involved in NC development and in NCPs (Antonaci and Wheeler, 2022).

These miRNAs include *miR-219* and *miR-196a*, which have previously been described in our lab as important for the correct development of *Xenopus*' NC development (Godden et al., 2022). The miRNAs that have been described from the literature are shown in Fig. 21, where different steps of NC development are highlighted in the squared boxes, starting from induction, ranging to the differentiation into various derivatives.

The presence in this list of some of these miRNAs was quite unexpected, since they have not previously been associated with NC biology. One miRNA in particular, *miR-208*, caught our attention since it's an established cardiac-specific miRNA in the adult organism (Zhao et al., 2020). In particular, it is a well-known biomarker to test cardiac damage (Ji et al., 2009). Despite its extensive medical use, not much was known about the role that it plays during embryogenesis. Of course, the fact that this miRNA flagged up as potentially involved in NC development could have been caused by the presence of false positives in the bioinformatical approach.

In order to test this, we had to perform *in vivo* analysis on developing embryos. However, only some of them were eventually tested *in vivo* in *Xenopus* as part of this project. These miRNAs were *xtr-miR-10b*, *xtr-miR-208*, *xtr-miR-218-2*, and *xtr-miR-204-1*. Among these, for the first three we performed a simple loss-of-function and phenotypic analysis experiment, while for *xtr-miR-204-1* we carried out an extensive analysis which include rescue experiments, several controls, as well as analysis of genes that are potentially regulated by the levels of *xtr-miR-204-1*.

Concerning *xtr-miR-10b*, we observed interesting NC-specific phenotypes, which included both craniofacial malformations and changes in the shape of the melanocytes. Unfortunately, after the version of *Xenopus tropicalis* genome was updated (from V9.0 to V10.0), we saw that *xtr-miR-10b* genomic locus falls within the same transcript of *hoxd4*, specifically in its 5' UTR. Because of the nature of our CRISPR/Cas9 knock-down experiment, which removes the entire genomic locus that hosts the miRNA gene, we could not exclude the fact that the observed phenotypes were partially, or even completely, caused by the loss of an important regulatory element in *hoxd4* mRNA.

Considering that miR-10 family includes three members in *Xenopus tropicalis* (*xtr-10a/b/c*) which possess almost the same sequence, morpholinos could target the other

isoforms as well. Also, a possible rescue experiment to test the specificity of the morpholino would also rescue any of the other miR-10 family member, since the seed sequence is exactly the same among all the three of them (Fig. 46).

This leads to another possible strategy with respect to investigating the role of *xtr-miR-10b* only, reducing to the minimum the effect on *hoxd4* or to any of the other miR-10 family members. This possibility includes the direct mutagenesis of the seed sequence of *xtr-miR-10b-5p* and *xtr-miR-10b-3p* only, leaving intact everything else in the genome. This way, the 5' UTR of *hoxd4* would have only a maximum of 16bp mutated (8bp for each seed sequence).

Using this strategy, we would still face the problem of the choice of which seed sequence to insert, instead of the ones of *xtr-miR-10b*. The first possible answer is the seed sequence of our control miRNA: *cel-miR-39-3p*. From our rescue experiments we already know that the overexpression of this miRNA does not cause any visible phenotype in *Xenopus* embryos. However, this is not necessarily true for *cel-miR-39-5p*. We have conducted no experiments on this miRNA therefore, before using it for such experiment, it would be necessary to perform an overexpression experiment to determine the effect of this miRNA during *Xenopus* embryogenesis.

Ideally, to test such an effect, it could be possible to inject in *Xenopus tropicalis* embryos the *pri-xtr-miR-10b* with the mutated seed sequences (*cel-miR-39-3p* and *cel-miR-39-5p*), and observe if this synthetic miRNA causes any visible phenotype. If not, it would be likely that any visible phenotype on embryos that have been genetically modified to lose the wild-type seed sequence of *xtr-miR-10b* would be due to the loss of *xtr-miR-10b* itself, and not to any other effect on *xtr-miR-10a/b* or *hoxd4*.

**Xtr-miR-10a-5p** U**ACCCUGUA**GAUCCGAAUUUGUG  
**Xtr-miR-10b-5p** U**ACCCUGUA**GAACCGAAUUUGU  
**Xtr-miR-10c-5p** C**ACCCUGUA**GAAUCGAAUUUGU

**Fig. 46: Members of the miR-10 family in *Xenopus tropicalis*.** Sequence of the mature miRNAs belonging to the miR-10 family in *Xenopus tropicalis*. In red, there is the seed sequence while, underlined, there are the different nucleotides. It is possible to appreciate that most nucleotides are identical within the three members, and the seed sequence (and, by extension, the possible targets) is exactly the same.

*Xtr-miR-208* was one of the most interesting miRNAs that was flagged up in the bioinformatic approach, which identified miRNAs that have an enriched pool of craniosynostosis-associated genes that is higher than expected (see 3.2). Reason for this include the fact that this miRNA has always been associated with cardiac biology (Zhao et al., 2020). It's locus in the genome, within an intron of *myh6* gene, which encodes for a cardiac muscle myosin subunit, is closely related to the cardiac physiology.

For this reason, we were very interested in studying the role that this miRNA plays during embryo development, considering that not much is known about the role of this miRNA, especially in the context of developmental biology. To date, there are 119 articles on PubMed shown when the key word, "miR-208", is used and almost all of them are addressed to cardiac failure, cancer, or hiPSCs reprogramming to cardiac myocytes. None of the articles talk about a role for this miRNA during embryogenesis.

However, from the LNA-WISH data using *xtr-miR-208-5p* probe, we observed an early expression of this miRNA in *Xenopus tropicalis* tailbuds, which starts being visible around stage NF28, indicating that this miRNA is expressed very early in development (Chapter 3, Fig. 20A). It was interesting to observe extension defects on *Xenopus* tadpoles (Chapter 3, Fig. 20), and these defects are likely to be attributed to problems during the elongation of the musculature. This highlights a likely involvement of this miRNA in the development of tissues that are different from the heart itself.

For the aim of this thesis, however, the lack of NC-specific phenotypes was a reason to stop pursuing the investigation of the biological role of *miR-208* during development. This result might be explained by the presence of false-positives within the results of the

bioinformatical analysis. This does not mean that this miRNA is not worth to be studied in the context of embryogenesis. On the contrary, the observation of such a striking phenotype should be further investigated. In fact, many of the congenital muscular dystrophies do not have any molecular diagnosis, and studying *miR-208* biology might help filling this knowledge gap.

*Xtr-miR-218-2* is localised inside an intron of the *slit3* gene. This gene is part of the SLIT/ROBO pathway, which has been associated with axon guidance and neurogenesis (Rothberg et al., 1988). However, this pathway has been more recently associated with kidney and heart development (Fan et al., 2012; Medioni et al., 2010). However, since this miRNA was one of the most specific from the NC-induced *Xenopus* animal caps produced by Dr Ward in our laboratory (Ward et al., 2018), we decided to pursue the phenotypic analysis of this miRNA.

Indeed, the observed edema, following *xtr-miR-218-2* knock-down experiment was definitely singular and unexpected. Confirmation of such phenotype following rescue experiment would definitely highlight a novel role for this miRNA during embryogenesis. This function would fit with the role of the SLIT/ROBO pathway during (at least) nephrogenesis. However, similarly to *xtr-miR-208* knock-down experiment, edema is not a phenotype that is usually associated with NC developmental defects. Therefore, this miRNA was also discarded from the possible miRNAs of interest for this study.

Of note, one of the novel miRNAs discovered by Dr Ward in her small RNA-seq analysis, *xla-miR-nov-12a1* was not considered for further analysis due to the lack of conservation with other species, including *Xenopus tropicalis*. However, when we searched for the genomic location of this novel miRNA in the genome of *Xenopus laevis*, we noticed that this is also localised inside an intron of a protein coding gene, *slit2*. From this, we can suggest that at least two of the three slit family genes are expressed in the NC-induced animal caps produced by Dr Ward in our lab, and that the introns of these genes were processed by the microprocessor complex in order to synthesise miRNAs. It is possible that the three-dimensional shape of the intron of *slit2* is recognised as a miRNA by the microprocessor, and therefore processed accordingly (Fig. 47).

However, from these data, we cannot tell if this miRNA is a subproduct of the processing of this intron, or if it plays an actual biological role during *Xenopus laevis* development. To clarify this, this miRNA should be further investigated in this species, which we could not do since we have not tested our miRNA CRISPR-KD approach in *Xenopus laevis*.

However, since this *xla-miR-nov-12a-1* is not conserved in *Xenopus tropicalis*, nor in *Homo sapiens* we suggest that, even if this miRNA plays a role in *Xenopus laevis* development, this would be specific for this species.

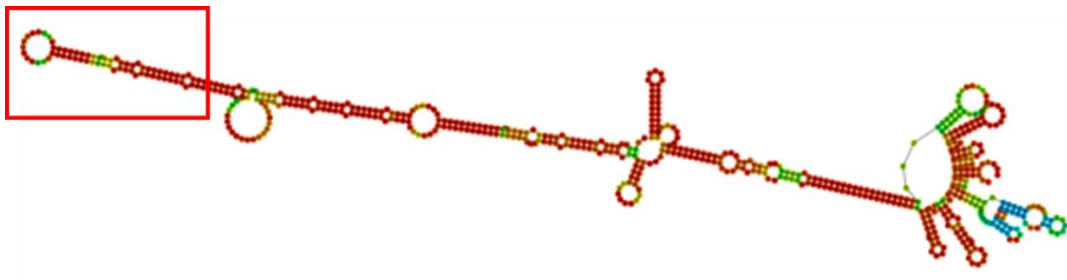


**Fig. 47: 3-D structure of *slit2* intron that hosts *xla-miR-nov-12a-1*.** Vienna RNA-fold structure of part of the intron that hosts *xla-miR-nov-12a-1*. As highlighted in the red box, the portion of the intron that hosts this novel miRNA possess the typical hairpin shape that is recognised by the microprocessor.

In conclusion, while most of the preliminary knock-downs of the selected miRNAs displayed interesting phenotypes affecting *Xenopus tropicalis* developing embryos, only *xtr-miR-10b* showed NC-specific phenotypes (craniofacial malformations and change in the melanocytes shape), however, due to its position in the genome, within the 5' UTR of *hoxd4*, we were unable to study this miRNA with ease. The other miRNAs that were identified throughout the bioinformatical and literature approach (*nov-miR-12a*, *xtr-miR-21/590*, *xtr-miR-23*, *xtr-miR-24*, *xtr-miR-99/100*, *xtr-miR-130b/c*, *xtr-miR-132/212*, *xtr-miR-139*, *xtr-miR-143*, *xtr-miR-145*, *xtr-miR-147b*, *xtr-miR-187*, *xtr-miR-194*, *xtr-miR-202*, *xtr-miR-210*, *xtr-miR-217*, *xtr-miR-338-3*, *xtr-miR-425*, *xtr-miR-455*, and *xtr-miR-499a*) should still be considered for further investigation during *Xenopus tropicalis* embryogenesis.

## 6.2 The dual role of *xtr-miR-204-1* during development

The most promising result that we observed, following knock-down of one of the selected miRNAs, was undoubtedly the effect of loss of *xtr-miR-204-1*. This miRNA was selected

for mainly two reasons: it is one of the most specific miRNAs expressed in the NC-induced animal caps produced in our lab, by Dr Ward, and because of its high expression in the adult melanocytes, which are NC-derived cells, other than in the RPE (Adijanto et al., 2012; Ward et al., 2018).

Given the expression of this miR-211 in the adult organisms (RPE and melanocytes), following its knock-down we predicted the first tissues where we expected an impairment during development, were the eye, and the pigment cells. Eventually, both these predictions came to reality, to different extents.

Firstly, we did not observe a critical reduction in the melanocyte population, nor a change in the shape of the melanocytes in the *xtr-miR-204-1* knocked-down embryos. What we observed, was a noticeable reduction in the NC markers *snai2* and *sox10* in these cells, at tadpole stages. The downstream effect of the loss of these two genes in these cells during development is still to be addressed.

The second and major phenotype that we observed was a severe effect on the development of the eye. In particular, we observed two separate phenotypes: colobomas and eye growth defects. These phenotypes, which we are observed in human conditions as well, with a frequency of ~1:3000 live birth child, can both lead to loss of vision, for different reasons. In the case of coloboma, the loss of vision can be caused by the inability of the iris to properly contract (mydriasis) or relax (miosis) following variations in the environmental lights. This can lead to an excess of light passing through the pupil which can, eventually, damage the retina. In the case of microphthalmia, the reduced size of the eye often result in a failure of the eye to extrude from the eyelid. This can be surgically corrected. However, in some cases, the eye is still not functional (Williamson and FitzPatrick, 2014).

Following a number of experimental controls, performed in order to confirm that the observed phenotypes were to be attributed to the loss of *xtr-miR-204-1* itself, and not to other unpredicted variables, we came across what we can consider the most exciting result of this project.

Following the rescue experiments (Chapter 4.5, Chapter 4.7), we noticed that the two different phenotypes could be attributed to the two different strands (guide and

passenger) of the mature miRNA itself, and not just to the loss of the guide strand, as we expected. In particular, while *xtr-miR-204-1-5p* rescue experiment resulted in the sole rescue of the coloboma phenotypes, we observed that *xtr-miR-204-1-3p* resulted in the rescue of microphthalmia and anophthalmia phenotypes only.

From these results, we suggest that, in the context of eye development in *Xenopus tropicalis*, *xtr-miR-204-1-5p* (guide strand) is involved in the closure of the choroid fissure, and that loss of this miRNA may result in colobomas. On the other hand, *xtr-miR-204-1-3p* (passenger strand) is involved in the growth of the eye itself, and that loss of this miRNA (as well as its overexpression, as shown in Chapter 4.6) might result in microphthalmia or anophthalmia.

This was quite surprising since we are not aware of any other miRNA that acts in a similar fashion during embryogenesis. However, this does not mean that *xtr-miR-204-1* is the only miRNA whose action is dependent on both guide and passenger strands. On the contrary, this might suggest that other miRNAs might act in ways that we, as a scientific community, still have to elucidate.

Here, we propose a hypothesis in which both, guide and passenger strand of a miRNA can play a functional role in the context of developmental biology, which is shown in Fig. 48.

It is still to elucidate if the action of the two strands of *xtr-miR-204-1* are acting in the same cells, or if one of the two (or both) are secreted by the cell, and used by other cell types. Future work should be done to clarify these questions.

Another important take-home message from this work is that the effect of the loss of a miRNA might cause severe phenotypes in the developing embryo and to the adult organism. Therefore there is a question from the medical community as to whether miRNAs could be used as a diagnostic tool. It has been shown several times in the scientific literature that miRNA mutations can cause rare human conditions (Antonaci and Wheeler, 2022). However, to date, little effort has been made to include miRNAs polymorphisms in the panel to identify the genetic cause of a person's condition.

With this study, we also wanted to provide the scientific community with additional evidence about the importance of the RNAi pathway in the context of pathological conditions. We believe that it would be important to study *hsa-miR-211* biology during human eye development. The reason of this would be to include this miRNA in the screening for the genetic cause/s of congenital eye conditions in human.

However, as mentioned before in this work, none of this knowledge might prove useful for people living with NCPs, unless it is used by geneticists. Because of this, we would need tools, other than the whole exome sequencing (WES) (which is, to date, the most used tool to find genetic variants that are of medical interest). With this, we do not want to undervalue the importance of the WES as an incredibly powerful tool to identify the cause of human conditions, but it should be complemented with others.

Since costs for whole genome sequencing (WGS) are still too high to be able to perform this technique on a regular base to identify pathological variants, it will be necessary to investigate new methods to identify mutations affecting miRNAs on a genome-wide scale. Such methods might include specific panels of sequencing, or even microarray chips designed to cover the most important miRNA loci, in order to identify mutations in these genes.

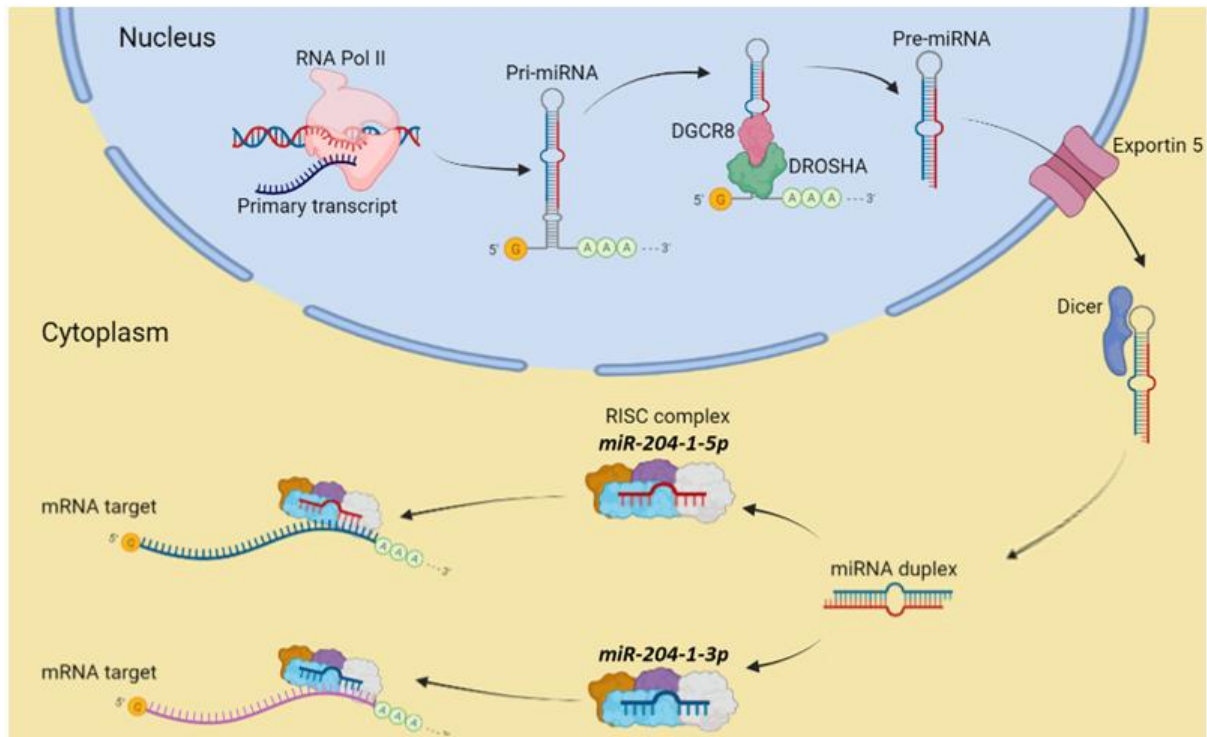


**Fig. 48: Proposed mechanism of action for *xtr-miR-204-1*.** Schematic representation of the proposed mechanism of action operated by *xtr-miR-204-1* in the context of *Xenopus*' eye development. Shortly, the miRNA is transcribed and processed in the nucleus as a normal miRNA. However, after the processing operated by Dicer in the cytoplasm, both *xtr-miR-204-1-5p* and *xtr-miR-204-1-3p* are loaded separately into different RISC complexes. These loaded complexes will have a different array of targets that they will then downregulate.

### 6.3 *Xtr-miR-204-1* GRN

While it is important to understand the importance and the role of *xtr-miR-204-1* during embryogenesis, it is equally important to determine what are the most important genes that are regulated by this miRNA.

To answer this question, we performed an extensive analysis of the possible targets, as well as genes that are involved in eye development, and tested their expression level/pattern in embryos that have been unilaterally injected to knock-down *xtr-mi-204-1*. The technique that we used to do so, the whole-mount in-situ hybridization (WISH), is an excellent semiquantitative technique that allows us to determine where and when a specific gene of interest is expressed in an embryo, by targeting the mRNA of that specific gene.

A large number of probes directed to genes of interest were synthesised and assessed in *Xenopus tropicalis*, in control (injected with Cas9 protein) and knocked-down (injected with Cas9 protein and gRNAs) embryos, in order to determine which genes might be involved in the regulation operated by *xtr-miR-204-1*. By doing so, we identified several genes whose expression was altered in the knocked-down side of the embryos, in comparison to the uninjected side of the same embryo.

This list includes (but is not limited to) genes that are known to cause, in human, the same phenotypes that we observed in *Xenopus*, linking the two species and proving, once more, the importance of using frog in research (Table 4).

Firstly, we observed a downregulation of the master regulator of eye development, the highly conserved transcription factor *pax6*. This gene is essential for early eye development, and we observed a strong reduction of its expression, at late tailbud stage, following knock-down of *xtr-miR-204-1*. It is important to note that when mutated, *PAX6* can cause both coloboma and microphthalmia, in human (Wawersik et al., 2000; Williamson and FitzPatrick, 2014). Given that the expression of *pax6* was analysed in tadpoles lacking both *xtr-miR-204-1-5p* (guide strand) and *xtr-miR-204-1-3p* (passenger strand), it is impossible to assess which of these strands is important for the expression of *pax6*. It is not to be excluded that both passenger and guide strands might be regulating *pax6* expression. To assess this, further experiments will be necessary.

Another gene whose expression was affected by loss of *xtr-miR-204-1*, is one of its computationally predicted targets: *tfap2a*. This gene is also a key regulator of several aspects of NC-development, from its early induction to late migration. Because of this, it is not surprising that mutations affecting this gene can cause, in human, a syndromic condition; the Branchio-oculo-facial syndrome (BOFS) (Jin et al., 2023; Thomeer et al., 2010). One of the phenotypes of this syndrome is coloboma. Interestingly, we have seen a disrupted expression of this gene, at late tadpole stage, indicating that this gene is subjected to the regulation operated by *xtr-miR-204-1* (Chapter 5, Fig. 32). What is more interesting, is that the disruption of the expression of this gene is not limited to the optic region, but extends to the branchial arches as well, indicating a deeper and yet unexplored role of this miRNA during *Xenopus tropicalis* development. This deregulation might have further effects on development that might be only visible later in

development, or even in the adult frog. It is not excluded that loss of *xtr-miR-204-1* might cause, in frogs as well as in human, a syndromic-like phenotype, but this might be visible only by growing stable knocked-out *Xenopus tropicalis* lines, if viable.

Another predicted target of *xtr-miR-204-1* which showed disrupted expression is another transcription factor, *hmx1*. This gene, which in human is also involved in a syndrome, the Oculo-auricular syndrome (OCACS), showed disrupted expression in the choroid fissure, in the trigeminal nerve, as well as in the otic vesicle. Also in this case, one of the signs of the OCACS is coloboma which is associated with a lack of closure of the choroid fissure (Gillespie et al., 2015). This is another indication suggesting that deregulation of *xtr-miR-204-1* might be involved in syndromic phenotypes that, before metamorphosis, cannot be visualised, apart from molecular assays such as WISH, and highlights the importance of, in the future, generating *Xenopus* stable *xtr-miR-204-1* knock-out lines.

Interestingly, not only genes expressed in different regions of the eye showed a different expression, in comparison to the wild-type half of the embryo. In particular, unexpected regions of the developing embryo, such as the otic vesicle, and even the pronephros, showed altered expression patterns or levels. For example, the genes *cox5a* and *ndrg3*, which are expressed in the pronephric tubule and duct, and that are both predicted targets of *xtr-miR-204-1*, showed an increased mRNA expression in this organ. This result is in line with the fact that *xtr-miR-204-1-3p* has been visualised by LNA-WISH in the pronephros (Chapter 4, Fig. 22). Also, considering that both these genes are computationally predicted targets of *xtr-miR-204-1* is a strong indicator that, at least in the developing pronephric kidney, *cox5a* and *ndrg3* are indeed directly targeted by *xtr-miR-204-1-5p*.

On the same line, another gene which is also expressed in the pronephric kidney, *pax2*, and that is not a predicted target of *xtr-miR-204-1*, showed a reduced expression in this organ, in comparison to the wild-type side of the embryo. *PAX2* gene is involved in the etiopathogenesis of a rare human condition called papillorenal syndrome, or renal-coloboma syndrome. This condition display colobomas and renal hypoplasia in people affected by it. Interestingly, while *PAX2* is the only gene that has been associated with papillorenal syndrome, still half of the people affected do not have a molecular diagnosis, opening the possibility on the involvement of *hsa-miR-211* in the

etiopathogenesis of this condition (Giovanella et al., 2023). However, the data produced by analysing the expression of *pax2* should be reinforced with more observations, in order to strengthen the statistics behind it. In any case, it is a promising result that, if confirmed, would reinforce the hypothesis that *xtr-miR-204-1* is expressed and acts in the developing kidney of *Xenopus tropicalis*.

Importantly, when we tried to analyse the expression pattern of NC-specific genes, such as *sox10* and *snai2*, we observed a deregulation of these genes. For example, the melanocytes of the embryos that were knocked-down for *xtr-miR-204-1* displayed a severe reduction in the expression of both *sox10* and *snai2*. This suggests that this miRNA is also expressed in the melanocytes (probably co-transcribed along with *trpm1*), and that plays a role in the maturation of these cells. It is yet to be assessed if the action exerted by *xtr-miR-204-1* in the developing melanocytes could produce pathological phenotypes in the adult frog, like an increased chance of developing melanomas. If that would be confirmed, then it would be useful to investigate if such action could also be played by *hsa-miR-211* in human melanocytes.

An observation that we could extrapolate, following knock-down of *xtr-miR-204-1*, we have seen the deregulation of many different genes, whose mutations can produce the same phenotype, in human (see *pax6*, *tfap2a* or *hmx1*, mutations of these genes can all produce coloboma). Considering that, except for some of these markers such as *sox10* in the melanocytes, we have never seen an “on/off” effect on the expression of these genes. This suggests to us that the observed phenotypes on eye development of knocked-down embryos is likely to be attributed to a combination of perturbations that start with the deregulation of *xtr-miR-204-1*. In other words, if the binding between *hmx1* mRNA and *xtr-miR-204-1-5p* would be disrupted, maybe because of a mutation in the 3' UTR of *hmx1* gene, we could probably still appreciate coloboma phenotype on knocked down tadpoles, because *xtr-miR-204-1* could still bind *tfap2a* mRNA. This reinforces the theory that miRNAs have the potential to regulate dozens, if not hundreds of genes within the same cell type, but they do not have the potential to completely turn on/off the expression of a specific gene on their own.

In conclusion, we were able to identify several genes whose expression is directly or indirectly affected by *xtr-miR-204-1*. Some of these genes, such as *pax6*, or *tfap2a* have

been directly associated with human conditions that affect the eyes. Some others, such as *cox5a* and *ndrg3*, were expressed in tissues where we did not observe any phenotype, up to the stage of development that we explored, but their de-regulation might be affecting downstream developmental processes, such as the functionality of the kidneys in the adult frog and other genes, such as *snai2* and *sox10*, which are important for the NC development, are downregulated in a tissue-specific context. With this study, we are increasing our knowledge of the biology of *xtr-miR-204-1* in the context of embryo development, highlighting its several layers of regulation that extend to different tissues.

It is also interesting to point out the fact that different pronephric markers, such as *ndrg3*, *cox5a* and *pax2* show different behaviours, with the first two being overexpressed (likely because direct targets of *xtr-miR-204-1*) and the latter being downregulated. This suggests that the organogenesis of the pronephric kidney is still occurring, however, the functionality of it should be further investigated.

#### **6.4 Future work**

The main goal of this project was to identify novel miRNAs that are involved in different aspects of the NC biology. Through bioinformatical approaches, we managed to shortlist approximately twenty four potential miRNAs that answer this question. During the course of this project, however, only four of these miRNAs were tested by performing preliminary knock-down experiments, and only one of those four, *xtr-miR-204-1* was explored more in depth.

This leaves us with twenty miRNAs that should still be tested in *Xenopus*, and that might play a role in the NC-GRN: *nov-miR-12a*, *xtr-miR-21/590*, *xtr-miR-23*, *xtr-miR-24*, *xtr-miR-99/100*, *xtr-miR-130b/c*, *xtr-miR-132/212*, *xtr-miR-139*, *xtr-miR-143*, *xtr-miR-145*, *xtr-miR-147b*, *xtr-miR-187*, *xtr-miR-194*, *xtr-miR-202*, *xtr-miR-210*, *xtr-miR-217*, *xtr-miR-338-3*, *xtr-miR-425*, *xtr-miR-455*, and *xtr-miR-499a*. In the future, it would be useful to validate the bioinformatical analysis by assessing the role of these miRNA during NC development.

Similarly, even if the tissue involved is not the NC, it would be good to assess more deeply the three miRNAs that have been knocked down during this project: *xtr-miR-10b*, *xtr-miR-208* and *xtr-miR-218-2*. Despite the fact that the knock-down of these miRNAs did not

produce visible NC phenotype (with the exception of *xtr-miR-10b*), they did produce other unexpected phenotypes. Because of this, it might be important to validate the preliminary experiments by carrying out several control experiments, such as rescues with miRNA mimics, or genotyping to control the efficacy of the CRISPR-Cas9 deletion, and then to investigate which genes are regulated, directly and indirectly, by these miRNAs. These experiments might provide useful tools to investigate the aetiopathogenesis of some human conditions for which there is currently no genetic explanation.

When we move forward to *xtr-miR-204-1*, the miRNA that we better characterised during this project, there are several experiments that could be performed in order to better understand its biological functions. The first experiment that could be carried out is to knock it down and to let the tadpoles grow after metamorphosis, and to assess the phenotypes caused by the lack of this miRNA in the adult organism. It seems that tissues other than the eyes are potentially affected by lack of *xtr-miR-204-1*. These tissues involve melanocytes, the kidneys, otic vesicle and the first branchial arches. One might imagine that, in the adult organism, these tissues might be affected in some ways that are not visible while the embryos are still at tadpole stage. However, by WISH, we have observed the deregulation of several genes involved in the etiopathogenesis of syndromic disorders, such as *tfap2a*, *hmx1*, and *pax2*. It is possible that the knock-down of *xtr-miR-204-1* could produce similar phenotypes in the adult frogs, by modulating the expression of all of these genes. (Table 4).

Gene name	Syndrome/Condition	Phenotypes-excluding coloboma/microphthalmia
Hmx1	Oculoauricular syndrome	Abnormal ear cartilage, microcornea, cataract
Pax2	Papillorenal syndrome	Vesicoureteral reflux, renal abnormalities
Pax6	Microphthalmia, coloboma	
Snai2	Waardenburg syndrome	Hearing loss, lack of pigmentation
Sox10	Waardenburg syndrome	Hearing loss, lack of pigmentation
Tfap2a	Branchio-oculofacial syndrome	Facial dysorfism, hearing loss, cleft palate
Trpm1	Congenital stationary night blindness	Night blindness, loss of sharpness, myopia, nystagmus, strabismus
Vax2	Astigmatism	Astigmatism

**Table 4: Syndromes and conditions associated with mutations in the genes that are regulated by *xtr-miR-204-1*.** The table shows the genes that are regulated (directly or indirectly) by *xtr-miR-204-1*. The third column shows the phenotypes associated with such conditions, without including colobomas or microphthalmias. It is important to note that not all of these signs and symptoms have to be present at once, in order to be diagnosed with such condition. For example, in the case of congenital stationary night blindness, it can manifest by night blindness alone, without loss of sharpness, myopia, nystagmus, and strabismus.

The use of stable lines might also elucidate another important aspect that, by using an F<sub>0</sub>, cannot be assessed, which is how penetrant the observed phenotypes are. Since the knock-downs embryos produced by using our CRISPR-Cas9 strategy are highly heterogeneous in their mosaicism (Chapter 4, Fig. 24B), it is impossible to address this point without further analysis. Following the knock-down experiments, we could observe, on average, 30% of the embryos with colobomas and 15% of the embryos with microphthalmia/anophthalmia. However, we can speculate that these percentages would be much higher than this, if the embryos were completely knocked out for *xtr-miR-204-1*. However, some conditions are not fully penetrant (incomplete penetrance). This is usually due to compensatory mechanisms that the cells and, in general, the whole organism uses to maintain the physiology of the body.

In this specific case, it is simple to speculate what such a mechanism might be; following knock-out of *xtr-miR-204-1*, the cells might overexpress the other member of the family, *xtr-miR-204-2*. In this case, the seed sequence of *xtr-miR-204-1-5p* is exactly the same as the seed sequence of *xtr-miR-204-2-5p*, therefore, the predicted targets should be the same, and the compensatory mechanism might allow an incomplete penetrance of the observed phenotypes.

However, the seed sequence of *xtr-miR-204-1-3p* and *xtr-miR-204-2-3p* is not the same, in fact, three of the eight nucleotides of the seed sequence of these two mature miRNAs differ, which means that the predicted targets are different from each other. This can be easily confirmed by the fact that the number of predicted targets of *hsa-miR-211-3p* is 4814 transcripts, while the number of predicted targets of *hsa-miR-204-3p* is 5753. This simple comparison indicates a completely different set of predicted targets of these two miRNAs (Fig. 49).

In this study, we demonstrated that the passenger strand of *xtr-miR-204-1* (*xtr-miR-204-1-3p*) is indeed involved in the regulation of the eye growth during development. Without an obvious candidate for a compensatory mechanism that could rescue the knock-out of *xtr-miR-204-1-3p* it might be possible that, in a context of *xtr-miR-204-1* complete knock-out, we might observe a lower than expected number of colobomas, due to the compensation provided by *xtr-miR-204-1-5p*, and a high number of microphthalmia phenotypes, that cannot be rescued by the overexpression of *xtr-miR-204-2-3p*, since this miRNA has a different sequence from *xtr-miR-204-1-3p*.

As a matter of fact, if *xtr-miR-204-2* would be used as a compensatory mechanism to mitigate the absence of *xtr-miR-204-1*, we might be able to observe some other different phenotypes, due to the overexpression of *xtr-miR-204-2-3p*. This possibility arises from the fact that the overexpression of *xtr-miR-204-1-3p* can, itself, induce microphthalmia in the developing tadpoles (Chapter 4, Fig. 27B). However, these speculations should be supported by more experiments, other than the generation of stable knock-down lines of *xtr-miR-204-1*. One of such experiments could be the silencing of *xtr-miR-204-2-3p* by using a morpholino approach, in the context of *xtr-miR-204-1* knock-down, and a control experiment in which only *xtr-miR-204-1-3p* is overexpressed by using a miRNA mimic. These experiments would provide us with information about the compensatory mechanism operated by *xtr-miR-204-2*, in case *xtr-miR-204-1* is knocked down.

We could further the investigation about the effect of the guide strand and passenger strand of *xtr-miR-204-1*, by performing rescue experiments with each of the mature miRNAs (*xtr-miR-204-2-5p* or *xtr-miR-204-1-3p*) and perform WISH to analyse the rescue of the expression pattern of the genes investigated in “Chapter 5: *Xtr-miR-204-1* Gene Regulatory Network”. This would tell us, among all the genes whose expression is deregulated following knock-down of *xtr-miR-204-1*, which are the ones controlled by *xtr-miR-204-1-5p*, and which ones are controlled by *xtr-miR-204-1-3p*.

However, this is an incredibly laborious task, which requires doubling the number of injections for each sample, resulting in thousands of injections, with the result of analysing the role of the two mature miRNA strands on only about ten genes.

There is another possibility, which will provide an incredibly higher amount of information with less experimental effort. This would be to perform bulk RNA-seq on embryos that have been rescued with either the guide miRNA or with the passenger miRNA. In this context, we could have four samples, including 1) wild-type embryos, 2) *xtr-miR-204-1* knock-down, 3) *xtr-miR-204-1* knock-down rescued with *xtr-miR-204-1-5p* and 4) *xtr-miR-204-1* knock-down rescued with *xtr-miR-204-1-3p*.

This way, we would be able to determine, on a transcriptome level, the effect of the absence of *xtr-miR-204-1* from a developing embryo by using the comparison of wild-type embryos with knocked-down embryos. More interestingly, we would be able to determine the effect of the individual miRNAs (guide and passenger strand) on the affected genes. For example, we observed, by WISH, that *pax6* expression is reduced following knock-down of *xtr-miR-204-1*. If, following rescue, we would observe an increase of *pax6* mRNA only on the embryos that have been rescued with *xtr-miR-204-1-3p*, we could say that it is the passenger strand of *xtr-miR-204-1* regulating the expression of *pax6*. This experiment would allow us to have a global view of the role of *xtr-miR-204-1* during *Xenopus tropicalis* embryogenesis.

Another aspect that we could not investigate about the biology of *xtr-miR-204-1* is its possible involvement in another, less studied, pathway, the RNA activation (RNAa). By using this pathway, miRNAs can move back to the nucleus, where they promote the expression of specific genes by binding to their promoters and, thus, facilitating the attachment of the RNA PolIII. However, so far, only a few miRNAs have been shown to be able to play a role in this pathway and, at the moment, there are no bioinformatical tools able to predict potential miRNA binding sites to the promoter of a gene (Portnoy et al., 2016; Ramchandran and Chaluvally-Raghavan, 2017). Interestingly, we manually found several binding sites of *xtr-miR-204-1* in the promoter of *trpm1*. If future experiments would explain why, following *xtr-miR-204-1* knock-down, we observed a reduction in *trpm1* expression (Chapter 5, Fig. 36), it would highlight an exciting positive feedback-loop between the expression of *trpm1*, which leads to *xtr-miR-204-1* expression, which enhances *trpm1* expression. Finally, it would prove that RNAa is an important process in developmental biology, and might initiate a new exciting field of research within this field.

The dissection of the role of *xtr-miR-204-1* mature miRNAs, the understanding of its GRN, and the generation of a stable knock-out line would lead us into a better understanding of the biology of this miRNA, but the ultimate goal for such research should always be addressed to a better understanding of human conditions, and on how to provide them with better care.

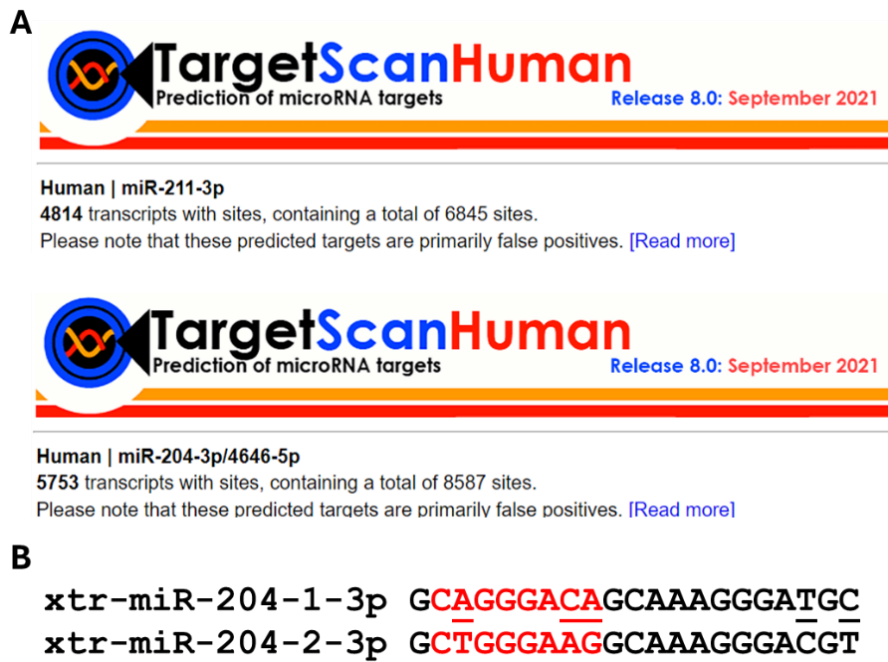


**Fig. 49: Comparison between the passenger strand of miR-204 family members: A)** TargetScan8.0 prediction of the numbers of targets of human *hsa-miR-211-3p* (4814 predicted targets) and human *hsa-miR-204-3p* (5753 predicted targets). **B)** Comparison of the mature miR-204-3p family members in *Xenopus tropicalis*. *Xtr-miR-204-1-3p* on top and *xtr-miR-204-2-3p* on the bottom. In red there are the seed sequences, while underlined there are the differences between the two strands.

This is the reason why, in addition to the above experiments, it would be important to understand the role of *hsa-miR-211* in human eye development. To do so, we would need to use different models than those used in our studies. We know that miR-204 family is highly conserved, as well as the TRPM genes, across vertebrates. This means that it is possible to investigate the role of these miRNAs using human cell lines. The most obvious cell type to investigate would be a retina cell line, such as ARPE-19, a human derived RPE cell line. However, thank to this study, we have found out that the eye is not the only developing tissue affected by the lack of *xtr-miR-204-1*. Other tissues, such as

melanocytes and the kidneys are affected as well. Therefore, it would be interesting to investigate other cell lines as well, such as A375 (a melanoma cell line).

The investigation of the role of *hsa-miR-211* in the context of these cell types would provide a useful insight into the biology of this miRNA on differentiated tissues, however, it might not be indicative of the effect on the differentiation of these tissues. For example, the role of *xtr-miR-204-1* on kidney development might extend to its organogenesis only, and not to the homeostasis of the fully developed organ.

To address this question, it would be necessary to study the dynamics of development on human, which is possible to do thank to the technology of the hiPSCs. In particular, it would be necessary to knock-down/out *hsa-miR-211* in the undifferentiated PSCs, and then differentiate them into the tissues of interest, in order to assess if the presence or absence of *hsa-miR-211* is necessary for the correct differentiation of these tissues.

Finally, it could be possible to include *hsa-miR-211* in the screening for the determination of specific human conditions, such as coloboma or even some of the syndromes listed in Table 4. Some of those conditions still remain without a molecular diagnosis, and *hsa-miR-211* might provide an answer to some of the people and families that are affected by such diseases. That might provide them with better care from clinicians but, most importantly, might give these people an answer about the reason why such conditions happened to them. This knowledge can, on its own, provide an important psychological help to both families and people directly affected by these conditions.

## **Acknowledgments**

I must admit, during the writing of this thesis, this is probably the most complicated part to write. Not because I don't know whom to thank, but because in writing these lines, I feel the tremendous responsibility of not forgetting anyone who made this journey possible.

I cannot start with anyone else, but with my family. My parents and my siblings are the real reason why I never freaked out and why I have always been so positive about everything. Whatever it is going to happen, I know they will be there to help and support me, no matter what.

A huge thanks goes to my supervisor, Grant, who has given me all the freedom I needed in the lab, supported every crazy side-project, and never put more pressure on me than I could handle.

The fellowship of the Indie, Anna, Andrea, Elien, Victoria, Audun, the MVPs of my UK experience. From the very first moment, they were there to provide the best mental support anyone could ever have. Each one of you deserves a page in these acknowledgments. But I will just say that if the snail eventually managed to climb the stairs, it is also thanks to you, guys.

I also want to thank Geoff for all the help he gave me, even after saying, "not my problem." Andrea, for all the support and suggestions during these years. Tim, for the endless discussions about everything, like why mammals lost the eye bones (I still don't know it, by the way).

A special thank you to the whole Münsterberg group, especially to Magdina, who is one of the most fun and brilliant people I have ever had the pleasure to meet. Emily, who is by far the kindest bully I have ever seen in my life. Shahrzad, I loved your positive energy, no matter what. And then Rafeeq, Raphi, Jennifer, Shannon and everyone who made my lab experience better. I also want to thank the NEUcrest ESRs, in particular Anna, William, and Irina, for being such amazing people.

As you can see from the fact that I switched to "single spacing" between the lines, I am running short of space on this page, but the people who helped me getting through the PhD are many more and, as I expected, now I feel guilty for not giving enough credit to all of them.

However, these last lines are dedicated to Amy. From the very beginning, when you thought I was shy while I just had no clue how to communicate in English, till now that I am writing these words at the end of this journey, you have always been there. No matter what, no matter the challenge, we have always faced it together, and while we were together, nothing looked too scary to be faced.

Thank you.

## **References**

A Vega-Lopez, G., J Aybar, M., 2018. Neurocristopathies: How New Discoveries in Neural Crest Research Changed our Understanding. *Cell & Developmental Biology* 07.

Adijanto, J., Castorino, J.J., Wang, Z.X., Maminishkis, A., Grunwald, G.B., Philp, N.J., 2012. Microphthalmia-associated transcription factor (MITF) promotes differentiation of human retinal pigment epithelium (RPE) by regulating microRNAs-204/211 expression. *J Biol Chem* 287, 20491-20503.

Agarwal, P., Wylie, J.N., Galceran, J., Arkhitko, O., Li, C., Deng, C., Grosschedl, R., Bruneau, B.G., 2003. Tbx5 is essential for forelimb bud initiation following patterning of the limb field in the mouse embryo. *Development* 130, 623-633.

Altmann, C.R., Chow, R.L., Lang, R.A., Hemmati-Brivanlou, A., 1997. Lens induction by Pax-6 in *Xenopus laevis*. *Dev Biol* 185, 119-123.

Alves, C.L., Elias, D., Lyng, M.B., Bak, M., Ditzel, H.J., 2018. SNAI2 upregulation is associated with an aggressive phenotype in fulvestrant-resistant breast cancer cells and is an indicator of poor response to endocrine therapy in estrogen receptor-positive metastatic breast cancer. *Breast Cancer Res* 20, 60.

Antonaci, M., Godden, A.M., Wheeler, G.N., 2023. Determining miRNA Expression Patterns in *Xenopus*. *Methods Mol Biol* 2630, 145-154.

Antonaci, M., Wheeler, G.N., 2022. MicroRNAs in neural crest development and neurocristopathies. *Biochem Soc Trans* 50, 965-974.

Ashery-Padan, R., Marquardt, T., Zhou, X., Gruss, P., 2000. Pax6 activity in the lens primordium is required for lens formation and for correct placement of a single retina in the eye. *Genes Dev* 14, 2701-2711.

Avellino, R., Carrella, S., Pirozzi, M., Risolino, M., Salierno, F.G., Franco, P., Stoppelli, P., Verde, P., Banfi, S., Conte, I., 2013. miR-204 targeting of Ankrd13A controls both mesenchymal neural crest and lens cell migration. *PLoS One* 8, e61099.

Ayers, D., Mestdagh, P., Van Maerken, T., Vandesompele, J., 2015. Identification of miRNAs contributing to neuroblastoma chemoresistance. *Comput Struct Biotechnol J* 13, 307-319.

Bachetti, T., Bagnasco, S., Piumelli, R., Palmieri, A., Ceccherini, I., 2021. A Common 3'UTR Variant of the PHOX2B Gene Is Associated With Infant Life-Threatening and Sudden Death Events in the Italian Population. *Front Neurol* 12, 642735.

Bailey, A.P., Bhattacharyya, S., Bronner-Fraser, M., Streit, A., 2006. Lens specification is the ground state of all sensory placodes, from which FGF promotes olfactory identity. *Dev Cell* 11, 505-517.

- Bakiri, L., Macho-Maschler, S., Custic, I., Niemiec, J., Guio-Carrion, A., Hasenfuss, S.C., Eger, A., Muller, M., Beug, H., Wagner, E.F., 2015. Fra-1/AP-1 induces EMT in mammary epithelial cells by modulating Zeb1/2 and TGFbeta expression. *Cell Death Differ* 22, 336-350.
- Barbieri, A.M., Broccoli, V., Bovolenta, P., Alfano, G., Marchitello, A., Mocchetti, C., Crippa, L., Bulfone, A., Marigo, V., Ballabio, A., Banfi, S., 2002. Vax2 inactivation in mouse determines alteration of the eye dorsal-ventral axis, misrouting of the optic fibres and eye coloboma. *Development* 129, 805-813.
- Barbieri, A.M., Lupo, G., Bulfone, A., Andreazzoli, M., Mariani, M., Fougerousse, F., Consalez, G.G., Borsani, G., Beckmann, J.S., Barsacchi, G., Ballabio, A., Banfi, S., 1999. A homeobox gene, vax2, controls the patterning of the eye dorsoventral axis. *Proc Natl Acad Sci U S A* 96, 10729-10734.
- Bartel, D.P., 2004. MicroRNAs: genomics, biogenesis, mechanism, and function. *Cell* 116, 281-297.
- Belecky-Adams, T.L., Adler, R., Beebe, D.C., 2002. Bone morphogenetic protein signaling and the initiation of lens fiber cell differentiation. *Development* 129, 3795-3802.
- Bergsland, M., Werme, M., Malewicz, M., Perlmann, T., Muhr, J., 2006. The establishment of neuronal properties is controlled by Sox4 and Sox11. *Genes Dev* 20, 3475-3486.
- Bernstein, E., Kim, S.Y., Carmell, M.A., Murchison, E.P., Alcorn, H., Li, M.Z., Mills, A.A., Elledge, S.J., Anderson, K.V., Hannon, G.J., 2003. Dicer is essential for mouse development. *Nat Genet* 35, 215-217.
- Bertani-Torres, W., Lezirovitz, K., Alencar-Coutinho, D., Pardono, E., da Costa, S.S., Antunes, L.D.N., de Oliveira, J., Otto, P.A., Pingault, V., Mingroni-Netto, R.C., 2023. Waardenburg Syndrome: The Contribution of Next-Generation Sequencing to the Identification of Novel Causative Variants. *Audiol Res* 14, 9-25.
- Biagioni, F., Bossel Ben-Moshe, N., Fontemaggi, G., Yarden, Y., Domany, E., Blandino, G., 2013. The locus of microRNA-10b: a critical target for breast cancer insurgence and dissemination. *Cell Cycle* 12, 2371-2375.
- Blixt, A., Mahlapuu, M., Aitola, M., Pelto-Huikko, M., Enerback, S., Carlsson, P., 2000. A forkhead gene, FoxE3, is essential for lens epithelial proliferation and closure of the lens vesicle. *Genes Dev* 14, 245-254.
- Blum, M., Ott, T., 2018. Xenopus: An Undervalued Model Organism to Study and Model Human Genetic Disease. *Cells Tissues Organs* 205, 303-313.
- Bohnsack, B.L., Kahana, A., 2013. Thyroid hormone and retinoic acid interact to regulate zebrafish craniofacial neural crest development. *Dev Biol* 373, 300-309.

Bohnsack, B.L., Kasprick, D.S., Kish, P.E., Goldman, D., Kahana, A., 2012. A zebrafish model of axenfeld-rieger syndrome reveals that pitx2 regulation by retinoic acid is essential for ocular and craniofacial development. *Invest Ophthalmol Vis Sci* 53, 7-22.

Bondurand, N., Sham, M.H., 2013. The role of SOX10 during enteric nervous system development. *Dev Biol* 382, 330-343.

Bower, M., Salomon, R., Allanson, J., Antignac, C., Benedicenti, F., Benetti, E., Binenbaum, G., Jensen, U.B., Cochat, P., DeCramer, S., Dixon, J., Drouin, R., Falk, M.J., Feret, H., Gise, R., Hunter, A., Johnson, K., Kumar, R., Lavocat, M.P., Martin, L., Moriniere, V., Mowat, D., Murer, L., Nguyen, H.T., Peretz-Amit, G., Pierce, E., Place, E., Rodig, N., Salerno, A., Sastry, S., Sato, T., Sayer, J.A., Schaafsma, G.C., Shoemaker, L., Stockton, D.W., Tan, W.H., Tenconi, R., Vanhille, P., Vats, A., Wang, X., Warman, B., Weleber, R.G., White, S.M., Wilson-Brackett, C., Zand, D.J., Eccles, M., Schimmenti, L.A., Heidet, L., 2012. Update of PAX2 mutations in renal coloboma syndrome and establishment of a locus-specific database. *Hum Mutat* 33, 457-466.

Bronner, M.E., LeDouarin, N.M., 2012. Development and evolution of the neural crest: an overview. *Dev Biol* 366, 2-9.

Brownell, I., Dirksen, M., Jamrich, M., 2000. Forkhead Foxe3 maps to the dysgenetic lens locus and is critical in lens development and differentiation. *Genesis* 27, 81-93.

Burns, A.J., Douarin, N.M., 1998. The sacral neural crest contributes neurons and glia to the post-umbilical gut: spatiotemporal analysis of the development of the enteric nervous system. *Development* 125, 4335-4347.

Castro-Perez, E., Singh, M., Sadangi, S., Mela-Sanchez, C., Setaluri, V., 2023. Connecting the dots: Melanoma cell of origin, tumor cell plasticity, trans-differentiation, and drug resistance. *Pigment Cell Melanoma Res* 36, 330-347.

Chambers, B.E., Gerlach, G.F., Clark, E.G., Chen, K.H., Levesque, A.E., Leshchiner, I., Goessling, W., Wingert, R.A., 2019. Tfp2a is a novel gatekeeper of nephron differentiation during kidney development. *Development* 146.

Chapnik, E., Sasson, V., Blueloch, R., Hornstein, E., 2012. Dgcr8 controls neural crest cells survival in cardiovascular development. *Dev Biol* 362, 50-56.

Chiang, C., Litingtung, Y., Lee, E., Young, K.E., Corden, J.L., Westphal, H., Beachy, P.A., 1996. Cyclopia and defective axial patterning in mice lacking Sonic hedgehog gene function. *Nature* 383, 407-413.

Chipman, L.B., Pasquinelli, A.E., 2019. miRNA Targeting: Growing beyond the Seed. *Trends Genet* 35, 215-222.

Chow, R.L., Altmann, C.R., Lang, R.A., Hemmati-Brivanlou, A., 1999. Pax6 induces ectopic eyes in a vertebrate. *Development* 126, 4213-4222.

- Chow, R.L., Lang, R.A., 2001. Early eye development in vertebrates. *Annu Rev Cell Dev Biol* 17, 255-296.
- Chubanov, V., Kottgen, M., Touyz, R.M., Gudermann, T., 2024. TRPM channels in health and disease. *Nat Rev Nephrol* 20, 175-187.
- Conte, I., Hadfield, K.D., Barbato, S., Carrella, S., Pizzo, M., Bhat, R.S., Carissimo, A., Karali, M., Porter, L.F., Urquhart, J., Hateley, S., O'Sullivan, J., Manson, F.D., Neuhauss, S.C., Banfi, S., Black, G.C., 2015. MiR-204 is responsible for inherited retinal dystrophy associated with ocular coloboma. *Proc Natl Acad Sci U S A* 112, E3236-3245.
- Cui, Y.Z., Man, X.Y., 2023. Biology of melanocytes in mammals. *Front Cell Dev Biol* 11, 1309557.
- Cvekl, A., Mitton, K.P., 2010. Epigenetic regulatory mechanisms in vertebrate eye development and disease. *Heredity (Edinb)* 105, 135-151.
- Delaloy, C., Liu, L., Lee, J.A., Su, H., Shen, F., Yang, G.Y., Young, W.L., Ivey, K.N., Gao, F.B., 2010. MicroRNA-9 coordinates proliferation and migration of human embryonic stem cell-derived neural progenitors. *Cell Stem Cell* 6, 323-335.
- Diehl, A.G., Zarepari, S., Qian, M., Khanna, R., Angeles, R., Gage, P.J., 2006. Extraocular muscle morphogenesis and gene expression are regulated by Pitx2 gene dose. *Invest Ophthalmol Vis Sci* 47, 1785-1793.
- Dixon, M.J., Marazita, M.L., Beaty, T.H., Murray, J.C., 2011. Cleft lip and palate: understanding genetic and environmental influences. *Nat Rev Genet* 12, 167-178.
- Dolinska, M.B., Kovaleva, E., Backlund, P., Wingfield, P.T., Brooks, B.P., Sergeev, Y.V., 2014. Albinism-causing mutations in recombinant human tyrosinase alter intrinsic enzymatic activity. *PLoS One* 9, e84494.
- Donner, A.L., Episkopou, V., Maas, R.L., 2007. Sox2 and Pou2f1 interact to control lens and olfactory placode development. *Dev Biol* 303, 784-799.
- Dressler, G.R., Woolf, A.S., 1999. Pax2 in development and renal disease. *Int J Dev Biol* 43, 463-468.
- Du, Q., de la Morena, M.T., van Oers, N.S.C., 2019. The Genetics and Epigenetics of 22q11.2 Deletion Syndrome. *Front Genet* 10, 1365.
- Eccles, M.R., He, S., Legge, M., Kumar, R., Fox, J., Zhou, C., French, M., Tsai, R.W., 2002. PAX genes in development and disease: the role of PAX2 in urogenital tract development. *Int J Dev Biol* 46, 535-544.
- Fabian, M.R., Sonenberg, N., Filipowicz, W., 2010. Regulation of mRNA translation and stability by microRNAs. *Annu Rev Biochem* 79, 351-379.

Fan, X., Li, Q., Pisarek-Horowitz, A., Rasouly, H.M., Wang, X., Bonegio, R.G., Wang, H., McLaughlin, M., Mangos, S., Kalluri, R., Holzman, L.B., Drummond, I.A., Brown, D., Salant, D.J., Lu, W., 2012. Inhibitory effects of Robo2 on nephrin: a crosstalk between positive and negative signals regulating podocyte structure. *Cell Rep* 2, 52-61.

Fan, Y., Hackland, J., Baggiolini, A., Hung, L.Y., Zhao, H., Zumbo, P., Oberst, P., Minotti, A.P., Hergenreder, E., Najjar, S., Huang, Z., Cruz, N.M., Zhong, A., Sidharta, M., Zhou, T., de Stanchina, E., Betel, D., White, R.M., Gershon, M., Margolis, K.G., Studer, L., 2023. hPSC-derived sacral neural crest enables rescue in a severe model of Hirschsprung's disease. *Cell Stem Cell* 30, 264-282 e269.

Faure, S., de Santa Barbara, P., Roberts, D.J., Whitman, M., 2002. Endogenous patterns of BMP signaling during early chick development. *Dev Biol* 244, 44-65.

Feng, R., Wen, J., 2015. Overview of the roles of Sox2 in stem cell and development. *Biol Chem* 396, 883-891.

Francia, S., Michelini, F., Saxena, A., Tang, D., de Hoon, M., Anelli, V., Mione, M., Carninci, P., d'Adda di Fagagna, F., 2012. Site-specific DICER and DROSHA RNA products control the DNA-damage response. *Nature* 488, 231-235.

Fu, X., Zhang, H., Chen, Z., Yang, Z., Shi, D., Liu, T., Chen, W., Yao, F., Su, X., Deng, W., Chen, M., Yang, A., 2019. TFAP2B overexpression contributes to tumor growth and progression of thyroid cancer through the COX-2 signaling pathway. *Cell Death Dis* 10, 397.

Furuta, Y., Hogan, B.L., 1998. BMP4 is essential for lens induction in the mouse embryo. *Genes Dev* 12, 3764-3775.

Gage, P.J., Rhoades, W., Prucka, S.K., Hjalt, T., 2005. Fate maps of neural crest and mesoderm in the mammalian eye. *Invest Ophthalmol Vis Sci* 46, 4200-4208.

Garcia-Castro, M.I., Marcelle, C., Bronner-Fraser, M., 2002. Ectodermal Wnt function as a neural crest inducer. *Science* 297, 848-851.

Gessert, S., Bugner, V., Tecza, A., Pinker, M., Kuhl, M., 2010. FMR1/FXR1 and the miRNA pathway are required for eye and neural crest development. *Dev Biol* 341, 222-235.

Gillespie, R.L., Urquhart, J., Lovell, S.C., Biswas, S., Parry, N.R., Schorderet, D.F., Lloyd, I.C., Clayton-Smith, J., Black, G.C., 2015. Abrogation of HMX1 function causes rare oculoauricular syndrome associated with congenital cataract, anterior segment dysgenesis, and retinal dystrophy. *Invest Ophthalmol Vis Sci* 56, 883-891.

Giovanella, S., Pasini, A., Ligabue, G., Testa, F., Mori, G., Tagliafico, E., Magistroni, R., 2023. PAX2/Renal Coloboma Syndrome Expresses Extreme Intrafamilial Phenotypic Variability. *Nephron* 147, 120-126.

Giusti, J., Pinhal, D., Moxon, S., Campos, C.L., Munsterberg, A., Martins, C., 2016. MicroRNA-10 modulates Hox genes expression during Nile tilapia embryonic development. *Mech Dev* 140, 12-18.

Godden, A.M., Antonaci, M., Ward, N.J., van der Lee, M., Abu-Daya, A., Guille, M., Wheeler, G.N., 2022. An efficient miRNA knockout approach using CRISPR-Cas9 in *Xenopus*. *Dev Biol* 483, 66-75.

Goding, C.R., Arnheiter, H., 2019. MITF-the first 25 years. *Genes Dev* 33, 983-1007.

Goljanek-Whysall, K., Mok, G.F., Fahad Alrefaei, A., Kennerley, N., Wheeler, G.N., Munsterberg, A., 2014. myomiR-dependent switching of BAF60 variant incorporation into Brg1 chromatin remodeling complexes during embryo myogenesis. *Development* 141, 3378-3387.

Goos, J.A.C., Mathijssen, I.M.J., 2019. Genetic Causes of Craniosynostosis: An Update. *Mol Syndromol* 10, 6-23.

Goudreau, G., Petrou, P., Reneker, L.W., Graw, J., Loster, J., Gruss, P., 2002. Mutually regulated expression of Pax6 and Six3 and its implications for the Pax6 haploinsufficient lens phenotype. *Proc Natl Acad Sci U S A* 99, 8719-8724.

Grigoryan, E.N., 2022. Self-Organization of the Retina during Eye Development, Retinal Regeneration In Vivo, and in Retinal 3D Organoids In Vitro. *Biomedicines* 10.

Grocott, T., Johnson, S., Bailey, A.P., Streit, A., 2011. Neural crest cells organize the eye via TGF-beta and canonical Wnt signalling. *Nat Commun* 2, 265.

Grocott, T., Lozano-Velasco, E., Mok, G.F., Munsterberg, A.E., 2020. The Pax6 master control gene initiates spontaneous retinal development via a self-organising Turing network. *Development* 147.

Haddad, A., Mohiuddin, S.S., 2024. Biochemistry, Citric Acid Cycle, StatPearls, Treasure Island (FL) ineligible companies. Disclosure: Shamim Mohiuddin declares no relevant financial relationships with ineligible companies.

Harding, P., Moosajee, M., 2019. The Molecular Basis of Human Anophthalmia and Microphthalmia. *J Dev Biol* 7.

Harris, M.L., Erickson, C.A., 2007. Lineage specification in neural crest cell pathfinding. *Dev Dyn* 236, 1-19.

Hochgreb-Hagele, T., Bronner, M.E., 2013. A novel FoxD3 gene trap line reveals neural crest precursor movement and a role for FoxD3 in their specification. *Dev Biol* 374, 1-11.

Hockman, D., Chong-Morrison, V., Green, S.A., Gavriouchkina, D., Candido-Ferreira, I., Ling, I.T.C., Williams, R.M., Amemiya, C.T., Smith, J.J., Bronner, M.E., Sauka-Spengler, T., 2019. A genome-wide assessment of the ancestral neural crest gene regulatory network. *Nat Commun* 10, 4689.

- Hovland, A.S., Rothstein, M., Simoes-Costa, M., 2020. Network architecture and regulatory logic in neural crest development. *Wiley Interdiscip Rev Syst Biol Med* 12, e1468.
- Huang, S., Song, J., He, C., Cai, X., Yuan, K., Mei, L., Feng, Y., 2022. Genetic insights, disease mechanisms, and biological therapeutics for Waardenburg syndrome. *Gene Ther* 29, 479-497.
- Huang, T., Liu, Y., Huang, M., Zhao, X., Cheng, L., 2010. Wnt1-cre-mediated conditional loss of Dicer results in malformation of the midbrain and cerebellum and failure of neural crest and dopaminergic differentiation in mice. *J Mol Cell Biol* 2, 152-163.
- Huang, X.H., Li, J.L., Li, X.Y., Wang, S.X., Jiao, Z.H., Li, S.Q., Liu, J., Ding, J., 2021. miR-208a in Cardiac Hypertrophy and Remodeling. *Front Cardiovasc Med* 8, 773314.
- Huang, Y., Fliegert, R., Guse, A.H., Lu, W., Du, J., 2020. A structural overview of the ion channels of the TRPM family. *Cell Calcium* 85, 102111.
- Hutchins, E.J., Bronner, M.E., 2018. Draxin acts as a molecular rheostat of canonical Wnt signaling to control cranial neural crest EMT. *J Cell Biol* 217, 3683-3697.
- Hutchins, E.J., Kunttas, E., Piacentino, M.L., Howard, A.G.A.t., Bronner, M.E., Uribe, R.A., 2018. Migration and diversification of the vagal neural crest. *Dev Biol* 444 Suppl 1, S98-S109.
- Hyer, J., Kuhlman, J., Afif, E., Mikawa, T., 2003. Optic cup morphogenesis requires pre-lens ectoderm but not lens differentiation. *Dev Biol* 259, 351-363.
- Jang, S.M., Kim, J.W., Kim, C.H., An, J.H., Johnson, A., Song, P.I., Rhee, S., Choi, K.H., 2015. KAT5-mediated SOX4 acetylation orchestrates chromatin remodeling during myoblast differentiation. *Cell Death Dis* 6, e1857.
- Ji, X., Takahashi, R., Hiura, Y., Hirokawa, G., Fukushima, Y., Iwai, N., 2009. Plasma miR-208 as a biomarker of myocardial injury. *Clin Chem* 55, 1944-1949.
- Jia, Q., Hu, S., Jiao, D., Li, X., Qi, S., Fan, R., 2020. Synaptotagmin-4 promotes dendrite extension and melanogenesis in alpaca melanocytes by regulating Ca(2+) influx via TRPM1 channels. *Cell Biochem Funct* 38, 275-282.
- Jin, C., Luo, Y., Liang, Z., Li, X., Kolat, D., Zhao, L., Xiong, W., 2023. Crucial role of the transcription factors family activator protein 2 in cancer: current clue and views. *J Transl Med* 21, 371.
- Jin, Y., Birlea, S.A., Fain, P.R., Gowan, K., Riccardi, S.L., Holland, P.J., Mailloux, C.M., Sufit, A.J., Hutton, S.M., Amadi-Myers, A., Bennett, D.C., Wallace, M.R., McCormack, W.T., Kemp, E.H., Gawkrödger, D.J., Weetman, A.P., Picardo, M., Leone, G., Taieb, A., Jouary, T., Ezzedine, K., van Geel, N., Lambert, J., Overbeck, A., Spritz, R.A., 2010. Variant of TYR and autoimmunity susceptibility loci in generalized vitiligo. *N Engl J Med* 362, 1686-1697.
- Jing, J.S., Li, H., Wang, S.C., Ma, J.M., Yu, L.Q., Zhou, H., 2018. NDRG3 overexpression is associated with a poor prognosis in patients with hepatocellular carcinoma. *Biosci Rep* 38.

Kasai, A., Kakihara, S., Miura, H., Okada, R., Hayata-Takano, A., Hazama, K., Niu, M., Shintani, N., Nakazawa, T., Hashimoto, H., 2016. Double In situ Hybridization for MicroRNAs and mRNAs in Brain Tissues. *Front Mol Neurosci* 9, 126.

Kastriti, M.E., Faure, L., Von Ahsen, D., Boudierlique, T.G., Bostrom, J., Solovieva, T., Jackson, C., Bronner, M., Meijer, D., Hadjab, S., Lallemand, F., Erickson, A., Kaucka, M., Dyachuk, V., Perlmann, T., Lahti, L., Krivanek, J., Brunet, J.F., Fried, K., Adameyko, I., 2022. Schwann cell precursors represent a neural crest-like state with biased multipotency. *EMBO J* 41, e108780.

Kelly, L.E., El-Hodiri, H.M., 2016. *Xenopus laevis* Nkx5.3 and sensory organ homeobox (SOHo) are expressed in developing sensory organs and ganglia of the head and anterior trunk. *Dev Genes Evol* 226, 423-428.

Kim, J.W., Lemke, G., 2006. Hedgehog-regulated localization of Vax2 controls eye development. *Genes Dev* 20, 2833-2847.

Krichevsky, A.M., Sonntag, K.C., Isacson, O., Kosik, K.S., 2006. Specific microRNAs modulate embryonic stem cell-derived neurogenesis. *Stem Cells* 24, 857-864.

Krispin, S., Nitzan, E., Kassem, Y., Kalcheim, C., 2010. Evidence for a dynamic spatiotemporal fate map and early fate restrictions of premigratory avian neural crest. *Development* 137, 585-595.

Lachke, S.A., Maas, R.L., 2010. Building the developmental oculome: systems biology in vertebrate eye development and disease. *Wiley Interdiscip Rev Syst Biol Med* 2, 305-323.

Lackey, A.E., Muzio, M.R., 2021. DiGeorge Syndrome, StatPearls, Treasure Island (FL).

Lamouille, S., Xu, J., Derynck, R., 2014. Molecular mechanisms of epithelial-mesenchymal transition. *Nat Rev Mol Cell Biol* 15, 178-196.

Lattanzi, W., Barba, M., Di Pietro, L., Boyadjiev, S.A., 2017. Genetic advances in craniosynostosis. *Am J Med Genet A* 173, 1406-1429.

Lee, R.C., Feinbaum, R.L., Ambros, V., 1993. The *C. elegans* heterochronic gene *lin-4* encodes small RNAs with antisense complementarity to *lin-14*. *Cell* 75, 843-854.

Li, F., Zhou, M.W., Liu, N., Yang, Y.Y., Xing, H.Y., Lu, Y., Liu, X.X., 2019a. MicroRNA-219 Inhibits Proliferation and Induces Differentiation of Oligodendrocyte Precursor Cells after Contusion Spinal Cord Injury in Rats. *Neural Plast* 2019, 9610687.

Li, H., Xie, H., Liu, W., Hu, R., Huang, B., Tan, Y.F., Xu, K., Sheng, Z.F., Zhou, H.D., Wu, X.P., Luo, X.H., 2009. A novel microRNA targeting HDAC5 regulates osteoblast differentiation in mice and contributes to primary osteoporosis in humans. *J Clin Invest* 119, 3666-3677.

Li, J., Perfetto, M., Materna, C., Li, R., Thi Tran, H., Vleminckx, K., Duncan, M.K., Wei, S., 2019b. A new transgenic reporter line reveals Wnt-dependent Snai2 re-expression and cranial neural crest differentiation in *Xenopus*. *Sci Rep* 9, 11191.

- Li, S., Wang, S., Guo, Z., Wu, H., Jin, X., Wang, Y., Li, X., Liang, S., 2016. miRNA Profiling Reveals Dysregulation of RET and RET-Regulating Pathways in Hirschsprung's Disease. *PLoS One* 11, e0150222.
- Lima Cunha, D., Arno, G., Corton, M., Moosajee, M., 2019. The Spectrum of PAX6 Mutations and Genotype-Phenotype Correlations in the Eye. *Genes (Basel)* 10.
- Lingam, G., Sen, A.C., Lingam, V., Bhende, M., Padhi, T.R., Xinyi, S., 2021. Ocular coloboma-a comprehensive review for the clinician. *Eye (Lond)* 35, 2086-2109.
- Liu, C., Luo, Y.P., Chen, J., Weng, Y.H., Lan, Y., Liu, H.B., 2023. Functional polymorphism in miR-208 is associated with increased risk for ischemic stroke. *BMC Med Genomics* 16, 176.
- Liu, H., Lei, C., He, Q., Pan, Z., Xiao, D., Tao, Y., 2018. Nuclear functions of mammalian MicroRNAs in gene regulation, immunity and cancer. *Mol Cancer* 17, 64.
- Liu, H., Tan, B.C., Tseng, K.H., Chuang, C.P., Yeh, C.W., Chen, K.D., Lee, S.C., Yung, B.Y., 2007. Nucleophosmin acts as a novel AP2alpha-binding transcriptional corepressor during cell differentiation. *EMBO Rep* 8, 394-400.
- Liu, J., Qiu, J., Zhang, Z., Zhou, L., Li, Y., Ding, D., Zhang, Y., Zou, D., Wang, D., Zhou, Q., Lang, T., 2021a. SOX4 maintains the stemness of cancer cells via transcriptionally enhancing HDAC1 revealed by comparative proteomics study. *Cell Biosci* 11, 23.
- Liu, W., Lagutin, O.V., Mende, M., Streit, A., Oliver, G., 2006. Six3 activation of Pax6 expression is essential for mammalian lens induction and specification. *EMBO J* 25, 5383-5395.
- Liu, Y., Semina, E.V., 2012. pitx2 Deficiency results in abnormal ocular and craniofacial development in zebrafish. *PLoS One* 7, e30896.
- Liu, Y., Xia, J., Zhou, Y., Shao, S., 2021b. High expression of NDRG3 correlates with poor prognosis in gastric cancer patients. *Rev Esp Enferm Dig* 113, 524-528.
- Livesey, F.J., Cepko, C.L., 2001. Vertebrate neural cell-fate determination: lessons from the retina. *Nat Rev Neurosci* 2, 109-118.
- Lorusso, C., De Summa, S., Pinto, R., Danza, K., Tommasi, S., 2020. miRNAs as Key Players in the Management of Cutaneous Melanoma. *Cells* 9.
- Lotfollahzadeh, S., Taherian, M., Anand, S., 2021. Hirschsprung Disease, StatPearls, Treasure Island (FL).
- Lukoseviciute, M., Gavriouchkina, D., Williams, R.M., Hochgreb-Hagele, T., Senanayake, U., Chong-Morrison, V., Thongjuea, S., Repapi, E., Mead, A., Sauka-Spengler, T., 2018. From Pioneer to Repressor: Bimodal foxd3 Activity Dynamically Remodels Neural Crest Regulatory Landscape In Vivo. *Dev Cell* 47, 608-628 e606.

Luo, J., Fang, H., Wang, D., Hu, J., Zhang, W., Jiang, R., 2024. Molecular Mechanism of SOX18 in Lipopolysaccharide-Induced Injury of Human Umbilical Vein Endothelial Cells. *Crit Rev Immunol* 44, 1-12.

Lv, N., Wang, Y., Zhao, M., Dong, L., Wei, H., 2021. The Role of PAX2 in Neurodevelopment and Disease. *Neuropsychiatr Dis Treat* 17, 3559-3567.

Ma, X.R., Xu, Y.L., Qian, J., Wang, Y., 2019. Long non-coding RNA SNHG15 accelerates the progression of non-small cell lung cancer by absorbing miR-211-3p. *Eur Rev Med Pharmacol Sci* 23, 1536-1544.

Macdonald, R., Barth, K.A., Xu, Q., Holder, N., Mikkola, I., Wilson, S.W., 1995. Midline signalling is required for Pax gene regulation and patterning of the eyes. *Development* 121, 3267-3278.

Marathe, H.G., Watkins-Chow, D.E., Weider, M., Hoffmann, A., Mehta, G., Trivedi, A., Aras, S., Basuroy, T., Mehrotra, A., Bennett, D.C., Wegner, M., Pavan, W.J., de la Serna, I.L., 2017. BRG1 interacts with SOX10 to establish the melanocyte lineage and to promote differentiation. *Nucleic Acids Res* 45, 6442-6458.

Marcon, C.R., Maia, M., 2019. Albinism: epidemiology, genetics, cutaneous characterization, psychosocial factors. *An Bras Dermatol* 94, 503-520.

Martik, M.L., Bronner, M.E., 2017. Regulatory Logic Underlying Diversification of the Neural Crest. *Trends Genet* 33, 715-727.

Martik, M.L., Bronner, M.E., 2021. Riding the crest to get a head: neural crest evolution in vertebrates. *Nat Rev Neurosci* 22, 616-626.

Massaad, E., Tfayli, H., Awwad, J., Nabulsi, M., Farra, C., 2019. Char Syndrome a novel mutation and new insights: A clinical report. *Eur J Med Genet* 62, 103607.

Mayor, R., Theveneau, E., 2013. The neural crest. *Development* 140, 2247-2251.

Medioni, C., Bertrand, N., Mesbah, K., Hudry, B., Dupays, L., Wolstein, O., Washkowitz, A.J., Papaioannou, V.E., Mohun, T.J., Harvey, R.P., Zaffran, S., 2010. Expression of Slit and Robo genes in the developing mouse heart. *Dev Dyn* 239, 3303-3311.

Mercuri, R.L.V., Conceicao, H.B., Guardia, G.D.A., Goldstein, G., Vibranovski, M.D., Hinske, L.C., Galante, P.A.F., 2023. Retro-miRs: novel and functional miRNAs originating from mRNA retrotransposition. *Mob DNA* 14, 12.

Michels, K., Bohnsack, B.L., 2023. Ophthalmological Manifestations of Axenfeld-Rieger Syndrome: Current Perspectives. *Clin Ophthalmol* 17, 819-828.

Moe, A., Dimogkioka, A.R., Rapaport, D., Ojemyr, L.N., Brzezinski, P., 2023. Structure and function of the *S. pombe* III-IV-cyt c supercomplex. *Proc Natl Acad Sci U S A* 120, e2307697120.

Mok, G.F., Lozano-Velasco, E., Munsterberg, A., 2017. microRNAs in skeletal muscle development. *Semin Cell Dev Biol* 72, 67-76.

Monsoro-Burq, A.H., Fletcher, R.B., Harland, R.M., 2003. Neural crest induction by paraxial mesoderm in *Xenopus* embryos requires FGF signals. *Development* 130, 3111-3124.

Montagna, D.R., Duarte, A., Todero, M.F., Ruggiero, R.A., Isturiz, M., Rearte, B., 2020. Meta-tyrosine modulates the immune response induced by bacterial endotoxins. *Immunobiology* 225, 151856.

Moreno, C.S., 2020. SOX4: The unappreciated oncogene. *Semin Cancer Biol* 67, 57-64.

Mui, S.H., Hindges, R., O'Leary, D.D., Lemke, G., Bertuzzi, S., 2002. The homeodomain protein Vax2 patterns the dorsoventral and nasotemporal axes of the eye. *Development* 129, 797-804.

Murchison, E.P., Hannon, G.J., 2004. miRNAs on the move: miRNA biogenesis and the RNAi machinery. *Curr Opin Cell Biol* 16, 223-229.

Mustarde, J.C., 1963. Epicanthus and Telecanthus. *Br J Plast Surg* 16, 346-356.

Nieto, M.A., Huang, R.Y., Jackson, R.A., Thiery, J.P., 2016. Emt: 2016. *Cell* 166, 21-45.

O'Brien, J., Hayder, H., Zayed, Y., Peng, C., 2018. Overview of MicroRNA Biogenesis, Mechanisms of Actions, and Circulation. *Frontiers in Endocrinology* 9.

Oliver, G., Loosli, F., Koster, R., Wittbrodt, J., Gruss, P., 1996. Ectopic lens induction in fish in response to the murine homeobox gene Six3. *Mech Dev* 60, 233-239.

Onuma, Y., Takahashi, S., Asashima, M., Kurata, S., Gehring, W.J., 2002. Conservation of Pax 6 function and upstream activation by Notch signaling in eye development of frogs and flies. *Proc Natl Acad Sci U S A* 99, 2020-2025.

Ooi, C.Y., Carter, D.R., Liu, B., Mayoh, C., Beckers, A., Lalwani, A., Nagy, Z., De Brouwer, S., Decaestecker, B., Hung, T.T., Norris, M.D., Haber, M., Liu, T., De Preter, K., Speleman, F., Cheung, B.B., Marshall, G.M., 2018. Network Modeling of microRNA-mRNA Interactions in Neuroblastoma Tumorigenesis Identifies miR-204 as a Direct Inhibitor of MYCN. *Cancer Res* 78, 3122-3134.

Perri, P., Ponzoni, M., Corrias, M.V., Ceccherini, I., Candiani, S., Bachetti, T., 2021. A Focus on Regulatory Networks Linking MicroRNAs, Transcription Factors and Target Genes in Neuroblastoma. *Cancers (Basel)* 13.

Piacentino, M.L., Li, Y., Bronner, M.E., 2020. Epithelial-to-mesenchymal transition and different migration strategies as viewed from the neural crest. *Curr Opin Cell Biol* 66, 43-50.

Pingault, V., Zerad, L., Bertani-Torres, W., Bondurand, N., 2022. SOX10: 20 years of phenotypic plurality and current understanding of its developmental function. *J Med Genet* 59, 105-114.

Pla, P., Monsoro-Burq, A.H., 2018. The neural border: Induction, specification and maturation of the territory that generates neural crest cells. *Dev Biol* 444 Suppl 1, S36-S46.

Plouhinec, J.L., Zakin, L., Moriyama, Y., De Robertis, E.M., 2013. Chordin forms a self-organizing morphogen gradient in the extracellular space between ectoderm and mesoderm in the *Xenopus* embryo. *Proc Natl Acad Sci U S A* 110, 20372-20379.

Pontoriero, G.F., Deschamps, P., Ashery-Padan, R., Wong, R., Yang, Y., Zavadil, J., Cvekl, A., Sullivan, S., Williams, T., West-Mays, J.A., 2008. Cell autonomous roles for AP-2alpha in lens vesicle separation and maintenance of the lens epithelial cell phenotype. *Dev Dyn* 237, 602-617.

Portnoy, V., Lin, S.H., Li, K.H., Burlingame, A., Hu, Z.H., Li, H., Li, L.C., 2016. saRNA-guided Ago2 targets the RITA complex to promoters to stimulate transcription. *Cell Res* 26, 320-335.

Purcell, P., Oliver, G., Mardon, G., Donner, A.L., Maas, R.L., 2005. Pax6-dependence of Six3, Eya1 and Dach1 expression during lens and nasal placode induction. *Gene Expr Patterns* 6, 110-118.

Raap, M., Gierendt, L., Kreipe, H.H., Christgen, M., 2021. Transcription factor AP-2beta in development, differentiation and tumorigenesis. *Int J Cancer* 149, 1221-1227.

Ramchandran, R., Chaluvally-Raghavan, P., 2017. miRNA-Mediated RNA Activation in Mammalian Cells. *Adv Exp Med Biol* 983, 81-89.

Rastrelli, M., Tropea, S., Rossi, C.R., Alaibac, M., 2014. Melanoma: epidemiology, risk factors, pathogenesis, diagnosis and classification. *In Vivo* 28, 1005-1011.

Rehman, S., Ahmed, D., 2023. Embryology, Kidney, Bladder, and Ureter, StatPearls, Treasure Island (FL) ineligible companies. Disclosure: Danish Ahmed declares no relevant financial relationships with ineligible companies.

Robinson, M.L., 2006. An essential role for FGF receptor signaling in lens development. *Semin Cell Dev Biol* 17, 726-740.

Rose, A.B., 2018. Introns as Gene Regulators: A Brick on the Accelerator. *Front Genet* 9, 672.

Roth, S.A., Hald, O.H., Fuchs, S., Lokke, C., Mikkola, I., Flaegstad, T., Schulte, J., Einvik, C., 2018. MicroRNA-193b-3p represses neuroblastoma cell growth via downregulation of Cyclin D1, MCL-1 and MYCN. *Oncotarget* 9, 18160-18179.

Rothberg, J.M., Hartley, D.A., Walther, Z., Artavanis-Tsakonas, S., 1988. slit: an EGF-homologous locus of *D. melanogaster* involved in the development of the embryonic central nervous system. *Cell* 55, 1047-1059.

Sadaghiani, B., Thiebaud, C.H., 1987. Neural crest development in the *Xenopus laevis* embryo, studied by interspecific transplantation and scanning electron microscopy. *Dev Biol* 124, 91-110.

- Salim, U., Kumar, A., Kulshreshtha, R., Vivekanandan, P., 2022. Biogenesis, characterization, and functions of mirtrons. *Wiley Interdiscip Rev RNA* 13, e1680.
- Saliminejad, K., Khorram Khorshid, H.R., Soleymani Fard, S., Ghaffari, S.H., 2019. An overview of microRNAs: Biology, functions, therapeutics, and analysis methods. *J Cell Physiol* 234, 5451-5465.
- Sato, T.S., Handa, A., Priya, S., Watal, P., Becker, R.M., Sato, Y., 2019. Neurocristopathies: Enigmatic Appearances of Neural Crest Cell-derived Abnormalities. *Radiographics* 39, 2085-2102.
- Sauka-Spengler, T., Bronner-Fraser, M., 2006. Development and evolution of the migratory neural crest: a gene regulatory perspective. *Curr Opin Genet Dev* 16, 360-366.
- Sauka-Spengler, T., Bronner-Fraser, M., 2008. A gene regulatory network orchestrates neural crest formation. *Nat Rev Mol Cell Biol* 9, 557-568.
- Schell, G., Roy, B., Prall, K., Dwivedi, Y., 2022. miR-218: A Stress-Responsive Epigenetic Modifier. *Noncoding RNA* 8.
- Schorle, H., Meier, P., Buchert, M., Jaenisch, R., Mitchell, P.J., 1996. Transcription factor AP-2 essential for cranial closure and craniofacial development. *Nature* 381, 235-238.
- Seal, S., Monsoro-Burq, A.H., 2020. Insights Into the Early Gene Regulatory Network Controlling Neural Crest and Placode Fate Choices at the Neural Border. *Front Physiol* 11, 608812.
- Seberg, H.E., Van Otterloo, E., Loftus, S.K., Liu, H., Bonde, G., Sompallae, R., Gildea, D.E., Santana, J.F., Manak, J.R., Pavan, W.J., Williams, T., Cornell, R.A., 2017. TFAP2 paralogs regulate melanocyte differentiation in parallel with MITF. *PLoS Genet* 13, e1006636.
- Sheedy, P., Medarova, Z., 2018. The fundamental role of miR-10b in metastatic cancer. *Am J Cancer Res* 8, 1674-1688.
- Shi, J., Severson, C., Yang, J., Wedlich, D., Klymkowsky, M.W., 2011. Snail2 controls mesodermal BMP/Wnt induction of neural crest. *Development* 138, 3135-3145.
- Shiels, A., 2020. TRPM3\_miR-204: a complex locus for eye development and disease. *Hum Genomics* 14, 7.
- Simoës-Costa, M., Bronner, M.E., 2013. Insights into neural crest development and evolution from genomic analysis. *Genome Res* 23, 1069-1080.
- Simoës-Costa, M., Bronner, M.E., 2015. Establishing neural crest identity: a gene regulatory recipe. *Development* 142, 242-257.
- Smits, J.P.H., Qu, J., Pardow, F., van den Brink, N.J.M., Rodijk-Olthuis, D., van Vlijmen-Willems, I., van Heeringen, S.J., Zeeuwen, P., Schalkwijk, J., Zhou, H., van den Bogaard, E.H., 2023. The

aryl hydrocarbon receptor regulates epidermal differentiation through transient activation of TFAP2A. *bioRxiv*.

Snyman, M., Walsdorf, R.E., Wix, S.N., Gill, J.G., 2024. The metabolism of melanin synthesis-From melanocytes to melanoma. *Pigment Cell Melanoma Res*.

Song, N., Schwab, K.R., Patterson, L.T., Yamaguchi, T., Lin, X., Potter, S.S., Lang, R.A., 2007. *pygopus 2* has a crucial, Wnt pathway-independent function in lens induction. *Development* 134, 1873-1885.

Stallings, R.L., 2009. MicroRNA involvement in the pathogenesis of neuroblastoma: potential for microRNA mediated therapeutics. *Curr Pharm Des* 15, 456-462.

Steimle, J.D., Moskowitz, I.P., 2017. TBX5: A Key Regulator of Heart Development. *Curr Top Dev Biol* 122, 195-221.

Su, M., Miao, F., Jiang, S., Shi, Y., Luo, L., He, X., Wan, J., Xu, S., Lei, T.C., 2020. Role of the p53-TRPM1/miR-211-MMP9 axis in UVB-induced human melanocyte migration and its potential in repigmentation. *Int J Mol Med* 45, 1017-1026.

Svoronos, A.A., Engelman, D.M., Slack, F.J., 2016. OncomiR or Tumor Suppressor? The Duplicity of MicroRNAs in Cancer. *Cancer Res* 76, 3666-3670.

Takahashi, K., Yamanaka, S., 2006. Induction of pluripotent stem cells from mouse embryonic and adult fibroblast cultures by defined factors. *Cell* 126, 663-676.

Thatcher, E.J., Bond, J., Paydar, I., Patton, J.G., 2008. Genomic organization of zebrafish microRNAs. *BMC Genomics* 9, 253.

Theveneau, E., Mayor, R., 2012a. Cadherins in collective cell migration of mesenchymal cells. *Curr Opin Cell Biol* 24, 677-684.

Theveneau, E., Mayor, R., 2012b. Neural crest delamination and migration: from epithelium-to-mesenchyme transition to collective cell migration. *Dev Biol* 366, 34-54.

Thomeer, H.G., Crins, T.T., Kamsteeg, E.J., Buijsman, W., Cruysberg, J.R., Knoers, N.V., Cremers, C.W., 2010. Clinical presentation and the presence of hearing impairment in branchio-oculo-facial syndrome: a new mutation in the TFAP2A gene. *Ann Otol Rhinol Laryngol* 119, 806-814.

Timme-Laragy, A.R., Karchner, S.I., Hahn, M.E., 2012. Gene knockdown by morpholino-modified oligonucleotides in the zebrafish (*Danio rerio*) model: applications for developmental toxicology. *Methods Mol Biol* 889, 51-71.

Tsang, S.H., Sharma, T., 2018. Congenital Stationary Night Blindness. *Adv Exp Med Biol* 1085, 61-64.

Twigg, S.R., Wilkie, A.O., 2015. A Genetic-Pathophysiological Framework for Craniosynostosis. *Am J Hum Genet* 97, 359-377.

Usman, N., Sur, M., 2021. CHARGE Syndrome, StatPearls, Treasure Island (FL).

Uwanogho, D., Rex, M., Cartwright, E.J., Pearl, G., Healy, C., Scotting, P.J., Sharpe, P.T., 1995. Embryonic expression of the chicken Sox2, Sox3 and Sox11 genes suggests an interactive role in neuronal development. *Mech Dev* 49, 23-36.

Vega-Lopez, G.A., Cerrizuela, S., Aybar, M.J., 2017. Trunk neural crest cells: formation, migration and beyond. *Int J Dev Biol* 61, 5-15.

Vega-Lopez, G.A., Cerrizuela, S., Tribulo, C., Aybar, M.J., 2018. Neurocristopathies: New insights 150 years after the neural crest discovery. *Dev Biol* 444 Suppl 1, S110-S143.

Wang, X., Chan, A.K., Sham, M.H., Burns, A.J., Chan, W.Y., 2011. Analysis of the sacral neural crest cell contribution to the hindgut enteric nervous system in the mouse embryo. *Gastroenterology* 141, 992-1002 e1001-1006.

Wang, X., Rong, S., Sun, Y., Yin, B., Yang, X., Lu, X., Sun, H., Yan, Y., Sun, G., Liang, Y., Wang, P., Xie, S., Li, Y., 2023. NDRG3 regulates imatinib resistance by promoting beta-catenin accumulation in the nucleus in chronic myelogenous leukemia. *Oncol Rep* 50.

Ward, N.J., Green, D., Higgins, J., Dalmay, T., Munsterberg, A., Moxon, S., Wheeler, G.N., 2018. microRNAs associated with early neural crest development in *Xenopus laevis*. *BMC Genomics* 19, 59.

Wawersik, S., Purcell, P., Maas, R.L., 2000. Pax6 and the genetic control of early eye development. *Results Probl Cell Differ* 31, 15-36.

Weigele, J., Bohnsack, B.L., 2020. Genetics Underlying the Interactions between Neural Crest Cells and Eye Development. *J Dev Biol* 8.

White, R.M., Cech, J., Ratanasirintrao, S., Lin, C.Y., Rahl, P.B., Burke, C.J., Langdon, E., Tomlinson, M.L., Mosher, J., Kaufman, C., Chen, F., Long, H.K., Kramer, M., Datta, S., Neuberg, D., Granter, S., Young, R.A., Morrison, S., Wheeler, G.N., Zon, L.I., 2011. DHODH modulates transcriptional elongation in the neural crest and melanoma. *Nature* 471, 518-522.

Wigle, J.T., Chowdhury, K., Gruss, P., Oliver, G., 1999. Prox1 function is crucial for mouse lens-fibre elongation. *Nat Genet* 21, 318-322.

Williams, A.L., Bohnsack, B.L., 2020. The Ocular Neural Crest: Specification, Migration, and Then What? *Front Cell Dev Biol* 8, 595896.

Williamson, K.A., FitzPatrick, D.R., 2014. The genetic architecture of microphthalmia, anophthalmia and coloboma. *Eur J Med Genet* 57, 369-380.

Williamson, K.A., Yates, T.M., FitzPatrick, D.R., 1993. SOX2 Disorder, in: Adam, M.P., Feldman, J., Mirzaa, G.M., Pagon, R.A., Wallace, S.E., Bean, L.J.H., Gripp, K.W., Amemiya, A. (Eds.), *GeneReviews*((R)), Seattle (WA).

Winter, J., Jung, S., Keller, S., Gregory, R.I., Diederichs, S., 2009. Many roads to maturity: microRNA biogenesis pathways and their regulation. *Nat Cell Biol* 11, 228-234.

Wu, H., Zhao, J., Fu, B., Yin, S., Song, C., Zhang, J., Zhao, S., Zhang, Y., 2017. Retinoic acid-induced upregulation of miR-219 promotes the differentiation of embryonic stem cells into neural cells. *Cell Death Dis* 8, e2953.

Wu, Q., Zhao, J., Zheng, Y., Xie, X., He, Q., Zhu, Y., Wang, N., Huang, L., Lu, L., Hu, T., Zeng, J., Xia, H., Zhang, Y., Zhong, W., 2021. Associations between common genetic variants in microRNAs and Hirschsprung disease susceptibility in Southern Chinese children. *J Gene Med* 23, e3301.

Wuebben, E.L., Rizzino, A., 2017. The dark side of SOX2: cancer - a comprehensive overview. *Oncotarget* 8, 44917-44943.

Wulf, A.M., Moreno, M.M., Paka, C., Rampasekova, A., Liu, K.J., 2021. Defining Pathological Activities of ALK in Neuroblastoma, a Neural Crest-Derived Cancer. *Int J Mol Sci* 22.

Xiao, Y., MacRae, I.J., 2019. Toward a Comprehensive View of MicroRNA Biology. *Mol Cell* 75, 666-668.

Xing, F., Song, Z., He, Y., 2018. MiR-219-5p inhibits growth and metastasis of ovarian cancer cells by targeting HMGA2. *Biol Res* 51, 50.

Xu, J., Zhang, R., Zhao, J., 2017. The Novel Long Noncoding RNA TUSC7 Inhibits Proliferation by Sponging MiR-211 in Colorectal Cancer. *Cell Physiol Biochem* 41, 635-644.

Yang, J., Sheng, Y.Y., Wei, J.W., Gao, X.M., Zhu, Y., Jia, H.L., Dong, Q.Z., Qin, L.X., 2018. MicroRNA-219-5p Promotes Tumor Growth and Metastasis of Hepatocellular Carcinoma by Regulating Cadherin 1. *Biomed Res Int* 2018, 4793971.

Zacharias, A.L., Lewandoski, M., Rudnicki, M.A., Gage, P.J., 2011. Pitx2 is an upstream activator of extraocular myogenesis and survival. *Dev Biol* 349, 395-405.

Zehir, A., Hua, L.L., Maska, E.L., Morikawa, Y., Cserjesi, P., 2010. Dicer is required for survival of differentiating neural crest cells. *Dev Biol* 340, 459-467.

Zhao, F., Bosserhoff, A.K., Buettner, R., Moser, M., 2011. A heart-hand syndrome gene: *Tfap2b* plays a critical role in the development and remodeling of mouse ductus arteriosus and limb patterning. *PLoS One* 6, e22908.

Zhao, R., Trainor, P.A., 2023. Epithelial to mesenchymal transition during mammalian neural crest cell delamination. *Semin Cell Dev Biol* 138, 54-67.

Zhao, X., Wang, Y., Sun, X., 2020. The functions of microRNA-208 in the heart. *Diabetes Res Clin Pract* 160, 108004.

Zhong, C., Zhou, Y.K., Yang, S.S., Zhao, J.F., Zhu, X.L., Chen, H.H., Chen, P.C., Huang, L.Q., Huang, X., 2015. Developmental expression of the N-myc downstream regulated gene (NdrG) family during *Xenopus tropicalis* embryogenesis. *Int J Dev Biol* 59, 511-517.

Zhu, Y., Lin, A., Zheng, Y., Xie, X., He, Q., Zhong, W., 2020. miR-100 rs1834306 A>G Increases the Risk of Hirschsprung Disease in Southern Chinese Children. *Pharmgenomics Pers Med* 13, 283-288.

Zuber, M.E., Gestri, G., Viczian, A.S., Barsacchi, G., Harris, W.A., 2003. Specification of the vertebrate eye by a network of eye field transcription factors. *Development* 130, 5155-5167.



# An efficient miRNA knockout approach using CRISPR-Cas9 in *Xenopus*<sup>☆</sup>

Alice M. Godden<sup>a</sup>, Marco Antonaci<sup>a,1</sup>, Nicole J. Ward<sup>a,1</sup>, Michael van der Lee<sup>a</sup>,  
Anita Abu-Daya<sup>b</sup>, Matthew Guille<sup>b</sup>, Grant N. Wheeler<sup>a,\*</sup>

<sup>a</sup> School of Biological Sciences, University of East Anglia, Norwich Research Park, Norwich, NR4 7TJ, United Kingdom

<sup>b</sup> King Henry Building, King Henry I St, Portsmouth, PO1 2DY, United Kingdom

## ARTICLE INFO

**Keywords:**  
miRNAs  
Neural crest  
Pigment  
Craniofacial  
CRISPR-Cas9  
*Xenopus*

## ABSTRACT

In recent years CRISPR-Cas9 knockouts (KO) have become increasingly utilised to study gene function. MicroRNAs (miRNAs) are short non-coding RNAs, 20–22 nucleotides long, which affect gene expression through post-transcriptional repression. We previously identified miRNAs-196a and -219 as implicated in the development of *Xenopus* neural crest (NC). The NC is a multipotent stem-cell population, specified during early neurulation. Following EMT, NC cells migrate to various points in the developing embryo where they give rise to a number of tissues including parts of the peripheral nervous system, pigment cells and craniofacial skeleton. Dysregulation of NC development results in many diseases grouped under the term neurocristopathies. As miRNAs are so small, it is difficult to design CRISPR sgRNAs that reproducibly lead to a KO. We have therefore designed a novel approach using two guide RNAs to effectively ‘drop out’ a miRNA. We have knocked out miR-196a and miR-219 and compared the results to morpholino knockdowns (KD) of the same miRNAs. Validation of efficient CRISPR miRNA KO and phenotype analysis included use of whole-mount *in situ* hybridization of key NC and neural plate border markers such as *Pax3*, *Xhe2*, *Sox10* and *Snail2*, q-RT-PCR and Sanger sequencing. To show specificity we have also rescued the knockout phenotype using miRNA mimics. MiRNA-219 and miR-196a KO's both show loss of NC, altered neural plate and hatching gland phenotypes. Tadpoles show gross craniofacial and pigment phenotypes.

## 1. Introduction

MiRNAs are short non-coding, single stranded RNAs, approximately 20–22 nucleotides in length (Alberti and Cochella, 2017; Lee et al., 1993; Shah et al., 2017). MiRNAs are initially transcribed by RNA polymerase II as a pri-miRNA stem-loop structure from the genome, which undergoes processing to form a mature miRNA (Agarwal et al., 2015; Alberti and Cochella, 2017; Bartel, 2004; Inui et al., 2010).

MiRNAs are highly conserved between species with many orthologues discovered (Bartel, 2004). The miRNA database and repository, miRbase, currently has 2,656 mature miRNA sequences across all species. It is thought that there are >2,300 different miRNAs in humans alone (Alles et al., 2019). Recent reports suggest that 60% of all protein coding

genes in mammals are regulated by one or more miRNAs (Li et al., 2018). Within the human genome, it is estimated that up to 2% of genes encode for miRNAs (Miska, 2005). MiRNAs are implicated in development of various tissues in vertebrates, including chick, mouse, frog and fish (Mok et al., 2017; Ward et al., 2018); as well as in invertebrates like the worm and fruit fly (Chandra et al., 2017). Efficient methods to KO one or more miRNAs are therefore required.

The NC has the potential to differentiate into many different cell types and it contributes to many tissues. The NC can migrate all over the body and become parts of the peripheral nervous system, craniofacial skeleton and pigment (Aoto et al., 2015; Cheung and Briscoe, 2003; Hatch et al., 2016). How this occurs depends on niches and environments that have the right cocktail of gene expression patterns, signals or transcription

**Abbreviations:** INDEL, Insertion deletion (mutation); miRNAs, MicroRNAs; KD, Knockdown; KO, Knockout; NC, Neural crest; NF, Nieuwkoop and Faber; sgRNA, single guide RNA; MO, Morpholino.

\* This work was supported by UKRI Biotechnology and Biological Sciences Research Council Norwich Research Park Biosciences Doctoral Training Partnership grants to AG (BB/M011216/1) and NW (BB/J014524/1). MA has received funding from the European Union's Horizon 2020 research and innovation programme under the Marie Skłodowska-Curie grant agreement No. 860635. The European *Xenopus* Resource Centre is supported by the Wellcome Trust (101480Z) and BBSRC BB/K019988/1.

\* Corresponding author.

E-mail address: [grant.wheeler@uea.ac.uk](mailto:grant.wheeler@uea.ac.uk) (G.N. Wheeler).

<sup>1</sup> These authors contributed equally to this work.

<https://doi.org/10.1016/j.ydbio.2021.12.015>

Received 30 July 2021; Received in revised form 15 December 2021; Accepted 23 December 2021

Available online 27 December 2021

0012-1606/© 2022 The Authors. Published by Elsevier Inc. This is an open access article under the CC BY license (<http://creativecommons.org/licenses/by/4.0/>).

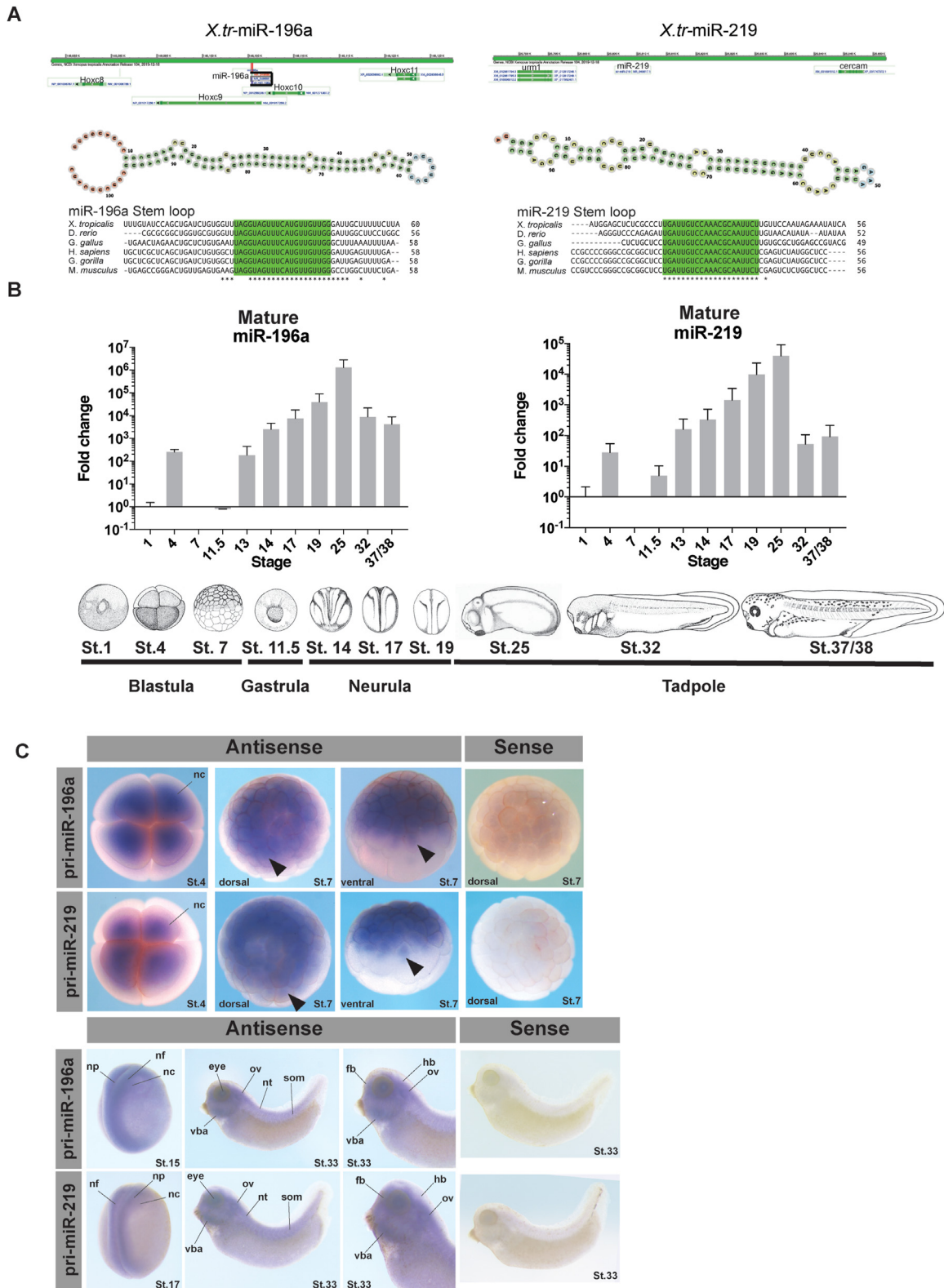


**Fig. 1.** Conservation, location, spatial and temporal expression of miR-196a and miR-219 in *X. tropicalis*. (A) miRNA genomic locations and stem-loop structures of miRNAs. Bottom-conservation of mature miRNAs as indicated by “\*”. miRNA stem loop structures were predicted computationally using Vienna RNA fold tool: [http://rna.tbi.univie.ac.at/forna/forna.html?id=RNAfold/vCiQTz5Wd4&file=cent\\_probs.json](http://rna.tbi.univie.ac.at/forna/forna.html?id=RNAfold/vCiQTz5Wd4&file=cent_probs.json) (B) *X. laevis* developmental profile of miR-196a and miR-219 by qRT PCR. Fold change is represented as mean ± SD normalised to snU6 at St.1, and biological replicates with undetermined values are excluded. Ten embryos (three biological replicates) were pooled to extract total RNA for cDNA synthesis. For each biological replicate three technical replicates were conducted. *Xenopus* embryo pictures at Nieuwkoop and Faber stages are shown. The neural crest generally begins to appear at NF st. 12.5/13. (C) Spatial expression of pri-miR-196a and pri-miR-219 by whole-mount *in situ* hybridisation in *X. tropicalis* embryos with sense and anti-sense expression. Embryos show expression from St.4 with global expression in NC, at St.7 expression is seen in cell nucleus, at neurula stages expression is in NC and neural tissues, and at tadpole stages can be seen in craniofacial tissues. Abbreviations: nf-neural fold, np-neural plate, nc- NC, vba-ventral branchial arches, ov-otic vesicle, nt-neural tube, som-somites, fb-forebrain, hb-hindbrain.

factors (Sauka-Spengler and Bronner-Fraser, 2008). miRNAs have been suggested to play a role in NC development with Dicer KD experiments in mouse leading to NC cell death by apoptosis (Zehir et al., 2010). We have found that miR-219 and miR-196a are enriched in NC tissue, with miR-219 almost exclusively expressed in NC explants; others have also identified miR-196a implicated in eye development and NC through morpholino miRNA-KD experiments (Gessert et al., 2010; Ward et al., 2018).

CRISPR in recent years has been increasingly used in manipulating gene expression. CRISPR-Cas9 utilizes a highly specific targeted nuclease to induce genomic editing by non-homologous end joining or homology-directed repair. CRISPR is an efficient technology that can rapidly generate KO samples for analysis (Ran et al., 2013). In *X. tropicalis*, Nakayama and colleagues laid the foundation and set out a simple CRISPR pipeline and use of mutations in the tyrosinase gene to generate albinism phenotypes, targeting the start codon, leading to frameshift mutation and KO (Nakayama et al., 2013). CRISPR can be used to analyse gene function, and to replicate human disease mutations to generate mosaic targeted mutant F0's and lines in *Xenopus* embryos (Feehan et al., 2019; Macken et al., 2021; Naert et al., 2017, 2020; Naert and Vleminckx, 2018; Nakayama et al., 2013).

As part of our ongoing work of looking at miRNAs in NC development we have developed a novel method to KO miRNAs quickly and efficiently in *X. tropicalis* embryos and analyse the phenotype generated transiently in the F0 population. Using this method we have begun to more clearly investigate the role of miR-196a and miR-219 in NC development.

## 2. Results and discussion

### 2.1. miRNA expression profiling

We previously identified miRNAs expressed in NC tissue through RNA-sequencing experiments on Wnt/Noggin induced animal-caps (Ward et al., 2018). Here we focus on two miRNAs identified in our earlier study; miR-196a which is located within the *Hoxc* cluster, in *Hoxc9*, and miR-219 which is located intergenically. Both miRNAs have a pri-miRNA stem-loop structure that is highly conserved among the animal kingdom (Fig. 1A). The initial aim was to identify when and where miR-196a and miR-219 are expressed in the developing *Xenopus* embryo. To understand when the miRNAs were expressed, q-RT-PCR was employed. Both miRNAs have a very similar profile with expression peaking initially at Nieuwkoop and Faber (NF) St.4 before dropping at gastrula stages of development and then increasing at late-gastrula and early neurula stages. Expression peaks at St.25 before dropping at tadpole stages (Fig. 1B).

Mature miRNAs are short 20–22 nucleotides long (Bartel, 2004). Due to this they are too short to detect with a standard *in situ* hybridisation probe (Thompson et al., 2007). We have previously used LNA modified *in situ* probes to determine miRNA expression in *Xenopus* embryos; however, LNA probes for miR-196a and miR-219 produced no signal (not shown). Another approach is to generate an antisense pri-miRNA *in situ* probe by PCR from genomic DNA (Walker and Harland, 2008). Using this method we looked at the expression of miR-196 and miR-219. For miR-196a and miR-219, expression is very similar (Fig. 1C). Expression can be seen with the antisense probes but not in sense. At early embryonic stages miRNA expression peaks at St.4 of development. The q-RT-PCR data indicates this at St. 4 and shows no expression at St.7. This is in contrast to the whole mount *in situ* hybridisation data which shows clear expression of miRNA. This could be explained by the fact that the *in situ* hybridisation experiment shows precursory miRNA expression, and q-RT-PCR shows mature miRNA expression. This may explain why the St.7 expression profile for both pri-miR-196a and pri-miR-219 are localized to the cell nucleus (Bartel, 2004). St. 4 expression however is ubiquitous across the upper level of cells, in the dorsal and ventral animal cells (Fig. 1B–C).

At neurula stages, NF St. 15 and 17, expression is seen in neural folds,

neural plate and NC. At tadpole stage, NF St. 33, expression can be seen in craniofacial tissues, including NC derivatives, the otic vesicle and ventral branchial arches. Using LNA probes we also observed miR-196a and miR-219 expression in chick embryos in the neural tube, neural tissue and some expression in NC (Suppl. Fig. 1).

### 2.2. Developing and employing CRISPR-Cas9

CRISPR-Cas9 approaches have been developed in many species including *Xenopus* (Nakayama et al., 2013). To KO a miRNA in *X. tropicalis*, the technical limitation of generating a viable embryo with a clean KO is that designing a sgRNA close to or in the miRNA is difficult due to their small size. In addition an insertion/deletion (INDEL) mutation could lead to generation of a novel miRNA as well as losing the original miRNA (Bhattacharya and Cui, 2017). This was the main concern when an individual sgRNA was implemented to mutate the mature miRNA (Suppl. Fig. 4). Here it was shown that one sgRNA could not significantly disrupt the mature miRNA enough to alter the processing or structure of the pri-miRNA, and thus the mature miRNA would like have been potentially expressed or have become a novel miRNA with an altered sequence to its parent.

Other ways to KD miRNA expression by CRISPR include targeting the DROSHA and DICER processing sites within the miRNA under study (Chang et al., 2016). Again, this is not always possible due to sgRNA design limitations due to the NGG PAM design for Cas9 used in this study (Wilson et al., 2018). By designing sgRNAs flanking the stem-loop of the miRNA, it was predicted they would simultaneously create double-stranded breaks in the genome to “drop-out”, the entire miRNA stem-loop, and give a clean miRNA KO (Fig. 2A and Table 1).

To be confident the miRNAs were knocked out, pairs of sgRNAs, Cas9 protein and GFP cRNA were co-injected into *X. tropicalis* embryos into both blastomeres at the 2-cell stage to target whole embryo (Fig. 2A). Embryos expressing GFP on both sides were selected, and 5 St.14 neurulas were pooled to produce independent biological repeats. RNA was harvested to analyse miRNA expression by q-RT-PCR to evaluate sgRNA efficiency. The results showed that expression of both miRNAs was reduced in the treated samples, compared to control embryos injected with Cas9 protein and GFP cRNA tracer. miR-196a sgRNAs resulted in a 67% reduction of miR-196a expression and miR-219 sgRNAs reduced miR-219 expression by 93% as compared to control samples (Fig. 2B). Differences in efficiency could be due to the nature of CRISPR (Ran et al., 2013).

Next, we identified the types of INDEL generated using the two guide-RNAs approach. Genomic DNA was extracted from individual *X. tropicalis* embryos injected with CRISPR reagents and a GFP capped RNA tracer into one blastomere at 2-cell stage of development. Cas9 + tracer was used as a negative control. PCR was carried out to amplify the stem-loop of the miRNA (Fig. 2A). As expected, we detected wild-type (WT) miRNA in all samples as only half the gDNA could have been mutated. For the miR-KO samples an extra smaller band was seen on the gel (Fig. 2C and D). For miR-196a, the WT miRNA band is 815 bp. The sgRNAs should lead to the deletion of 467 bp and release a fragment of approximately 300 bp if a CRISPR event was successful. For miR-219 the WT miRNA should be 847 bp, and the CRISPR-released fragment is expected to be 260 bp or smaller, as seen in the gel (Fig. 2 C & D). Amplified products were then gel extracted and sent for Sanger sequencing (Fig. 2 C' & D'). For miR-196a a nested PCR was carried out using primer set 3 (Table 2). Stem-loops for each miRNA are shown by red text (Fig. 2 C' & D') and as expected the “drop-out” bands do not contain the miRNA. This confirms the successful CRISPR deletion of miRNA stem-loops. The WT and Cas9 control group bands were also extracted and sent for sequencing. The sequencing all showed wild-type miRNA sequences for these. This to our knowledge, is the first time this approach with two sgRNAs has been used in *Xenopus* embryos, though Kretov et al. (2020) do report a similar approach in Zebrafish (Kretov et al., 2020).

Some embryos were left to develop into tadpoles for phenotype

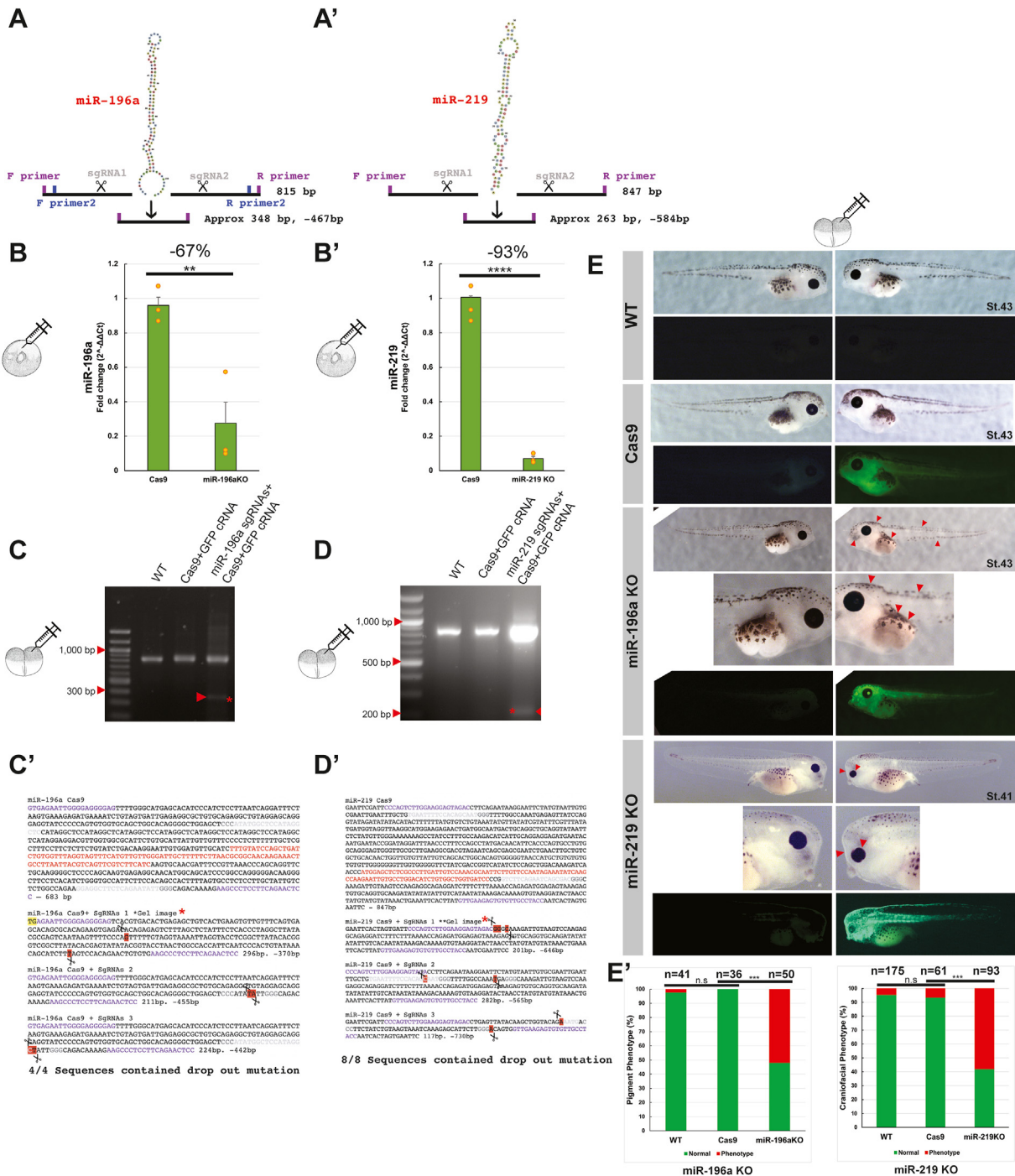


**Fig. 2. CRISPR-Cas9 approach for knocking out miRNAs in *X. tropicalis* and validation strategies.** (A-A') Schematic showing the approach taken with use of two sgRNAs for miR-196a (A) and miR-219 (A'). (B) Q-RT-PCR validation of miR-KO, with individual data points from biological repeats shown in orange. MiR-196a KO showed a 67% reduction in expression (B), and miR-219 KO showed a 93% reduction in expression following CRISPR-Cas9 treatment (B'). Embryos were injected at the 1 cell stage, bar charts show mean  $\pm$  S.E.M. Experiments were conducted with biological and technical triplicate. (C–D) PCR/nested PCR validation of gDNA miRNA regions from embryos injected into one cell at 2 cell stage of development, with KO's showing an extra smaller band in the fourth lane of each gel. (C'–D') Sanger sequencing validation of miRNA KO's and CRISPR events. Cas9+GFP control samples were also harvested, genomic DNA extracted, PCR amplified and subcloned. Purple text highlights primers used for cloning, red text shows miRNA stem-loop. Yellow highlight shows a mis-match, and red highlight with scissors icons show where CRISPR events occurred, grey text shows sgRNA. WT and Cas9 sequences show miRNA WT sequence, whereas Cas9+sgRNAs show 3 repeats of mutated sequences, with significantly shorter sequences. (E) Phenotype analysis of miRNA KO embryos, representative embryos are shown. Embryos were co-injected with CRISPR-reagents a GFP capped RNA tracer into one cell at a two cell stage of development. Embryos are imaged on left and right sides. WT had no injection, Cas9 protein was co-injected with GFP crRNA and miR-KO were pairs of sgRNAs, Cas9 protein and GFP crRNA tracer. The fluorescent side of miR-196a KO embryo red arrows indicate a pigment phenotype, and for miR-219 KO, the red arrows indicate a strong craniofacial phenotype, with smaller eyes, branchial arch and flattened face features. (E') Bar charts show count data of yes/no phenotypes for miR-196a KO (pigment loss) and miR-219 KO (craniofacial disfigurement), with chi-squared tests for statistical significance. There was a significant difference between Cas9 and miR-196a KO groups  $p = 2.22 \times 10^{-7}$  and between Cas9 and miR-219 KO  $p = 1.1 \times 10^{-10}$ . Embryo phenotypes were blind counted on three biological repeats on embryos from different *Xenopus* parents.

**Table 1**  
SgRNA sequences used. Common oligo taken from (Nakayama et al., 2013).

SgRNA (sgRNA) Oligo	Sequence 5' to 3'
sg219-5	taatacgaactactataGGTGAATTTCCACAGCAATgttttagagctagaa
sg219-9	taatacgaactactataGGGTCTTCAGAATCAGCGACgttttagagctagaa
sg196-4	taatacgaactactataGGGAGGCTTCTCAGAATATgttttagagctagaa
sg196-7	taatacgaactactataGGGAGCCTATGGAGCCATATgttttagagctagaa
Common oligo (reverse primer)	AAAAGCACCGACTCGGTGCCACTTTTTCAAGTTGATAACGGACTAGCCTTATTTAACTTGCTATTCTAGCTCTAAAAC

**Table 2**  
Table of primers and sequences. Primers used for sequencing and PCR of genomic DNA. Designed using Primer3.

Primer	Sequence 5' to 3'
219 R3	GGTAGGCAACACTCTTCAAC
219 R4	GAAGGCTGTATTTAGCCCTGGC
219 6F	CCCAGTCTTGGGAAGGAGTAGAC
196 F3	GTGAGAATTGGGGAGGGGAG
196 R3	AGGAGTTCTGAAGGAGGGCTTC
196 F7	CAGCCAGCACTTACAGGTT
196 R7	GGAGTTCTGAAGGAGGGCTT
196 F5	TTCAGGACACTTGTCTGGC
196 R5	TGAGCTTCCGGTTTAGGGG

analysis. Embryos were targeted with CRISPR reagents on one side only for comparison with the non-injected side as an internal control. WT and Cas9 embryos look morphologically normal on both sides. However, miR-196a tadpoles on the “crispant” (CRISPR-mutated) side show pigment phenotypes, with a reduction in pigment seen along the cranial, dorsal and medial abdominal regions, as indicated by red arrows (Fig. 2E). MiR-219 tadpoles show gross craniofacial impairments; with smaller eyes and flattened anterior nasal region, as shown by the red arrows (Fig. 2E). Blind counts of the phenotypes showed that over 50% of embryos carried the respective pigment and craniofacial phenotypes (Fig. 2E'). These phenotypes suggest a possible role for miR-196a and miR-219 in NC development (Collazo et al., 1993; Lukoseviciute et al., 2018; Petratou et al., 2021; Scerbo and Monsoro-Burq, 2020; Spokony et al., 2002).

To validate the specificity of the miRNA CRISPR KO, a novel rescue experiment was developed (Suppl. Fig. 5). To do this a miRNA mimic was used to rescue the miRNA KO. As a control experiment for this, a control miRNA mimic was used. This was *C. elegans* miRNA, cel-miR-39-3p, as recommended by the manufacturer. This was chosen as a miRNA that should not have an effect on *Xenopus* development, and not rescue our miR-219 KO.

In Supp Fig. 5A, miRNA mimic was tested for phenotype on its own at a dose of 11  $\mu$ M to see if overexpression of miRNA would induce phenotype. For miR-219 mimic this led to minor craniofacial phenotypes as indicated by the black arrow (Suppl. Fig. 5A and B). In contrast, the overexpression of control mimic miRNA alone did not have a significant impact on embryo phenotype (Suppl. Fig. 5B). To rescue the CRISPR KO of miR-219 the miR-219 miRNA mimic was co-injected into the embryo along with the CRISPR reagents (Suppl. Fig. 5C and D). Craniofacial phenotype were observed in miR-219 KO and miR-219 KO + control mimic groups. The phenotype was not observed as much in miR-219 KO + miR-219 mimic group and is indicative of a successful rescue of loss of miR-219. This suggests specificity for our novel miRNA KO and rescue experimental design. This is significant as the only currently known reported use of a miRNA mimic used to rescue phenotypes in developing embryos was reported in Zebrafish to overexpress miR-9 to alter and reduce mRNA expression of VEGF-alpha (Madelaine et al., 2017).

MiRNAs can be produced from independent genes or encoded in intronic regions of the genome. They are most commonly found in intergenic, intronic regions of the genome, and rarely found in exonic regions (Olena and Patton, 2010). The proposed CRISPR method in this paper works for intergenic and intronic miRNAs, this was not tested on

exonic miRNAs, as these are extremely rare, but could be used with caution. We show this by knocking out miR-196a which is located in a *Hoxc* intron and miR-219, which is intergenic (Fig. 1A).

### 2.3. Exploring miRNA phenotypes

To verify if our miRNAs were implicated in the development of NC, we determined the expression of key markers Sox10, Snail2 for NC, Pax3 for neural plate and Xhe2 for hatching gland (Fig. 3). In addition, we compared the efficiency of our CRISPR KO approach versus morpholino (Table 3) mediated KD of the miRNAs. Control and optimization experiments for miRNA-morpholino KD can be seen in Suppl. Fig. 2.

For miR-196a, KO and KD led to distinct reduction in Sox10 expression. For Snail2, miR-196 KO and KD led to a reduction and shift in expression. For Pax3 expression a slight reduction and shift in profile was observed and finally Xhe2 expression was expanded following miR-196a KO and KD, (Fig. 3A–B). For miR-219 KO and KD, Sox10 expression was markedly decreased. Like with miR-196 KD, Snail2 expression following miR-219 KD was reduced, but miR-219 KO showed more of a shift in profile with slight reduction. Following miR-219 KO and KD, Pax3 expression was greatly increased and expanded (Fig. 3A–B). Section data showed miR-219 KD led to Pax3 expansion over the superficial ectoderm but not following miR-196a KD (Suppl. Fig. 3). Phenotypes shown by *in situ* hybridisation were more prevalent for miRNA-KD than KO. This could be due to potential mosaicism of CRISPR events seen in F0 embryos thus leading to variable miRNA levels between embryos (Naert et al., 2020).

Q-RT-PCR was conducted to quantify the phenotypic change in expression of the above markers across the whole embryo, and to compare the efficacy of CRISPR experiments in comparison to morpholino (MO) experiments knocking down mRNA expression for neural crest, neural plate border and hatching gland markers (Fig. 3B). Q-RT-PCR was carried out on crispant samples, as described previously, injecting CRISPR reagents into one blastomere at the 1 cell stage. For mRNA expression, all the Q-RT-PCR data was in agreement with the *in situ* data including for the miR-219 KO on Pax3, which was shown to be increased in expression though this was not significant (Fig. 3B). Reasons for this could be that the whole embryo was used for RNA extraction. In Suppl. Fig. 3 the sections of the Pax3 embryos following miR-219 KD show that the expansion of Pax3 is shifted and limited to the superficial ectoderm (Suppl. Fig. 3). The MO KD q-RT-PCR data seen alongside the CRISPR KO data for miRNAs in Fig. 3B panel b, d, f and h show the same trends in mRNA expression for Sox10, Snail2, Pax3 and Xhe2 respectively. The data indicate that miR-196a and miR-219 could be involved in early regulation of NC development. Additionally the lab has shown Eya1 to be a direct target of miR-219 by luciferase assay (Ward and Wheeler, unpublished results). Using MO KD, q-RT-PCR also showed changes in expression following loss of miRNA (Suppl. Fig. 6). Loss of miR-196a led to loss of Eya1, loss of miR-219 led to enrichment of Eya1; further supporting the work to show Eya1 is a target of miR-219.

The incidence rate of phenotypes can be seen in Fig. 3B a,c,e and g; with the observed phenotypes clearly occurring in the experimental groups. Broadly miRNA KD and KO phenotype incidence were similar between morpholino and CRISPR, although miR-196a morpholino had a higher rate of phenotype incidence for Sox10 and Pax3. Q-RT-PCR profiles match the *in situ* data, with NC markers showing significant

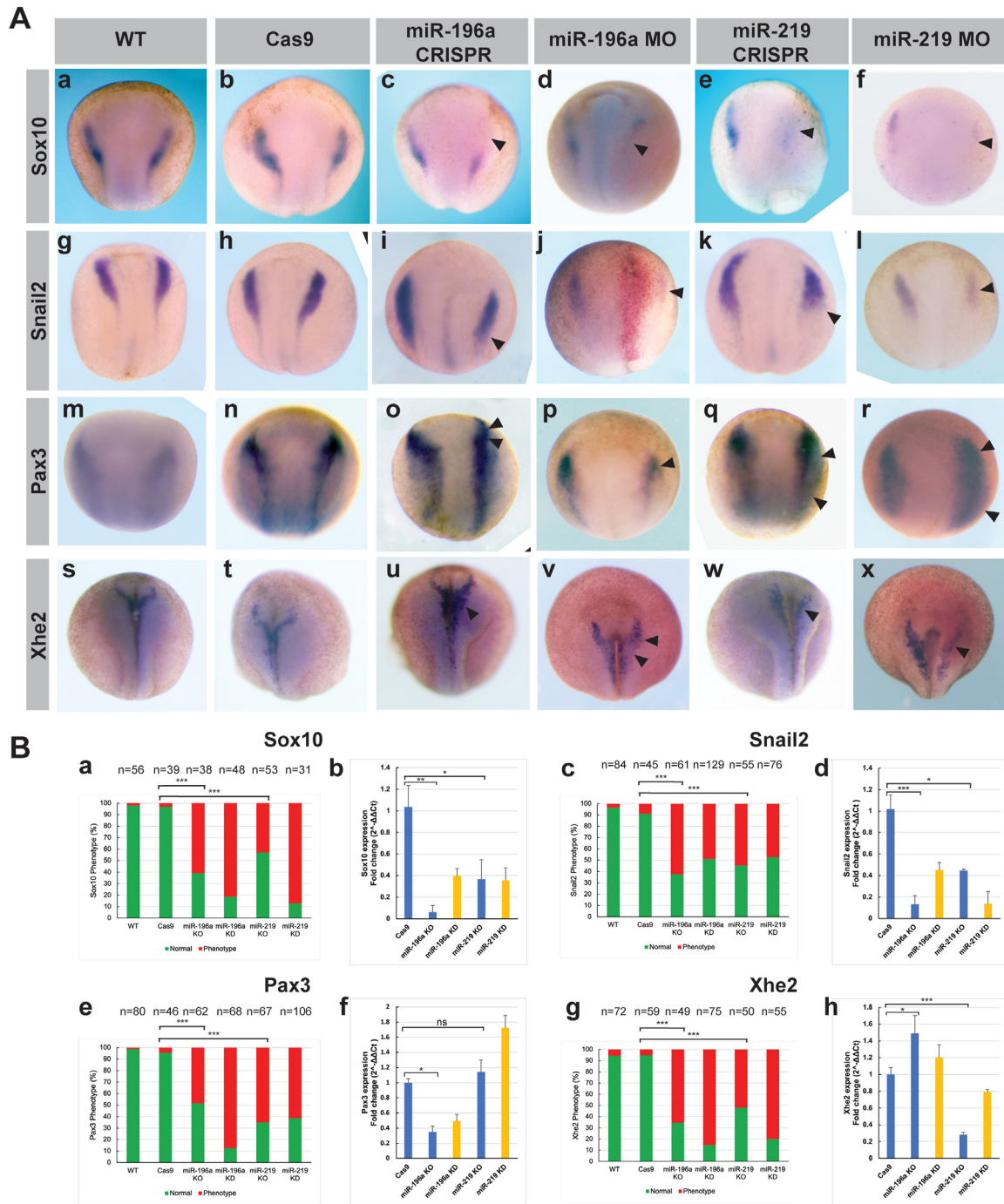


**Fig. 3. Analysis of key NC, neural plate and hatching gland markers after miRNA KO and KD.** (A) Whole mount *in situ* hybridisation profiles on neurula stage *Xenopus* embryos of Sox10, Snail2, Pax3 and Xhe2. CRISPR-Cas9 was carried out in *X. tropicalis* embryos with GFP cRNA as a tracer and morpholino-KD was carried out in *X. laevis* embryos with lacZ cRNA as a tracer. Embryos for whole mount *in situ* hybridisation were injected with tracer at 4-cell stage of development into the right dorsal blastomere. Panel A, a-f show Sox10 expression following CRISPR and MO experiments. Panel A g-l show Snail2 expression following CRISPR and MO experiments. Panel A m-r show Pax3 expression following CRISPR and MO experiments. Panel A, s-x shows Xhe2 expression following CRISPR and MO experiments. Overall phenotypes show a reduction of NC and altered neural plate and hatching gland profiles. (B) Phenotype analysis for individual markers. a, c, e and g show count data of yes/no phenotype presence. Chi-squared statistical tests were carried out on three biological repeats of whole mount *in situ* hybridisation on embryos from different frogs. b, d, f and h, Q-RT-PCR results of mRNA expression analysis following CRISPR KO and MO KD. Normalised to U6 expression, RNA was pooled from 5 individual neurula embryos for one biological sample, Q-RT-PCR was carried out with biological and technical triplicates. The Q-RT-PCR data supports phenotypes shown in (A). Panel B, a-b show Sox10 expression following CRISPR KO and MO KD. Panel B, c-d show Snail2 expression following CRISPR KO and MO KD. Panel B, e-f show Pax3 expression following CRISPR KO and MO KD. Panel B, g-h show Xhe2 expression following CRISPR KO and MO KD experiments. Panel B, a,c,e and g show phenotype count data. Panel B, b,d,f and h show q-RT-PCR expression of mRNAs following miRNA KO and KD. Abbreviations for phenotype and q-RT-PCR bar charts in (B): miR-KO refers to CRISPR miRNA KO and miR-KD refers to MO KD of miRNA. Phenotypes for miRNA KD/KO: Sox10 phenotype is a reduction in expression, Snail2 is a reduction/shift in profile, Pax3 phenotype is a shift/reduced profile for miR-196a and an expansion for miR-219 experiments, finally, Xhe2 is an increased profile for miR-196a and a reduced profile for miR-219 experiments respectively. Statistical significance: Sox10 Cas9 vs miR-196a KO  $p = 4.02 \times 10^{-8}$ , Cas9 vs miR-219 KO  $p = 1.04 \times 10^{-5}$ , Snail2 Cas9 vs miR-196a KO  $p = 6.15 \times 10^{-9}$ , Cas9 vs miR-219 KO  $p = 4.07 \times 10^{-7}$ , Pax3 Cas9 vs miR-196a KO  $p = 7.19 \times 10^{-7}$ , Cas9 vs miR-219 KO  $p = 2.29 \times 10^{-8}$ , Xhe2 Cas9 vs miR-196a KO  $p = 7.19 \times 10^{-7}$ , Cas9 vs miR-219 KO  $p = 2.29 \times 10^{-8}$ .

**Table 3**  
Injected morpholino sequence data.

Morpholino	Sequence
miR-196a MO	5'-CAATCCCAACAACATGAACTACCT-3'
miR-196a Mismatch	5'-CATTGCCAAGAACATCAAAGTACCT-3'
miR-219 MO	5'-AGAATTGCGTTTGGACAATCAAGGG-3'
miR-219 Mismatch	5'-ACAATTGCCTTTCGAGAATCAACGG-3'

decreases in expression, more notably for miR-196a. Pax3 expansion for miR-219 KO was not statistically significant, but miR-196a KO led to significant reduction in expression. Xhe2 showed significant expansion for miR-196a KO and significant decrease in miR-219 KO. These results show that miRNAs are likely to be implicated in the development of the *Xenopus* NC and can be analysed through use of CRISPR to KO miRNAs.

The loss of Sox10 expression shown in Fig. 3A for miR-196a and miR-219 KD and KO supports the phenotypes shown in the tadpoles in Fig. 2E. The tadpole phenotypes for miR-196a show loss of pigment, and for miR-219 show craniofacial abnormalities, which is significant as Sox10 is involved in trunk NC to produce pigmentation (Aoki et al., 2003) and is disrupted in neurocristopathies affecting cranial NC (Devotta et al., 2016). The craniofacial phenotypes in Fig. 2E included flattened fronto-nasal regions, and smaller eyes, as indicated by the red arrows.

Snail2 expression is downregulated following loss of miRNA (Fig. 3A). This could mean that miRNA KO and KD is leading to a loss of NC differentiation, and may help explain the craniofacial phenotypes seen in miR-219 KO tadpoles (Fig. 2E), (Li et al., 2019). The loss of pigment phenotype seen following miR-196a KO (Fig. 2E) is typical of problems in trunk NC development (Abu-Elmagd et al., 2006). This is also supported by Snail2<sup>-/-</sup> mice that show patchy pigmentation phenotypes (Shi et al., 2011).

The loss of Pax3 seen in Fig. 3A following loss of miR-196a also supports the pigment phenotype seen in Fig. 2E, as Pax3 is essential for the development of pigment (Kubic et al., 2008). Waardenburg syndrome type 1 and 3 are caused by Pax3 gene mutations, and type 2 and 4 are affected by Sox10 and MITF levels and mutations. Pax3 and Sox10 regulate expression of MITF and thus melanocyte development (BONDURAND et al., 2000). As expected, our results follow this by showing reduced Pax3 and Sox10 expression following miR-196a loss (Fig. 3A) which led to pigment loss in tadpoles (Fig. 2E). The expansion of Pax3 following loss of miR-219 (Fig. 3A), could be affecting NC specification leading to the loss of NC induction expression of Snail2 and Sox10 seen in Fig. 3A (McKeown et al., 2005; Monsoro-Burq et al., 2005).

The expansion of Pax3 observed in superficial ectoderm (Suppl Fig. 3) following miR-219 KD could also be indicative of increased neural pluripotency (Chalmers et al., 2002). *Xenopus* neural plate border region can give rise to placodal ectoderm, hatching gland and NC. The hatching gland marker Xhe2 demarcates this. Xhe2 expression is affected by Pax3 expression (Hong and Saint-Jeannet, 2007, 2014). MiR-196a and miR-219 KO and KD experiments show altered Pax3 expression states, therefore as expected Xhe2 expression was also affected. In contrast to results seen in (Hong and Saint-Jeannet, 2014), Pax3 expansion does not lead to expanded Xhe2 in our work. This could be due to the other signals that mediate Xhe2 like Zic1. Further work is required to investigate more markers across neural plate and neural derivatives.

### 3. Conclusions

One drawback of CRISPR gene-editing is finding sgRNAs that are effective especially when studying miRNAs. As mentioned, a challenge with CRISPR experiments is that with a short target sequence the number of sgRNAs that can be designed is limited (Najah et al., 2019). With the advent of more Cas9 nucleases with broader PAM recognition sequences more designs could be generated (Kim et al., 2020). Furthermore new sgRNA design tools are making sgRNA design easier and more robust (Hsu et al., 2021). However, using sgRNAs flanking the miRNA stem-loop

expands the potential for identifying and generating optimal sgRNAs. Using a pair of sgRNAs leads to a complete loss of the miRNA in the majority of embryos. The method described is a quick and efficient way to KO specific miRNAs in independent genes or within introns. With the generation of lines of frogs, time would be saved from laborious injections of morpholinos and controls thus more ambitious and technically demanding experiments would be more realistic.

This work shows that miRNAs miR-196a and miR-219 are expressed in NC and neural tissue. Phenotype analysis shows that the miRNAs are important for NC and hatching gland development. This body of work establishes a protocol and controls for CRISPR experiments for knocking out and rescuing miRNAs in embryo development and puts forward CRISPR as not only a tool to rival use of morpholinos in embryo research but also to potentially replace in certain instances.

## 4. Materials and methods

### 4.1. *Xenopus* husbandry

All experiments were carried out in accordance with relevant laws and institutional guidelines at the University of East Anglia, with full ethical review and approval, compliant to UK Home Office regulations. Embryos were generated as described in (Harrison et al., 2004; Williams et al., 2017). *X. tropicalis* embryos obtained by priming females up to 72 h before use with 10 ui chorulon and induced on the day of use with 200ui. Eggs were collected manually and fertilised in vitro. Embryos were de-jellied in 2% L-cysteine, incubated at 23°C and microinjected in 3% Ficoll into 1 cell at the 2–4 cell stage in the animal pole. Embryos were left to develop at 23°C. Embryo staging is according to Nieuwkoop and Faber (NF) normal table of *Xenopus* development (Nieuwkoop and Faber, 1967). GFP/LacZ capped RNA for injections was prepared using the SP6 mMMESSAGE mMACHINE kit, 5 ng was injected per embryo.

### 4.2. CRISPR-Cas9

SgRNAs were designed using CRISPRscan (<https://www.crisprscan.org/>), (Moreno-Mateos et al., 2015). miRNA sequences were attained from miRbase (<http://www.mirbase.org/>); under accession numbers: Xtr-miR-219 MI0004873, Xtr-miR-196a MI0004942. SgRNAs were designed up and downstream of the miRNA stem-loop. miRNA stem loop structures were predicted computationally using Vienna RNA fold tool ([http://rna.tbi.univie.ac.at/forna/forna.html?id=RNAfold/vCiQTz5Wd4&file=cent\\_probs.json](http://rna.tbi.univie.ac.at/forna/forna.html?id=RNAfold/vCiQTz5Wd4&file=cent_probs.json)).

### 4.3. Embryo injection

Embryos were injected using a 10 nL calibrated needle. For *X. laevis* 10 nL injections, for *X. tropicalis* 4.2 nL injections were used. Cas9 protein was added to a 3 µL reaction volume, to give a final concentration of 2.4 mM (New England Biolabs, #M0646M, EnGen Cas9 NLS 20 µM). 300 pg of sgRNAs along with 5 ng of GFP capped RNA were co-injected into the *X. tropicalis* embryos simultaneously at 2–4 cell stage of development. For q-RT-PCR both sides of embryo were targeted, for gene expression and morphological analysis phenotypes 1 side of the embryo was targeted, with embryos injected at 4 cell stage into one dorsal blastomere for whole-mount *in situ* experiments and morphological analysis.

### 4.4. CRISPR validation

Embryos were left to develop until tadpole stages and underwent phenotype scoring. Embryos were then frozen on dry ice before genomic DNA extraction. Genomic DNA was isolated using PureLink Genomic DNA Mini Kit, K1820-00 (Invitrogen, California, USA), according to manufacturers guidelines and then quantified using a Nanodrop 1000. Genotyping PCRs were conducted and products underwent gel extraction before subcloning and sanger sequencing. CRISPR rescue experiments

utilised an LNA miRNA mimic from Qiagen. They were ordered at 5 nmol with no labelling and desalting. Before use they were diluted in 75  $\mu$ L of nuclease free water to give a concentration of 66.7  $\mu$ M and stored in small aliquots at  $-20^{\circ}$ C. Qiagen could not provide a molecular weight for the mimic. The approximate molecular weight using the following formula:

$$\text{Molecular weight} = 320.5 \times \text{Number of nucleotides of RNA.}$$

For the miR-219 mimic this equated to 6730.5 therefore:

$$66.7 \mu\text{M} = 448.9 \text{ ng} / \mu\text{L}$$

$$6.67 \mu\text{M} = 44.9 \text{ ng} / \mu\text{L}$$

$$1 \mu\text{M} = 6.73 \text{ ng} / \mu\text{L}$$

MiRCURY LNA miRNA mimics were used to replace miRNA in CRISPR miRNA-219 KO embryos in rescue experiments. MiR-219 mimic was used from (Qiagen, 339173 YM0047076-ADA, MIMAT0000276); hsa-miR-219a-5p miRCURY LNA miRNA Mimic, compatible and fully aligning with *Xenopus* miR-219, Xtr-miR-219 sequence: 5'UGAUU-GUCCAAACGCAAUUCU. A negative control miRNA mimic recommended by Qiagen was used (Qiagen, 331973 YM00479902-ADA); Negative control (cel-miR-39-3p), sequence 5'UCACCGGGUGUAAAUCAGCUUG. Mimics were used at a final concentration of 11  $\mu$ M dose with CRISPR reagents as described above, or 11  $\mu$ M alone +5 ng GFP cRNA tracer.

#### 4.4.1. Morpholinos

Morpholino dose was optimized to 60 ng for miRNAs; morpholino and lacZ capped RNA tracer were injected at 4 cell stage of embryo development into the right dorsal blastomere.

#### 4.5. Phenotype statistical analysis

Chi-squared test for association was used to test phenotype yes or no categories for morpholino injected embryos to see if there was a relationship between two categorical values. Excel was used to collate and tabulate data. IBM SPSS v25 to carry out chi-squared test. Statistical significance is reported as;  $p < 0.05 = *$ ,  $p < 0.01 = **$ ,  $p < 0.001 = ***$ .

#### 4.6. CDNA synthesis

MiRCURY LNA RT kit (Qiagen, Cat No./ID: 339340) was used to produce cDNA for q-RT-PCR. 50 ng of RNA was used to generate cDNA according to manufacturers instructions. cDNA was produced on a thermocycler with the following programme:  $42^{\circ}$ C for 60 min and  $95^{\circ}$ C for 5 min cDNA was diluted 1:40 for q-RT-PCR. CDNA can be stored at  $-20^{\circ}$ C. To produce cDNA for mRNA q-RT-PCR the following recipe was used: 500 ng of total RNA was added in 9  $\mu$ L of nuclease free water, plus 2  $\mu$ L of random primers (Promega, C1181). This was then incubated at  $70^{\circ}$ C for 10 min. A mastermix was prepared as follows per sample: 4  $\mu$ L of 5X buffer, 2  $\mu$ L of DTT, 1  $\mu$ L of dNTPs, 1  $\mu$ L of Superscript II (Invitrogen, 18064014), 1  $\mu$ L of nuclease free water or RNasin (Promega, N2611). qRT-PCR reactions were set up in 10  $\mu$ L volume containing 4  $\mu$ L cDNA, 1  $\mu$ L primer (10  $\mu$ M for standard oligo primers), and 5  $\mu$ L SybrGreen (Applied Biosystems 4309155).

#### 4.7. Q-RT-PCR

Embryos were frozen on dry ice before RNA extraction. For miRNA and mRNA quantification total RNA was extracted from five St.14 *X. tropicalis* embryos, embryos were homogenised with a micropestle and RNA was extracted according to manufacturers guidance, Quick-RNA Mini prep plus kit (Zymo, Cat no. R1058). Samples were eluted in 25  $\mu$ L of nuclease free water; RNA concentration and purity quantified on a Nanodrop 1000 and 1  $\mu$ L was checked on a 2% agarose gel. All q-RT-PCR's were performed with triplicate biological and technical repeats.

Primers for q-RT-PCR were found in the literature and some were

**Table 4**

Q-RT PCR Primers used for *X. tropicalis* embryos. miRCURY LNA miRNA PCR primers, Qiagen. mRNA primers were ordered as standard oligos.

Primer name	Sequence 5' to 3'	Product code/Accession number for design
xtr-miR-196a	UAGGUAGUUUUAUGUUGUUGG	YP02103491 (Qiagen)
ipu-miR-219a	AGAAUUGUGCCUGGACAUCUGU	YP02101832 (Qiagen)
U6 snRNA	CTCGCTTCGGCAGCACA	YP00203907 (Qiagen)
hsa-miR-219a-5p	UGAUUUGUCCAAACGCAAUUCU	YP00204780 (Qiagen)
EEF1Alpha F X.tr	CCCAACTGATAAGCCTCTGCG	PMID 23559567(Dhorne-Pollet et al., 2013)
EEF1Alpha R X.tr	CATGCCTGGCTTAAGGACAC	PMID 23559567 (Dhorne-Pollet et al., 2013)
Sox10 F X.tr	GATGGGTCTCTGAAGCTGA	Self designed NM_001100221.1
Sox10 R X.tr	GGTAGGGGGTCCATGACTTT	Self designed NM_001100221.1
Snail2 F X.tr	CCCCATTCCTGTATGAGCGG	PMID: 32713114, (Wang et al., 2020)
Snail2 R X.tr	TGAAGCAGTCTGTCCACAC	PMID: 32713114, (Wang et al., 2020)
Xhe2 F2 X.tr	CGCCACCTCTTTTCCCATCCA	Self designed NM_001044399.1
Xhe2 R2 X.tr	TTTGGGCCACAGACTCCTT	Self designed NM_001044399.1
Pax3 F X.tr	TACAGCATGGAGCCTGTAC	PMID: 24055059 (Gentsch et al., 2013)
Pax3 R X.tr	TCCTTTATGCAATATCTGGCTTC	PMID: 24055059 (Gentsch et al., 2013)
EEF1Alpha F X.la	ACCCTCCTCTTGCTGTTTT	PMID: (24360908) (Bae et al., 2014)
EEF1Alpha R X.la	TTTGGTTTTCGTGCTTTCT	PMID: (24360908) (Bae et al., 2014)
Eya1 F X.la	ATGACACCAAATGGCAGAGA	PMID: 17409353 (Hong and Saint-Jeannet, 2007)
Eya1 R X.la	GGGAAAACCTGGTGTGCTTGT	PMID: 17409353 (Hong and Saint-Jeannet, 2007)
Pax3 F X.la	CAAGCTCACAGAGCGCGAGT	PMID: 29038306 (Figueiredo et al., 2017)
Pax3 R X.la	AGCTGGCATAGCTGCAGGAGG	PMID: 29038306 (Figueiredo et al., 2017)
Sox10 F X.la	CTATTACTGACACACGCGGAGG	PMID (32494672) (Scerbo and Monsoro-Burq, 2020)
Sox10 R X.la	ACCTCTCATCTCTGAATCCTGC	PMID(32494672) (Scerbo and Monsoro-Burq, 2020)
Snail2 F X.la	CACACGTTACCTGCGTATG	PMID: 29038306 (Figueiredo et al., 2017)
Snail2 R X.la	TCTGTCTGCGAATGCTCTGT	PMID: 29038306 (Figueiredo et al., 2017)
Xhe2 F X.la	CATGTCTAATGGCGTTGTG	PMID: (24360908) (Bae et al., 2014)
Xhe2 R X.la	TGCTGGATGATCCCCATATT	PMID: (24360908) (Bae et al., 2014)

designed using primer blast (<https://www.ncbi.nlm.nih.gov/tools/primer-blast/>), (Ye et al., 2012). Primers were designed to generate 100 bp products with a melting temperature of between 59 and 62  $^{\circ}$ C. Primers used are listed in Table 4.

#### 4.8. Whole-mount *in situ* hybridisation & Riboprobe synthesis

Standard *in situ* hybridisations and probe synthesis were carried out according to (Harrison et al., 2004; Monsoro-Burq, 2007; Sive et al., 2007). In brief, Whole-mount *in situ* hybridisation (WISH) with LNA probes was carried out with probes hybridised at  $50^{\circ}$ C at a concentration of 1  $\mu$ g/mL, overnight with embryos, before stringency washes with graded SSC washes, blocking and incubation overnight with anti-DIG antibody fragments (Roche, 11093274910). MAB washes then removed unbound antibody prior to colour development with NBT/BCIP. The LNA WISH experiments were carried out according to Ahmed et al.

**Table 5**  
Riboprobe synthesis and capped RNA plasmids information.

Clone name	Antibiotic resistance	Backbone	Antisense RE	Antisense Polymerase	Source
Pax3	Ampicillin	pBSK	BglII	SP6	M.G. Sargent
Sox10	Ampicillin	pBSK	EcoRI	T3	J.P. Saint-Jeannet
Snail2	Ampicillin	pCS107	EcoRI/ BamHI	T7	EXRC
Xhe2	Ampicillin	pBSK	XbaI	T7	A.H.Monsoro-Burq
GFP2	Ampicillin	pCS	NotI (sense)	SP6 (sense)	M. Walmsely
LacZ	Ampicillin	pCS	NotI (sense)	SP6 (sense)	M. Walmsely

(2015) and Sweetman et al. (2006). Probe synthesis experiments involved digestion of plasmid with appropriate restriction enzyme to produce antisense product which was then transcribed by respective polymerase, (Table 5).

### Acknowledgements

We would like to acknowledge the technical support from the team at the European Xenopus Resource Centre at the University of Portsmouth. We would also like to thank Dr. Timothy Grocott for chick embryo expertise, Dr. Paige Paddy and Dr. Tracey Swingler for q-RT-PCR advice and Dr. Benjamin Rix for useful CRISPR discussions. We thank Prof. Monsoro-Burq (Orsay), Prof. Saint-Jeannet (New York), Dr. Sargent (MRC) and Dr. Walmsely (Nottingham) for sharing plasmids. We would like to acknowledge Prof. Andrea Münsterberg (UEA) and Dr. Simon Moxon (UEA) for help with experimental design.

### Appendix A. Supplementary data

Supplementary data to this article can be found online at <https://doi.org/10.1016/j.ydbio.2021.12.015>.

### References

- Abu-Elmagd, M., Garcia-Morales, C., Wheeler, G.N., 2006. Frizzled7 mediates canonical Wnt signaling in neural crest induction. *Dev. Biol.* 298, 285–298.
- Agarwal, V., Bell, G.W., Nam, J.W., Bartel, D.P., 2015. Predicting effective microRNA target sites in mammalian mRNAs. *Elife* 4.
- Ahmed, A., Ward, N.J., Moxon, S., Lopez-Gomollon, S., Viaut, C., Tomlinson, M.L., Patrushev, I., Gilchrist, M.J., Dalmay, T., Dotlic, D., et al., 2015. A database of microRNA expression patterns in *Xenopus laevis*. *PLoS One* 10, e0138313.
- Alberti, C., Cochella, L., 2017. A framework for understanding the roles of miRNAs in animal development. *Development* 144, 2548–2559.
- Alles, J., Fehlmann, T., Fischer, U., Backes, C., Galata, V., Minet, M., Hart, M., Abu-Halima, M., Grasser, F.A., Lenhof, H.P., et al., 2019. An estimate of the total number of true human miRNAs. *Nucleic Acids Res.* 47, 3353–3364.
- Aoki, Y., Saint-Germain, N., Gyda, M., Magner-Fink, E., Lee, Y.H., Credidio, C., Saint-Jeannet, J.P., 2003. Sox10 regulates the development of neural crest-derived melanocytes in *Xenopus*. *Dev. Biol.* 259, 19–33.
- Aoto, K., Sandell, L.L., Butler Tjaden, N.E., Yuen, K.C., Watt, K.E., Black, B.L., Durnin, M., Trainor, P.A., 2015. Mef2c-F10N enhancer driven beta-galactosidase (LacZ) and Cre recombinase mice facilitate analyses of gene function and lineage fate in neural crest cells. *Dev. Biol.* 402, 3–16.
- Bae, C.J., Park, B.Y., Lee, Y.H., Tobias, J.W., Hong, C.S., Saint-Jeannet, J.P., 2014. Identification of Pax3 and Zic1 targets in the developing neural crest. *Dev. Biol.* 386, 473–483.
- Bartel, D.P., 2004. MicroRNAs: genomics, biogenesis, mechanism, and function. *Cell* 116, 281–297.
- Bhattacharya, A., Cui, Y., 2017. Systematic prediction of the impacts of mutations in MicroRNA seed sequences. *J Integr Bioinform* 14.
- Bondurand, N., Pingault, V., Goerich, D.E., Lemort, N., Sock, E., Le Caignec, C., Wegner, M., Goossens, M., 2000. Interaction among SOX10, PAX3 and MITF, three genes altered in Waardenburg syndrome. *Hum. Mol. Genet.* 9, 1907–1917.
- Chalmers, A.D., Welchman, D., Papalopulu, N., 2002. Intrinsic differences between the superficial and deep layers of the *Xenopus* ectoderm control primary neuronal differentiation. *Dev. Cell* 2, 171–182.
- Chandra, S., Vimal, D., Sharma, D., Rai, V., Gupta, S.C., Chowdhuri, D.K., 2017. Role of miRNAs in development and disease: lessons learnt from small organisms. *Life Sci.* 185, 8–14.

- Chang, H., Yi, B., Ma, R., Zhang, X., Zhao, H., Xi, Y., 2016. CRISPR/cas9, a novel genomic tool to knock down microRNA in vitro and in vivo. *Sci. Rep.* 6, 22312.
- Cheung, M., Briscoe, J., 2003. Neural crest development is regulated by the transcription factor Sox9. *Development* 130, 5681–5693.
- Collazo, A., Bronner-Fraser, M., Fraser, S.E., 1993. Vital dye labelling of *Xenopus laevis* trunk neural crest reveals multipotency and novel pathways of migration. *Development* 118, 363–376.
- Devotta, A., Juraver-Geslin, H., Gonzalez, J.A., Hong, C.S., Saint-Jeannet, J.P., 2016. Sf3b4-depleted *Xenopus* embryos: a model to study the pathogenesis of craniofacial defects in Nager syndrome. *Dev. Biol.* 415, 371–382.
- Dhorne-Pollet, S., Thelie, A., Pollet, N., 2013. Validation of novel reference genes for RT-qPCR studies of gene expression in *Xenopus tropicalis* during embryonic and post-embryonic development. *Dev. Dynam.* 242, 709–717.
- Feehan, J.M., Stanar, P., Tam, B.M., Chiu, C., Moritz, O.L., 2019. Generation and analysis of *Xenopus laevis* models of retinal degeneration using CRISPR/Cas9. *Methods Mol. Biol.* 1834, 193–207.
- Figueiredo, A.L., Maczkowiak, F., Borday, C., Pla, P., Sittewelle, M., Pegoraro, C., Monsoro-Burq, A.H., 2017. PFKFB4 control of AKT signaling is essential for premigratory and migratory neural crest formation. *Development* 144, 4183–4194.
- Gentsch, G.E., Owens, N.D., Martin, S.R., Piccinelli, P., Faial, T., Trotter, M.W., Gilchrist, M.J., Smith, J.C., 2013. In vivo T-box transcription factor profiling reveals joint regulation of embryonic neuromesodermal bipotency. *Cell Rep.* 4, 1185–1196.
- Gessert, S., Bugner, V., Tecza, A., Pinker, M., Kuhl, M., 2010. FMRI/FXR1 and the miRNA pathway are required for eye and neural crest development. *Dev. Biol.* 341, 222–235.
- Harrison, M., Abu-Elmagd, M., Grocott, T., Yates, C., Gavrilovic, J., Wheeler, G.N., 2004. Matrix metalloproteinase genes in *Xenopus* development. *Dev. Dynam.* 231, 214–220.
- Hatch, V.L., Marin-Barba, M., Moxon, S., Ford, C.T., Ward, N.J., Tomlinson, M.L., Desanlis, I., Hendry, A.E., Hontelez, S., van Kruijsbergen, I., et al., 2016. The positive transcriptional elongation factor (P-TEFb) is required for neural crest specification. *Dev. Biol.* 416, 361–372.
- Hong, C.S., Saint-Jeannet, J.P., 2007. The activity of Pax3 and Zic1 regulates three distinct cell fates at the neural plate border. *Mol. Biol. Cell* 18, 2192–2202.
- Hong, C.S., Saint-Jeannet, J.P., 2014. Xhe2 is a member of the astacin family of metalloproteases that promotes *Xenopus* hatching. *Genesis* 52, 946–951.
- Hsu, J.Y., Grunewald, J., Szalay, R., Shih, J., Anzalone, A.V., Lam, K.C., Shen, M.W., Petri, K., Liu, D.R., Keith Joung, J., et al., 2021. PrimeDesign software for rapid and simplified design of prime editing guide RNAs. *Nat. Commun.* 12, 1034.
- Inui, M., Martello, G., Piccolo, S., 2010. MicroRNA control of signal transduction. *Nat. Rev. Mol. Cell Biol.* 11, 252–263.
- Kim, H.K., Lee, S., Kim, Y., Park, J., Min, S., Choi, J.W., Huang, T.P., Yoon, S., Liu, D.R., Kim, H.H., 2020. High-throughput analysis of the activities of xCas9, SpCas9-NG and SpCas9 at matched and mismatched target sequences in human cells. *Nat. Biomed. Eng.* 4, 111–124.
- Kretov, D.A., Walawalkar, I.A., Mora-Martín, A., Shafiq, A.M., Moxon, S., Cifuentes, D., 2020. Ago2-Dependent processing allows miR-451 to evade the global MicroRNA turnover elicited during erythropoiesis. *Mol. Cell* 78, 317–328 e316.
- Kubic, J.D., Young, K.P., Plummer, R.S., Ludvik, A.E., Lang, D., 2008. Pigmentation PAX-ways: the role of Pax3 in melanogenesis, melanocyte stem cell maintenance, and disease. *Pigment Cell Melanoma. Res.* 21, 627–645.
- Lee, R.C., Feinbaum, R.L., Ambros, V., 1993. The *C. elegans* heterochronic gene lin-4 encodes small RNAs with antisense complementarity to lin-14. *Cell* 75, 843–854.
- Li, J., Perfetto, M., Materna, C., Li, R., Thi Tran, H., Vlemminck, K., Duncan, M.K., Wei, S., 2019. A new transgenic reporter line reveals Wnt-dependent Snai2 re-expression and cranial neural crest differentiation in *Xenopus*. *Sci. Rep.* 9, 11191.
- Li, Z., Xu, R., Li, N., 2018. MicroRNAs from plants to animals, do they define a new messenger for communication? *Nutr. Metab.* 15, 68.
- Lukoseviciute, M., Gavriouchkina, D., Williams, R.M., Hochgreb-Hagele, T., Senanayake, U., Chong-Morrison, V., Thongjuea, S., Repapi, E., Mead, A., Sauka-Spengler, T., 2018. From pioneer to repressor: bimodal foxD3 activity dynamically remodels neural crest regulatory landscape in vivo. *Dev. Cell* 47, 608–628 e606.
- Macken, W.L., Godwin, A., Wheway, G., Stals, K., Nazlamova, L., Ellard, S., Alfares, A., Aloraini, T., AlSubaie, L., AlFadhel, M., et al., 2021. Biallelic variants in COPB1 cause a novel, severe intellectual disability syndrome with cataracts and variable microcephaly. *Genome Med.* 13, 34.
- Madelaine, R., Sloan, S.A., Huber, N., Notwell, J.H., Leung, L.C., Skariah, G., Halluin, C., Pasca, S.P., Bejerano, G., Krasnow, M.A., et al., 2017. MicroRNA-9 couples brain neurogenesis and angiogenesis. *Cell Rep.* 20, 1533–1542.
- McKeown, S.J., Lee, V.M., Bronner-Fraser, M., Newgreen, D.F., Farlie, P.G., 2005. Sox10 overexpression induces neural crest-like cells from all dorsoventral levels of the neural tube but inhibits differentiation. *Dev. Dynam.* 233, 430–444.
- Miska, E.A., 2005. How microRNAs control cell division, differentiation and death. *Curr. Opin. Genet. Dev.* 15, 563–568.
- Mok, G.F., Lozano-Velasco, E., Munsterberg, A., 2017. microRNAs in skeletal muscle development. *Semin. Cell Dev. Biol.* 72, 67–76.
- Monsoro-Burq, A.H., 2007. A rapid protocol for whole-mount in situ hybridization on *Xenopus* embryos. *CSH Protoc.* 2007, pdb prot4809.
- Monsoro-Burq, A.H., Wang, E., Harland, R., 2005. Msx1 and Pax3 cooperate to mediate FGF8 and WNT signals during *Xenopus* neural crest induction. *Dev. Cell* 8, 167–178.
- Moreno-Mateos, M.A., Vejnar, C.E., Beaudoin, J.D., Fernandez, J.P., Mis, E.K., Khokha, M.K., Giraldez, A.J., 2015. CRISPRscan: designing highly efficient sgRNAs for CRISPR-Cas9 targeting in vivo. *Nat. Methods* 12, 982–988.
- Naert, T., Tulkens, D., Edwards, N.A., Carron, M., Shaidani, N.I., Whizla, M., Boel, A., Demuyck, S., Horb, M.E., Coucke, P., et al., 2020. Maximizing CRISPR/Cas9 phenotype penetrance applying predictive modeling of editing outcomes in *Xenopus* and zebrafish embryos. *Sci. Rep.* 10, 14662.

- Naert, T., Van Nieuwenhuysen, T., Vlemminckx, K., 2017. TALENs and CRISPR/Cas9 fuel genetically engineered clinically relevant *Xenopus tropicalis* tumor models. *Genesis* 55.
- Naert, T., Vlemminckx, K., 2018. Methods for CRISPR/Cas9 *Xenopus tropicalis* tissue-specific multiplex genome engineering. *Methods Mol. Biol.* 1865, 33–54.
- Najah, S., Saulnier, C., Pernodet, J.L., Bury-Mone, S., 2019. Design of a generic CRISPR-Cas9 approach using the same sgRNA to perform gene editing at distinct loci. *BMC Biotechnol.* 19, 18.
- Nakayama, T., Fish, M.B., Fisher, M., Oomen-Hajagos, J., Thomsen, G.H., Grainger, R.M., 2013. Simple and efficient CRISPR/Cas9-mediated targeted mutagenesis in *Xenopus tropicalis*. *Genesis* 51, 835–843.
- Nieuwkoop, P., Faber, J., 1967. *Normal Table of Xenopus Laevis (Daudin): A Systematical and Chronological Survey of the Development from the Fertilized Egg till the End of Metamorphosis*. Garland Publishing, New York.
- Olena, A.F., Patton, J.G., 2010. Genomic organization of microRNAs. *J. Cell. Physiol.* 222, 540–545.
- Petratou, K., Spencer, S.A., Kelsh, R.N., Lister, J.A., 2021. The MITF paralogue *tfec* is required in neural crest development for fate specification of the iridophore lineage from a multipotent pigment cell progenitor. *PLoS One* 16, e0244794.
- Ran, F.A., Hsu, P.D., Wright, J., Agarwala, V., Scott, D.A., Zhang, F., 2013. Genome engineering using the CRISPR-Cas9 system. *Nat. Protoc.* 8, 2281–2308.
- Sauka-Spengler, T., Bronner-Fraser, M., 2008. A gene regulatory network orchestrates neural crest formation. *Nat. Rev. Mol. Cell Biol.* 9, 557–568.
- Scerbo, P., Monsoro-Burq, A.H., 2020. The vertebrate-specific *VENTX/NANOG* gene empowers neural crest with ectomesenchyme potential. *Sci. Adv.* 6, Press.
- Shah, V.V., Soibam, B., Ritter, R.A., Benham, A., Oomen, J., Sater, A.K., 2017. MicroRNAs and ectodermal specification I. Identification of miRs and miR-targeted mRNAs in early anterior neural and epidermal ectoderm. *Dev. Biol.* 426, 200–210.
- Shi, J., Severson, C., Yang, J., Wedlich, D., Klymkowsky, M.W., 2011. *Snail2* controls mesodermal BMP/Wnt induction of neural crest. *Development* 138, 3135–3145.
- Sive, H.L., Grainger, R.M., Harland, R.M., 2007. Synthesis and purification of digoxigenin-labeled RNA probes for in situ hybridization. *CSH Protoc.* 2007, pdb prot4778.
- Spokony, R.F., Aoki, Y., Saint-Germain, N., Magner-Fink, E., Saint-Jeannet, J.P., 2002. The transcription factor *Sox9* is required for cranial neural crest development in *Xenopus*. *Development* 129, 421–432.
- Sweetman, D., Rathjen, T., Jefferson, M., Wheeler, G., Smith, T.G., Wheeler, G.N., Munsterberg, A., Dalmay, T., 2006. FGF-4 signaling is involved in *mir-206* expression in developing somites of chicken embryos. *Dev. Dynam.* 235, 2185–2191.
- Thompson, R.C., Deo, M., Turner, D.L., 2007. Analysis of microRNA expression by in situ hybridization with RNA oligonucleotide probes. *Methods* 43, 153–161.
- Walker, J.C., Harland, R.M., 2008. Expression of microRNAs during embryonic development of *Xenopus tropicalis*. *Gene Expr. Patterns* 8, 452–456.
- Wang, C., Qi, X., Zhou, X., Sun, J., Cai, D., Lu, G., Chen, X., Jiang, Z., Yao, Y.G., Chan, W.Y., et al., 2020. RNA-Seq analysis on *ets1* mutant embryos of *Xenopus tropicalis* identifies *microseminoprotein beta* gene 3 as an essential regulator of neural crest migration. *Faseb. J.* 34, 12726–12738.
- Ward, N.J., Green, D., Higgins, J., Dalmay, T., Munsterberg, A., Moxon, S., Wheeler, G.N., 2018. microRNAs associated with early neural crest development in *Xenopus laevis*. *BMC Genom.* 19, 59.
- Williams, R.M., Winkfein, R.J., Ginger, R.S., Green, M.R., Schnetkamp, P.P., Wheeler, G.N., 2017. A functional approach to understanding the role of *NCKX5* in *Xenopus* pigmentation. *PLoS One* 12, e0180465.
- Wilson, L.O.W., O'Brien, A.R., Bauer, D.C., 2018. The current state and future of CRISPR-cas9 gRNA design tools. *Front. Pharmacol.* 9, 749.
- Ye, J., Coulouris, G., Zaretskaya, I., Cutcutache, I., Rozen, S., Madden, T.L., 2012. Primer-BLAST: a tool to design target-specific primers for polymerase chain reaction. *BMC Bioinf.* 13, 134.
- Zehir, A., Hua, L.L., Maska, E.L., Morikawa, Y., Cserjesi, P., 2010. *Dicer* is required for survival of differentiating neural crest cells. *Dev. Biol.* 340, 459–467.

## Review Article

# MicroRNAs in neural crest development and neurocristopathies

Marco Antonaci and  Grant N. Wheeler

School of Biological Sciences, University of East Anglia, Norwich Research Park, Norwich NR7 7TJ, U.K.

**Correspondence:** Grant N. Wheeler ([grant.wheeler@uea.ac.uk](mailto:grant.wheeler@uea.ac.uk))



The neural crest (NC) is a vertebrate-specific migratory population of multipotent stem cells that originate during late gastrulation in the region between the neural and non-neural ectoderm. This population of cells give rise to a range of derivatives, such as melanocytes, neurons, chondrocytes, chromaffin cells, and osteoblasts. Because of this, failure of NC development can cause a variety of pathologies, often syndromic, that are globally called neurocristopathies. Many genes are known to be involved in NC development, but not all of them have been identified. In recent years, attention has moved from protein-coding genes to non-coding genes, such as microRNAs (miRNA). There is increasing evidence that these non-coding RNAs are playing roles during embryogenesis by regulating the expression of protein-coding genes. In this review, we give an introduction to miRNAs in general and then focus on some miRNAs that may be involved in NC development and neurocristopathies. This new direction of research will give geneticists, clinicians, and molecular biologists more tools to help patients affected by neurocristopathies, as well as broadening our understanding of NC biology.

## Introduction

Since their discovery in 1993, miRNAs have been associated with a number of physiological and pathological processes [1]. These small RNA molecules (~22 nt) comprise ~1–5% of the RNA species in cells but, as a single miRNA can target many genes and many genes can be targeted by multiple miRNAs, it has been estimated that ~30% of human genes are regulated by miRNAs. As the regulation operated by these elements is subtle and can be subject to additive effects when more than one miRNA is targeting the same mRNA, it is not surprising that these elements have been mainly associated with highly regulated biological processes such as development. In recent years, more and more evidence is pointing in this direction, but many gaps still need to be filled. In particular, more effort is needed in order to include miRNAs in the gene regulatory networks (GRN) that orchestrate the development of different tissues. Together with evidence that links miRNAs and pathological conditions such as cancer and cardiac diseases, a broader understanding of their role in biological processes is required. In this review, we give an insight of what is known about miRNAs during different steps of NC development. We also stress the reason why such knowledge could be beneficial for people affected by diseases of the NC, so-called neurocristopathies (NCP), and for the clinicians treating them. Finally, we suggest further investigations in this direction can be applicable to other aspects of biology, including cancer biology, and might help the development of new innovative drugs for treating these conditions.

## Neural crest

The Neural Crest (NC), sometimes referred as the ‘fourth germ layer’, is a multipotent population of cells that originate in the region between the neural and non-neural ectoderm of the developing embryo as the neural plate develops [2,3]. The NC is specific to vertebrates and required for the

Received: 18 October 2021  
 Revised: 23 March 2022  
 Accepted: 24 March 2022

Version of Record published:  
 6 April 2022

formation of an astonishing number of cells and tissues, such as the craniofacial skeleton, dentine in the teeth, chondrocytes, cardiac septa, the peripheral nervous system, adrenal medulla, and pigment cells [4–6].

To allow the formation of the NC, a complex GRN of secreted growth factors and transcription factors is required. NC formation starts with neural induction, a process orchestrated by a gradient of BMP signalling. Additional signalling by Wnt leads to the transcription of specifiers for the neural plate border (NPB). FGF and Notch signalling are also involved in the expression of NPB specifiers, although these two factors play different roles among various species [2,7–9].

The combined action of these signalling pathways leads to the expression of NPB specifiers, including (but not limited to): *Pax3/7*, *Zic1*, *nMyc*, *Tfap2* and *Dlx5/6* [2,7,10,11]. A precise balance between neural and non-neural ectoderm, at this stage, is fundamental for the correct formation of NC tissue [2,12]. The next step leading to the formation of NC tissue is the expression of NC specifiers such as *FoxD3* and *Snail/2*. Their expression is enabled by the action of the NPB specifiers [2,9,13].

One of the most extraordinary properties of NC cells is their ability to undergo an epithelial to mesenchymal transition (EMT), a property that allows neural crest cells (NCCs) to migrate throughout the developing embryo. EMT requires two steps: delamination and dispersion. Initially, NCCs detach from the neural tube, they then separate from each other to start their migration to the rest of the embryo in a coordinated manner [5,14,15]. To allow the movement of NCCs through the embryo, it is necessary to modulate the activity of cell adhesion molecules, metalloproteinases and the extracellular matrix [2,13,16].

It is important to emphasise that not all the actors involved in NC development have been discovered, and that the GRN that orchestrates this process is constantly being updated [2,3,17]. In addition, other gene regulatory mechanisms, such as the regulation operated by non-coding RNA, need to be considered.

## MicroRNAs

MicroRNAs (miRNAs) are short RNA molecules of ~22 nt involved in the post-transcriptional control of gene regulation. They act mainly as repressors of gene expression by binding to the 3' UTR of targeted mRNAs and either cause stalling of the ribosome, or directly promote degradation of the targeted mRNAs [18].

MiRNAs were first discovered in *C. elegans* by Lee and colleagues in 1993 [1]. Since then, an increasing number of miRNAs have been characterised, together with evidence of their important roles in regulating gene expression.

The synthesis of miRNAs has been well covered in other reviews [19]. It starts with the action of RNA-Polymerase II, which transcribes a longer primary transcript, called a pri-miRNA. In most cases, the pri-miRNA has stem loops that are recognised by the RNase III, DROSHA, which together with DGCR8, cleaves the pri-miRNA and generates a smaller product of ~70 nt. This RNA molecule, called the pre-miRNA, is exported to the cytoplasm by the action of Exportin 5. Here, the pre-miRNA is cleaved again by another RNase III, Dicer, which generates a double stranded RNA molecule of ~22 nt. Generally, only one strand of RNA is used as mature miRNA, while the other is degraded [20].

The mature miRNA is loaded into the RNA-induced silencing complex (RISC), which is then guided to mRNA targets and allows pairing between the 'seed' sequence of the miRNA (~7 nt) and the 3' UTR of the target mRNA. This pairing leads to reduced expression by two mechanisms: the removal of the poly-A tail of the mRNA and the subsequent degradation by exonuclease activity, or the blocking of translation by stalling the ribosome. The stalled ribosome then moves to subcellular organelles called P-bodies. Here, the complex can either be stored or degraded [21–24].

Although this is the main mechanism of biosynthesis of miRNAs, other non-canonical mechanisms are known. For example, Dicer-independent processing of miRNAs can occur using short hairpin RNAs (shRNAs) as substrate. In this case AGO2 completes their maturation instead of Dicer [25]. Other non-canonical mechanisms of miRNA biogenesis occur with miRNAs located in introns of transcribed genes (mirtrons) that can be produced during the splicing process and exported by Exportin 5 [26]. Another example is the methylation of the guanosine in position 7 of the capped pre-miRNA, or '7-methylguanosine capped pre-miRNA' [27]. This post-transcriptional modification allows the miRNA to be exported directly to the cytoplasm by Exportin 1. In both cases (mirtrons and 7-methylguanosine capped pre-miRNA), the nascent pre-miRNA is not processed by DROSHA/DGCR8.

A different mechanism of action of miRNAs is the so-called RNA activation (RNAa). RNAa is a pathway that promotes the synthesis of mRNA, instead of repressing the translation. This mechanism is mediated by AGO1 that, once it loads the miRNA, is internalised in the nucleus and binds the promoter of specific genes,

using the miRNA as guide. This mechanism creates a DNA–RNA duplex (R-loop) in proximity of the promoter that enhances the binding of the RNA-Polymerase II to the DNA [28].

It is important to note that many different miRNAs can target one specific mRNA and specific miRNAs can target more than one mRNA. This mechanism allows for the intricate regulation of gene expression, in particular the presence of more than one miRNA on a single mRNA could generate a stronger silencing effect [18].

## The role of miRNAs in NC development

A role for miRNAs during development was first noted in 2003, when Bernstein and colleagues deleted Dicer in mice, observing early embryonic lethality [29]. Other groups have gone on to show miRNAs to be important in many developmental processes, such as, for example, muscle development [30].

MiRNAs associated with the NC have previously been reviewed by Weiner and colleagues [31]. Here we summarise what is known and look at more recent literature (see Figure 1 and Table 1). A role for miRNAs in NC development was originally shown by knocking out and knocking down Dicer in mice, thus disrupting miRNA biogenesis. It was observed that a NC-specific knockout of Dicer using a Wnt1-CRE is lethal [32]. This effect was due to extensive NC cell death that led to the absence of NC-derived tissues [33]. Similar effects were observed following NC-specific inactivation of DGCR8, an important co-factor of the endonuclease DROSHA. In addition, cardiac defects associated with a defect in the NC were noted [34]. It is important to note that DGCR8 is one of the genes deleted in DiGeorge Syndrome, a Neurocristopathy (NCP) that affects 1 : 4000 children [35].

Many individual miRNAs have now been associated with aspects of NC development. One of the first studies was carried out by Gessert and colleagues [36]. They found that miR-130a, miR-219, miR-23b, miR200b, miR-96 and miR-196a are involved in eye and NC development in *Xenopus laevis*. By using a morpholino approach, they further showed that miR-130a, miR-219 and miR-23b are essential for the correct development of the eye, while the knock-down of miR-200b, miR-96 and miR-196a cause, other than eye phenotypes, craniofacial defects often associated with NC defects.

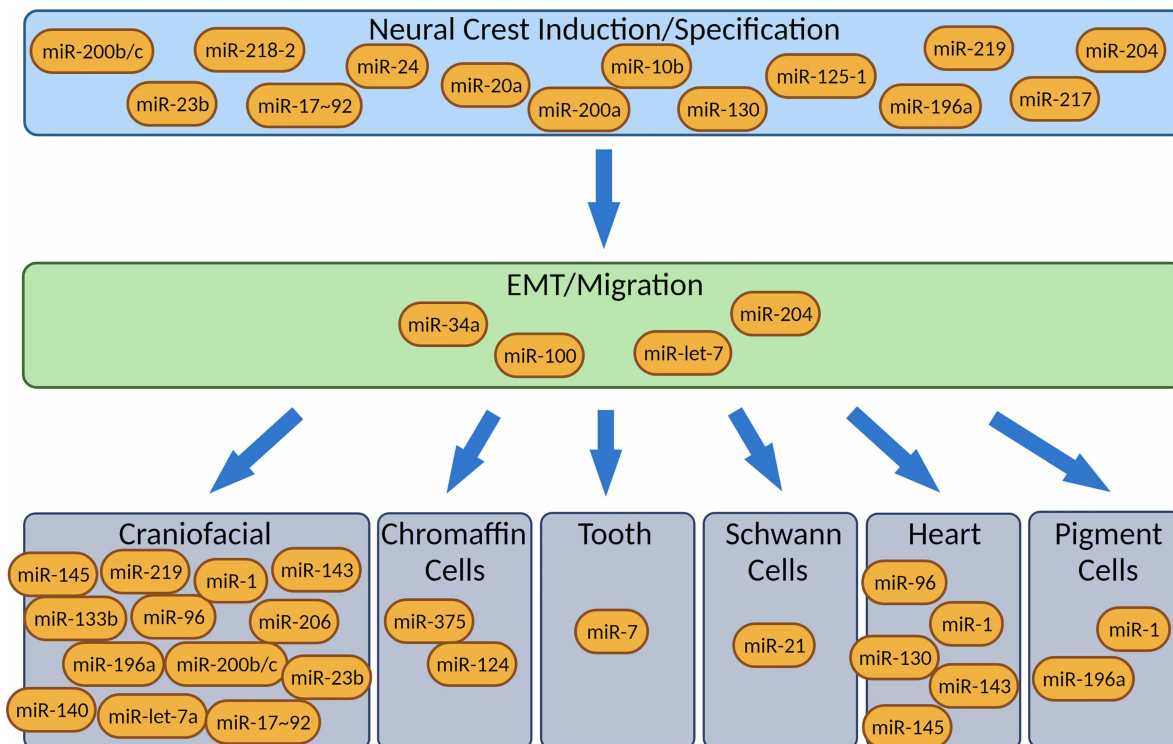


**Figure 1.** MiRNAs described in this review and where they act during Neural Crest development, from induction to differentiation.

**Table 1. Neurocristopathies and associated miRNAs, with possible implicated targets**

Part 1 of 2

Neurocristopathy	Symptoms	miRNA or miRNA-related genes	Implicated target/s	Involvement in NC development	Reference
CHARGE Syndrome	Coloboma; Heart defects; Atresia choanae; Growth retardation; Genital abnormalities; Ear abnormalities	let-7	<i>chd7</i>	Chondrocyte differentiation	[66]
Cleft palate	Incomplete fusion of the bilateral palatal shelves	miR-140	<i>pdgfra</i>	Chondrocyte differentiation	[67]
		miR-17~92	<i>tbx1, tbx3</i>	Induction, chondrocyte differentiation	
		miR-200b	<i>smad2, snai2, zeb1, zeb2</i>	Specification	
Congenital central hypoventilation syndrome	CNS development delay; Hypoxic crisis	miR-204	<i>phox2b</i>	Specification and migration	[58]
Craniosynostosis	Premature fusion of two or more skull bones	miR-23b miR-133b	<i>smad3, smad5, egfr, fgfr1</i>	Induction Chondrocyte differentiation	[68]
Hirschsprung Disease	Swollen belly; Vomiting; Chronic constipation; Fatigue	miR-100	<i>ednrb</i>	EMT [69]	[70]
		miR-206	<i>scpr</i>	Orofacial development	[63]
		miR-214	<i>plagl2</i>		[21]
		miR-483	<i>fn1</i>		[71]
		miR-124	<i>sox9</i>	Sympathoadrenal development	[72]
DiGeorge Syndrome	Behaviour problems; Hearing problems; Feeding problems; Congenital heart defects; Hypoparathyroidism	DGCR8	iRNA pathway	General	[73]
Melanoma	Skin tumours	miR-32 miR-579-3p	<i>mcl1, mitf, braf, mdm2</i> (predicted)		[50]
		miR-200c	<i>bmi1, zeb2, tubb3, abcg5, mdr1</i>	Specification	
		miR-7 miR-21	<i>egfr, igf1r, craf, pten</i>	Tooth development Schwann cells differentiation [74]	
		miR-638 miR-34a	<i>tp53inp2, bcl2, cdk6, e2f3, mycn</i>	EMT	
		miR-100 miR-125b miR-192 miR-193b	<i>trim71, bak1, bcl2, e2f3, zeb2</i>	EMT [69]	
		miR-193b	<i>cdk6, mcl1, bmi1</i> (predicted)	Orofacial development	
		miR-514a	<i>nf1</i>		
		miR-17~92	<i>cdkn1a</i>	Induction, chondrocyte differentiation	[49]
Neuroblastoma	Sympathetic nervous system (peripheral ganglia and adrenal medulla) tumours	miR-34a	<i>e2f3, mycn, bcl2, cdk6</i>	EMT	
		miR-204	<i>bcl2, ntrk2</i>	Specification and migration	[53]
		miR-193b	<i>mycn, mcl1, ccnd1</i>	Orofacial development	[51]
		miR-188 miR-125-1	<i>kif1b</i> (predicted) <i>e2f3, mcl1</i> (predicted)	Specification	[52]

Continued

**Table 1. Neurocristopathies and associated miRNAs, with possible implicated targets**

Part 2 of 2

Neurocristopathy	Symptoms	miRNA or miRNA-related genes	Implicated target/s	Involvement in NC development	Reference
Neurofibromatosis	Peripheral nerves and Schwann cells tumour	miR-501	<i>bcl2, e2f3, cdk6, ntrk2</i> (predicted)		
		let-7b	<i>lin28b</i>	Chondrocyte differentiation	[75]
		miR-143	<i>bcl2, fgf1, igfbp5, camk1d</i>	Cardiac differentiation	
		miR-145	<i>tgfr2, apc, cmc</i>	Cardiac differentiation	
		miR-135	<i>lzts1, lats2, ndr2, btrc</i>		
		miR-889	<i>apc</i>		
		miR-128	<i>nf1</i>		[76]
		miR-137	<i>nf1</i>		
		miR-103	<i>nf1</i>		

In 2013, Avellino and colleagues investigated the role of miR-204 during NC migration. They found that by modulating the expression of miR-204 in Medaka fish embryos, they were able to increase or reduce NCC migration. They also demonstrated that *Ankrd13A* is a direct target of miR-204 and an important modulator of NCC migration [37]. It is worth noting that, among the human *in-silico* predicted targets of miR-204, there is *Ankrd13C*, a paralog of *Ankrd13A*, and other genes involved in motility and extracellular matrix stability, such as the metalloprotease, *Adamts9*, the cadherins, *Cdh4* and *Cdh11*, and the collagen, *Col5A3*. If these *in-silico* targets were validated in NCCs, it would mean that miR-204 is able to regulate NC migration by targeting several key proteins involved in this process.

These results were partially confirmed by Ward and colleagues [38]. In this study *Xenopus laevis* embryonic organoids, often termed ‘animal caps’ were induced to become either NC or neural tissue by injection of Wnt1 and Noggin mRNA (to induce NC) or with Noggin alone (to induce neural tissue). The resulting induced-animal caps were then subjected to small RNA next generation sequencing and differential analysis carried out to identify miRNAs specifically expressed in NC tissue. The most abundant miRNA species detected in NC-induced animal caps were miR-219, miR-196a, miR-218-2, miR-10b, miR-204a, miR-130b/c, miR-23, and miR-24, with miR-219 as the most enriched miRNA in NC-induced animal caps, followed by miR-196a. Further experiments using luciferase assays to validate targets of miR-219 found that *Eya1* is directly targeted by this miRNA (Ward and Wheeler, unpublished results). Other enriched miRNAs were miR-301a and miR-338-3, but these were also found to be expressed in blastula stage animal caps and could be involved in maintaining pluripotency of the blastula stage ectoderm and putative NC.

Recently, we developed an efficient method to knockout miRNAs using CRISPR/Cas9. To do this, we generate two sgRNAs flanking the miRNA sequence in the genome. Introduction of these sgRNAs plus Cas9 into the embryo leads to deletion of the whole miRNA pri-RNA sequence. Using this method, we have knocked out miR-219 and miR-196a, showing clear NC phenotypes, including craniofacial and pigment abnormalities [39]. The observed phenotype for miR-219 could be due to the direct down-regulation of *Pdgfra* and *Sox6* which have been shown to be targets of miR-219 in oligodendrocyte differentiation and myelination [40].

More recent work in chick, highlighted how miR-20a, miR-200a and miR-217 contribute to NC identity by inhibiting FGF pathway on different levels, reducing the levels of *Fgf4*, *Fgf13* and *Fgfr2* in the NC region [41]. In a similar way, other miRNAs have been shown to modulate other key pathways during NC development. For example, Bhattacharya and colleagues showed how the Wnt signalling pathway is modulated by the Lin28/miR-let-7 axis. In particular, high levels of Lin28a promoted by Wnt inhibit the activity of miR-let-7. When NCCs migrate away from the Wnt source, the level of Lin28a is reduced, and this results in an increased level of miR-let-7 activity. The effect leads to the repression of the NC multipotency factors, such as *Pax3/7*, *FoxD3* and *cMyc* [42].

A number of groups have reported a role for specific miRNAs during NC differentiation [31]. For example, Steeman and colleagues have shown that the highly conserved miR-145, which is transcribed together with

miR-143, plays a role during craniofacial development in zebrafish. They speculated that this might be caused by a direct interaction between miR-145 and *Sox9b* [43]. Zhao and colleagues, also working in zebrafish, have shown that miR-1 plays a role in NC development, as its knock-down produces defects during craniofacial, heart, melanocyte and iridophore development [44].

Other studies have revealed that miR-375 is up-regulated in chromaffin cells from the adrenal medulla, another NC-derived tissue involved in the synthesis of the catecholamines adrenaline and noradrenaline [45]. It has been observed that miR-375 acts as negative regulator of TH and DBH (two key enzymes involved in the synthesis of catecholamines). In particular, the authors showed that miR-375 targets *Sp1*, the regulator of TH and DBH, in response to stress [46]. Another study conducted by Shtukmaster and colleagues demonstrated that miR-124 is also expressed in developing sympathetic neurons and supports the maintenance of neuronal morphology in sympathoadrenal cells [47].

Figure 1 shows various miRNAs that have been so far identified to potentially play a role in NC specification, migration and differentiation. Future work needs to determine the specific effects of these miRNAs in NC development. In particular, at what point in NC development do they act and how are they regulated? Also, it will be necessary to validate functional and direct targets of the miRNAs involved in NC development. For example, a luciferase assay shows if there is a direct interaction between a miRNA and an mRNA under a non-physiological expression of both miRNA and mRNA, but it does not provide information about the spatial-temporal expression of those two molecules and whether they interact *in vivo*. To assess the role of a miRNA in the NC-GRN, it is necessary to investigate what factors regulates its expression and verify that the miRNA targets are expressed in the same tissue and at the same stage of development.

## miRNAs and neurocristopathies

Neurocristopathies (NCPs) are diseases that can arise due to problems occurring at any time during the development of the NC. These defects can affect a single NC-derived tissue as in albinism that only affects melanocytes, or they can be syndromic and affect several NC-derived tissues as in CHARGE syndrome, which causes coloboma, heart congenital defects and genital abnormalities [48].

MiRNAs are increasingly becoming associated with various NCPs (Table 1). Despite the fact that NCPs are among the most studied genetic diseases, the etiopathogenesis of many NCPs remains to be elucidated, and many factors involved are still to be discovered.

As mentioned before, a well characterised NCP that affects 1 in 4000 to 6000 live births is DiGeorge Syndrome (DGS). The pathology of this condition is characterised by a combination of phenotypes, including cardiac defects, abnormal facies, cleft palate and an absent or hypoplastic thymus. Other common symptoms are renal anomalies, hearing loss and skeletal abnormalities. DGS is often caused by a deletion of 22q11.2, a region that includes the gene that encodes for DGCR8, an important cofactor of DROSHA and essential for proper miRNA biogenesis [35]. The fact that loss of DGCR8 is associated with a syndromic NCP is a strong indication that the miRNA pathway plays an important role at many levels of NC-development.

In recent years, de-regulated miRNAs have been associated with different types of NCPs and NC-derived cancers (Table 1) [49–53]. Some types of cancers, in particular neuroblastoma (NB) and melanoma, are considered NCPs, as they derive from NC tissues. MiRNAs that promote tumour growth are called oncomiRs, while miRNAs known to suppress the malignancy of the tumoral mass are called anti-oncomiRs [54]. MiRNAs associated with NB aggressiveness include the cluster miR-17~92, which contains five miRNAs (miR-17, miR-18a, miR-19a, miR-20a and miR-92). The overexpression of this cluster in NB is associated with high proliferation and invasiveness, while down-regulation reduces the invasiveness and increases apoptosis in these cells. On the other hand, miR-34a has been shown to have a protective role, as the overexpression of this miRNA induces the arrest of cell proliferation and apoptosis in NB cells. This effect might be due to the targeting of *cdkn1a* by miR-17-p, while miR-34a is shown to directly target *E2F3*, which induces cell cycle progression [49]. MiRNAs have also been associated with melanoma. For example, miR-21 is considered an oncomiR, as its expression is often up-regulated in melanoma cells. Its actions involve the inhibition of cell differentiation and apoptosis. Moreover, knock-down of this miRNA in melanoma cells induces apoptosis and enhances the effectiveness of chemotherapy and radiotherapy. Also in this case, other miRNAs have been shown to have oncosuppressor activity. MiR-32 is one of these as it promotes the arrest of melanoma growth by inhibiting the expression of MCL-1 and, by doing so, the PI3K-AKT-mTOR pathways [50].

Given the increasing number of findings that associate an altered expression of miRNAs and cancer, research groups are starting to give particular attention to regions of DNA harbouring non-translated genes (miRNAs,

lncRNAs, piRNAs) and the non-coding regions of mRNAs which are, in fact, important post-transcriptional regulators via interaction with RNA-binding proteins and miRNAs [55,56]. This trend is providing insights into additional facets of gene regulation, mechanisms of development and mechanisms that lead to pathological conditions.

As an example, Bachetti and colleagues (2021) made an association between the miRNA-mediated regulation of *phox2B* and a pathological condition, congenital central hypoventilation syndrome (CCHS), an NCP that affects the correct development of the CNS and which can cause sudden infant death (SUID) via hypoxic crisis which occurs during sleep [57]. They observed a point mutation in the 3' UTR of *phox2B* [58]. This generates a potential new binding site for miR-204, which is already known to target *phox2b* mRNA in NB cells [59,60]. They speculated that the generation of this new binding site for miR-204 is the cause of the down-regulation of *phox2b* expression, and that could contribute to the occurrence of SUID [58].

Another NCP that has recently been associated with miRNAs is Hirschsprung Disease (HD), a condition characterised by absence of enteric ganglia. This condition impairs passing stool and can lead to a series of signs such as swollen belly, vomiting, chronic constipation, and fatigue [61]. In 2016, a differential miRNA expression analysis on colon tissue from HD patients was carried out. 168 differentially (up-regulated and down-regulated) expressed miRNAs were identified between Hirschsprung and healthy tissues [62]. In recent years, a number of miRNAs has been associated with HD, including miR-100, miR-206, miR-214 and miR-483. For example, a point mutation in the miR-100 gene has been shown to increase HD susceptibility in a southern China population [63].

These studies are leading the way for a new concept underpinning the diagnosis of rare diseases, in which clinicians analyse regions of the genome producing protein coding mRNAs and/or non-coding RNAs to make predictions. In the future, this approach might be used to treat these conditions before the appearance of symptoms, providing the families of these patients with an alternative that could actually cure the disease [64,65].

## Perspectives

- The GRN underlying the induction, migration and specification of the NC is under constant revision.
- Further studies that focus on the role of non-coding RNA species, such as miRNAs, during NC development are fundamental in order to increase our knowledge of the NC-GRN.
- Understanding the role of miRNAs in NC-development can provide clinicians with more powerful tools for the diagnosis of NCPs and other rare diseases.

## Competing Interests

The authors declare that there are no competing interests associated with the manuscript.

## Open Access

Open access for this article was enabled by the participation of University of East Anglia in an all-inclusive *Read & Publish* agreement with Portland Press and the Biochemical Society under a transformative agreement with JISC.

## Authors Contributions

The authors contributed equally to all the aspects of the preparation of the manuscript.

## Acknowledgements

The authors would like to thank Amy Kerr and Andrea Münsterberg for useful discussions and comments. M.A. is funded by the European Union's Horizon 2020 Research and Innovation Program under Marie Skłodowska-Curie (grant agreement No 860635, ITN NEUcrest). G.N.W. is funded by BBSRC grant number BB/T00715X/1

## Abbreviations

BMP, Bone Morphogenic Protein; CCHS, Congenital Central Hypoventilation Syndrome; DGS, DiGeorge syndrome; EMT, Epithelial to Mesenchymal Transition; FGF, Fibroblast Growth Factor; GRN, Gene Regulatory Network; lncRNA, long non-coding RNA; miRNA, microRNA; MMP, Matrix Metalloproteinases; mRNA, messenger RNA; NB, Neuroblastoma; NC, Neural Crest; NCCs, Neural Crest Cells; NCP, Neurocristopathy; NPB, Neural Plate Border; ORF, Open Reading Frame; piRNA, Piwi-interacting RNA; RISC, RNA Inducing Silencing Complex; sgRNA, short guide RNA; SUID, Sudden and Unexpected Infant Death; UTR, Untranslated Region.

## References

- Lee, R.C., Feinbaum, R.L. and Ambros, V. (1993) The *C. elegans* heterochronic gene *lin-4* encodes small RNAs with antisense complementarity to *lin-14*. *Cell* **75**, 843–854 [https://doi.org/10.1016/0092-8674\(93\)90529-Y](https://doi.org/10.1016/0092-8674(93)90529-Y)
- Simoës-Costa, M. and Bronner, M.E. (2015) Establishing neural crest identity: a gene regulatory recipe. *Development* **142**, 242–257 <https://doi.org/10.1242/dev.105445>
- Simoës-Costa, M. and Bronner, M.E. (2013) Insights into neural crest development and evolution from genomic analysis. *Genome Res.* **23**, 1069–1080 <https://doi.org/10.1101/gr.157586.113>
- Martik, M.L. and Bronner, M.E. (2017) Regulatory logic underlying diversification of the neural crest. *Trends Genet.* **33**, 715–727 <https://doi.org/10.1016/j.tig.2017.07.015>
- Mayor, R. and Theveneau, E. (2013) The neural crest. *Development* **140**, 2247–2251 <https://doi.org/10.1242/dev.091751>
- Theveneau, E. and Mayor, R. (2012) Neural crest delamination and migration: from epithelium-to-mesenchyme transition to collective cell migration. *Dev. Biol.* **366**, 34–54 <https://doi.org/10.1016/j.ydbio.2011.12.041>
- Hockman, D., Chong-Morrison, V., Green, S.A., Gavriouchkina, D., Candido-Ferreira, I., Ling, I.T.C. et al. (2019) A genome-wide assessment of the ancestral neural crest gene regulatory network. *Nat. Commun.* **10**, 4689 <https://doi.org/10.1038/s41467-019-12687-4>
- Hutchins, E.J. and Bronner, M.E. (2018) Draxin acts as a molecular rheostat of canonical Wnt signaling to control cranial neural crest EMT. *J. Cell Biol.* **217**, 3683–3697 <https://doi.org/10.1083/jcb.201709149>
- Hochgreb-Hagele, T. and Bronner, M.E. (2013) A novel FoxD3 gene trap line reveals neural crest precursor movement and a role for FoxD3 in their specification. *Dev. Biol.* **374**, 1–11 <https://doi.org/10.1016/j.ydbio.2012.11.035>
- Schlosser, G. and Ahrens, K. (2004) Molecular anatomy of placode development in *Xenopus laevis*. *Dev. Biol.* **271**, 439–466 <https://doi.org/10.1016/j.ydbio.2004.04.013>
- Barembaum, M. and Bronner, M.E. (2013) Identification and dissection of a key enhancer mediating cranial neural crest specific expression of transcription factor, Ets-1. *Dev. Biol.* **382**, 567–575 <https://doi.org/10.1016/j.ydbio.2013.08.009>
- Bhatt, S., Diaz, R. and Trainor, P.A. (2013) Signals and switches in mammalian neural crest cell differentiation. *Cold Spring Harb. Perspect. Biol.* **5**, a008326 <https://doi.org/10.1101/cshperspect.a008326>
- Piacentino, M.L., Li, Y. and Bronner, M.E. (2020) Epithelial-to-mesenchymal transition and different migration strategies as viewed from the neural crest. *Curr. Opin. Cell Biol.* **66**, 43–50 <https://doi.org/10.1016/j.ceb.2020.05.001>
- Battle, E., Sancho, E., Franci, C., Dominguez, D., Monfar, M., Baulida, J. et al. (2000) The transcription factor *snail* is a repressor of E-cadherin gene expression in epithelial tumour cells. *Nat. Cell Biol.* **2**, 84–89 <https://doi.org/10.1038/35000034>
- Cano, A., Perez-Moreno, M.A., Rodrigo, I., Locascio, A., Blanco, M.J., del Barrio, M.G. et al. (2000) The transcription factor *snail* controls epithelial-mesenchymal transitions by repressing E-cadherin expression. *Nat. Cell Biol.* **2**, 76–83 <https://doi.org/10.1038/35000025>
- Taneyhill, L.A. and Schiffmacher, A.T. (2017) Should I stay or should I go? Cadherin function and regulation in the neural crest. *Genesis* **55**, 10.1002/dvg.23028 <https://doi.org/10.1002/dvg.23028>
- Seal, S. and Monsoro-Burq, A.H. (2020) Insights into the early gene regulatory network controlling neural crest and placode fate choices at the neural border. *Front. Physiol.* **11**, 608812 <https://doi.org/10.3389/fphys.2020.608812>
- Bartel, D.P. (2004) MicroRNAs: genomics, biogenesis, mechanism, and function. *Cell* **116**, 281–297 [https://doi.org/10.1016/S0092-8674\(04\)00045-5](https://doi.org/10.1016/S0092-8674(04)00045-5)
- O'Brien, J., Hayder, H., Zayed, Y. and Peng, C. (2018) Overview of MicroRNA biogenesis, mechanisms of actions, and circulation. *Front. Endocrinol.* **9**, 402 <https://doi.org/10.3389/fendo.2018.00402>
- Krol, J., Loedige, I. and Filipowicz, W. (2010) The widespread regulation of microRNA biogenesis, function and decay. *Nat. Rev. Genet.* **11**, 597–610 <https://doi.org/10.1038/nrg2843>
- Wu, L., Yuan, W., Chen, J., Zhou, Z., Shu, Y., Ji, J. et al. (2019) Increased miR-214 expression suppresses cell migration and proliferation in hirschsprung disease by interacting with PLAGL2. *Pediatr. Res.* **86**, 460–470 <https://doi.org/10.1038/s41390-019-0324-9>
- Fabian, M.R., Sonenberg, N. and Filipowicz, W. (2010) Regulation of mRNA translation and stability by microRNAs. *Annu. Rev. Biochem.* **79**, 351–379 <https://doi.org/10.1146/annurev-biochem-060308-103103>
- Winter, J., Jung, S., Keller, S., Gregory, R.I. and Diederichs, S. (2009) Many roads to maturity: microRNA biogenesis pathways and their regulation. *Nat. Cell Biol.* **11**, 228–234 <https://doi.org/10.1038/ncb0309-228>
- Murchison, E.P. and Hannon, G.J. (2004) miRNAs on the move: miRNA biogenesis and the RNAi machinery. *Curr. Opin. Cell Biol.* **16**, 223–229 <https://doi.org/10.1016/j.ceb.2004.04.003>
- Yang, J.S., Maurin, T., Robine, N., Rasmussen, K.D., Jeffrey, K.L., Chandwani, R. et al. (2010) Conserved vertebrate miR-451 provides a platform for Dicer-independent, Ago2-mediated microRNA biogenesis. *Proc. Natl Acad. Sci. U.S.A.* **107**, 15163–15168 <https://doi.org/10.1073/pnas.1006432107>
- Ruby, J.G., Jan, C.H. and Bartel, D.P. (2007) Intronic microRNA precursors that bypass Drosha processing. *Nature* **448**, 83–86 <https://doi.org/10.1038/nature05983>
- Xie, M., Li, M., Vilborg, A., Lee, N., Shu, M.D., Yartseva, V. et al. (2013) Mammalian 5'-capped microRNA precursors that generate a single microRNA. *Cell* **155**, 1568–1580 <https://doi.org/10.1016/j.cell.2013.11.027>

- 28 Ramchandran, R. and Chaluvally-Raghavan, P. (2017) miRNA-mediated RNA activation in mammalian cells. *Adv. Exp. Med. Biol.* **983**, 81–89 [https://doi.org/10.1007/978-981-10-4310-9\\_6](https://doi.org/10.1007/978-981-10-4310-9_6)
- 29 Bernstein, E., Kim, S.Y., Carmell, M.A., Murchison, E.P., Alcorn, H., Li, M.Z. et al. (2003) Dicer is essential for mouse development. *Nat. Genet.* **35**, 215–217 <https://doi.org/10.1038/ng1253>
- 30 Mok, G.F., Lozano-Velasco, E. and Munsterberg, A. (2017) microRNAs in skeletal muscle development. *Semin. Cell Dev. Biol.* **72**, 67–76 <https://doi.org/10.1016/j.semcdb.2017.10.032>
- 31 Weiner, A.M.J. (2018) MicroRNAs and the neural crest: from induction to differentiation. *Mech. Dev.* **154**, 98–106 <https://doi.org/10.1016/j.mod.2018.05.009>
- 32 Zehir, A., Hua, L.L., Maska, E.L., Morikawa, Y. and Cserjesi, P. (2010) Dicer is required for survival of differentiating neural crest cells. *Dev. Biol.* **340**, 459–467 <https://doi.org/10.1016/j.ydbio.2010.01.039>
- 33 Huang, T., Liu, Y., Huang, M., Zhao, X. and Cheng, L. (2010) Wnt1-cre-mediated conditional loss of Dicer results in malformation of the midbrain and cerebellum and failure of neural crest and dopaminergic differentiation in mice. *J. Mol. Cell Biol.* **2**, 152–163 <https://doi.org/10.1093/jmcb/mjq008>
- 34 Chapnik, E., Sasson, V., Belloch, R. and Hornstein, E. (2012) Dgcr8 controls neural crest cells survival in cardiovascular development. *Dev. Biol.* **362**, 50–56 <https://doi.org/10.1016/j.ydbio.2011.11.008>
- 35 Lackey, A.E. and Muzio, M.R. (2021) *DiGeorge Syndrome*, StatPearls, Treasure Island, FL
- 36 Gessert, S., Bugner, V., Tecza, A., Pinker, M. and Kuhl, M. (2010) FMR1/FXR1 and the miRNA pathway are required for eye and neural crest development. *Dev. Biol.* **341**, 222–235 <https://doi.org/10.1016/j.ydbio.2010.02.031>
- 37 Avellino, R., Carrella, S., Pirozzi, M., Risolino, M., Salierno, F.G., Franco, P. et al. (2013) miR-204 targeting of Ankrd13A controls both mesenchymal neural crest and lens cell migration. *PLoS ONE* **8**, e61099 <https://doi.org/10.1371/journal.pone.0061099>
- 38 Ward, N.J., Green, D., Higgins, J., Dalmay, T., Munsterberg, A., Moxon, S. et al. (2018) microRNAs associated with early neural crest development in *Xenopus laevis*. *BMC Genomics* **19**, 59 <https://doi.org/10.1186/s12864-018-4436-0>
- 39 Godden, A.M., Antonaci, M., Ward, N.J., van der Lee, M., Abu-Daya, A., Guille, M. et al. (2021) An efficient miRNA knockout approach using CRISPR-Cas9 in *Xenopus*. *Dev. Biol.* **483**, 66–75 <https://doi.org/10.1016/j.ydbio.2021.12.015>
- 40 Dugas, J.C., Cuellar, T.L., Scholze, A., Ason, B., Ibrahim, A., Emery, B. et al. (2010) Dicer1 and miR-219 Are required for normal oligodendrocyte differentiation and myelination. *Neuron* **65**, 597–611 <https://doi.org/10.1016/j.neuron.2010.01.027>
- 41 Copeland, J. and Simoes-Costa, M. (2020) Post-transcriptional tuning of FGF signaling mediates neural crest induction. *Proc. Natl Acad. Sci. U.S.A.* **117**, 33305–33316 <https://doi.org/10.1073/pnas.2009997117>
- 42 Bhattacharya, D., Rothstein, M., Azambuja, A.P. and Simoes-Costa, M. (2018) Control of neural crest multipotency by Wnt signaling and the Lin28/let-7 axis. *eLife* **7**, e40556 <https://doi.org/10.7554/eLife.40556>
- 43 Steeman, T.J., Rubiolo, J.A., Sanchez, L.E., Calcaterra, N.B. and Weiner, A.M.J. (2021) Conservation of zebrafish MicroRNA-145 and its role during neural crest cell development. *Genes (Basel)* **12**, 1023 <https://doi.org/10.3390/genes12071023>
- 44 Zhao, N., Qin, W., Wang, D., Raquel, A.G., Yuan, L., Mao, Y. et al. (2021) MicroRNA-1 affects the development of the neural crest and craniofacial skeleton via the mitochondrial apoptosis pathway. *Exp. Ther. Med.* **21**, 379 <https://doi.org/10.3892/etm.2021.9810>
- 45 Dutt, M., Wehrle, C.J. and Jialal, I. (2022) *Physiology, Adrenal Gland*, StatPearls, Treasure Island, FL
- 46 Gai, Y., Zhang, J., Wei, C., Cao, W., Cui, Y. and Cui, S. (2017) miR-375 negatively regulates the synthesis and secretion of catecholamines by targeting Sp1 in rat adrenal medulla. *Am. J. Physiol. Cell Physiol.* **312**, C663–C672 <https://doi.org/10.1152/ajpcell.00345.2016>
- 47 Shtukmaster, S., Narasimhan, P., El Faitwri, T., Stubbusch, J., Ernsberger, U., Rohrer, H. et al. (2016) MiR-124 is differentially expressed in derivatives of the sympathoadrenal cell lineage and promotes neurite elongation in chromaffin cells. *Cell Tissue Res.* **365**, 225–232 <https://doi.org/10.1007/s00441-016-2395-9>
- 48 Vega-Lopez, G.A., Cerrizuela, S., Tribulo, C. and Aybar, M.J. (2018) Neurocristopathies: new insights 150 years after the neural crest discovery. *Dev. Biol.* **444**, S110–S143 <https://doi.org/10.1016/j.ydbio.2018.05.013>
- 49 Stallings, R.L. (2009) MicroRNA involvement in the pathogenesis of neuroblastoma: potential for microRNA mediated therapeutics. *Curr. Pharm. Des.* **15**, 456–462 <https://doi.org/10.2174/138161209787315837>
- 50 Lorusso, C., De Summa, S., Pinto, R., Danza, K. and Tommasi, S. (2020) miRNAs as key players in the management of cutaneous melanoma. *Cells* **9**, 415 <https://doi.org/10.3390/cells9020415>
- 51 Roth, S.A., Hald, O.H., Fuchs, S., Lokke, C., Mikkola, I., Flaegstad, T. et al. (2018) MicroRNA-193b-3p represses neuroblastoma cell growth via downregulation of Cyclin D1, MCL-1 and MYCN. *Oncotarget* **9**, 18160–18179 <https://doi.org/10.18632/oncotarget.24793>
- 52 Ayers, D., Mestdagh, P., Van Maerken, T. and Vandesompele, J. (2015) Identification of miRNAs contributing to neuroblastoma chemoresistance. *Comput. Struct. Biotechnol. J.* **13**, 307–319 <https://doi.org/10.1016/j.csbj.2015.04.003>
- 53 Ooi, C.Y., Carter, D.R., Liu, B., Mayoh, C., Beckers, A., Lalwani, A. et al. (2018) Network modeling of microRNA-mRNA interactions in neuroblastoma tumorigenesis identifies miR-204 as a direct inhibitor of MYCN. *Cancer Res.* **78**, 3122–3134 <https://doi.org/10.1158/0008-5472.CAN-17-3034>
- 54 Svoronos, A.A., Engelman, D.M. and Slack, F.J. (2016) Oncomir or tumor suppressor? The duplicity of microRNAs in cancer. *Cancer Res.* **76**, 3666–3670 <https://doi.org/10.1158/0008-5472.CAN-16-0359>
- 55 Mignone, F. and Pesole, G. (2018) mRNA untranslated regions (UTRs). *eLS*, 1–6 <https://doi.org/10.1002/9780470015902.a0005009.pub3>
- 56 Chatterjee, S. and Pal, J.K. (2009) Role of 5'- and 3'-untranslated regions of mRNAs in human diseases. *Biol. Cell* **101**, 251–262 <https://doi.org/10.1042/BC20080104>
- 57 Matera, I., Bachetti, T., Puppo, F., Di Duca, M., Morandi, F., Casiraghi, G.M. et al. (2004) PHOX2B mutations and polyalanine expansions correlate with the severity of the respiratory phenotype and associated symptoms in both congenital and late onset Central Hypoventilation syndrome. *J. Med. Genet.* **41**, 373–380 <https://doi.org/10.1136/jmg.2003.015412>
- 58 Bachetti, T., Bagnasco, S., Piumelli, R., Palmieri, A. and Ceccherini, I. (2021) A common 3'UTR variant of the PHOX2B gene is associated With infant life-threatening and sudden death events in the Italian population. *Front. Neurol.* **12**, 642735 <https://doi.org/10.3389/fneur.2021.642735>
- 59 Bachetti, T., Di Zanni, E., Ravazzolo, R. and Ceccherini, I. (2015) miR-204 mediates post-transcriptional down-regulation of PHOX2B gene expression in neuroblastoma cells. *Biochim. Biophys. Acta* **1849**, 1057–1065 <https://doi.org/10.1016/j.bbaggm.2015.06.008>

- 60 Perri, P., Ponzone, M., Corrias, M.V., Ceccherini, I., Candiani, S. and Bachetti, T. (2021) A focus on regulatory networks linking MicroRNAs, transcription factors and target genes in neuroblastoma. *Cancers (Basel)* **13**, 5528 <https://doi.org/10.3390/cancers13215528>
- 61 Lotfollahzadeh, S., Taherian, M. and Anand, S. (2021) *Hirschsprung Disease*, StatPearls, Treasure Island, FL
- 62 Li, S., Wang, S., Guo, Z., Wu, H., Jin, X., Wang, Y. et al. (2016) miRNA profiling reveals dysregulation of RET and RET-regulating pathways in hirschsprung's disease. *PLoS ONE* **11**, e0150222 <https://doi.org/10.1371/journal.pone.0150222>
- 63 Gunadi, Budi, N.Y.P., Kalim, A.S., Santiko, W., Musthofa, F.D., Iskandar, K. et al. (2019) Aberrant expressions of miRNA-206 target, FN1, in multifactorial Hirschsprung disease. *Orphanet. J. Rare Dis.* **14**, 5 <https://doi.org/10.1186/s13023-018-0973-5>
- 64 Hydbring, P. and Badalian-Very, G. (2013) Clinical applications of microRNAs. *F1000Res.* **2**, 136 <https://doi.org/10.12688/f1000research.2-136.v1>
- 65 Hanna, J., Hossain, G.S. and Kocerha, J. (2019) The potential for microRNA therapeutics and clinical research. *Front. Genet.* **10**, 478 <https://doi.org/10.3389/fgene.2019.00478>
- 66 Evsen, L., Li, X., Zhang, S., Razin, S. and Doetzlhofer, A. (2020) let-7 miRNAs inhibit CHD7 expression and control auditory-sensory progenitor cell behavior in the developing inner ear. *Development* **147**, dev183384 <https://doi.org/10.1242/dev.183384>
- 67 Schoen, C., Aschrafi, A., Thonissen, M., Poelmans, G., Von den Hoff, J.W. and Carels, C.E.L. (2017) MicroRNAs in palatogenesis and cleft palate. *Front. Physiol.* **8**, 165 <https://doi.org/10.3389/fphys.2017.00165>
- 68 Ding, H.L., Hooper, J.E., Batzel, P., Eames, B.F., Postlethwait, J.H., Artinger, K.B. et al. (2016) MicroRNA profiling during craniofacial development: potential roles for Mir23b and Mir133b. *Front. Physiol.* **7**, 281 <https://doi.org/10.3389/fphys.2016.00281>
- 69 Chen, D., Sun, Y., Yuan, Y., Han, Z., Zhang, P., Zhang, J. et al. (2014) miR-100 induces epithelial-mesenchymal transition but suppresses tumorigenesis, migration and invasion. *PLoS Genet.* **10**, e1004177 <https://doi.org/10.1371/journal.pgen.1004177>
- 70 Zhu, Y., Lin, A., Zheng, Y., Xie, X., He, Q. and Zhong, W. (2020) miR-100 rs1834306 A>G increases the risk of Hirschsprung disease in southern Chinese children. *Pharmacogenomics Pers. Med.* **13**, 283–288 <https://doi.org/10.2147/PGPM.S265730>
- 71 Wang, G., Guo, F., Wang, H., Liu, W., Zhang, L., Cui, M. et al. (2017) Downregulation of microRNA-483-5p promotes cell proliferation and invasion by targeting GFRA4 in hirschsprung's disease. *DNA Cell Biol.* **36**, 930–937 <https://doi.org/10.1089/dna.2017.3821>
- 72 Mi, J., Chen, D., Wu, M., Wang, W. and Gao, H. (2014) Study of the effect of miR124 and the SOX9 target gene in hirschsprung's disease. *Mol. Med. Rep.* **9**, 1839–1843 <https://doi.org/10.3892/mmr.2014.2022>
- 73 Du, Q., de la Morena, M.T. and van Oers, N.S.C. (2019) The genetics and epigenetics of 22q11.2 deletion syndrome. *Front. Genet.* **10**, 1365 <https://doi.org/10.3389/fgene.2019.01365>
- 74 Ni, Y., Zhang, K., Liu, X., Yang, T., Wang, B., Fu, L. et al. (2014) miR-21 promotes the differentiation of hair follicle-derived neural crest stem cells into Schwann cells. *Neural Regen. Res.* **9**, 828–836 <https://doi.org/10.4103/1673-5374.131599>
- 75 Amiras, A., Verdijk, R.M., van Kuijk, P.F., Kartal, P., Vriends, A.L.M., French, P.J. et al. (2020) Deregulated microRNAs in neurofibromatosis type 1 derived malignant peripheral nerve sheath tumors. *Sci. Rep.* **10**, 2927 <https://doi.org/10.1038/s41598-020-59789-4>
- 76 Paschou, M. and Doxakis, E. (2012) Neurofibromin 1 is a miRNA target in neurons. *PLoS ONE* **7**, e46773 <https://doi.org/10.1371/journal.pone.0046773>



# Chapter 11

## Determining miRNA Expression Patterns in *Xenopus*

Marco Antonaci, Alice M. Godden, and Grant N. Wheeler

### Abstract

Whole-mount in situ hybridization (WISH) is a technique that enables temporal and spatial visualization of RNA molecules in an embryo or whole tissue by using a complementary labelled probe. MicroRNAs are short noncoding RNAs of 20–25 nt in length mainly involved in posttranscriptional regulation of gene expression. In this chapter, we describe how to visualize miRNAs in *Xenopus laevis* or *tropicalis* by WISH using two different approaches: LNA-WISH to visualize mature miRNAs and pri-miRNA-WISH to visualize the immature form of miRNAs, the pri-miRNAs.

**Key words** WISH, miRNA, *Xenopus*, Development, Expression pattern

---

## 1 Introduction

One of the most important goals in developmental biology is to determine where and when a gene is expressed. *Xenopus laevis* and *Xenopus tropicalis* are powerful model species which have been used to identify several fundamental biological processes in development. This is due to the relative ease from which the eggs can be collected and fertilized and by the large numbers of eggs that a single frog can lay (over hundreds in a single use). This, combined with the fact that many human diseases can be modelled in *Xenopus* species [1], makes this animal an excellent model to study genetic diseases and basic embryonic development. A well-established technique to visualize the expression of a gene during development is whole-mount in situ hybridization (WISH). The general idea of WISH is to use a digoxigenin-labelled RNA probe that pairs with the RNA of interest. Following hybridization with this probe, the sample is incubated with an alkaline phosphatase-labelled anti-digoxigenin antibody. The color reaction occurs by incubating the sample with dyes that upon dephosphorylation will generate a

---

Marco Antonaci and Alice M. Godden have contributed equally to this chapter

Tamas Dalmay (ed.), *MicroRNA Detection and Target Identification: Methods and Protocols*, Methods in Molecular Biology, vol. 2630, [https://doi.org/10.1007/978-1-0716-2982-6\\_11](https://doi.org/10.1007/978-1-0716-2982-6_11), © The Author(s), under exclusive license to Springer Science+Business Media, LLC, part of Springer Nature 2023

colored precipitate. This color reaction therefore only occurs in the regions of the sample where the RNA target is expressed [2, 3]. As a “good” probe is usually 250–1000 nt in length, and mature miRNAs are around 20–25 nt in length [4], alternative approaches have been developed in order to visualize their expression. The first involves the use of locked nucleic acid (LNA) probes to stain mature miRNAs [5, 6]. A second approach generates a probe that pairs with the unprocessed form of the miRNA of interest (primary miRNA or pri-miRNA) [7, 8]. Pri-miRNAs’ length can be very different from a minimum range of 80–120 nt for isolated miRNAs. Clustered miRNAs, such as the ones in the group miR-17–92 can have primary transcripts longer than 1 kb. Probes that bind these transcripts can be used the same way as probes for mRNAs. In this chapter, we will discuss how to carry out an LNA-WISH and a pri-miRNA WISH on *Xenopus* embryos.

---

## 2 Materials

### 2.1 Collection of *Xenopus* Species Embryos

1. PMSG.
2. Chorulon: hcG.
3. 1× MMR—100 mM NaCl, 2 mM KCl, 1 mM MgCl<sub>2</sub>, 2 mM CaCl<sub>2</sub>, 5 mM HEPES, pH 7.5 (*see Note 1*).
4. 0.1× MMR—10 mM NaCl, 0.2 mM KCl, 0.1 mM MgCl<sub>2</sub>, 0.2 mM CaCl<sub>2</sub>, 0.5 mM HEPES, pH 7.5 (*see Note 1*).
5. 0.05× MMR—5 mM NaCl, 0.1 mM KCl, 50 μM MgCl<sub>2</sub>, 0.1 mM CaCl<sub>2</sub>, 250 μM HEPES, pH 7.5 (*see Note 1*).
6. 2% L-cysteine pH 7.5 in MMR (1× for *X. laevis*, 0.1× for *X. tropicalis*) (*see Note 2*).
7. *Xenopus laevis* or *tropicalis* frozen sperm.

### 2.2 Fixation of *Xenopus* Species Embryos

1. 10× MEM salts—1 M MOPS, 20 mM EGTA, 10 mM MgSO<sub>4</sub>, pH 7.4, in DEPC-H<sub>2</sub>O (*see Note 3*).
2. MEMFA—3.7% formaldehyde, in 1× MEM salts (*see Note 4*).
3. 100% ethanol.
4. DEPC-PBS—137 mM NaCl, 2.7 mM KCl, 10 mM Na<sub>2</sub>HPO<sub>4</sub>, 1.8 mM KH<sub>2</sub>PO<sub>4</sub> in DEPC-H<sub>2</sub>O (*see Note 1*).

### 2.3 Whole Mount *In Situ* Hybridization

1. PBST—0.1% Tween 20 in 1× PBS.
2. 75% ethanol in DEPC-PBST.
3. 50% ethanol in DEPC-PBST.
4. 25% ethanol in DEPC-PBST.
5. Proteinase K solution—20 μg/mL Proteinase K in DEPC-PBST (*see Note 2*).

6. RNase A solution—1 µg/mL RNase A in 2× SSC (*see Note 2*).
7. Fixing solution—3.7% formaldehyde in DEPC-PBST (*see Note 4*).
8. 2× SSC—0.3 M NaCl, 30 mM Na citrate, pH 7, in dH<sub>2</sub>O (*see Note 5*).
9. 0.2× SSC—30 mM NaCl, 3 mM Na citrate, pH 7, in dH<sub>2</sub>O (*see Note 5*).
10. Hybridization buffer—50% formamide, 25% 20× SSC, 1 mg/mL torula RNA, 100 µg/mL heparin, 1× Denhardt's, 0.1% Tween 20, 0.1% Chaps, 10 mM EDTA in DEPC-H<sub>2</sub>O (*see Note 6*).
11. Probe buffer—1 µg/mL DIG-labelled probe in hybridization buffer (*see Notes 6 and 7*).
12. MAB—0.1 M maleic acid, 150 mM NaCl in dH<sub>2</sub>O (*see Note 1*).
13. Blocking solution—2% Boehringer Blocking Reagent (BBR) in MAB.
14. Antibody solution—1:3000 α-DIG (anti-digoxigenin-AP Fab fragments, Sigma-Aldrich, REF: 11093274910) in blocking solution (*see Note 2*).
15. NTMT—100 mM Tris-HCl pH 9.5, 100 mM NaCl, 50 mM MgCl<sub>2</sub>, 1% Tween 20 (*see Note 2*).
16. NBT—50 mg/mL nitro blue tetrazolium in 70% dimethylformamide (DMF) (*see Note 8*).
17. BCIP—50 mg/mL 5-bromo-4-chloro-3-indolyl-phosphate in dimethylformamide (DMF) (*see Note 8*).
18. Color solution—0.09% NBT, 0.35% BCIP in NTMT (*see Notes 2 and 8*).
19. Imaging plate—2% agarose in dH<sub>2</sub>O (*see Note 9*).
20. 100% methanol (*see Note 10*).

---

### 3 Methods

#### 3.1 Collection of *Xenopus laevis* Eggs

1. Females of *Xenopus laevis* are primed with an injection of 200 U (200 µL) PMSG onto one lymph sac 3 to 7 days before egg collection (*see Note 11*). Frogs are not fed during this time.
2. Induction is then performed ~16 h before egg collection with an injection of 500 U (500 µL) of Chorulon onto one lymph sac.
3. Once the first eggs are naturally released, frogs are gently squeezed in order to collect eggs in a petri dish.

### 3.2 Fertilization of *Xenopus Laevis* Eggs

1. *Xenopus laevis* frozen sperm is collected from the  $-80\text{ }^{\circ}\text{C}$  in dry ice and thawed for 30 s in a  $37\text{ }^{\circ}\text{C}$  water bath doing an “8” movement (*see* **Note 12**).
2.  $125\text{ }\mu\text{L}$  of  $0.1\times$  MMR is added to the frozen sperm and gently mixed with a precut tip; the mixture is then pipetted on the eggs.
3. The eggs are then incubated at  $18\text{ }^{\circ}\text{C}$  for 10 min. After this incubation, the dish is flooded with  $0.1\times$  MMR and incubated for 20 min more at  $18\text{ }^{\circ}\text{C}$ . At this point, fertilized eggs will turn with the animal pole (pigmented side) on the top and vegetal pole (nonpigmented side) on the bottom.
4. The embryos are de-jellied by removing  $0.1\times$  MMR and adding 2% cysteine for 7 min. During this incubation, it is useful to gently swirl the embryos. At the end of the 7 min, cysteine is removed by washing the embryos a minimum of three times with  $1\times$  MMR and then a minimum of three more times with  $0.1\times$  MMR.

### 3.3 Collection of *Xenopus Tropicalis* Eggs

1. Females of *Xenopus tropicalis* are primed with an injection of 10 U ( $100\text{ }\mu\text{L}$ ) Chorulon onto one lymph sac 24–72 h before egg collection. Frogs are not fed during this time.
2. Induction is then performed  $\sim 5$  h before egg collection with an injection of 200 U ( $200\text{ }\mu\text{L}$ ) of Chorulon onto one lymph sac.
3. Once the first eggs are naturally released, frogs are gently squeezed in order to collect eggs in a petri dish.

### 3.4 Fertilization of *Xenopus Tropicalis* Eggs

1. *Xenopus tropicalis* frozen sperm is collected from the  $-80\text{ }^{\circ}\text{C}$  and thawed for 30 s in a  $37\text{ }^{\circ}\text{C}$  water bath doing an “8” movement (*see* **Note 12**).
2.  $125\text{ }\mu\text{L}$  of  $0.1\times$  MMR is added to the frozen sperm and gently mixed with a precut tip; the mixture is then pipetted on the eggs.
3. The eggs are incubated at  $25\text{ }^{\circ}\text{C}$  for 20 min. After this incubation, the dish is flooded with  $0.05\times$  MMR and incubated for 30 min more at  $25\text{ }^{\circ}\text{C}$ . At this point, fertilized eggs will contract the pigmentation on the animal pole, making it darker than the one of unfertilized eggs.
4. The embryos are then de-jellied by removing  $0.05\times$  MMR and adding 2% cysteine for 7 min at  $25\text{ }^{\circ}\text{C}$ . At the end of the 7 min, cysteine is removed by washing the embryos a minimum of three times with  $0.1\times$  MMR and a minimum of three times with  $0.05\times$  MMR.

### 3.5 Fixation of *Xenopus* Species Embryos

1. Fertilised embryos develop at 16–21 °C (*X. laevis*) or 25 °C (*X. tropicalis*). Once they reach the desired stage, embryos are collected and fixed in MEMFA for 2 h at RT with gentle rocking, or overnight at 4 °C on gentle rocking.
2. Once fixed, embryos are washed three times with 100% Ethanol. At this point, it is possible to proceed with the WISH protocol, or the embryos can be stored at –20 °C indefinitely.

### 3.6 LNA-Wish

All steps are carried out at room temperature and with gentle rocking, unless specified (*see* **Notes 13, 14, 15, and 16**).

1. Wash with 75% ethanol in DEPC-PBST for 5 min (*see* **Notes 17 and 18**).
2. Wash with 50% ethanol in DEPC-PBST for 5 min.
3. Wash with 25% ethanol in DEPC-PBST for 5 min.
4. Wash twice with DEPC-PBST for 5 min.
5. Treat with Proteinase K solution, guidelines for the incubation time on **Table 1**, no rocking.
6. Wash twice with DEPC-PBST for 5 min.
7. Treat with fixing solution for 20 min.
8. Wash twice with DEPC-PBST for 5 min.
9. Treat with preheated hybridization buffer (54 °C) until the embryos settle to the bottom of the vial, no rocking.
10. Replace the hybridization buffer with some new hybridization buffer and incubate at 54 °C for at least 3 h.
11. Incubate with the LNA-probe solution overnight at 54 °C (*see* **Note 19**).
12. Wash with hybridization buffer once for 10 min at 54 °C.
13. Wash three times with 2× SSC for 20 min at 54 °C.
14. Wash twice with 0.2× SSC for 30 min at 54 °C.
15. Wash with MAB for 10 min.
16. Block in blocking solution for at least 1 h.
17. Incubate in the antibody solution overnight at 4 °C (*see* **Note 20**).

**Table 1**

**Time in minutes of incubation with Proteinase K solution. This is a guideline; every time a new batch of Proteinase K is prepared, it should be tested with known probes on different stages of development. The staging is performed according to the standard Nieuwkoop and Faber staging system**

Stage (NF)	1–10	10.5–12	13–16	17–20	21–25	26–30	31–33	34–36	37–40	41–45
Time (min)	0.5	1	2	3	4	5	6	8	18	20

18. Wash twice with MAB for 5 min.
19. Wash six times with MAB for 30 min.
20. Wash with MAB overnight at 4 °C.
21. Wash three times with MAB for 5 min.
22. Wash twice with NTMT solution for 10 min.
23. Incubate in color solution protected from light. At this point, keep the embryos in color solution until the control LNA-probe starts developing color. It is possible to replace the Color solution if the solution starts changing color from pale yellow to purple. This will speed the reaction and reduce the background staining.
24. Stop the solution by washing three times with PBST (*see Note 21*).
25. It is possible to remove some of the background by incubating the embryos overnight at 4 °C in 100% methanol. Embryos can be stored at –20 °C indefinitely.
26. Rehydrate by washing twice with PBS for 10 min.
27. Acquire images on a 2% agarose plate with PBS (*see Fig. 1*).

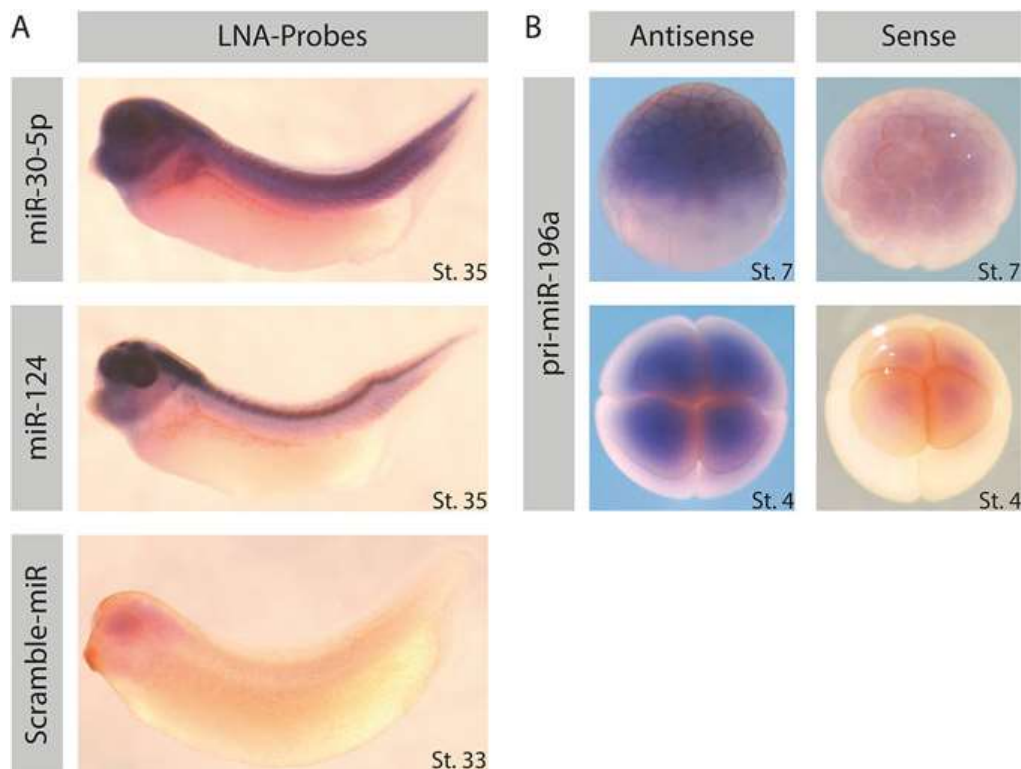


**Fig. 1** Example of LNA-WISH and pri-miRNA WISH. (a) LNA-WISH: from top to bottom, expression of xtr-miR-30-5p, xtr-miR-124, and control, scramble miRNA at tailbud stages. (b) Pri-miRNA-WISH on xtr-miR-196a. On the left side, WISH on xtr-miR-196a anti-sense probe at NF stage 7 (top) and NF stage 4 (bottom). On the right side, WISH on xtr-miR-196a sense probe at NF stage 7 (top) and NF stage 4 (bottom)

**3.7 Pri-MIRNA WISH**

All steps are carried out at room temperature and with gentle rocking, unless specified (*see* **Notes 13, 14, 15, 16, and 22**).

1. Wash with 75% ethanol in DEPC-PBST for 5 min (*see* **Notes 17 and 18**).
2. Wash with 50% ethanol in DEPC-PBST for 5 min.
3. Wash with 25% ethanol in DEPC-PBST for 5 min.
4. Wash twice with DEPC-PBST for 5 min.
5. Treat with Proteinase K solution, guidelines for the incubation time on **Table 1**, no rocking.
6. Wash twice with DEPC-PBST for 5 min.
7. Treat with fixing solution for 20 min.
8. Wash twice with DEPC-PBST for 5 min.
9. Treat with preheated hybridization buffer (60 °C) until the embryos settle to the bottom of the vial, no rocking.
10. Replace the hybridization buffer with some new hybridization buffer and incubate at 60 °C for at least 1 h.
11. Incubate with the probe solution overnight at 60 °C.
12. Wash with hybridization buffer once for 10 min at 60 °C.
13. Wash three times with 2× SSC for 20 min at 60 °C.
14. Treat with RNase A solution for 30 min at 37 °C.
15. Wash with 2× SSC for 10 min.
16. Wash twice with 0.2× SSC for 30 min at 60 °C.
17. Wash with MAB for 10 min.
18. Block in blocking solution for at least 1 h.
19. Incubate in the antibody solution overnight at 4 °C (*see* **Note 20**).
20. Wash twice with MAB for 5 min.
21. Wash six times with MAB for 30 min.
22. Wash with MAB overnight at 4 °C.
23. Wash three times with MAB for 5 min.
24. Wash twice with NTMT solution for 10 min.
25. Incubate in color solution protected from light. Keep checking the embryos every 20–30 min until a signal is seen. It is possible to replace the color solution if the solution starts changing color from pale yellow to purple. This will speed the reaction and reduce the background staining.
26. Stop the solution by washing three times with PBST (*see* **Note 21**).

27. It is possible to remove some of the background by incubating the embryos overnight at 4 °C in 100% methanol.
28. Rehydrate by washing twice with PBS for 10 min.
29. Acquire images on a 2% agarose plate with PBS.

---

## 4 Notes

1. MMR, DEPC-PBST, and MAB can be prepared as stock solution of 10× and stored at 4 °C.
2. 2%, MEMFA, Proteinase K solution, RNase A solution, fixing solution, antibody solution, NTMT, and color solution should be prepared fresh.
3. MEM salts are photosensitive and should be stored at 4 °C wrapped in aluminum foil.
4. MEMFA and fixation solution contain formaldehyde, which is toxic; handle with care.
5. SSC can be prepared as stock solution of 20× and stored at 4 °C.
6. Hybridization buffer and probe buffer contain formamide, which is toxic; handle with care. Both can be prepared in advance and stored at −20 °C.
7. LNA probes need to be prehybridized against a mixture of different stage embryos up to six times before first use in order to minimize background staining. Both LNA probe and pri-miRNA probe can be used multiple times and stored at −20 °C. Usually, probes that have been used at least 1–2 times show cleaner staining.
8. Color solution, BCIP, and NBT contain dimethylformamide, or DMF. All are toxic; handle with care.
9. A thicker agarose layer on the plate will show a nicer blue background during the acquisition of the picture.
10. Methanol is toxic; handle with care.
11. An alternative to the use of PMSG is to prime *X. laevis* with a diluted Chorulon, injecting 50 U/frog of Chorulon in the same way.
12. For more detailed information on how to use frozen sperm to fertilize *Xenopus* eggs, see <https://xenopusresource.org/using-frozen-sperm-4>.
13. Fixed embryos are particularly fragile; while changing solution, it is better to leave a bit of the previous solution but not to ruin the embryos, rather than removing all of it.
14. Embryos should never be let to dry.

15. The whole experiment can be performed in glass vials, but is also possible to use normal 2-mL tubes and, before the color reaction, transfer the embryos in glass vials. This way it will be possible to look at the embryos during the color reaction.
16. Usually, 10–15 embryos per sample are a good number for each WISH.
17. Usually, 0.5–1 mL of solution is enough to completely cover all the embryos.
18. While rocking, glass vials can be kept standing. This can be optimal since, if they get stuck on the lid of the vial, they will not be in contact with the solution and will dry out.
19. LNA probes should be used 4–6 times before they lose their nonspecific staining. Before starting an experiment, it should be better to perform mock LNA-WISH with that specific probe, in order to obtain the best results.
20. After the incubation with primary antibody, the use of DEPC-treated solutions is no longer necessary.
21. It is possible to stop and restart the color reaction by washing three times with PBST and leaving the embryos *on* at 4 °C. The day after, it is possible to incubate again twice with NTMT and then start again the color reaction.
22. For the list of primers used to produce xtr-miR-219 pri-miRNA probe, see Godden et al. [7].

---

## Acknowledgements

We would like to thank the members of the Wheeler and Munsterberg labs, both past and present, who have contributed to the development of these protocols.

---

## Funding

MA is funded by the European Union's Horizon 2020 research and innovation program under the Marie Skłodowska-Curie grant agreement no. 860635. AMG was supported by UKRI Biotechnology and Biological Sciences Research Council Norwich Research Park Biosciences Doctoral Training Partnership grants (BB/M011216/1).

## References

1. Tandon P, Conlon F, Furlow JD, Horb ME (2017) Expanding the genetic toolkit in *Xenopus*: approaches and opportunities for human disease modeling. *Dev Biol* 426(2):325–335
2. Dakou E, Vanbekbergen N, Corradi S, Kemp CR, Willems E, Leyns L (2014) Whole-mount in situ hybridization (WISH) optimized for gene expression analysis in mouse embryos and Embryoid bodies. In: Nielsen BS (ed) *In situ hybridization protocols*. New York, Springer New York, pp 27–40
3. Harland RM (1991) In situ hybridization: an improved whole-mount method for *Xenopus* embryos. *Methods Cell Biol* 36:685–695
4. Lu TX, Rothenberg ME (2018) MicroRNA. *J Allergy Clin Immunol* 141(4):1202–1207
5. Darnell DK, Antin PB (2014) LNA-based in situ hybridization detection of mRNAs in embryos. *Methods Mol Biol* 1211:69–76
6. Ahmed A, Ward NJ, Moxon S, Lopez-Gomollon S, Viaut C, Tomlinson ML et al (2015) A database of microRNA expression patterns in *Xenopus laevis*. *PLoS One* 10(10): e0138313
7. Godden AM, Antonaci M, Ward NJ, van der Lee M, Abu-Daya A, Guille M et al (2012) An efficient miRNA knockout approach using CRISPR-Cas9 in *Xenopus*. *Dev Biol.* 483:66–75
8. Walker JC, Harland RM (2008) Expression of microRNAs during embryonic development of *Xenopus tropicalis*. *Gene Expr Patterns* 8(6): 452–456



## An Efficient CRISPR-Cas9 Method to Knock Out miRNA Expression in *Xenopus Tropicalis*

Alice M. Godden, Marco Antonaci, and Grant N. Wheeler

### Abstract

In recent years CRISPR-Cas9 knockouts (KO) have become increasingly utilized to study gene function. MicroRNAs (miRNAs) are short noncoding RNAs, 20–25 nucleotides long, which affect gene expression through posttranscriptional repression. As miRNAs are so small and due to the limitations of known PAM sequences, it is difficult to design CRISPR sgRNAs that reproducibly lead to a KO. We have therefore developed a novel approach using two guide RNAs to effectively “drop out” a miRNA. Validation of efficient CRISPR miRNA KO and phenotype analysis included use of q-RT-PCR and Sanger sequencing. To show specificity of the phenotype, we provide a protocol to use miRNA mimics to rescue the KO phenotype.

**Key words** CRISPR-Cas9, *Xenopus tropicalis*, Knock-out, Micro RNA, Rescue

---

### 1 Introduction

Recently, CRISPR-Cas9 gene editing has become increasingly popular and more mainstream for manipulating gene expression in model organisms such as *Xenopus*. CRISPR-Cas9 utilizes a highly specific targeted nuclease to induce genomic editing by nonhomologous end joining (NHEJ) or homology-directed repair (HDR). CRISPR therefore is an efficient method that can rapidly generate KO *Xenopus* embryos and lines of frogs for phenotype and genotype analysis [1, 2].

CRISPR genome editing works by using single-guide RNAs (sgRNAs) to target Cas9 endonuclease to induce genomic cleavage [3]. SgRNAs are part of the CRISPR RNA (crRNA) and are the region that is complementary to the genomic DNA (gDNA) that is being targeted. The sgRNA will bind to the genomic target region if it has a protospacer adjacent motif (PAM), NGG sequence, present. This helps guide the Cas9 endonuclease to its cleavage site. The PAM region can limit the sgRNA designs for the end

user; however, more Cas9 endonucleases are being engineered and refined, which will give the user more flexibility and sgRNA options [4]. Additionally, crRNA pairs with a trans-activating CRISPR RNA (tracrRNA) and recruits the Cas9 endonuclease to the target site for mutagenesis [2, 5]. *X. tropicalis* are a diploid species of *Xenopus* and so are the optimal *Xenopus* model for this project using targeted mutagenesis techniques such as CRISPR/Cas9 [2, 6]. Both mosaic knockouts and generation of stable lines could be achieved with this approach.

MiRNAs are short noncoding RNAs, 20–25 nucleotides long mainly involved in posttranscriptional regulation of gene expression [7]. To KO a miRNA in *X. tropicalis*, the technical limitation of generating a viable embryo with a clean KO is that designing a sgRNA close to or in the miRNA is difficult due to their small size. In addition an insertion/deletion (INDEL) mutation could lead to generation of a novel miRNA as well as losing the original miRNA [8]. In our approach we design sgRNAs flanking the stem-loop of the miRNA. These are predicted to simultaneously create double-strand breaks in the genome to “drop out” the entire miRNA stem-loop and give a clean miRNA KO (see also Godden et al., 2021). This method can be used to knock out miRNAs that are single genes, located in introns or part of multiple miRNA transcripts.

---

## 2 Materials

### 2.1 Embryo Acquisition

1. Chorulon: hcG, (Intervet).
2. 1× MMR: 100 mM NaCl, 2 mM KCl, 1 mM MgCl<sub>2</sub>, 2 mM CaCl<sub>2</sub>, 5 mM HEPES, pH 7.5.
3. BSA: 1.5% bovine serum albumin dissolved in 0.05x MMR.
4. Cysteine: 2% L-cysteine in 1× MMR, pH 7.8–8.0.
5. Ficoll: 3% Ficoll in 0.05× MMR.
6. Frozen sperm: obtained from the EXRC, Portsmouth.

### 2.2 Embryo Fixation

1. 10× MEM salts: 1 M MOPS, 20 mM EGTA, 10 mM MgSO<sub>4</sub>, pH 7.4.
2. MEMFA: 3.7% formaldehyde in MEM salts.
3. 10× PBS: 100 mM Na<sub>2</sub>HPO<sub>4</sub>H<sub>2</sub>O, 18 mM KH<sub>2</sub>PO<sub>4</sub>, 1.37 M NaCl, 27 mM KCl.
4. PBST: PBS, 0.1% Tween-20.

### 2.3 Embryo Injection

1. Harvard apparatus injector (Medical Systems Research); set the injector to the following parameters:  $P_{\text{out}} = 90$ ,  $P_{\text{balance}} = 0.6$  and  $P_{\text{inject}} = 16$ . For *X. tropicalis*, the maximum injection volume was 4.2 nL.

2. Glass capillaries: borosilicate standard wall with filament. OD 1 mM, ID 0.58 mM, 15 cM long, G100F-6, multichannel systems.
3. Cas9 protein, M0646M, EnGen Cas9 NLS 20  $\mu$ M, (New England Biolabs).
4. Capped RNA tracer generation: mMACHINE SP6 Transcription (Ambion).

#### **2.4 sgRNA Generation**

Guide RNAs are initially synthesized from PCR-amplified oligo sequences. These sequences contain the T7 promoter, the sgRNA sequence, and the CRISPR guide RNA assembly. The sequences to order as oligos are in Table 1. See Subheading 3.2.2 for sgRNA synthesis.

Materials for sgRNA synthesis:

1. GoTaq Green.
2. T7 MegaSHORTScript kit (Ambion).
3. PCR purification kit.
4. Nanodrop 1000.
5. Custom oligos.

#### **2.5 MiRNA Mimics**

1. hsa-miR-219a-5p miRCURY LNA miRNA mimic, compatible with xtr-miR-219 sequence: 5' UGAUUGUCCAAACG CAAUUCU (339173 YM0047076-ADA, MIMAT0000276, Qiagen).
2. Negative-control miRNA mimic, as recommended by manufacturer, was cel-miR-39-3p, sequence 5' UCACCGGGU GUAAAUCAGCUUG (331973, YM00479902-ADA, Qiagen).

#### **2.6 Genomic DNA Isolation**

1. Micropestles and 1.5-mL Eppendorf tubes.
2. Vortex.
3. PureLink gDNA Mini Kit, K1820-00 (Invitrogen).
4. PCR primers for genotyping can be found in Table 3.

#### **2.7 Subcloning of PCR Products**

1. GeneJET Gel Extraction Kit (Thermo Scientific).
2. UV gel visualizer.
3. Agarose gel electrophoresis tanks and peripherals.
4. pGEM-T easy kit (Promega).
5. GoTaq G2 DNA polymerase.
6. PCR primers can be seen in Table 2. M13 primers are used for sequencing of subcloned products into pGEM-T plasmids.

**Table 1**

**SgRNA sequences used. Common oligo taken from [2]. The first part of the sequence is in lowercase if the T7 promoter sequence, the capital letter sequence is the sgRNA complementary binding region sequence, and the last lowercase sequence is for the tracrR part of the sgRNA assembly**

SgRNA (sgRNA) oligo	Sequence 5' to 3'
sg219-5	taatacgactcactataGGTGAATTTTCCACAGCAATggttttagagctagaa
sg219-9	taatacgactcactataGGGTCTTCAGAATCAGCGACggttttagagctagaa
sg219-8	taatacgactcactataGGGTGTGTTGGGGGGGTTGGggttttagagctagaa
sg219-10	taatacgactcactataGGAAAGATTGTAAGTCCAAGggttttagagctagaa
Common oligo (reverse primer)	AAAAGCACCGACTCGGTGCCACTTTTTCAAGTTGATAACGGAC TAGCCTTATTTTAACTTGCTATTTCTAGCTCTAAAAC

**Table 2**

**Table of primers and sequences. Primers used for sequencing and PCR of genomic DNA**

Primer	Sequence 5' to 3'
miR-219 R3	GGTAGGCAACACACTCTTCAAC
miR-219 R2	GCCCTGGCAATGCTGGAAATG
miR-219 R4	GAAGGCTGTATTTTAGCCCTGGC
miR-219 6F	CCCAGTCTTGGAAGGAGTAGAC

**Table 3**

**Primers used for miRNA q-RT-PCR**

Primer name	Sequence 5' to 3'	Product code/accession number for design
ipu-miR-219a (for use with miR-219 KO samples)	AGAAUUGUGCC UGGACAUCUGU	YP02101832 (Qiagen)
U6 snRNA	CTCGC TTCGGCAGCACA	YP00203907 (Qiagen)
hsa-miR-219a-5p (for use when miR-219 mimic has been used)	UGAUUG UCCAAACGCAAUUC U	YP00204780 (Qiagen)

## 2.8 qRT-PCR

1. Quick-RNA Miniprep Plus Kit (Zymo).
2. cDNA synthesis: miRCURY LNA RT kit (Qiagen).
3. SYBR Green qPCR Master mix (Applied Biosystems).

4. MicroAmp® Optical 96-Well Reaction Plate (Applied Biosystems) and plate seals.
5. Primers and product codes can be seen in Table 3.

---

### 3 Methods

#### 3.1 *Xenopus* Husbandry and Embryo Acquisition

1. Obtain *X. tropicalis* embryos by priming females up to 72 h before use with 10 U of Chorulon and induce on the day of use with 200 U of Chorulon [9, 10].
2. Collect eggs manually and fertilize in vitro.
3. Remove the jelly from the embryos in 2% L-cysteine, incubate at 26 °C, and microinject in 3% Ficoll into 1 cell at the 2–4 cell stage in the animal pole.
4. Leave embryos to develop at 26 °C. Embryo staging is according to Nieuwkoop and Faber (NF) normal table of *Xenopus* development [11].

#### 3.2 CRISPR-Cas9

##### 3.2.1 Design of sgRNA

1. Design sgRNAs to incorporate the T7 promoter, as in [2]. SgRNAs are designed using CRISPRScan (<https://www.crisprscan.org/>) [12]. MiRNA sequences can be obtained from miRbase (<http://www.mirbase.org/>). In this example we are using miR-219, accession number: Xtr-miR-219 MI0004873. SgRNAs are designed up- and downstream of the miRNA stem-loop. miRNA stem-loop structures can be predicted computationally using the Vienna RNA fold tool (<http://rna.tbi.univie.ac.at/forna/>) (Fig. 1) (see Note 2).

##### 3.2.2 Generation of sgRNAs and CRISPR Reagents

1. Capped GFP RNA to be used as a tracer for injections is prepared using the SP6 mMACHINE kit. Inject 5 ng per embryo.
2. sgRNAs are ordered as oligonucleotide templates (see Table 1). These templates are then amplified by PCR (with GoTaq polymerase) with the following thermocycler program: stage 1, 95 °C for 5 min (x1); stage 2, 95 °C for 20 s; 66 °C for 20 s (ramp) to 68 °C for 15 s (x13); and stage 3, 94 °C for 20 s and 58 °C for 20 s (x30). PCR reaction mix includes 10 µL GoTaq Green, 2 µL forward primer (sgRNA oligomer template), 0.4 µL reverse primer, and 7.6 µL nuclease-free water. Products are run on 2% agarose gel to check integrity.
3. The T7 MegaSHORTScript kit is used according to manufacturer's instructions to transcribe RNA from the PCR product template with T7 polymerase.
4. Transcription product is cleaned up with a PCR purification kit, run on a 2% agarose gel and is quantified on a Nanodrop 1000.

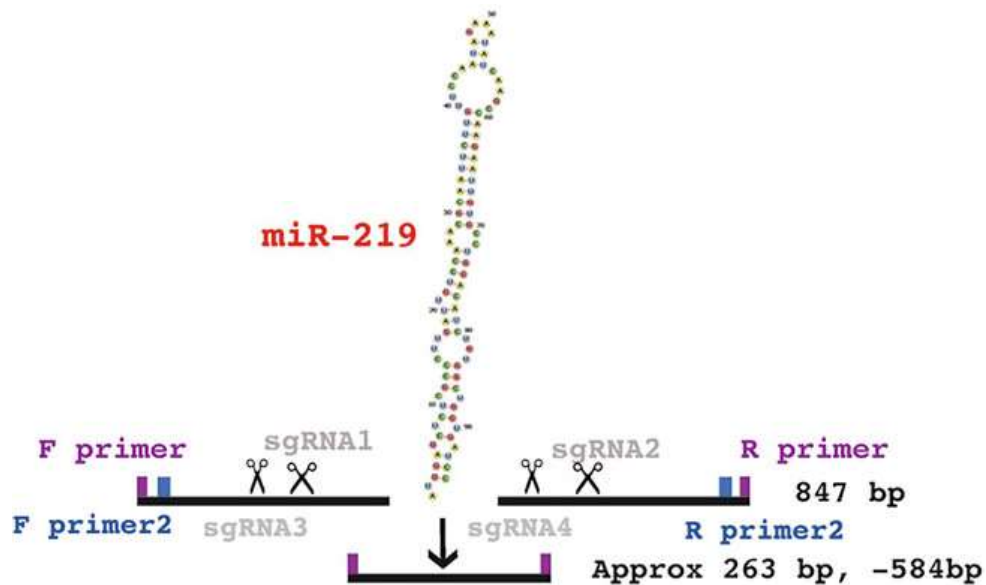


**Fig. 1** Schematic of sgRNA design and primer location around pri-miRNA stem-loop. In this example we show the primers required to KO miR-219, as used in [13]. This approach can target miRNAs in genic or intronic regions. It is best to design multiple sgRNAs, at least four, and select the most efficient two by experimentation as the best pair for miRNA KO. Primers for genome PCR are designed up- and downstream of the stem-loop outside of the sgRNA binding sites for genotyping. Multiple primers may need to be designed

5. CRISPR reagents for embryo injection are prepared as follows:

(a) CRISPR-KO cocktail:

sgRNAs are prepared to give a final concentration of 300 ng/ $\mu$ L (150 ng/ $\mu$ L each sgRNA), 500 ng/ $\mu$ L of GFP capped RNA tracer and Cas9 protein, and 0.8  $\mu$ L to give a final concentration of 2.4 mM and topped up to 3  $\mu$ L with nuclease-free water.

(b) CRISPR rescue cocktail:

As above, but with addition of miRNA mimic. Mimics are used at a final concentration of 11  $\mu$ M dose with CRISPR reagents to a final volume of 4  $\mu$ L.

### 3.2.3 Embryo Injection

1. Once *X. tropicalis* embryos have been fertilized, line up embryos in a gridded petri dish with Ficoll solution in the dish. Figure 2 shows example of how this would work.
2. Load CRISPR reagents into a glass capillary, by backfilling calibrated to 4.2 nL/injection.
3. Inject CRISPR reagents and GFP cRNA tracer with calibrated needle. See Note 3 for needle calibration. Harvard apparatus injector (Medical Systems Research) is set to the following parameters:  $P_{out} = 90$ ,  $P_{balance} = 0.6$ , and  $P_{inject} = 16$ . For *X. tropicalis*, the maximum injection volume is 4.2 nL.
4. Put embryos back in a 26 °C incubator for 2 h or until embryos have reached the 16–32 cell stage.



**Fig. 2** Microinjection setup of *Xenopus* embryos. (a) Microscope and micromanipulator setup. Harvard pli-100 injector is used, connected to a nitrogen gas supply system. (b, c) Embryos are lined up in rows in a gridded dish, with a minimal amount of Ficoll in to prevent embryo rupture upon injection

5. Once they have reached the 16–32 cell stage, gently remove Ficoll solution and replace with 0.05× MMR pre-warmed to 26 °C.
6. Leave embryos to develop in a 26 °C incubator until desired stages for morphological analysis are reached, or until tadpole stages for genotyping.
7. Select out GFP-positive from GFP-negative embryos after embryos have undergone gastrulation, as the level of fluorescence can be weaker during these stages, as it is obscured by lipids.

### 3.3 Genotyping and Sanger Sequencing

1. Once embryos reached the desired stage, they are imaged for phenotype analysis; to do this some embryos are fixed in MEMFA for 2 h at RT with gentle rocking.
2. After 2 h, MEMFA is removed and replaced with 2× 5-min washes of PBST and washed twice in 100% ethanol, before storage at –20 °C (if not needed for downstream analysis).
3. If embryos are needed for nucleic acid extraction, embryos were frozen individually in 1.5-mL Eppendorf tubes on dry ice for 30 min, before transfer to –80 °C.

4. Genomic DNA is extracted from individual embryos (*see Notes 1 and 4*).
5. Genomic DNA is then processed for genotyping PCRs. Further, 100 ng of template gDNA is used per PCR. Examples of primers are in Table 2. For wild-type samples, the PCR program is set up on the thermocycler as follows: stage 1, 95°C 5 min (X1); stage 2, 95°C for 20 s, 57 °C for 30 s, and 72°C for 30 s (X35); and stage 3, 72°C for 5 min (X1). For mutant samples, the following program is used: cycle 1, 98°C for 5 min (X1) and cycle 2, 95°C for 20 s, 57°C for 30 s, and 72°C for 10–30 s (X45) (*see Note 5*).
6. The PCR product is removed at the end of the program and incubated for 15 min with 1 µL of Taq polymerase (*see Note 6*).
7. PCR amplicons are run on a 2% agarose gel for 40 min at 90 V (*see Note 7*).
8. Bands are visualized and excised on a UV gel visualizer.
9. Gel bands are then purified using a gel extraction kit.
10. TA cloning kit with pGEM-T Easy Vector is used as recommended by manufacturer for subcloning PCR products.
11. Ligated construct is then transformed into DH5α onto X-Gal ampicillin plates.
12. Blue/white selection is used, with white colonies selected for colony PCR validation with M13 primers.
13. Successful subclones are then cultured in starter cultures of 50 mL LB media with 50 µL of ampicillin 10 mg/mL.
14. Plasmids are extracted from cultures using a Midi plasmid purification kit.
15. Samples are sent for Sanger sequencing, with 100 ng of plasmid and vector backbone primers (M13) at a concentration of 10 µM.
16. Resulting sequence products are then analyzed for deletions using sequence alignment tools on Clustal and SnapGene. Sequences are compared between wild type and KOs from sibling samples (*see Note 8*).

### **3.4 Q-RT-PCR Validation of miRNA KO**

1. To validate sgRNA efficiency and knockout of target miRNA, q-RT-PCR is needed. First, five embryos at a specific stage are pooled (*see Note 9*) and frozen on dry ice for 30 min before transfer to –80 °C.
2. RNA is extracted, from pooled samples, using a standard RNA extraction kit.
3. cDNA is synthesized using 50 ng of total RNA using miR-CURY LNA RT Kit (Qiagen). To generate the cDNA, a thermocycler is set with the following program: 42 °C for 60 min

and 95 °C for 5 min. cDNA was diluted 1:40 for q-RT-PCR. cDNA can be stored at –20 °C (*see Note 10*).

4. q-RT-PCR master mix is prepared as follows: SYBR Green PCR master mix (Applied Biosystems), 5 µL; miRNA-q-RT-PCR LNA primer, 1 µL; and cDNA template (1:40 diluted), 4 µL/well.
5. cDNA is pipetted on a MicroAmp® Optical 96-Well Reaction Plate, and then master mix is added and the plate spun down briefly. Plate and master mix are kept on ice, with cDNA thawed and kept on ice. Set up experiments with biological and technical triplicates.
6. q-RT-PCR is run on a 7500 standard PCR thermocycler (Applied Biosystems) using the following program: cycle 1, 50 °C for 2 min (X1), 95 °C for 10 s, 95 °C for 10 s, and 60 °C for 1 min (X45). Melt curve analysis was set to 95 °C for 15 s; 60 °C for 1 min; 95 °C 30 s, ramp rate 1%; 60 °C for 15 s.
7. Raw CT values are downloaded for analysis by the Delta Delta CT method to calculate fold change. U6 is used as housekeeper control reference for normalisation of miRNA expression.

### 3.5 miRNA Rescue Experiment

To validate specificity of miRNA KO, a novel rescue experiment was developed [13]. This needs to be carefully controlled, with use of a negative control miRNA mimic. This needs to be tested and injected into embryos alone to observe for any nonspecific phenotypes and dosed the same as experimental miRNA mimic, in this case the miR-219 mimic. The phenotype for your miRNA KO experiment should still be prevalent and unchanged in the control miRNA mimic-injected set of embryos, as in the miRNA KO. This phenotype observed in the miR KO and control miRNA mimic + miRNA KO group should then be rescued with experimental miRNA mimic + experimental miRNA KO. Careful phenotype analysis can be used to measure the extent of the rescue, along with q-RT-PCR.

---

## 4 Notes

1. *Xenopus* embryos are lipid-rich at younger neurula stages. When performing nucleic acid extractions, this can reduce your yield and 260:230 ratios. RNA 260:230 ratios can be low but generally do not interfere with the following experimental steps.
2. When designing sgRNAs, it is preferred to make sure they are at least 50 bp away from the start of the stem-loop structure to enable a clean dropout of the miRNA stem-loop and thus a clean miRNA KO. Likewise, if sgRNAs are designed far away

from the stem-loop, this could be suboptimal. When designing primers to amplify pri-miRNA, we have deliberately tried to design primers within 100–200 bp of the miRNA stem-loop. Shorter distances would reduce chance during Sanger sequencing of getting clean sequence data.

3. Needle calibration: capillaries were calibrated using a graticule eyepiece and measuring the size of the bubble generated carefully on a calibrated injector setup. The equipment we used in our lab was the Harvard apparatus injector (Medical Systems Research), and the injector was set to the following parameters:  $P_{\text{out}} = 90$ ,  $P_{\text{balance}} = 0.6$ , and  $P_{\text{inject}} = 16$ . Injections can be targeted at the right dorsal blastomere at the four-cell stage of development to target presumptive neural crest. For testing sgRNAs, the two-cell stage, injecting into one, blastomere is recommended so you can compare WT vs mutant PCR amplicons later on. For q-RT-PCR testing efficiency of sgRNAs, target both blastomeres at the two-cell stage of development to target the whole embryo.
4. Lower elution volumes recommended by nucleic acid extraction kits are recommended, 30  $\mu\text{L}$  minimum to maximize yield.
5. High-fidelity polymerases are recommended for detecting smaller mutations with higher accuracy.
6. Incubation with Taq polymerase is only necessary if proceeding to subclone PCR products for sequencing, into a TA vector. We find products have a better sequence quality if subcloned.
7. To bias the PCR towards the mutant, smaller miRNA KO amplicon, set up your PCR to generate a smaller amplicon. Set the elongation stage time to as short as possible. This is because the most abundant product, in our case WT if injecting/mutating half the embryo, will be amplified the most, and thus, the KO band will appear much weaker on a gel. To overcome this further, a nested PCR can be performed on gel extracted or purified products.
8. A good experiment to do is to genotype your own frog colony to identify your genome region of interest for your own miRNA to identify if your colony has any single-nucleotide polymorphisms compared to the current reference genome.
9. The stage chosen may vary depending on when the miRNA of interest is expressed; we had previously analyzed the temporal expression of our miRNAs and knew they were highly expressed enough at neurula stages to perform the analysis.
10. Keep cDNA in aliquots to avoid repeat freeze-thawing cycles as this will degrade your sample.

## Acknowledgements

We would like to acknowledge that AMG received technical support from the European *Xenopus* Resource Centre (EXRC), Portsmouth, UK, in the development of the CRISPR-Cas9 miRNA knockout method. We would like to thank Dr. Simon Moxon and Prof. Andrea Munsterberg for helpful discussions and the Wheeler and Munsterberg labs for support.

**Funding** This work was supported by UKRI Biotechnology and Biological Sciences Research Council Norwich Research Park Biosciences Doctoral Training Partnership grants to AMG (BB/M011216/1) and the European Union's Horizon 2020 research and innovation program under the Marie Skłodowska-Curie grant agreement no. 860635 to MA.

## References

1. Ran FA, Hsu PD, Wright J, Agarwala V, Scott DA, Zhang F (2013) Genome engineering using the CRISPR-Cas9 system. *Nat Protocols* 8(11):2281–2308
2. Nakayama T, Fish MB, Fisher M, Oomen-Hajagos J, Thomsen GH, Grainger RM (2013) Simple and efficient CRISPR/Cas9-mediated targeted mutagenesis in *Xenopus tropicalis*. *Genesis* 51(12):835–843
3. Cong L, Ran FA, Cox D, Lin S, Barretto R, Habib N et al (2013) Multiplex genome engineering using CRISPR/Cas systems. *Science* 339(6121):819–823
4. Kim HK, Lee S, Kim Y, Park J, Min S, Choi JW et al (2020) High-throughput analysis of the activities of xCas9, SpCas9-NG and SpCas9 at matched and mismatched target sequences in human cells. *Nat Biomed Eng* 4(1):111–124
5. Hwang WY, Fu Y, Reyon D, Maeder ML, Tsai SQ, Sander JD et al (2013) Efficient genome editing in zebrafish using a CRISPR-Cas system. *Nat Biotechnol* 31(3):227–229
6. Grainger RM (2012) *Xenopus tropicalis* as a model organism for genetics and genomics: past, present, and future. *Methods Mol Biol* 917:3–15
7. Bartel DP (2004) MicroRNAs: genomics, biogenesis, mechanism, and function. *Cell* 116(2):281–297
8. Bhattacharya A, Cui Y (2017) Systematic prediction of the impacts of mutations in MicroRNA seed sequences. *J Integr Bioinform* 14(1):20170001
9. Harrison M, Abu-Elmagd M, Grocott T, Yates C, Gavrilovic J, Wheeler GN (2004) Matrix metalloproteinase genes in *Xenopus* development. *Dev Dyn* 231(1):214–220
10. Williams RM, Winkfein RJ, Ginger RS, Green MR, Schnetkamp PP, Wheeler GN (2017) A functional approach to understanding the role of NCKX5 in *Xenopus* pigmentation. *PLoS One* 12(7):e0180465
11. Nieuwkoop P, Faber J (1967) Normal table of *Xenopus laevis* (Daudin): a systematical and chronological survey of the development from the fertilized egg till the end of metamorphosis. Garland Publishing, New York
12. Moreno-Mateos MA, Vejnar CE, Beaudoin JD, Fernandez JP, Mis EK, Khokha MK et al (2015) CRISPRscan: designing highly efficient sgRNAs for CRISPR-Cas9 targeting in vivo. *Nat Methods* 12(10):982–988
13. Godden AM, Antonaci M, Ward NJ, van der Lee M, Abu-Daya A, Guille M et al (2021) An efficient miRNA knockout approach using CRISPR-Cas9 in *Xenopus*. *Dev Biol* 483:66–75

## REVIEW

# Neural crest development and disorders: from patient to model system and back again – the NEUcrest conference

Marco Antonaci<sup>1,\*</sup>, Amy Kerr<sup>1</sup>, Merin Lawrence<sup>2</sup>, Francesca Lorenzini<sup>3</sup>, Nitin Narwade<sup>4</sup>, Chloé Paka<sup>5,6</sup> and Anna Magdalena Wulf<sup>6</sup>

## ABSTRACT

The neural crest (NC) is an embryonic multipotent and transitory population of cells that appears during late gastrulation/early neurulation in the developing embryos of vertebrate organisms. Often called “the fourth germ layer”, the NC is characterised by incredible mobility, which allows the NC cells to migrate throughout the whole embryo, giving rise to an astonishing number of different derivatives in the adult organism, such as craniofacial skeleton, adrenal gland, enteric nervous system and melanocytes. Because of these properties, neurocristopathies (NCPs), which is the term used to classify genetic diseases associated with NC developmental defects, are often syndromic and, taken all together, are the most common type of genetic disease. The NEUcrest consortium is an EU funded innovative training network (ITN) that aims to study the NC and NCPs. In March 2024, the early stage researchers (ESRs) in the NEUcrest consortium organised an in-person conference for well-established and early career researchers to discuss new advances in the NC and NCPs field, starting from the induction of the NC, and then moving on to migration and differentiation processes they undergo. The conference focused heavily on NCPs associated with each of these steps. The conference also included events, such as a round table to discuss the future of the NC research, plus a talk by a person living with an NCP. This 3-day conference aimed to bring together the past, present and future of this field to try and unravel the mysteries of this unique cell population.

**KEY WORDS:** Neural crest (NC), Neurocristopathies (NCPs), Development, Migration, Epithelial to mesenchymal transition (EMT)

## Introduction

The neural crest (NC) is a transient cell type that originates during late gastrulation/early neurulation of a developing embryo. During development, neural crest cells (NCCs) are induced at the neural plate border, and then undergo a process called epithelial to mesenchymal transition (EMT), which allows them to migrate throughout the embryo. These cells then differentiate into an

astonishing number of derivatives, which include (but are not limited to) craniofacial skeleton, teeth, melanocytes, enteric ganglia, and adrenal medulla (Fig. 1) (Bronner and LeDouarin, 2012). Such an incredible cell population is necessarily controlled by very complex gene regulatory networks (GRNs), which are constantly being updated with the addition of new transcription factors, signalling molecules and non-coding RNAs (Simoes-Costa and Bronner, 2013, 2015; Seal and Monsoro-Burq, 2020; Pla and Monsoro-Burq, 2018; Antonaci and Wheeler, 2022).

Diseases associated with problems during NC development are often syndromic, like Waardenburg syndrome (Huang et al., 2022), CHARGE syndrome (Usman and Sur, 2021), or DiGeorge syndrome (Lackey and Muzio, 2021). However, if the problem occurs later during NC development, it can give rise to NCPs with very specific phenotypes, such as Hirschsprung disease (Lotfollahzadeh et al., 2021), craniosynostosis (Goos and Mathijssen, 2019) or even give rise to some NC-specific cancer types, such as neuroblastoma (Wulf et al., 2021), pheochromocytoma (Gimenez-Roqueplo et al., 2023) and melanoma (Castro-Perez et al., 2023). Given this incredible heterogeneity of disorders, NCPs are, collectively, the most prevalent type of genetic diseases (Vega-Lopez et al., 2018).

Because of the high medical importance, and intriguing nature of the NCCs, in 2019 Professors Anne-Helene Monsoro-Burq, Karen Liu, Grant Wheeler and Gerhard Schlosser organised an innovative training network (ITN), funded by the EU program Horizon2020, NEUcrest – Training European Experts in Multiscale Studies on Neural Crest Development and Disorders: from Patient to Model System and Back again.

With a total of 11 beneficiaries, and nine associated partners (both in academia and industry), NEUcrest has the objective of training 15 early stage researchers (ESRs) and exploring different aspects of NC biology, from its physiology to pathological conditions (<https://neurest.curie.fr/index>) (Fig. 2).

The conference ‘Neural crest development and disorders: from patient to model system and back again’, held in the peninsula of Giens (France), at the Belambra Club, between the 3rd and the 6th of March 2024, celebrated the culmination of this program. Organised by selected members of the ESRs with help from the PIs, this in-person conference aimed to bring together well-established experts with scientists just starting their careers in this exciting field. Alongside talks from many invited speakers, this conference, gave the ESRs in the consortium the chance to present the results that they had obtained during the course of their PhD projects within the NEUcrest.

In this Meeting Report, we highlight the exciting content of this friendly conference of 100 people, in which established scientists from across the globe reunited with old friends, and young researchers had the chance of engaging for the first time with fellow scientists that they will, hopefully collaborate with in the future.

<sup>1</sup>School of Biological Sciences, University of East Anglia, Norwich Research Park, Norwich, NR7 7TJ, UK. <sup>2</sup>School of Biological and Chemical Sciences, University of Galway, Biomedical Sciences Building, Second Floor North, Newcastle Road, Galway, H91 W2TY, Ireland. <sup>3</sup>Experimental Cancer Biology Laboratory, CIBIO, University of Trento, Trento, Italy. <sup>4</sup>Cell plasticity in development and disease Unit, Instituto de Neurociencias, CSIC-UMH, Sant Joan de Alicante, 03550 Alicante, Spain. <sup>5</sup>STEMCELL Technologies UK Ltd, Cambridge, UK. <sup>6</sup>Centre for Craniofacial and Regenerative Biology, King’s College London, London, UK.

\*Author for correspondence (m.antonaci@uea.ac.uk)

© M.A., 0000-0002-5255-465X; M.L., 0009-0002-3934-3089; F.L., 0000-0002-1843-0151; N.N., 0000-0002-1368-307X

This is an Open Access article distributed under the terms of the Creative Commons Attribution License (<https://creativecommons.org/licenses/by/4.0>), which permits unrestricted use, distribution and reproduction in any medium provided that the original work is properly attributed.

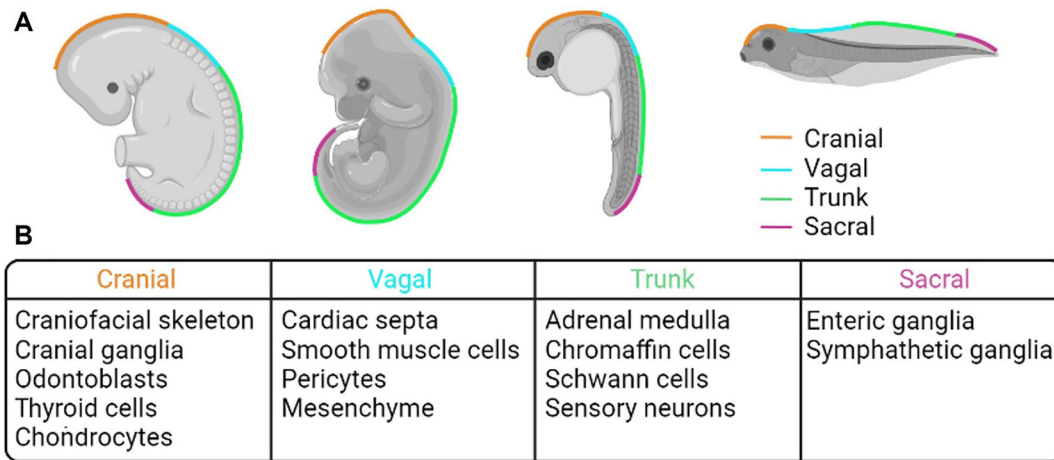


**Fig. 1. Neural crest contribution in the adult organism.** (A) NC separation in different animal models during embryogenesis (from left to right: human, mouse, zebrafish and frog). (B) Examples of NC contribution to the adult organism, specific for the different NC populations. All the NC populations give rise to melanocytes in the adult organism.

**From induction to differentiation: a neural crest trip**

As a conference opener and keynote speaker we had the honour of hosting Professor Marianne Bronner (Caltech, USA). She and her lab are one of the leading forces in to NC development in all of its facets (Martik and Bronner, 2021; Solovieva and Bronner, 2021; Tang and Bronner, 2020). Her presentation introduced the inspiring work that her lab is carrying out on the contribution of the NCCs to cardiac development. Using a variety of techniques, in zebrafish and chick embryos, they have found that *Tgif1* and its downstream targets are required to induce the cardiac identity of NCCs.

The way the NEUcrest conference was organised aimed to transport the attendees on a journey, following the developmental steps of the NCCs. Because of this, the early sessions were mainly focused on the induction and specification of the NC and as the conference progressed the talks shifted more towards differentiation of the NC.

One important aspect that emerged during the conference was that no matter the stage of NC development that the research group is investigating, a great importance is given to the medical impact that the research can lead to. The talk from Dr Anestis Tsakiridis

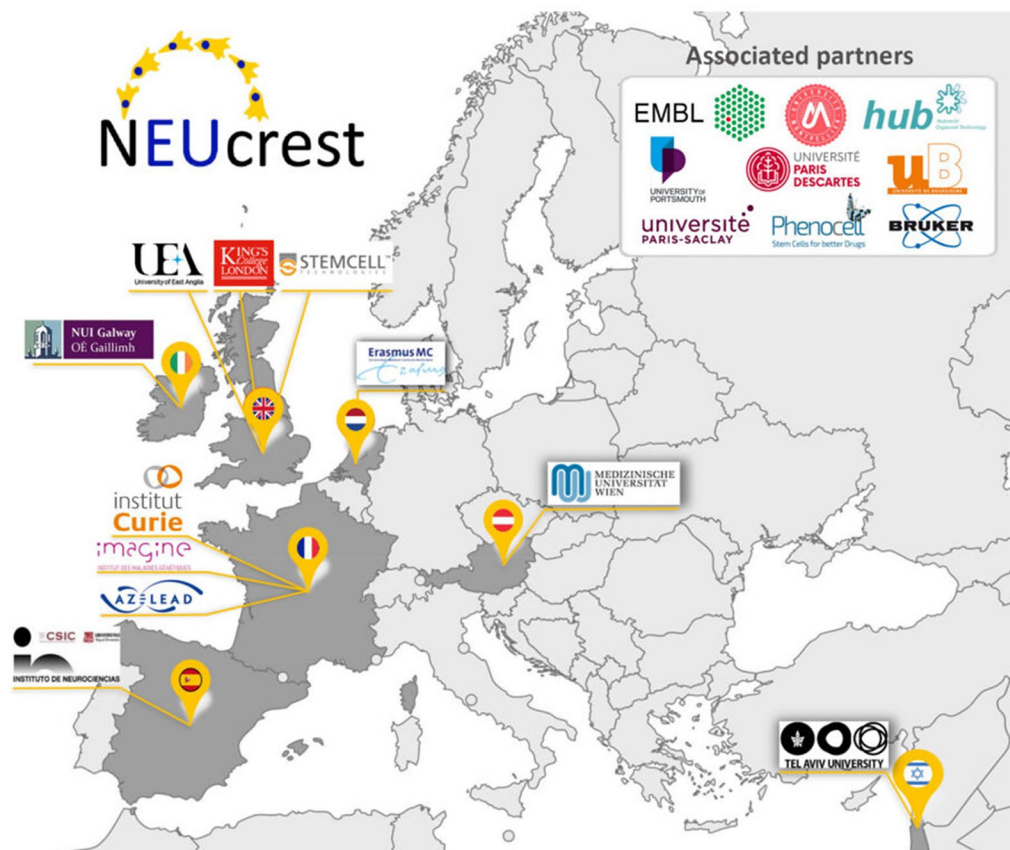


**Fig. 2. Map of the NEUcrest partners across the European territory.** Map showing all the partners (academic and industry) that are involved in the NEUcrest ITN. The countries in dark grey are the ones hosting the early stage researchers (ESRs).

(University of Sheffield, UK), was a perfect example of this. His lab is interested in the use of hiPSCs-induced NC with the aim of modelling human diseases, and to potentially use these reprogrammed cells to perform cell replacement therapy for people affected by Hirschsprung disease (Cooper et al., 2024). This neurocristopathy affects the enteric nervous system, generating several symptoms that range from severe constipation to malnutrition.

Historically speaking, developmental biology has focused much on transcription factors, whose expression and regulatory networks have been extensively studied for decades. Because of this, it was good to see that many of the talks were also diversified, pointing at different aspects of cell biology. Dr Eric Theveneau (Centre for Integrative Biology, France), one of the invited speakers, talked about the role that metalloproteases (and MMP14 in particular) play in NC delamination and migration (Barriga and Theveneau, 2020). Another example was given by Dr Ruth Palmer (University of Gothenburg, Sweden) and Anna Wulf (King's College London, UK), who both gave an insight into ALK (anaplastic lymphoma kinase) biology. ALK is the major player involved in the onset of neuroblastoma, a cancer of the sympatho-adrenal lineage which mostly affects children aged 5, or younger. While Palmer uses the *Drosophila* model to study pathological mutations in the *ALK* gene and its involvement in the DNA-damage response (Borenas et al., 2024), Wulf focused on its interaction with GSK3 (glycogen synthase kinase 3), and how the migration of NCCs is affected by pathological mutations of *ALK* (Wulf et al., 2021). The talk from another ESR, Marco Antonaci (University of East Anglia, UK), presented his data that show the dual role of *miR-204-1-5p* and *miR-204-1-3p* during the development of the eye (Antonaci and Wheeler, 2022). Also with the aim of studying human conditions, Dr Ruth Williams (University of Manchester, UK) talked about the role of the chromatin remodelling factor *Chd7*, the causative gene of CHARGE syndrome, using chicken embryos.

As Next Generation Sequencing progresses and becomes more and more accessible, the number of labs that are generating and processing this kind of data keeps increasing. The merging of different datasets produced by RNA, ATAC, ChIP, and Hi-C sequencing has the potential to drawing a clearer image of the molecular mechanisms that drive embryo development. A useful tool has been developed by Nitin Narwade, bioinformatician in Angela Nieto's lab (Institute of Neuroscience, Spain), which is capable of predicting cell fate trajectories in case of perturbation (introduction or removal) of a transcription factor from a still-undifferentiated cell type.

Speaking about cutting-edge technologies, it is impossible not to mention the contribution to the field (and to this conference) given by Professor Igor Adameyko. With his lab's single-cell OMICS, fate mapping and lineage tracing, he is currently one of the leading scientists when it comes to cell fate determination. Several people from his laboratories, located at the Medical University of Vienna (Austria) and at the Karolinska Institute (Sweden), presented their innovative data. One of the invited speakers, Dr Maria Elena Kastriti, is part of his team in Vienna. She presented data from one of her recent publications about the finding of a "hub state" of the Schwann cell precursors, that allows these cells to differentiate into a variety of cell type during mouse embryogenesis (Kastriti et al., 2022). Following that cell lineage, but looking at frog embryos, Amy Kerr (University of East Anglia, UK) presented her work on the characterisation of the development of the adrenal gland. She showed that chromaffin-like cells start appearing very early during development, and hinted that NCCs might be able to migrate even further than originally thought.

Also from the Adameyko lab, another ESR, Irina Poverennaya, introduced her bioinformatical analysis that highlighted the importance of ribosomal RNA and ribosomal assembly transcripts in NC fate decision. Next, Merin Lawrence (University of Galway, Ireland) presented her CUT&RUN data integrated with RNA-seq, aimed to shed light on the role of *SOX10* in placode and NC development.

### Ethical science, stem cells and animal models: the Yin and Yang of research

In the past years, the advent of stem cells and iPSCs technology has revolutionised the entirety of biological science. This is particularly true for the field of developmental biology. The possibility to produce, *in vitro*, NC-induced pluripotent stem cells (NC-iPSCs) has encouraged an increasing number of scientists to use less animals in their experiments. Of course, researchers are aware that the use of NC-iPSCs is not completely accurate in the recapitulation of the biological context of the NC development in a living organism. It is undeniable, though, that this model has the potential of reducing (but not completely replacing) the number of animals used in science every year.

In a society where the general opinion towards science is torn between the use or not of animals in science, it is important to make an effort and move towards this direction, whenever possible.

For this reason, an entire session of the NEUcrest conference was dedicated to research that uses biological models alternative to animals. During the session called 'Exploring neural crest biology with 3Rs strategies', speakers explained their research which gives particular importance to the 3Rs principles of *Replacement*, *Reduction* and *Refinement* of animals in research.

As an example of replacement, one of the ESRs, Ana Filipa Duarte (Erasmus Medical Centre, Rotterdam, Netherlands), described the generation of hiPSCs derived from a person affected by craniosynostosis. This person carries a potentially pathological variant on *FUZ* gene (*FUZ<sup>R284P</sup>*), which she reverted using CRISPR-prime editing, before further differentiation into the osteogenic lineage (Barrell et al., 2022).

Filipa was not the only NEUcrest member working on hiPSCs. Chloe Paka (Stemcell Technologies, UK) and William Bertani-Torres (Imagine Institute, France) are also modelling human neurocristopathies *in vitro*. Chloe, who works closely with Karen Liu's research team, has developed a cell line harbouring a mutation in *ALK* gene, that recapitulates a human mutation that has been found in patients with neuroblastoma. In a similar fashion, William is working on the characterization of a novel human mutation in *ADAMTS20* that has been found in a patient affected by Waardenburg syndrome (Bertani-Torres et al., 2023).

Similarly, Ayat Ahmed (a PhD student at the University of Heidelberg, Germany), also described work using hiPSCs-derived NC to generate cortical neurons or neural progenitor cells. Her aim was to investigate the role of the transcription factor *NR2F1* ('A gene to rule them all') and its long non-coding RNA (*lncNR2F1*) in chromatin organisation. By using high throughput techniques, such as Hi-C, 4C-seq, ATAC-seq and ChIP-seq, her goal is to shed light into the etiopathogenesis of the Bosh-Boonstra-Schaaf Optic Atrophy Syndrome (BBSOAS). This rare syndrome is caused by deletions or mutations in *NR2F1* locus, and causes typical craniofacial dysmorphism, autism spectrum disorder, and optic nerve atrophy.

Melanoma is a major cancer in Western society. Francesca Lorenzini (Azelead, Montpellier, France), presented beautiful

images generated during her PhD, using zebrafish embryos to study the microenvironment of melanomas by using patient-derived xenograft imaging (Marines et al., 2023).

### The urge for more cooperation between scientists and people affected by NCPs

A particularly special moment of the conference was the presentation of Charlotte Ashby, which was followed by a small discussion round. Charlotte lives with unicoronal Craniosynostosis and was invited to represent people living with these kinds of conditions. She talked about her experience, how it is to go through endless rounds of surgeries and medical discussions and also introduced the foundation she is part of: Headlines Craniofacial Support UK (<https://www.headlines.org.uk/>). Charlotte is a sociology graduate from the University of Bath and became the youngest-ever trustee of Headlines, at the age of 19.

Charlotte first talked about the troubles her parents encountered when she was a baby, regarding the initial struggle to find a diagnosis, and her parents having to watch their young child go through various medical procedures right after birth. Something that struck us in particular, was Charlottes admittance, that she didn't quite have a good understanding of her own diagnosis when she started being in charge of her own medical treatment courses as a young adult. It made all of us smile, but also reflect, to hear Charlotte opening's sentence: "I have to admit, before being invited at this conference, I had no idea what the neural crest was". It highlighted an old and deep-rooted problem between scientists and the general public, even with respect to those closely affected by scientific research.

Her knowledge of the condition was mostly based on her own reading and basic explanations of doctors but never went into great detail. She also told us that she was fascinated listening to some of our speakers, talks that were focused on background research on craniosynostosis and their work, and how much work is already being done.

Charlotte then introduced us to the work of Headlines. This charity was initially funded by a group of parents of children with craniosynostosis in 1993. It is currently run mostly by those living with craniosynostosis. Headlines is focused on providing support for people living with craniofacial conditions, raising awareness, educating people to improve public understanding of such conditions and facilitating research on craniosynostosis and other rare craniofacial conditions.

After the talk, there followed a question and discussion round with Charlotte, and the overall consensus seemed to be a wish on both sides to be more involved with each other. Researchers were keen to meet patients and to be able to explain their work. On the other hand, Headlines is interested in raising more awareness of the patient experience but also having more contact and events with researchers to create a greater understanding of such conditions.

Someone asked how many people in the room had worked with patients in any form before, and about 20% of the attendees raised their hand. Overall, this was a unique experience for both Charlotte and for all researchers in attendance and it added depth and meaning to the work presented at the conference. We are very grateful to Charlotte for bravely talking to a room full of scientists for the first time and allowing us to hear her story and about Headlines' work.

### Attendees at the conference: statistics

With its 95 participants, "Neural crest development and disorders: from patient to model system and back again" was a medium-small sized conference that aimed at creating a sense of community among the participants.

Using a combination of short talks and flash talks, 46 of the participants were given the opportunity to give an oral presentation. Also, with a total of 54 posters and eight invited speakers, more than half of the participants to the conference had the chance to present their work (either orally, or with a poster presentation). Of these oral presentations and posters, 12 were provided by the NEUcrest ESRs. This means that 60% of the participants had the chance to present their work, or the work conducted in their lab, through an oral or poster presentation (or both). Of these fractions, the NEUcrest ESRs accounted for 26% of the oral presentations, and 21% of the poster presentations (Fig. 4A). About the country of origin of the attendees, the biggest fraction of them was based in France, as expected (a total of 27 people), 58 people came from a European Country (other than France), and 10 attendees joined from extra European countries (USA and the Republic of China) (Fig. 4B).

Overall, given the length of the conference (2.5 days in total), it was expected that not so many people would have joined from countries other than European ones. However, people gave positive feedback to the organisers about the number of participants, and



**Fig. 3. Picture of Charlotte Ashby's talk, chaired by Professor Grant Wheeler (University of East Anglia, UK).** Charlotte Ashby was born with unicoronal craniosynostosis and became Headlines' youngest-ever trustee in 2020, at the age of 19. She runs the charity's Young Person's Network, which allows people aged 16-30 with craniofacial conditions to connect. Charlotte is passionate about advocating for young people and adults with craniofacial conditions and utilizing her experiences of growing up and living with a craniosynostosis to raise awareness of the condition.

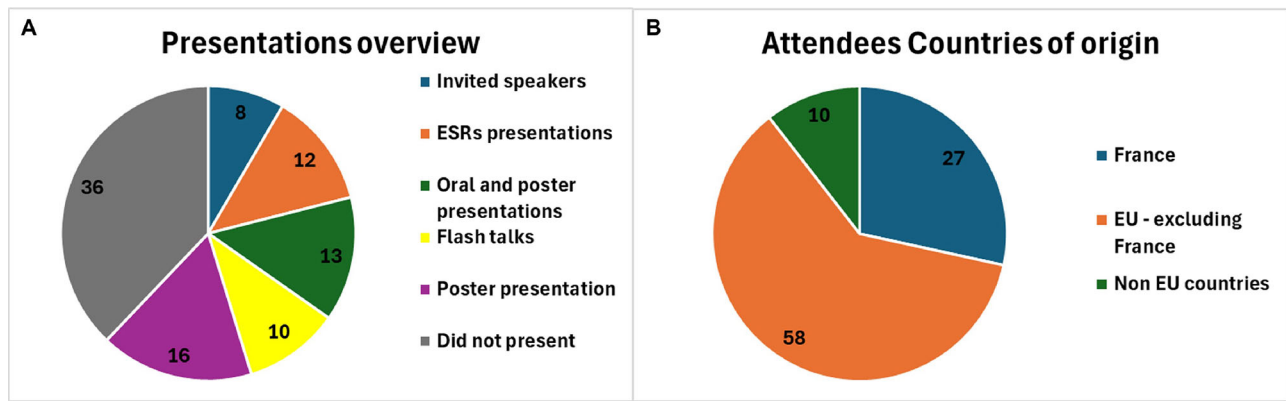


**Fig. 4. Attendees at the “Neural Crest Development and Disorders: From Patient to Model System and Back Again” conference.** (A) Breakdown of the number of attendees who had the chance of presenting their work through an oral presentation. Over half of the attendees had the possibility to present with an oral or poster presentation, or both. (B) Country of origin of the attendees. Most of them joined from a European country (58/95), with a prevalence of France institutions (27/95). In green, the number of attendees from extra European Countries (mainly USA and Republic of China).

said that they had the chance of talking with most of the other attendees during the breaks, or the evenings.

**Conclusion**

In March 2024, the conference: ‘Neural crest development and disorders: from patient to model system and back again’ was organised as final milestone and a celebration of the NEUcrest project. This conference, mainly organised by the early career researchers in the NEUcrest consortium, had different goals: to give the chance to young researchers to share their work to a community of experts in the field, and to interact with each other; to bridge the gap between scientist and people affected by rare conditions; discuss the evolution of the NC and, more broadly, the developmental biology field; lastly, to share with the scientific community the goals and achievements obtained by the NEUcrest consortium.

With discussions, sharing of ideas, point of views and vibrant debates, we believe these goals were achieved. Almost 100 participants from across the globe joined the conference. Most of them had the chance to share their results and ideas, either during the

poster sessions or during the oral presentations, kept short specifically to allow most people to give a talk, which included some excellent flash talks of 2-3 min each. Unfortunately, in this report, we have not been able to mention every talk from the attendees. Developmental Dynamics had kindly offered prizes of 250\$ each for the best talk and poster. These were awarded at the end of the conference to Dennis Pang (University of Hong Kong) for his poster titled: “Elucidating the mechanistic role of STRAP in regulating SNAI2 stability for proper onset of cranial neural crest epithelial to mesenchymal transition” and Sydney Arlis (University of Iowa) for her talk titled: “Defining the role of ISM1 in craniofacial development”.

While the future cannot be foreseen, after this conference we can at least predict the direction that this exciting field is taking: a more ethical science, with an increased level of resolution, but without forgetting clever experimental design and the reasons why we are asking our questions. Either way, with the exciting science that the attendees showed during the conference, we can be quite sure that the future of the neural crest research is in good hands.



**Fig. 5. Group picture of the attendees at the ‘Neural crest development and disorders: from patient to model system and back again’ conference.**

### Acknowledgements

The authors would like to thank all the members of the ITN NEUcrest and the organisers of the conference. In particular, we thank Patricia Noguez-Hellin for all the help she provided in preparing the conference. We would also like to thank Dr William Bertani-Torres and Ana Filipa Duarte for proofreading this document. Finally, the authors would like to thank Professor Grant Wheeler for his constant suggestions and advice on the writing of this report.

### Competing interests

The authors declare no competing or financial interests.

### Funding

The Neural Crest Development and Disorders: From Patient to Model System and Back Again conference was financed by the EU program Horizon 2020 (grant number 860635) NEUcrest – Training European Experts in Multiscale Studies on Neural Crest Development and Disorders: from Patient to Model System and Back again, and supported by the Société Française de Biologie du Développement, by The Company of Biologists, Developmental Dynamics, Institut Curie, and by the Routledge Taylor and Francis Group.

### References

- Antonaci, M. and Wheeler, G. N.** (2022). MicroRNAs in neural crest development and neurocristopathies. *Biochem. Soc. Trans.* **50**, 965-974. doi:10.1042/BST20210828
- Barrell, W. B., Adel Al-Lami, H., Goos, J. A. C., Swagemakers, S. M. A., Van Dooren, M., Torban, E., Van Der Spek, P. J., Mathijssen, I. M. J. and Liu, K. J.** (2022). Identification of a novel variant of the ciliopathic gene FUZZY associated with craniosynostosis. *Eur. J. Hum. Genet.* **30**, 282-290. doi:10.1038/s41431-021-00988-6
- Barriga, E. H. and Theveneau, E.** (2020). In vivo neural crest cell migration is controlled by "Mixotaxis". *Front. Physiol.* **11**, 586432. doi:10.3389/fphys.2020.586432
- Bertani-Torres, W., Lezirovitz, K., Alencar-Coutinho, D., Pardono, E., Da Costa, S. S., Antunes, L. D. N., De Oliveira, J., Otto, P. A., Pingault, V. and Mingroni-Netto, R. C.** (2023). Waardenburg syndrome: the contribution of next-generation sequencing to the identification of novel causative variants. *Audiol Res.* **14**, 9-25. doi:10.3390/audiolres14010002
- Borenas, M., Umapathy, G., Lind, D. E., Lai, W. Y., Guan, J., Johansson, J., Jennische, E., Schmidt, A., Kurhe, Y., Gabre, J. L. et al.** (2024). ALK signaling primes the DNA damage response sensitizing ALK-driven neuroblastoma to therapeutic ATR inhibition. *Proc. Natl. Acad. Sci. USA* **121**, e2315242121. doi:10.1073/pnas.2315242121
- Bronner, M. E. and Ledouarin, N. M.** (2012). Development and evolution of the neural crest: an overview. *Dev. Biol.* **366**, 2-9. doi:10.1016/j.ydbio.2011.12.042
- Castro-Perez, E., Singh, M., Sadangi, S., Mela-Sanchez, C. and Setaluri, V.** (2023). Connecting the dots: Melanoma cell of origin, tumor cell plasticity, trans-differentiation, and drug resistance. *Pigment Cell Melanoma Res.* **36**, 330-347. doi:10.1111/pcmr.13092
- Cooper, F., Souilhol, C., Haston, S., Gray, S., Boswell, K., Gogolou, A., Frith, T. J. R., Stavish, D., James, B. M., Bose, D. et al.** (2024). Notch signalling influences cell fate decisions and HOX gene induction in axial progenitors. *Development* **151**, dev202098. doi:10.1242/dev.202098
- Gimenez-Roqueplo, A. P., Robledo, M. and Dahia, P. L. M.** (2023). Update on the genetics of paragangliomas. *Endocr. Relat. Cancer* **30**, e220373. doi:10.1530/ERC-22-0373
- Goos, J. A. C. and Mathijssen, I. M. J.** (2019). Genetic causes of craniosynostosis: an update. *Mol. Syndromol.* **10**, 6-23. doi:10.1159/000492266
- Huang, S., Song, J., He, C., Cai, X., Yuan, K., Mei, L. and Feng, Y.** (2022). Genetic insights, disease mechanisms, and biological therapeutics for Waardenburg syndrome. *Gene Ther.* **29**, 479-497. doi:10.1038/s41434-021-00240-2
- Kastriti, M. E., Faure, L., Von Ahsen, D., Boudierlique, T. G., Bostrom, J., Solovieva, T., Jackson, C., Bronner, M., Meijer, D., Hadjab, S. et al.** (2022). Schwann cell precursors represent a neural crest-like state with biased multipotency. *EMBO J.* **41**, e108780. doi:10.15252/embj.2021108780
- Lackey, A. E. and Muzio, M. R.** (2021). *DiGeorge Syndrome*. Treasure Island, FL: StatPearls.
- Loffollahzadeh, S., Taherian, M. and Anand, S.** (2021). *Hirschsprung Disease*. Treasure Island, FL: StatPearls.
- Marines, J., Lorenzini, F., Kissa, K. and Fontenille, L.** (2023). Modelling 3D tumour microenvironment in vivo: a tool to predict cancer fate. *Curr. Issues Mol. Biol.* **45**, 9076-9083. doi:10.3390/cimb45110569
- Martik, M. L. and Bronner, M. E.** (2021). Riding the crest to get a head: neural crest evolution in vertebrates. *Nat. Rev. Neurosci.* **22**, 616-626. doi:10.1038/s41583-021-00503-2
- Pla, P. and Monsoro-Burq, A. H.** (2018). The neural border: Induction, specification and maturation of the territory that generates neural crest cells. *Dev. Biol.* **444** Suppl. 1, S36-S46. doi:10.1016/j.ydbio.2018.05.018
- Seal, S. and Monsoro-Burq, A. H.** (2020). Insights into the early gene regulatory network controlling neural crest and placode fate choices at the neural border. *Front. Physiol.* **11**, 608812. doi:10.3389/fphys.2020.608812
- Simoës-Costa, M. and Bronner, M. E.** (2013). Insights into neural crest development and evolution from genomic analysis. *Genome Res.* **23**, 1069-1080. doi:10.1101/gr.157586.113
- Simoës-Costa, M. and Bronner, M. E.** (2015). Establishing neural crest identity: a gene regulatory recipe. *Development* **142**, 242-257. doi:10.1242/dev.105445
- Solovieva, T. and Bronner, M.** (2021). Reprint of: schwann cell precursors: where they come from and where they go. *Cells Dev.* **168**, 203729. doi:10.1016/j.cdev.2021.203729
- Tang, W. and Bronner, M. E.** (2020). Neural crest lineage analysis: from past to future trajectory. *Development* **147**, dev193193. doi:10.1242/dev.193193
- Usman, N. and Sur, M.** (2021). *CHARGE Syndrome*. Treasure Island, FL: StatPearls.
- Vega-Lopez, G. A., Cerrizuela, S., Tribulo, C. and Aybar, M. J.** (2018). Neurocristopathies: new insights 150 years after the neural crest discovery. *Dev. Biol.* **444** Suppl. 1, S110-S143. doi:10.1016/j.ydbio.2018.05.013
- Wulf, A. M., Moreno, M. M., Paka, C., Rampasekova, A. and Liu, K. J.** (2021). Defining pathological activities of ALK in neuroblastoma, a neural crest-derived cancer. *Int. J. Mol. Sci.* **22**, 11718. doi:10.3390/ijms222111718